ROBUST CONTROL SYSTEM DESIGN

FOR A

FIXED-BED CATALYTIC REACTOR

Thesis by

Jorge Anibal Mandler

In Partial Fulfillment of the Requirements

for the Degree of

Doctor of Philosophy

California Institute of Technology

Pasadena, California

1987

(Submitted July 30, 1986)

Dedicated with love

to my dearest ones,

Silvia, Rafa and Mariana.

ACKNOWLEDGMENTS

I am grateful to Dr. John H. Seinfeld for his guidance, valuable advice and support throughout the years of my study and research at Caltech.

It is with deep appreciation that I acknowledge Dr. Manfred Morari, for his insight, wealth of ideas, enthusiasm and care that helped make this work possible. Working with him and being a member of his research group has been a privilege for me. I am specially thankful to my colleagues in this group, for the continuous interaction and enlightening discussions.

I am particularly indebted to Daniel E. Rivera for all his help, thoughtful suggestions, continuous encouragement and the many hours he dedicated on my behalf; to Sigurd Skogestad, who always answered gladly all my questions; and to Evanghelos Zafiriou, who *almost* always did. I have deeply enjoyed their friendship.

Chris Webb continues this project and I wish him (he deserves) the best. To John Doyle, many thanks for the brilliant theory.

Of the staff, I would like to thank Edith Huang, who throughout the years provided generous help in word-processing matters, George Griffith, for his kindness, and Betty Benjamin, for her patience.

The financial assistance of Caltech is gratefully acknowledged. Acknowledgment is made to the Donors of The Petroleum Research Fund, administered by the American Chemical Society, to the National Science Foundation and to the Department of Energy for the support of the research reported in this thesis.

Mario and Frida have been a constant source of love, affection, support, and encouragement. I appreciate this with all my heart. Silvia, the children and I have deeply enjoyed their visits. We feel them very close even if they are far away. We have also enjoyed being so close to Laura, Nestor and the children. Their company during these years has been very important to us.

When we arrived at Pasadena, David and Coty opened up their home to us and welcomed us as their children. This will always be remembered. I cannot exclude Vero, the Strauss family, Flora and Yaacov, Pedro and Nelly, Ana and Rodolfo, all the friends, all the people who always wished us the best. Finally, I cannot forget my parents and my elder brother, Raúl, who helped me and guided me in the early years.

Silvia, Rafael and Mariana deserved a little better during all this time. I hope that the many extra hours spent at Caltech (and also at the Technion) pay off in the form of a better future for all of us.

ABSTRACT

The design of control systems in the face of model uncertainty is addressed. A methodology for the design of robust control schemes is outlined, which employs the Structured Singular Value as an analysis tool and Internal Model Control as the synthesis framework. This methodology is applied to the design of control systems for a fixed-bed, laboratory, catalytic methanation reactor. The design procedure allows a clear insight on the fundamental limits to closed-loop performance and provides controllers with explicit stability and performance guarantees for the case of plant-model mismatch.

The overall controller design effort is initiated with a careful mathematical modeling of the system. The original nonlinear partial differential equations are converted through collocation techniques into a nonlinear ordinary-differential/algebraic equation system amenable to dynamic simulation. Interactive software is developed for the open- and closed-loop simulation of general non-linear differential-algebraic systems, which provides an efficient means to simulate the reactor model. Linearization and control-relevant model reduction techniques are applied to arrive at models appropriate for the control studies.

Both the single-input single-output and the multivariable case are addressed. Three different control configurations are investigated in the context of the single-pass operation of the reactor. In each case-study presented, the controller design procedure is divided into four steps: first, the definition of the control objectives, which not only leads to the selection of the appropriate control configuration but also determines the most adequate design techniques to employ; second, a nominal design step, in which the system-inherent limitations to the closed-loop performance are highlighted; third, a characterization of the uncertainty and the use of this information in the design of robust controllers; and, fourth, the evaluation of the designs through nonlinear simulations.

The thesis describes the first application of structured singular value-based analysis techniques to a chemical reactor system and is in essence the first comprehensive study of the application of robust control to fixed-bed reactors. The power of the new mathematical theory for robust control system design is demonstrated. It is shown that the design of control systems for complex, distributed systems such as the methanation reactor can be addressed in a practical way, and low-order controllers be adequately obtained, which possess near-optimal characteristics when applied in a realistic environment of uncertainty and unavailability of measurements.

TABLE OF CONTENTS

NOMENCLATURE

A,B,C,D	state-space quadruple
A_{ij}, B_{ij}	first and second derivative, respectively, of the Lagrange polynomial l_j evaluated at ζ_i
a_{ij}	heat transfer area per unit volume between phases i and j, cm^2/cm^3
C	classical multivariable controller
c	classical SISO controller
c_p	heat capacity, cal/g K
D_e	equivalent reactor diameter, cm
D_r	turbulent diffusivity for radial mass dispersion, cm^2/s
d	disturbance vector
d_p	diameter of catalysts particle, cm
E_a	activation energy, cal/gmol
e	error signal
e_m	multiplicative error
F	IMC filter (multivariable case)
F_P	total molar flow rate to the reactor, gmol/s
f	IMC filter (SISO case)
G	superficial mass flow velocity, g/cm^2 s
ΔH	heat of reaction, cal/gmol
h_{ij}	heat transfer coeff. between phase i and j, cal/s cm^2 K
K_{p_M}	equilibrium constant, atm^{-2} for methanation
K_1,K_2	methanation reaction rate constants, atm^{-1}
k_0	pre-exponential factor, gmol/s gcat atm^2
k	thermal conductivity, cal/s cm K
L	reactor length, cm

l_i	Lagrange polynomials
$\bar{l}_m$	bound on the multiplicative uncertainty
M	interconnection matrix
M′	interconnection matrix, analysis case
M_g	molecular weight of gas, g/gmol
N	number of interior axial collocation points
P	system transfer matrix
P	pressure, atm
$\hat{P}$	pseudopressure (mole change effect removed), atm
p	plant transfer function, SISO case
$\tilde{p}$	model transfer function
$\hat{p}$	reduced-order model transfer function
p_i	partial pressure of species i, atm
Pe	Peclet number
Q	multivariable IMC controller
q	SISO IMC controller
R	gas constant, 1.987 cal/gmol K
R_M	methanation reaction rate, gmol/s gcat
R'_M	normalized reaction rate
R_0,R_1	radius of thermal well and outer wall, respectively, cm
r	radial coordinate, cm
r	reference signals
r	normalized radial coordinate, r/R_1
S	sensitivity operator (multivariable case)
s	Laplace transform variable
t	time, s
t_d	time spent by catalyst on stream, h
T	temperature, K

U_{ij}	overall heat transfer coeff. between phase i and j, cal/s K
u	vector of *manipulated variables*
u_g	gas velocity, cm/s
V	volume, cm^3
v	input signals
W	multivariable weights
w	SISO weights
$\hat{w}$	weight defined by Eq. (30) of Chapter IV
x	state vector
x_i	mole fraction of species i
x_1	CO mole fraction
y	output vector
y_1	normalized CO mole fraction
z	axial coordinate, cm
z_i	zero of a transfer function

Greek letters

α	normalized axial dispersion
β	normalized radial dispersion
Γ	normalized convection coefficient (axial boundary condition)
Γ	smooth arc or branch of solutions
γ	normalized heat transfer coefficient
Δ	perturbation block (model uncertainty)
δ	moles of CO reacted per total inlet moles
δ_1	normalized heat of reaction
ϵ	void fraction, cm^3 void/cm^3 bed
ϵ	sensitivity function (SISO case)
ζ	normalized axial coordinate, z/L
H	complementary sensitivity operator (multivariable case)
η	complementary sensitivity function (SISO case)
Θ	normalized temperature, T/T_{REF}
κ	normalized convection parameter
κ	condition number
λ	IMC filter time-constant
μ	structured singular value
Π	uncertainty set
π	set of plants employed to define Π
ρ	density, g/cm^3
σ	singular value
σ_1	reaction coefficient
τ_d	time constant of first-order lag in disturbance model
ϕ_0	normalized radius of thermal well, R_0/R_1
ψ	dilution factor, cm^3 cat/cm^3 pellets

ω	frequency, rad/s
$\omega_1, \ldots, \omega_{10}$	coefficients of the radial collocation

Subscripts and Superscripts

A	all-pass
b	reactor bed
c	corresponding to the product concentration
D	discretization
d	disturbance model
exp	experimental
F	associated to the flow rate as manipulated variable
g	gas
i	input
in	conditions at reactor inlet
L	left
L	linear fractional transformation on the lower block
M	methanation reaction
M	minimum-phase
m	multiplicative
N	nonlinearity
o	output
out	outlet
REF	reference conditions
R	right
r	radial
s	solid (catalyst) phase
s	steady state
T	transpose
T	corresponding to the inlet temperature as manipulated variable
t	thermal well

U	linear fractional transformation on the upper block
w	cooling wall
z	axial
^	based on inlet conditions
^	reduced-order
~	nominal case
*	normalized variable
*	complex conjugate transpose

I. INTRODUCTION

This thesis addresses the control system design for a fixed-bed catalytic reactor system in which a highly exothermic reaction takes place. Temperature and concentration control of exothermic fixed-bed processes has traditionally been a difficult task. Major difficulties arise from the large time delays created by the slow propagation of temperature changes in the bed as a result of the thermal coupling between the fluid and the stationary masses. The unavailability in many cases of on-line, continuous measurements for the product concentrations, often the main control variables, complicates the controller implementation. The distributed parameter nature of the problem complicates the task of obtaining good low-order representations for use in the control system design. The main factor, however, affecting the synthesis of advanced control schemes for these reactor systems is constituted by the difficulties in obtaining accurate mathematical descriptions of these systems as a result of the large uncertainties that stem from the overall complexity of the chemical reaction and physical transport processes involved, and from the strongly nonlinear behavior. The issue of model uncertainty is a crucial one. In this context *robustness* of the control system is defined as the requirement that stability and acceptable control performance be maintained in the face of model uncertainty. In spite of its importance, the issue of robustness has seldom been adequately addressed in previous studies on fixed-bed reactor control or on the control of other complex chemical processes.

In the last fifteen years several attempts were made by different research groups in academia to cope with the difficulties associated with fixed-bed reactor control through the application of the so-called Modern Control Theory, which has its basis in stochastic optimal control and estimation theory (the Linear Quadratic Gaussian (LQG) approach). This includes works by Vakil *et al.* (1973), Jutan *et al.* (1977), Sorensen (1977), Silva *et al.* (1979), Sorensen *et al.* (1980) and Cinar (1984), among others. LQG constitutes the single most studied "non-traditional" synthesis

technique applied to reactor control in this period (Schnelle and Richards, 1986). In the late seventies, however, the inadequacy of Modern Control Theory to handle the crucial issue of robustness had become clear to the theoretical community. The LQG theory, which essentially restricts model uncertainty to additive noise, does not offer explicit robustness guarantees. Weighting matrices have to be varied in an obscure fashion in the hope of achieving some robustness which can be checked only through simulation (Garcia and Morari, 1982).

Other investigations on advanced control of fixed-bed reactors include, in addition to the LQG studies, the application of other state-space oriented methods, like modal control, which bases the controller calculation on eigenstructure assignment (Georgakis *et al.*, 1977, Bonvin *et al.*, 1983). This technique also fails to treat explicitly the fundamental aspect of feedback theory, i.e., plant uncertainty, or the issue of non-minimum phase behavior, both so frequent in chemical processes and so important for fixed-bed reactors, and that cannot be clearly addressed in the state-variable formulation (Horowitz, 1984). The inadequacy of the state-variable oriented framework, as opposed to input/output formulations, is also reflected by the fact that it has led to convoluted techniques. One example is a suggested approach to avoid state estimation in fixed-bed reactor control, based on altering, in some cases by relatively arbitrary means, discretization and/or model reduction procedures, in order to make the resulting state variables of the full- or reduced-order model correspond to the actual location of the available measurements (Bonvin *et al.*, 1983; Wong *et al.*, 1983). The relative complexity of the "modern" control schemes, combined with the lack of assurances about their performance in an environment of nonlinearities and uncertainty, are the main reasons explaining why these have not found their way in the chemical process industry.

Other recent studies on fixed-bed reactor control have included applications of different adaptive control schemes (Tremblay and Wright, 1977; Astrom, 1978;

Harris *et al.*, 1978) and of the frequency domain Nyquist array (Clement and Jorgensen, 1981) and characteristic loci (Foss *et al.*, 1980) methods. A more detailed review of recent applications of advanced control theories to fixed-bed reactor control will not be attempted. Suffice it here to say that very seldom, if ever, in the literature on fixed-bed reactor control, have the control schemes been *designed* to account explicitly for model uncertainty. At most, the designs have been tested for robustness only *a posteriori* (Jutan *et al.*, 1977; Bonvin *et al.*, 1983). This is in part, as previously suggested, a result of the fact that the available theory did not specifically address this problem, and in part also due to certain lack of awareness of the fact that the key issue in feedback design is model uncertainty, a fact emphasized for years by critics of the "modern" approach like Horowitz (1963; Horowitz and Shaked, 1975) and Shinnar (1976).

During the last decade, however, several developments started independently, which have brought the theory closer to practical problems. Only a short historical account of these developments is presented here, since the main issues of interest in the context of our studies are discussed along the lines of the treatment in Chapters III and IV.

In the theoretical community, a new interest in input/output (operator theoretic) methods has marked a return to an appreciation of classical control concepts and frequency domain techniques. It is in the frequency domain framework that the fundamental trade-offs of feedback controller design are best captured and made transparent to the eyes of the designer. In this framework, non-minimum phase effects are directly quantified. Frequency domain weights allow the direct specification of performance objectives, stability constraints, disturbance response and sensor noise response bandwidth.

The new direction has provided useful design techniques, including singular values as an analysis method, and singular value loop shaping as a synthesis

approach (Doyle, 1978; Doyle and Stein, 1981), that enable the systematic treatment of model uncertainty in multivariable systems without restricting it to be represented by additive noise. Another approach to synthesis which paralleled these developments and which applies to a similar description of uncertainty as the singular value approaches, is constituted by techniques for optimal control satisfying so-called H_∞ requirements. These techniques were introduced by Zames (1981) and Helton (1981) and developed further by others (e.g., Francis *et al.* (1984)).

The techniques of the last paragraph, however, still require rather restrictive assumptions about uncertainty. In particular, plant uncertainty must be modelled as a single "unstructured perturbation" (Doyle, 1984). This has prompted the development of a new framework for robustness analysis of systems with general structures of model uncertainty, which is based on a new mathematical tool called the structured singular value (SSV, μ) introduced by Doyle (1982). Doyle and coworkers (e.g., Doyle, 1984; Doyle and Chu, 1986) also introduced new solutions to the H_∞-optimal control problem as well as initial approaches to solve a so-called μ-synthesis problem, which results in optimal robust performance of the closed-loop system, or in other words, in the "best" possible controller in the face of model uncertainty[1] (Chapters III and IV).

In parallel to the developments of the last two paragraphs, which in many cases involve, to say the least, rather sophisticated mathematical concepts, in chemical process control the development of Internal Model Control (IMC) (Garcia and Morari, 1982; Morari, 1983a) and of the concept of dynamic resilience (best achievable closed-loop performance) (Morari, 1983b) generated a host of new results, and clarified with simplicity to the process control audience a large number of previously not so well understood issues. These include the concept of the existence of fundamental, system inherent limitations to the closed-loop performance, i.e.,

1. "Best," of course, depending on whether or not the assumptions inherent in the formalism are applicable to the particular problem under study.

independent of the choice of any controller, the simple notion that stability of the closed-loop system is not an issue when perfect models exist (provided that the plant is open-loop stable), and questions ranging from when decoupling is detrimental to performance (Holt and Morari, 1985), to the optimal tuning of PID controllers (Rivera *et al.*, 1986). Among the many IMC-related developments are new techniques for robust sampled-data controller design (Zafiriou and Morari, 1985), for control-relevant model reduction (Rivera and Morari, 1985), and for the design of decentralized control schemes (Grosdidier and Morari, 1986). The IMC controller design procedure, an input-output type of approach, explicitly takes into account robustness considerations and results in near-optimal controllers in the face of plant/model mismatch.

This thesis presents a methodology for the design of robust control schemes, which combines the insight, clarity and simplicity of the IMC design procedure with state-of-the-art analysis techniques based on the structured singular value. This methodology is applied and demonstrated on three case-studies of control of a fixed-bed, catalytic methanation reactor. The thesis, which describes the first application of structured singular value-based analysis techniques to a chemical reactor system, is in essence the first comprehensive study of the application of robust control to fixed-bed reactors. The thesis differs from previous work on fixed-bed reactor control in the emphasis placed in obtaining, as an inseparable part of the controller design procedure, explicit stability and performance guarantees, not only for the case in which it can be safely assumed that the reactor model accurately represents the true system, but, more importantly, for the more realistic case involving model uncertainty.

In addition to outlining a systematic approach to control system design that can be applied to any complex chemical process, the thesis is intended to provide further insight on the issue of fixed-bed reactor control. In particular, the main fun-

damental limitations to the achievable control performance are pinpointed for different cases of simple configurations, all involving single-pass operation. This insight can then serve as the basis for the study of more complex configurations, for example, involving heat and/or product recycle. The thesis is also intended to serve as a solid first basis for future experimental control studies to be carried out on the actual reactor unit.

Chapter II presents the main aspects of the extensive model development work for the reactor system carried out during the course of this project. Such type of work is a necessary prerequisite of any advanced control system design study. Chapters III and IV constitute the main core of the present thesis, addressing respectively the single-input single-output and the multivariable situation. While dealing specifically with the control design problem for the methanation reactor, in these chapters the design methodology is formulated and the general theoretical basis of the analysis and synthesis techniques employed is presented. Chapter V summarizes the software tools for control system design employed and also developed in this project. Chapter VI presents conclusions and suggestions for future work. A number of appendices detail the derivation of the reactor model employed for the control system design, the computer implementation of the models, the use of the software tools for analysis and synthesis and also include an account of preliminary investigations for a system configuration incorporating energy recycle.

REFERENCES

Astrom, K.J., 1978, Self-tuning control of a fixed-bed chemical reactor system. Report STU 78-3763, Lund Institute of Technology, Lund, Sweden.

Bonvin, D., R.G. Rinker and D.A. Mellichamp, 1983, On controlling an autothermal fixed-bed reactor at an unstable state - III. Model reduction and control strategies which avoid state estimation. *Chem. Engng Sci.* **38** , 607-618.

Cinar, A., 1984, Controller design for a tubular catalytic reactor. *Can. J. Chem. Engng* **62** , 746-754.

Clement, K. and S.B. Jorgensen, 1981, Experimental investigation of a fixed-bed chemical reactor control system designed by the direct Nyquist array method. Proceedings of the 8th IFAC World Congress, Kyoto, Japan.

Doyle, J.C., 1978, Robustness of multiloop linear feedback systems. Proceedings of the IEEE Conference on Decision and Control, San Diego, CA.

Doyle, J.C., 1982, Analysis of feedback systems with structured uncertainties. *IEE Proc.* **129** , D(6), 242-250.

Doyle, J.C., 1984, Lecture notes, ONR/Honeywell Workshop on Advances in Multivariable Control, Minneapolis, MN.

Doyle, J.C. and C.C. Chu, 1986, Robust control of multivariable and large scale systems. Technical report to A.F.O.S.R. for period July 1984/ October 1985.

Doyle, J.C. and G. Stein, 1981, Multivariable feedback design: concepts for a classical/ modern synthesis. *IEEE Trans. Automat. Contr.* **AC-26** , 4-16.

Foss, A.S., J.M. Edmunds and B. Kouvaritakis, 1980, Multivariable control system for two-bed reactors by the characteristic locus method. *Ind. Engng Chem. Fundam.* **19** , 109-117.

Francis, B.A., J.W. Helton and G. Zames, 1984, H_∞- optimal feedback controllers for

linear multivariable systems. *IEEE Trans. Automat. Contr.* **AC-29** , 888-900.

Garcia, C.E. and M. Morari, 1982, Internal Model Control - 1. A unifying review and some new results. *Ind. Engng Chem. Proc. Des. Dev.* **21** , 308-323.

Georgakis, C., R. Aris and N.A. Amundson, 1977, Studies in the control of tubular reactors - II. Stabilization by modal control. *Chem. Engng Sci.* **32** , 1371-1379.

Grosdidier, P. and M. Morari, 1986, Interaction measures for systems under decentralized control. *Automatica* , in press.

Harris, T.J., J.F. MacGregor and J.D. Wright, 1978, An application of self-tuning regulators to catalytic reactor control. Proceedings of the 1978 Joint Automatic Control Conference, Philadelphia, PA.

Helton, J.W., 1981, Broadbanding: gain equalization directly from data. *IEEE Trans. Circuits and Sys.* **28** , 1125-1137.

Holt, B.R. and M. Morari, 1985, Design of resilient processing plants - VI. The effect of right-half-plane zeros on dynamic resilience. *Chem. Engng Sci.* **40** , 59-74.

Horowitz, I.M., 1963, *Synthesis of Feedback Systems* , Academic Press, New York.

Horowitz, I.M., 1984, History of personal involvement in feedback control theory. *IEEE Control Systems Magazine* , Nov. 1984.

Horowitz, I.M. and U. Shaked, 1975, Superiority of transfer function over state-variable methods in linear time-invariant feedback system design. *IEEE Trans. Automat. Contr.* **AC-20** , 84-97.

Jutan, A., J.D. Wright and J.F. MacGregor, 1977, Multivariable computer control of a butane hydrogenolysis reactor: Part III. On-line linear quadratic stochastic control studies. *A.I.Ch.E. Journal* **23** , 751-758.

Morari, M., 1983a, Internal Model Control - Theory and applications. P.R.P.- Automation 5, 5th International IFAC/IMEKO Conference on Instrumentation and Auto-

mation in the Paper, Rubber, Plastics and Polymerization Industries, Antwerp, Belgium.

Morari, M., 1983b, Design of resilient processing plants - III. A general framework for the assessment of dynamic resilience. *Chem. Engng Sci.* **38** , 1881-1891.

Rivera, D.E. and M. Morari, 1985, Internal Model Control perspectives on model reduction. Proceedings of the 1985 American Control Conference, Boston, MA, 1293-1298.

Rivera, D.E., M. Morari and S. Skogestad, 1986, Internal Model Control - 4. PID controller design. *Ind. Engng Chem. Proc. Des. Dev.* **25** , 252-265.

Schnelle, P.D. and J.R. Richards, 1986, A review of industrial reactor control: difficult problems and workable solutions. Proceedings of the Third International Conference on Chemical Process Control, Asilomar, CA.

Shinnar, R., 1976, Process control research: an evaluation of present status and research needs. *A.I.Ch.E. Symposium Series 159* **72** , 155-166.

Silva, J.M., P.H. Wallman and A.S. Foss, 1979, Multi-bed catalytic reactor control systems: configuration development and experimental testing. *Ind. Engng Chem. Fundam.* **18** , 383-391.

Sorensen, J.P., 1977, Experimental investigation of the optimal control of a fixed-bed reactor. *Chem. Engng Sci.* **32** , 763-774.

Sorensen, J.P., S.B. Jorgensen and K. Clement, 1980, Fixed-bed reactor Kalman filtering and optimal control. *Chem. Engng Sci.* **35** , 1223-1230.

Tremblay, J.P. and J.D. Wright, 1977, Multivariable model reference adaptive control of a pilot scale packed-bed tubular reactor. 5th IFAC/IFIP International Conference on Digital Computer Applications to Process Control. The Hague, Netherlands.

Vakil, H.B., M.L. Michelsen and A.S. Foss, 1973, Fixed-bed reactor control with state estimation. *Ind. Engng Chem. Fundam.* **12** , 328-335.

Wong, C., D. Bonvin, D.A. Mellichamp and R.G. Rinker, 1983, On controlling an autothermal fixed-bed reactor at an unstable state - IV. Model fitting and control of the laboratory reactor. *Chem. Engng Sci.* **38** , 619-633.

Zafiriou E. and M. Morari, 1985, Robust digital controller design for multivariable systems. Paper 103f, 1985 Annual Meeting, A.I.Ch.E., Chicago, IL.

Zames, G., 1981, Feedback and optimal sensitivity: model reference transformations, multiplicative seminorms, and approximate inverses. *IEEE Trans. Automat. Contr.* **AC-26** , 301-320.

II. MODEL DEVELOPMENT FOR THE REACTOR SYSTEM

1. THE METHANATION REACTOR SYSTEM

This thesis addresses the control system design for a laboratory, fixed-bed, non-adiabatic methanation reactor. The reactor system under consideration is shown schematically in Fig. 1. The system, described by Strand and Seinfeld (1982), is currently under final stages of construction at the California Institute of Technology. This fully automated, completely instrumented experimental unit has been specifically designed as a test site for the study of fixed-bed reactor control.

The methanation reaction

$$CO + 3H_2 = CH_4 + H_2O \qquad (1)$$

was chosen mainly because it is a good example of a highly exothermic reaction. Temperature and concentration control of exothermic fixed-bed processes has traditionally been a difficult task. Among the major difficulties one can list the complexities and uncertainties associated with the dynamic behavior and the mathematical description of these systems, the intricacies of the nonlinear interactions between the thermal and reaction processes, the large time delays (created by the slow propagation of temperature changes in the bed) which impose fundamental limitations on the achievable closed-loop performance for certain configurations, and the unavailability in many cases of on-line, continuous measurements for the product concentrations, often the main control variables. The main objective of the research effort initiated with the construction of the experimental unit at Caltech is to understand how to best address these difficulties in the context of control system design. The control understanding obtained for the case of the laboratory (small pilot-plant)-scale unit may subsequently serve to draw conclusions for the case of larger-scale reactor systems and even for other chemical processes, plagued in many cases by essentially the same difficulties. A second objective of the research

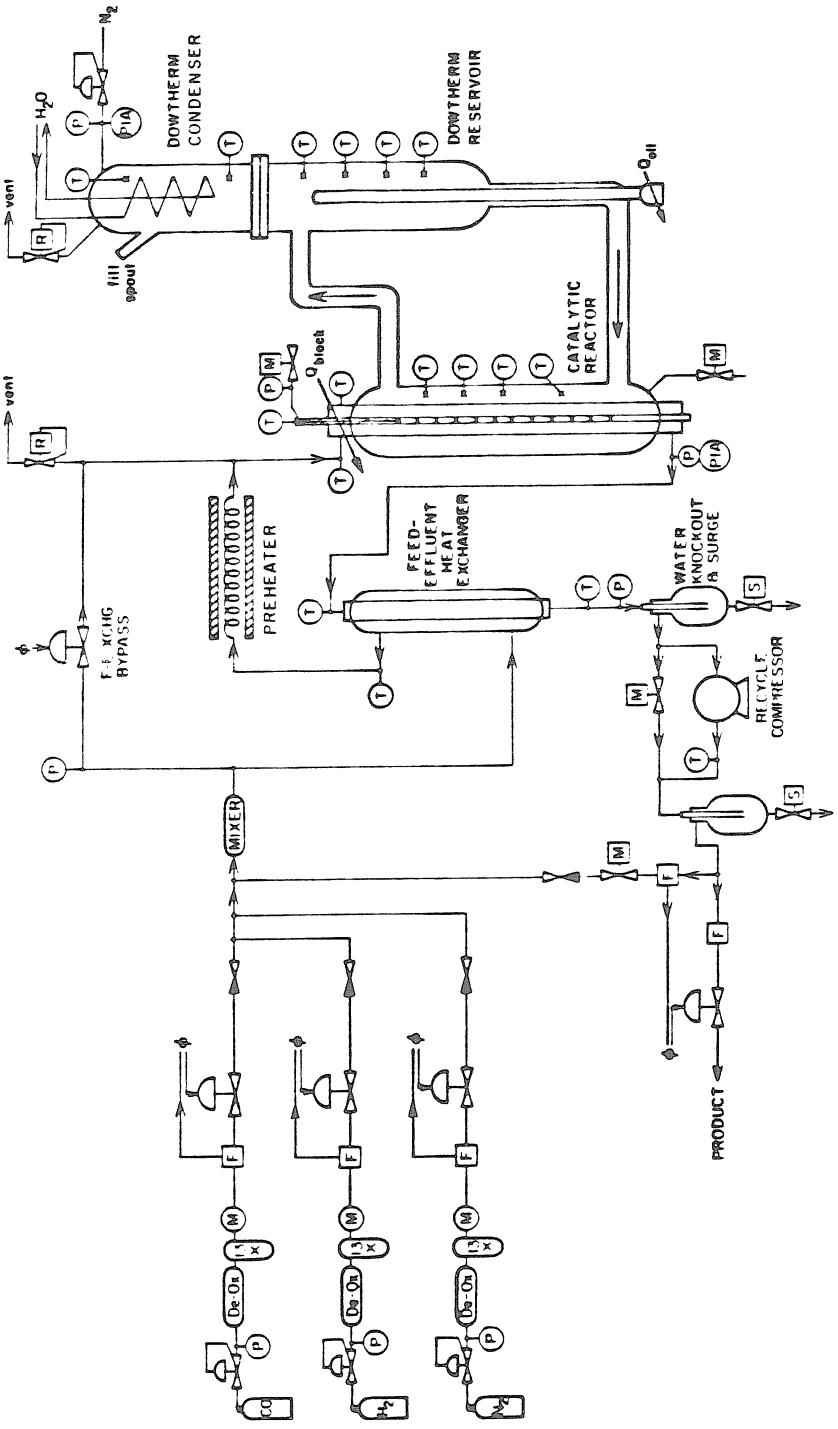

Figure 1 Process diagram of the experimental methanation reactor.

program is the evaluation and testing of advanced control schemes and the study of their applicability to complex chemical processes. The aforementioned difficulties make the methanation reactor system under study a very adequate one to serve this purpose. The emphasis in the present thesis is on theoretical studies. The modeling, simulation and control system design work carried out during the course of the present project lay the framework and provide the necessary basis for future experimental control studies on the actual reactor unit.

The main features of the reactor system are briefly summarized in what follows. Fig. 2 shows an expanded section of the reactor bed. The bed is a 1.194 cm radius, 30 cm length stainless steel tube filled with 0.8-1.0 mm nickel on alumina catalyst particles mixed with inert filling. The reaction is cooled by high temperature boiling oil circulating through natural convection in the outer reactor jacket. The oil is expected to boil in the jacket and circulate, countercurrently to the flow of the gases, from the jacket to a condenser and back. The reactor wall temperature is expected (and assumed in this work) to be independent of length. The reactor is a one tube version of a type of reactors employed in exothermic reactions. These reactors consist of a large number (up to several thousands) of tubes enclosed in a cooling oil shell (Froment and Bischoff, 1979).

Along the central axis of the reactor runs a 0.159 cm radius thermal well containing thermocouples for temperature measurements at various axial positions. Additional thermocouples allow direct measurement of the gas temperature at the reactor inlet and outlet. A dedicated on-line gas chromatograph provides periodic concentration measurements. Current implementation does not allow continuous outlet concentration measurements.

Mass flow controllers permit rapidly setting the flow rates of the different inlet streams. In single-pass operation, fast setting of the reactor inlet temperature is done through local control of the heat load of an electrical preheater and of the

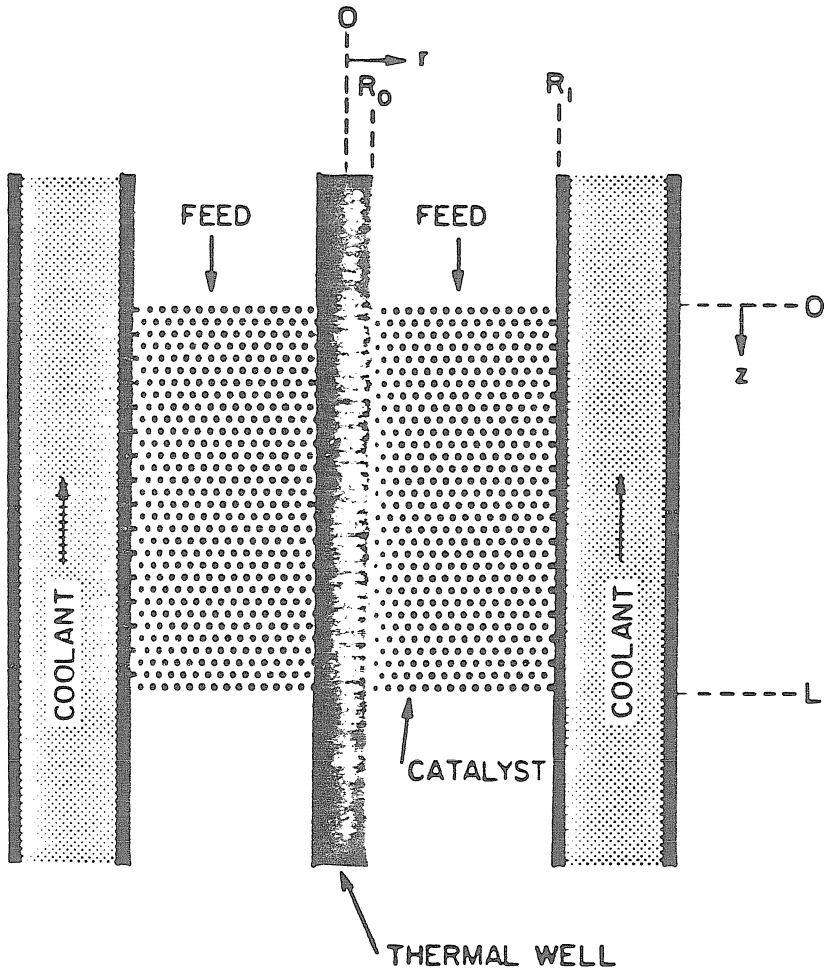

Figure 2 Expanded section of the reactor bed (Khanna, 1984).

ratio of material diverted through a bypass around this preheater. The oil temperature in the reactor jacket and therefore the reactor wall temperature can be varied slowly and only over a limited range by changing the pressure of nitrogen above the oil in the condenser.

The reactor bed is characterized by the following important ratios: i) reactor length to equivalent diameter $L/D_e \approx 15$; ii) reactor length to diameter of catalyst particle $L/d_p \approx 300$; iii) reactor diameter to particle diameter $D_e/d_p \approx 20$. The ratio of the heat capacities between the solid-phase and the gas-phase is of interest for the control studies, since it approximates the ratio between the speeds of the concentration wave and the thermal wave (Friedly, 1972). This ratio equals 61 for the system. All important physical parameters of the bed, together with the investigated operating conditions for the single-pass operation of the reactor are given in Table A1 of Appendix A.

The experimental system includes a countercurrent feed-effluent heat exchanger to recycle the heat generated by the reaction. This heat exchanger can be bypassed. Product recycle can also be implemented, adding to the flexibility of this experimental system for control studies. Feed-effluent heat exchange and product recycle are common features of many industrial reactors and are very interesting from the point of view of control system design, since the positive feedback of heat or mass can lead to the occurrence of multiple steady states, instabilities and in general to increased complexity in the dynamic behavior of the overall process.

Prior to any study on the control of the reactor on a configuration involving heat or product recycle, it is necessary to have first a solid understanding of the phenomena associated with the reactor bed itself. This thesis therefore focuses on the modeling, simulation and control system design for the reactor bed alone, i.e., the study of the single-pass operation of the reactor system. This study serves as a basis for the study of more complex configurations, which is left open as a subject

of future research. Initial investigations on possible control configurations for the reactor/feed-effluent heat exchanger system are presented in Appendix D.

2. MATHEMATICAL MODELS

Detailed mathematical models for the reactor bed and the feed-effluent heat exchanger have been derived from fundamental principles. The effort spent in modeling is justified when it comes to obtaining a real understanding of the system under consideration. Whereas it is true that process transfer functions for the control system design can be rapidly obtained from system identification experiments (see Section 6), only through mathematical modeling can detailed *a priori* information about the steady-state and dynamic system behavior be obtained. This information can then be used for the process design, optimization and the control system design.

Dynamic models derived from fundamental principles are required in order to be able to integrate process control considerations at an early stage in the design of a new process. Even for an already existing plant, mathematical models are essential for an evaluation of the influence of different operating conditions, modes of operation or the values of certain parameters on the system behavior and on the achievable control quality (i.e., the concept of dynamic resilience, as described by Morari (1983)), and for a clear understanding of the effect of various measured or unmeasured disturbances. Especially if the system is complex or strongly nonlinear, the effort in deriving an accurate mathematical model pays off as demonstrated in this thesis by the understanding and awareness (obtained before any possibly risky experiments) of different phenomena that may occur in the system. Having these models allows us to design controllers for the regulation of variables not easily measurable continuously, and puts us on a relatively solid ground for an appropriate characterization of the different sources of uncertainty. The knowledge

obtained from the models can be employed for properly designing the transfer function identification experiments, which in turn are most appropriate for a final validation of the modeling assumptions.

2.1 Mathematical Model of the Reactor Bed

The mathematical model for the reactor bed is based on the model developed by Khanna (1984). Extensive work beyond that of Khanna's has been carried out in order to arrive at the final computer implementation of the model as presented in this thesis. The new implementation differs significantly from the previous one and is a very appropriate one for the control studies. The model has been incorporated into the framework of a computer-aided control system design package. The solution algorithms have been replaced and a significant reduction in the simulation times over the previous implementation has been achieved. Interactive graphics have been incorporated that facilitate visualizing the results. A new, convenient analytic linearization procedure has been implemented.

The dimensionless quantities have been redefined in order to appropriately couple the reactor-bed model to models of other elements in the system like the feed-effluent heat exchanger (Appendix D) or the recycle line. The previous set was found to be inadequate for the case in which the steady-state values at the reactor inlet are not known *a priori*, as it occurs for the inlet temperature when the heat exchanger is used. The reactor model has been simplified for the initial analysis by considering the methanation reaction as the only significant reaction occurring in the system. This is justified by the results of kinetic experiments carried out in our laboratory (Chiang, 1983; Webb, 1986), which show that the steam-shift reaction

$$CO + H_2O = CO_2 + H_2 \ , \tag{2}$$

the second major reaction possible in the system, is much less important than the methanation reaction. The experiments of Chiang, corroborated later by those of Webb, also suggest the following rate expression for the CO methanation reaction over a nickel catalyst (evaluated at 513 K):

$$R_M = \frac{0.0217\ p_{CO}\ p_{H_2}\ t_d^{-0.3}(1-\upsilon)}{(1 + 110\ p_{CO} + 2.32\ p_{H_2})^2} \quad \left(\frac{\text{moles}}{\text{sec gcat}}\right) \ , \tag{3}$$

where t_d, measured in hours, accounts for a long-term deactivation effect, the partial pressures are measured in atmospheres and

$$\upsilon = \frac{p_{CH_4} p_{H_2O}}{p_{CO}(p_{H_2})^3}\ \frac{1}{K_{p_M}} \ . \tag{4}$$

The factor $(1-\upsilon)$ was included by us in order to reduce the rate to zero at equilibrium. This has been suggested by Vatcha (1976). The rate expression of Eq. (3) is a global rate expression, based on bulk gas conditions. The activation energy was measured at 37 kcal/mol. This rate expression is employed throughout the present thesis. This reaction kinetics and the operating conditions selected for the case of single-pass operation (Table A1, Appendix A) are close to the actual ones expected for the laboratory experimental system and differ from those employed by Khanna (1984; Khanna and Seinfeld, 1982,1986). The latter give rise to profiles significantly milder than the profiles obtained in our case. The rate expression in our case shows that the CO is a strong inhibitor in almost the entire range of concentrations. This has an important effect on the steady-state and dynamic behavior of the reactor.

Khanna (1984) discusses in detail the different considerations in the formulation of the mathematical model for the reactor bed and the validity of different assumptions. A similar discussion will not be attempted here. In short, the model:

- incorporates axial and radial dispersion of mass and energy;
- involves a two-dimensional, heterogeneous analysis;
- accounts for temperature, pressure and mole dependencies of gas density, average molecular weight, heat capacity and heats of reaction;
- incorporates the effects of axial pressure gradients;
- includes the dynamics of the axial central thermal well.

Among the major assumptions underlying the model:

- the reactor wall temperature is equal to the cooling fluid temperature and is independent of length along the reactor;
- the concentrations employed in the model are those in the gas phase; this requires that the mass transfer effects resulting from possible inter- and/or intraparticle limitations be included in the rate expressions; this is actually done when employing global rate expressions, but care has then to be taken that the flow conditions around the particles in the reactor where the kinetic experiments are carried out reproduce those expected for the catalyst particles in the actual reactor;
- the gas properties are functions of temperature, pressure and total moles as dictated by the ideal gas law;
- there is no radial velocity, and the axial velocity across the radius of the bed is uniform; the validity of the latter assumption and its effect on the results should be further verified in the experimental system since the value of 20 for the ratio D_e/d_p is a relatively low value for the assumption to be entirely justified.

The mathematical relationships for the reactor model are given in what follows in terms of dimensional quantities.

Energy balance for the catalyst phase:

$$(1-\epsilon)\rho_s c_{p_s}\frac{\partial T_s}{\partial t} = k_{zs}\frac{\partial^2 T_s}{\partial z^2} + \frac{k_{rs}}{r}\frac{\partial}{\partial r}\left[r\frac{\partial T_s}{\partial r}\right] - h_{sg}a_{sg}(T_s-T_g) + (-\Delta H_M)\bar{R}_M \qquad (5)$$

$$\begin{aligned}
r = R_0 \qquad & k_{rs}\frac{\partial T_s}{\partial r} = h_{ts}(T_s-T_t)\\
r = R_1 \qquad & -k_{rs}\frac{\partial T_s}{\partial r} = h_{ws}(T_s-T_w)\\
z = 0 \qquad & k_{zs}\frac{\partial T_s}{\partial z} = h_{sg}(T_s-T_g)\\
z = L \qquad & -k_{zs}\frac{\partial T_s}{\partial z} = h_{sg}(T_s-T_g) \quad .
\end{aligned}$$

The heat of reaction is taken as a linear function of temperature.

Energy balance for the gas phase:

$$\epsilon\rho_g c_{p_g}\frac{\partial T_g}{\partial t} = -\epsilon G c_{p_g}\frac{\partial T_g}{\partial z} + k_{zg}\frac{\partial^2 T_g}{\partial z^2} + \frac{k_{rg}}{r}\frac{\partial}{\partial r}\left[r\frac{\partial T_g}{\partial r}\right] - h_{sg}a_{sg}(T_g-T_s) \qquad (6)$$

$$\begin{aligned}
r = R_0 \qquad & k_{rg}\frac{\partial T_g}{\partial r} = h_{tg}(T_g-T_t)\\
r = R_1 \qquad & -k_{rg}\frac{\partial T_g}{\partial r} = h_{wg}(T_g-T_w)\\
z = 0 \qquad & k_{zg}\frac{\partial T_g}{\partial z} = h_{sg}(T_g-T_s) - G c_{p_g}\epsilon(T_{in_r}-T_g)\\
z = L \qquad & -k_{zg}\frac{\partial T_g}{\partial z} = h_{sg}(T_g-T_s) \quad .
\end{aligned}$$

Energy balance for the thermal well:

$$\rho_t c_{p_t}\frac{\partial T_t}{\partial t} = k_{zt}\frac{\partial^2 T_t}{\partial z^2} + h_{ts}a_{ts}(T_{s_{r=R_0}} - T_t) + h_{tg}a_{tg}(T_{g_{r=R_0}} - T_t) \qquad (7)$$

$$z = 0 \qquad T_t = T_{in_r}$$

$$z = L \qquad \frac{\partial T_t}{\partial z} = 0 \quad .$$

Species balance for the CO:

$$\rho_g \frac{\partial \hat{x}_1}{\partial t} = -G\frac{\partial \hat{x}_1}{\partial z} + \frac{D_r}{r}\frac{\partial}{\partial r}\left[r\rho_g \frac{\partial \hat{x}_1}{\partial r} + \frac{2\rho_g \hat{x}_1 r}{1-2\delta}\frac{\partial \delta}{\partial r}\right] - \frac{\bar{R}_M \hat{M}_g}{\epsilon} \tag{8}$$

$$r = R_0, R_1 \qquad D_r \frac{\partial \hat{x}_1}{\partial r} = 0$$

$$z = 0 \qquad \hat{x}_1 = \hat{x}_{1_{in}}$$

with

$$\bar{R}_m = R_m \rho_s \psi(1-\epsilon)$$

$$\delta = \frac{x_{1_0} - x_1}{1 - 2x_1} \tag{9}$$

$$\hat{x}_1 = x_1(1-2\delta)$$

where ψ is a dilution factor that accounts for the presence of inert material mixed with the catalyst in the bed, and δ is the number of moles of CO reacted per total inlet moles.

Additional relationships:

$$\rho_g = \frac{M_g P}{RT_g} = \frac{\hat{M}_g \hat{P}}{RT_g} \tag{10}$$

with

$$\hat{M}_g = M_g(1 - 2\delta)$$

and

$$\hat{P} = P(1 - 2\delta)^{-1} \quad .$$

The pseudopressure defined by the last relationship is convenient for use in the analysis since the effect of mole changes is explicitly removed (Khanna, 1984). Changes in $\hat{P}$ are basically due to pressure drop through the bed, and a linear profile such as

$$\hat{P} = \left[\frac{\hat{P}_{z=L} - \hat{P}_{z=0}}{L}\right] z + \hat{P}_{z=0} \qquad (11)$$

may be used to define the pseudo-pressure as a function of axial position. Alternatively, correlations such as the Blake-Kozeny or the Ergun equations (Bird *et al.*, 1960) can be used for describing the pressure drop across the packed bed as a function of the flow rate.

Radial temperature gradients are important in this system, since heat is removed continuously from the catalytic bed into the outer jacket. The radial dispersion of energy is retained in the model since this process governs the radial flow of energy through the bed to the jacket. For finite values of the radial mass dispersion coefficients, and for strong reaction conditions the temperature gradients may lead to significant radial concentration gradients. On the other hand, for mild reaction conditions the radial concentration gradients may be small as reported by Khanna (1984).

Compared to the convective terms the axial mass dispersion terms are relatively small and therefore can be safely neglected to simplify the model as has been done in Eq. (8). The exclusion of these terms has been tested to affect neither the steady-state nor the dynamic behavior of the model. The axial dispersion of energy terms are relatively more important and are kept in the model since it has been shown that retaining the axial dispersion terms in the main dynamic equations improves the structural characteristics of the PDE model for its numerical solution

by lumping techniques such as orthogonal collocation (Bonvin, 1980). The main dynamic equations in the reactor model (corresponding to the slowest modes of the system) are the energy balances for the catalyst phase and for the thermal well. The inclusion of the axial dispersion/conduction terms in these equations requires only marginal extra effort in the solution by means of orthogonal collocation as the discretization procedure.

3. NUMERICAL SOLUTION

Discretization of the partial differential equations. The numerical solution of the coupled set of nonlinear partial differential equations describing the reactor bed is carried out through orthogonal collocation (Villadsen and Stewart, 1967; Finlayson, 1972; Villadsen and Michelsen, 1978). By means of this technique the nonlinear partial differential equations are transformed into a combined system of nonlinear ordinary differential equations on time and nonlinear algebraic equations, which is then amenable for solution as a standard initial value problem. The advantage of the use of orthogonal collocation for the "early lumping" of the partial differential equations resides in the fact that relatively low order models[1] can be directly obtained, which preserve the main dynamic features of the actual process, and which, after appropriate linearizations, can be directly employed as state-space models for the control system design. The relative simplicity of the approach makes it very attractive, especially for complex distributed parameter systems such as the packed-bed reactor. The whole body of finite-dimensional ordinary differential equation control theory can then be applied to these systems. A large number of applications of the orthogonal collocation procedure for distributed parameter chemical reaction systems have been reported in the literature (for example, Georgakis *et al.*, 1977; Jutan *et al.*, 1977; Bonvin *et al.*, 1983). The pro-

1. Low order models by comparison with what would be obtained, for the same accuracy of the resulting model, by means of other techniques such as finite differences.

cedure is, however, not exempt from problems. The main difficulties experienced in this application, along with ways to cope with them are presented later on in the discussion.

The discretization procedure employed is similar to that of Khanna (1984), although certain differences exist, which are pointed out through the discussion. Only an outline of the procedure is given here; full details are presented in Appendix A.

After appropriate nondimensionalization of the model, the energy balance equations are first discretized in the radial direction, employing a quadratic representation for the radial temperature profiles. In most cases the representation of the temperature profiles by a quadratic is adequate, and it allows employing only one interior point for the radial collocation. This is most advantageous, since the number of resulting discretized equations remains the same as the number of original PDE's. On the other hand, because of the zero-flux radial boundary conditions for the concentration equation, using one interior radial collocation point for the discretization of this equation forces the resulting "discretized" radial concentration profiles to be flat. Although under mild reaction conditions the concentrations may be indeed close to constant along the radial direction (as in several examples presented by Khanna (1984)), for strongly exothermic reactions with high activation energies and strong reaction conditions, the assumption of radially uniform concentrations may not be valid. For these cases it is then necessary to discretize the concentration equation, employing at least two interior collocation points. The current implementation, however, does not include this extension because, unfortunately, each extra radial collocation point for the concentration equation increases the dimensionality of the final model by N+1 equations (where N is the number of interior axial collocation points) and complicates the treatment significantly. In addition, the major conclusions regarding the control studies

should not be strongly affected by the assumption of flat concentration profiles, at least for the operating conditions under consideration.

The next step in the solution procedure is the discretization of the partial differential equations resulting from the first step, by applying orthogonal collocation in the axial direction. The axial profiles are assumed to be of the general form

$$y(\varsigma,\tau) = \sum_{i=0}^{N+1} l_i(\varsigma) y_i(\tau) \tag{12}$$

where ς and τ are, respectively, dimensionless distance and time, y is temperature or concentration, y_i is the temperature or concentration at the collocation point i, and l_i are Lagrange polynomials of degree N based on the collocation points ς_j:

$$l_i(\varsigma) = \prod_{j=0\, j\neq i}^{N+1} \left(\frac{\varsigma-\varsigma_j}{\varsigma_i-\varsigma_j} \right) \quad i=0,1,...,N+1 \quad . \tag{13}$$

The N interior collocation points ς_j, j=1,...,N are selected to be the roots of an Nth degree Legendre polynomial (Villadsen and Michelsen, 1978).

Because only one Lagrangian is non-zero at a collocation point (it actually equals unity) and since the residual obtained when replacing Eq. (12) in the differential equations is set to be zero at the collocation points, the coefficient of this Lagrangian is equal to the solution at that point, namely,

$$y|_{\varsigma=\varsigma_i} = y_i \quad . \tag{14}$$

The first and second derivatives with respect to distance are replaced in the PDE's by

$$\left(\frac{\partial y}{\partial \varsigma} \right)_{\varsigma=\varsigma_i} = \sum_{j=0}^{N+1} l_j^{(1)}(\varsigma_i)\, y_j(\tau) \tag{15}$$

$$\left(\frac{\partial^2 y}{\partial \zeta^2}\right)_{\zeta=\zeta_i} = \sum_{j=0}^{N+1} l_j^{(2)}(\zeta_i)\, y_j(\tau) \qquad (16)$$

where $l_j^{(1)}(\zeta_i)$ and $l_j^{(2)}(\zeta_i)$, corresponding to the first and second derivatives of the Lagrange polynomials, are functions only of the collocation points and can be evaluated *a priori*. After applying Eqs (14)-(16) each PDE is replaced by a system of ordinary differential equations on time, one equation for each collocation point. It is seen that in this formulation the first and second derivatives with respect to distance are functions of the solution at each one of the collocation points.

If only one interior radial collocation point is used for the concentration equation, and after simple algebraic manipulations allowing for the explicit solution of some of the variables, the resulting discretized reactor model consists of 4N+1 nonlinear ordinary differential equations coupled with 4 algebraic equations (of which one is nonlinear). The algebraic equations correspond to the axial boundary conditions in Eqs (5) and (6). Because under some conditions steep axial profiles have been encountered, we have employed in general 12 interior axial collocation points, which makes the total number of equations 53. In this thesis it is shown that in spite of the large system dimensionality, both simulations and sound control system designs for this model and even larger order ones can be carried out with reasonable ease.

In the previous formulation by Khanna (1984), the continuity equation was explicitly included in the model for the calculation of the linear gas velocity u_g as a function of time and axial position. This resulted in N+1 additional nonlinear algebraic equations in the discretized model, which increased to 66 the total number of equations for the case of 12 collocation points. The explicit inclusion of the continuity equation is, however, not necessary because of the use of the total mass flow rate G (invariant along the reactor) in the model formulation, and because u_g is simply given by $u_g = G/\rho_g$. The N+1 nonlinear algebraic equations resulting from

the continuity equation were therefore excluded from the model and the treatment simplified considerably. Most of the simulations presented in this thesis were actually carried out before this change was implemented.

Steady-state solution of the reactor model. Several techniques are available for solution of the steady-state operating profiles. Steady-state solutions are required not only for system analysis, but also for defining the operating points around which to linearize the system to obtain an "equivalent" set of linear state-space models that can be employed for control system design.

At steady state, the discretized model equations resulting from the orthogonal collocation procedure become a system of nonlinear algebraic equations. This system can be solved by a number of techniques, such as the Newton method or Powell's algorithm (Powell, 1970). This approach was found to converge with no major difficulties for cases in which the profiles are relatively smooth. This, however, was not the case for conditions leading to steep profiles, for which rather severe difficulties were in some cases encountered in trying to solve the system of nonlinear algebraic equations. The reasons for these difficulties and ways to circumvent them are described in detail in Section 4.

Dynamic simulation of the reactor model. By means of the collocation techniques the PDE reactor model is converted as stated previously into a system of nonlinear ordinary differential and algebraic equations. The solution of this mixed system of equations is carried out employing code (called SNTEG) for the open- or closed-loop simulation of general linear or nonlinear dynamic systems, which uses powerful, state-of-the-art software (DASSL (Petzold, 1982)) for the solution of implicit systems of differential/algebraic equations. SNTEG is described separately in Chapter V. Suffice it here to say that for the dynamic simulations the nonlinear reactor model is implemented as a subroutine that is linked to this general code

(Appendix B).

All open- and closed-loop dynamic simulations reported in this thesis have been carried out employing SNTEG. Very significant reductions in computation time have been achieved over the previous implementation of the reactor model. For example, for a 300 sec simulation of a 66-equation version of the nonlinear reactor model, the CPU-time was 143 sec with SNTEG (Chapter V). The small CPU-times facilitate the control studies since they allow easy-to-carry out simulations in which the controllers are tested directly on the full nonlinear model, which thus serves in the simulation as "the actual plant." By contrast, a 50 sec simulation for a 41-equation version of the nonlinear model with milder kinetics required almost 5 hours of CPU-time with the previous implementation (Khanna, 1984).

A simulation example is shown in Fig. 3. Plotted are the CO concentration profiles corresponding to the open-loop system response to a -25% step-change in the inlet CO concentration. The system is initially at a steady state of partial conversion. The plots show the progress of the concentration front along the reactor immediately after the step-change occurs at the inlet. The front leaves the reactor just after 1.5 sec (the residence time). The reduction in the CO levels after the step-change causes the reaction rate to increase and this causes a further (although small for this example) reduction in the concentrations. In this particular example a new steady state of partial conversion is reached after about 100 sec. Because there is no axial mass dispersion included in the model, the actual shape of the front should be a step. The smoother profiles observed, as well as the small ripples appearing in the profiles are both a result of the approximation introduced by the discretization technique. The location of the front at different instants of time is, on the other hand, reasonably predicted by the discretized model.

Fig. 4 shows the open-loop outlet temperature response (for the nonlinear model) to a small step-change in the inlet temperature. As expected from physical

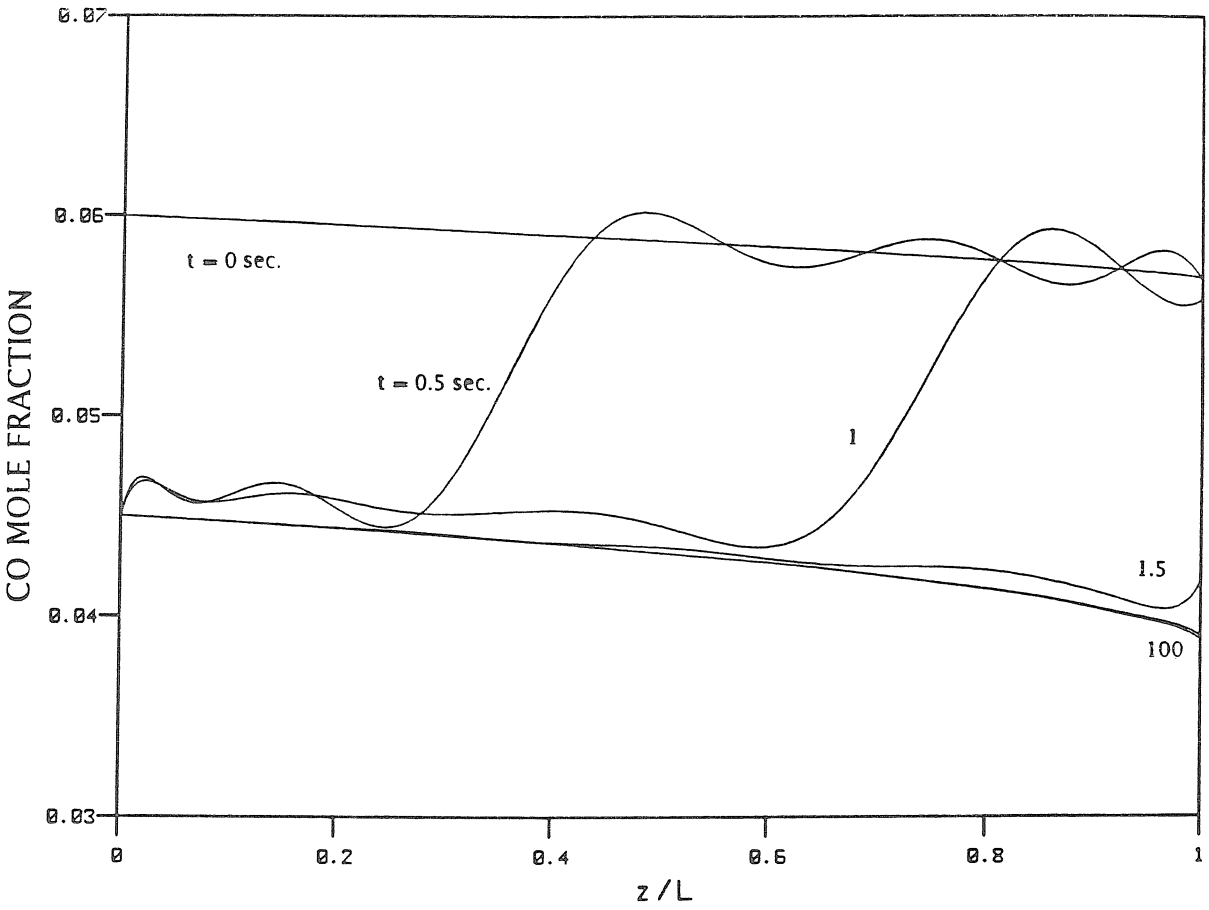

Figure 3 Open-loop time evolution of the CO concentration profile following a -25% step-change in the inlet CO concentration (nonlinear model).

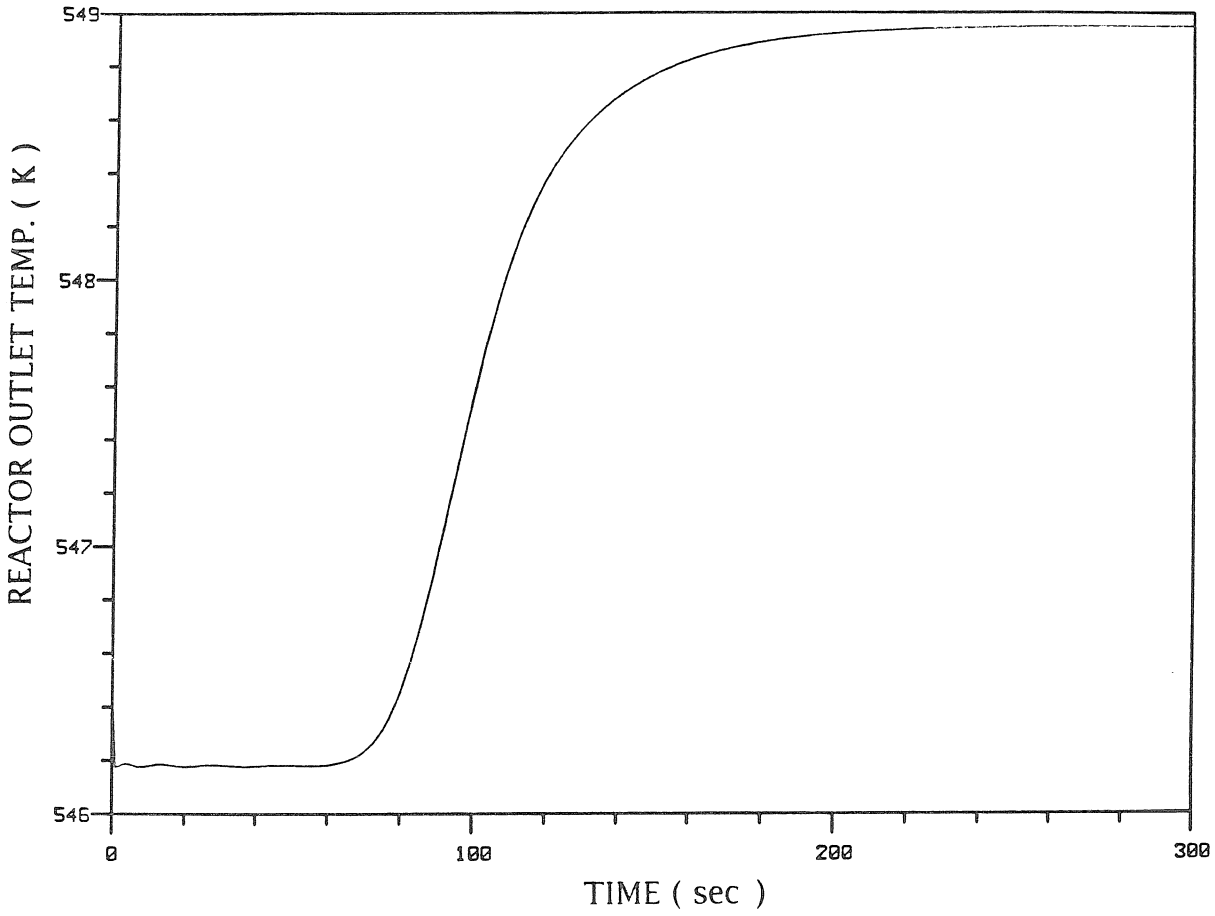

Figure 4 Open-loop outlet temperature response to a 2 K step-change in the inlet temperature (nonlinear model).

considerations, a time delay is observed in the response. This delay is approximately equal to 60 sec, which is consistent with the range of values expected for the flow rate and physical properties on which the simulation is based. The existence of this delay significantly affects the control system design (Chapter III), and it is important that the delay be adequately predicted by the model. It is apparent that the main dynamic features of the system are indeed adequately predicted by the orthogonal collocation model employed.

4. BEHAVIOR OF THE NONLINEAR REACTOR MODEL; NUMERICAL PROBLEMS

Because of the strong exothermicity and autocatalytic nature of the reaction and the high activation energy, the reactor is, under certain conditions, extremely sensitive, and a situation as depicted in Fig. 5 arises. Fig. 5a shows steady-state relationships between the reactor inlet and outlet temperatures for different values of the inlet CO concentration. Each point in these curves corresponds to a different steady-state solution of the reactor model. Curves relating the reactor inlet temperature with the exit conversion have a similar shape as those in Fig. 5a. It is observed that a small change in the operating conditions (for example, in the inlet temperature) which in certain regimes has negligible effect, in other regimes leads to extremely large changes in the profiles (and therefore in the outlet temperature or conversion). This effect is referred to as a high parametric sensitivity of the process (Bilous and Amundson, 1956).

The effect shown in Fig. 5 has also been interpreted, for models including axial dispersion, as the existence of an ignition temperature at which the system "jumps" from a steady state of partial conversion to another steady state of large or complete (equilibrium) conversion (Fig. 5b , Puszynski *et al.*, 1981). The upper steady states show in general the presence of hot spots close to the reactor entrance, and very sharp temperature and concentration profiles. Under certain

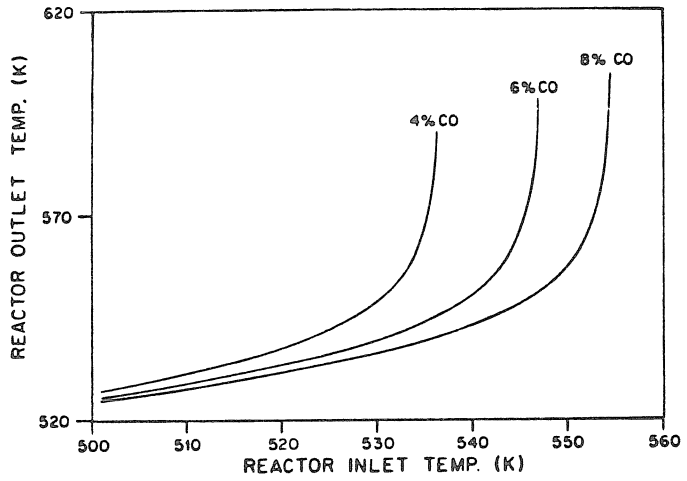

a

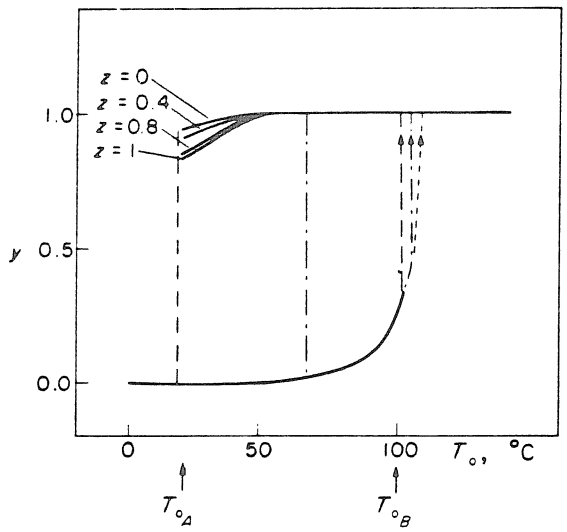

b

Figure 5 a) Steady-state relationships, for the methanation reactor, between the outlet and inlet temperatures for different inlet CO concentrations. b) Dependence of exit conversion on inlet temperature for a non-adiabatic fixed-bed reactor. Region of multiplicity; ----, general model including axial and radial dispersion terms; _.._.._, axial dispersion model; ....., piston flow model (Source: Puszynski *et al.* , 1981).

conditions, regions of steady-state multiplicity may exist; that is, for the same values of the parameters and operating conditions more than one steady-state solution may be found.

The steady-state multiplicity and hysteresis phenomena cannot be explained for models excluding axial dispersion terms. Puszynski *et al.* (1981) related the multiplicity and parametric sensitivity concepts and pointed out that as soon as a high parametric sensitivity region occurs, the axial derivatives are very large, and as a result the axial dispersion terms must be included. The authors indicated that multiple steady states can occur in nonadiabatic tubular reactors with exothermic reactions. This occurrence is supported by high values of the activation energy and the heat of reaction and by a large intensity of cooling at the walls, and is also affected by the contact time and the reaction kinetics. In the upper steady states, very sharp temperature and concentration profiles may occur not only axially but also radially.

The simulation results suggest, for our model, the occurrence of similar phenomena as those reported by Puszynski *et al.* (1981) for a similar reactor model. Numerical difficulties, however, prevented us so far from obtaining, through orthogonal collocation techniques, the steady-state profiles corresponding to the upper steady-state region, or from proving the existence of multiple steady states. These difficulties, and approaches to circumvent them are described in what follows.

Refer to Fig. 5a and consider trying to solve for the steady state corresponding to 6% CO and $T_{in} = 550$ K , starting with a profile obtained with $T_{in} = 540$ K as the initial guess. Clearly, since both profiles are completely different (although the inlet conditions are relatively close), the first problem that is encountered in trying to solve directly the system of nonlinear algebraic equations is that of a poor initial guess. With poor initial guesses most standard methods fail to arrive at the correct

solution or even to converge to any solution.

To address the problem of obtaining good initial guesses for the profiles, the use of continuation techniques was investigated. Fig. 5a was obtained by means of a pseudo arc-length continuation procedure for continuation about regular points and normal limit points (Keller, 1977). The technique allows one to solve non-linear problems of the form

$$G(x,\lambda) = 0 \quad , \tag{17}$$

where x is the solution vector and λ is a parameter, and to obtain the dependence x vs λ even in the case in which folds (normal limit points) and therefore multiple solutions might appear (Fig. 6). The technique is based on using the arc length s of the solution curve as the independent parameter, and then stepping slowly on s (rather than on λ) to obtain good initial guesses for the solution of both x and λ. The application of this technique (with $\lambda = T_{in}$) allowed obtaining the almost vertical sections of the branches in Fig. 5a. The technique, however, did not succeed in going beyond the upper points in the curves of Fig. 5a, suggesting that, for the system of nonlinear algebraic equations resulting at steady state from the collocation, there exist singularity phenomena of a greater complexity than that of folds, which are not captured by the procedure employed. The procedure was also applied with similar results to a model obtained by discretizing in the axial direction through finite-differences instead of orthogonal collocation.

In order to arrive at the upper steady states, the use of more sophisticated continuation procedures (for continuation past singular points, or bifurcation points (Keller, 1977)) was not attempted, but instead dynamic simulation was employed. The procedure involves integrating the nonlinear dynamic model from a known initial steady state to one in the upper regime, to which the system is driven by an appropriate change in one or more of the system inputs.

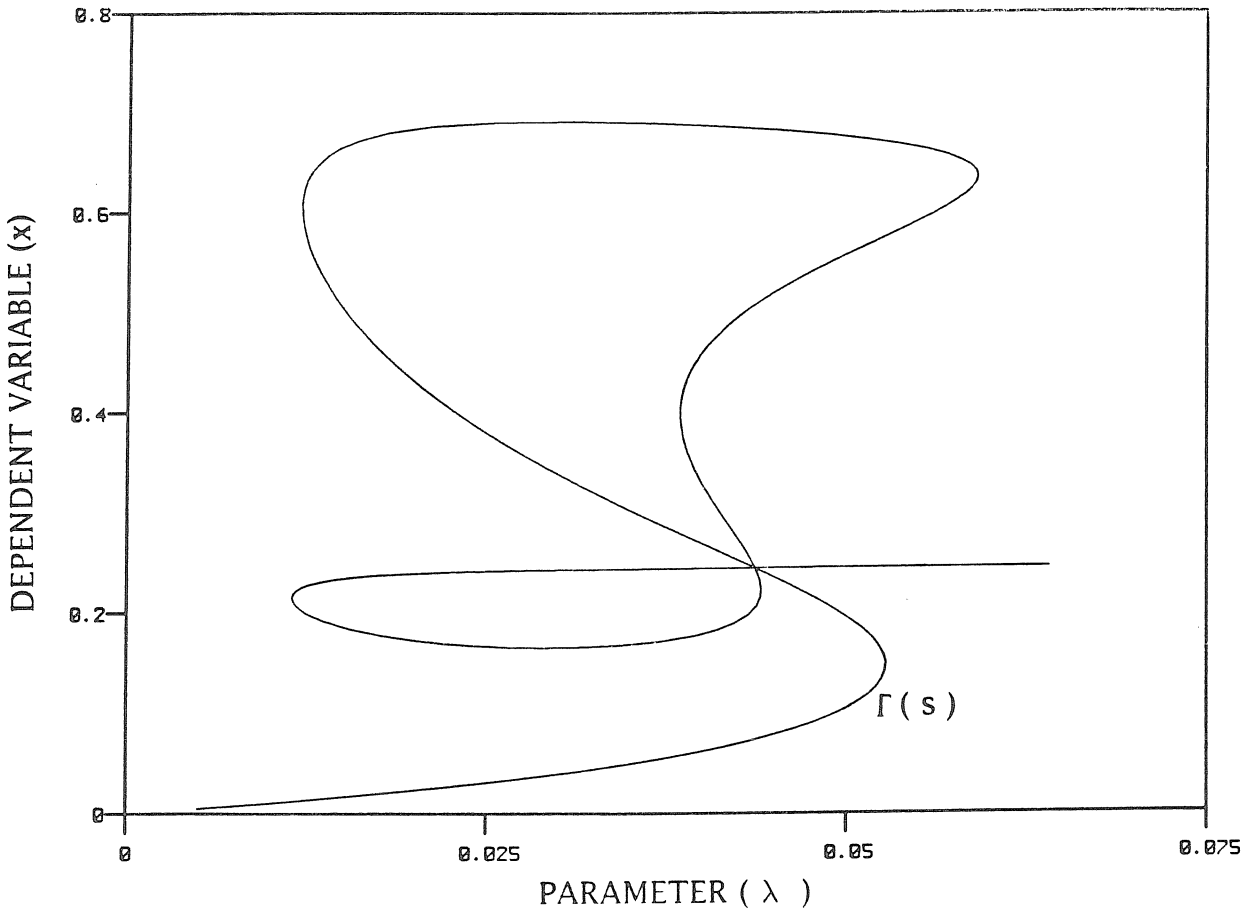

Figure 6 Dependence of the solution of a nonlinear system on a parameter. Example illustrating the occurrence of folds and multiple solutions. The system, used as an example by Kubicek (1976), consists of 4 coupled nonlinear algebraic equations. Solution obtained through a technique proposed by Keller (1977).

After a number of trials it was found that the most appropriate types of input changes for approaching the upper steady-state region are ramps in the inlet temperature leveling off at a desired value. The results are depicted in Fig. 7. In Fig. 7a the ramp in the inlet temperature is relatively flat (slope of 0.08 K/sec). At about 230 sec the temperature and conversion have not significantly increased along the inlet and middle sections of the reactor. However, close to the reactor exit the temperature and concentrations have reached a level at which suddenly something analogous to a chain reaction develops: the higher reaction rates cause the temperature and conversion to increase very fast and this causes in turn a strong acceleration of the reaction; this process stops only when the equilibrium conversion is achieved. This behavior is a result of the strong exothermicity of the reaction, the high value of the activation energy and the autocatalytic nature of the reaction rate. In Fig. 7b the ramp is steep enough (slope of 0.4 K/sec) to cause the same process to occur much closer to the reactor entrance. The very fast development of a sharp hot spot close to the inlet is then observed. Fig. 7c shows the evolution of the concentration profiles for the same ramp as that of Fig. 7b. Note the rapid reduction in the CO levels, which occurs at a pace even faster than the movement of the concentration front.

Although the curves of Fig. 7 show the approach to the upper steady-state region, they do not actually show steady-state profiles. The simulations eventually "stopped" before the new steady-state profiles could be reached. The reason for the numerical difficulties encountered lies in the steepness of the expected profiles. It is most certain that the final steady-state profiles for the conditions of Fig. 7 (corresponding to a final inlet temperature 40 K higher than that of the initial steady state) would show very sharp hot spots and very steep reductions in the CO concentration close to the reactor inlet.

The inability of simple orthogonal collocation to describe accurately profiles

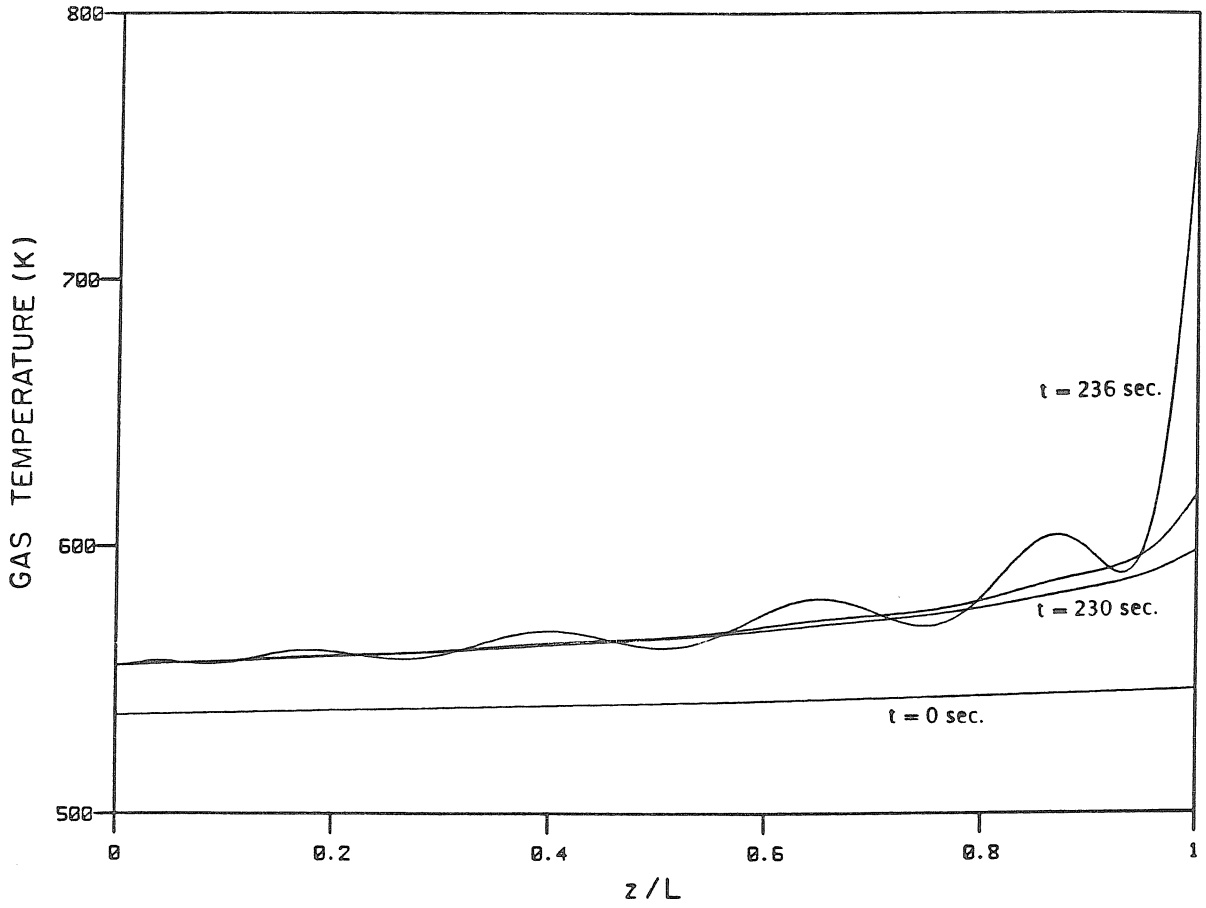

a

Figure 7 a) Open-loop time evolution of the gas temperature profile following a ramp-change in the inlet temperature, with a slope of 0.08 K/sec.

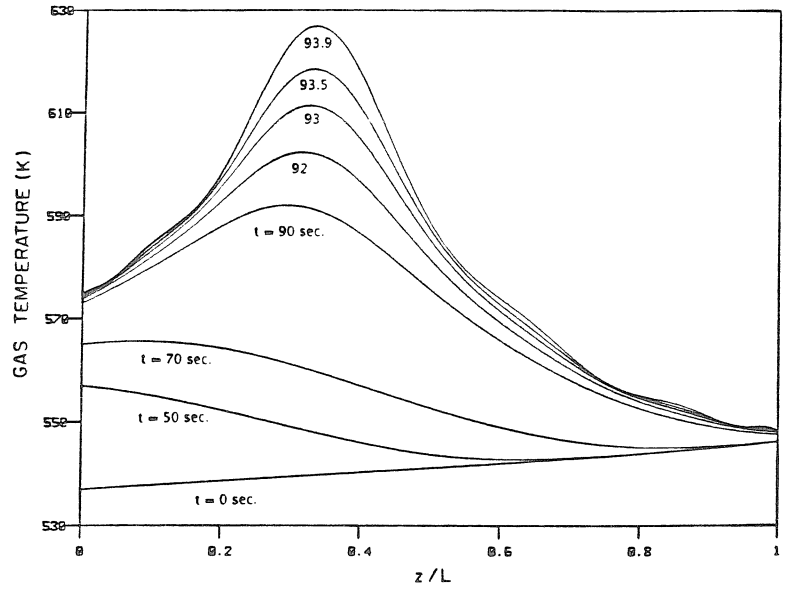

b

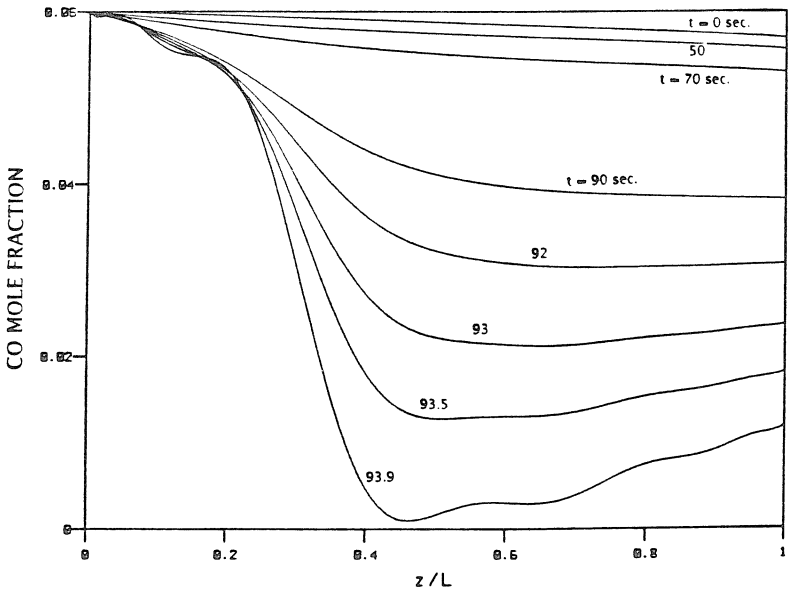

c

Figure 7 b) Open-loop time evolution of the gas temperature profile following a ramp-change in the inlet temperature, with a slope of 0.4 K/sec. The ramp levels off when the inlet temperature reaches 577 K. c) Evolution of the CO concentration profiles for the same ramp as in b).

with very sharp gradients is well known. It is not surprising then that singularities or spurious solutions arise when conditions resulting in steep profiles are encountered. Orthogonal collocation involves fitting a single polynomial to the entire profile, and if sharp changes are concentrated in a small region of the domain of solution, a very large number of collocation points may be needed so that enough are placed within that region to provide an accurate representation of the solution. As a result most of the collocation points are wasted in regions characterized by smooth concentration profiles, and high order interpolating polynomials result which easily give rise to spurious oscillations. This "rippling" effect, an artifact of the use of this procedure, starts to be observed in the steepest curves of Fig. 7.

A procedure called orthogonal collocation on finite elements has been proposed to address the case of very steep profiles in some regions of the domain of solution (Carey and Finlayson, 1975). This technique allows the discretization points to be concentrated in the small region where the gradients are steepest, thus limiting the total number of collocation points in the whole domain. The integration domain is subdivided into a suitable number of finite elements and orthogonal collocation is applied separately to each one of these elements. Appropriate continuity conditions are to be satisfied at the boundary discretization points between any two elements, called internal nodes. The number and location of the finite elements are selected so that the degree of the interpolating polynomials used inside each element is low enough to avoid oscillations.

A major difficulty in the use of the above technique arises from the fact that in general one does not know *a priori* where the steep profile actually occurs, and therefore it is difficult to define appropriately the different subdomains. This is especially true in the case of dynamic simulations, since the sharp fronts move. An extension of the technique, called orthogonal collocation on finite elements with moving boundaries has been proposed that specifically addresses this problem

(Jensen and Finlayson, 1980; Garza-Garza and Dudukovic, 1982). Gardini *et al.* (1985) have proposed, in the context of fixed-bed reactor simulation, ad-hoc procedures for updating the position of the finite element boundaries during the integration in order to follow the movement of the steep fronts. The use of this recently developed technique or of related ones should be investigated in future work on the modeling of the reactor system.

For the initial series of control studies involving single-pass operation of the reactor, operation around a steady state of partial conversion seems to provide more interesting control problems than those arising in system operation under complete conversion. The regulation of the product (CH_4) concentration around a set-point value is not an issue when all the reactant is consumed at the very entrance of the reactor. For this regime of "upper steady states," the product concentration is fixed by the inlet reactant concentration (because all the reactant is consumed), and changes in the inlet temperature or the flow rate over a long range do not affect its value. In addition, steady states of complete conversion may involve very high temperatures which should be avoided because of possible damage to the system. From these considerations it was decided to carry out the initial series of control studies for the system operated under partial conversion (around 15%). Challenging control problems arise in this case. These are mainly related to trying to avoid the drift of the reactor to an upper steady state of complete conversion following sustained disturbances. Chapters III and IV address this problem in detail.

For the regime of lower steady states the description by means of orthogonal collocation of both the steady-state and dynamic system behavior is accurate enough to justify its adoption. Phenomena observed with the model, like the high sensitivity under certain conditions and the steep concentration profiles, have been corroborated by employing other solution procedures like three-points-centered

finite differences with a very large number of grid points. These effects, therefore, are not by themselves an artifact of the use of the orthogonal collocation procedure.

5. DEVELOPMENT OF LINEAR STATE-SPACE MODELS FOR THE CONTROL STUDIES

5.1 General Procedure

The control system analysis and synthesis techniques employed throughout the present thesis are based on the characterization of the system under study by means of a nominal plant (model) plus an uncertainty description which accounts for the expected mismatch between the model and the actual plant. The uncertainty is characterized in the form of perturbations to the nominal plant, which are known only to within norm-bounds.

The analysis and synthesis techniques apply to systems described by finite dimensional linear time-invariant models. Section 3 describes the procedure employed for obtaining, from the distributed parameter system descriptions, finite dimensional nonlinear models. The next step in the development of models appropriate for the control studies is the linearization of these nonlinear models in order to arrive at state-space descriptions of the general form

$$\begin{aligned} \dot{x}(t) &= Ax(t) + Bu(t) \qquad x(0) = x_0 \\ y(t) &= Cx(t) + Du(t) \ , \end{aligned} \tag{18}$$

where x is the state vector, u is the vector of system inputs (manipulated variables and disturbances), y is the vector of system outputs and A, B, C and D are constant matrices, functions of the model parameters and of the reference (steady-state) conditions around which the linearization is carried out. The resulting mathematical description is then accurate for small perturbations around the steady state.

Unfortunately, the research in stability analysis and feedback controller design for general nonlinear systems has not reached a stage in which rigorous approaches exist for practical application to systems such as the reactor. Therefore, although not rigorous, the use of linear approximations to the nonlinear models constitutes the only feasible alternative. Clearly, in going from the nonlinear to the linearized descriptions, further mismatch is introduced between the resulting models and the actual plants. In the simulation studies considered in this thesis, the main source of uncertainty arises from the use of linearized models. The robust controllers, even though designed on the basis of linearized models, are expected to maintain closed-loop stability and reasonable performance when applied to the nonlinear model. As will be clear from the results of Chapters III and IV, the treatment of a nonlinear system by means of robust linear controller design methods yields reasonable results in many instances.

The uncertainty resulting from the system nonlinearity is characterized as parameter variations of the linearized model. To account for the model uncertainty, we assume that the dynamic behavior of the nonlinear plant is described not by a single linear time-invariant model but by a family Π of linear time-invariant models, referred to as the "uncertainty set." This set Π is a set of possible plants to which the actual plant is assumed to belong.

Several procedures may be employed for defining the set Π. One such procedure is described in what follows. This procedure involves a linearization of the nonlinear model not only around the steady state that corresponds to the nominal operating conditions, but also around "steady states" corresponding to conditions along the expected trajectory of the closed-loop system following a disturbance or set-point change. Each linearization results in a different state-space model (namely, in different values for the elements of A, B, C and D). From a number of such linearizations a set π of models is obtained, which serves as a basis for

defining the set Π employed in the control system design. The "operating conditions" on the basis of which these linearizations are carried out are defined by expected values of the disturbances to the system and of the manipulated variables. This approach is by nature an iterative procedure since the trajectory of the closed-loop system is not known *a priori*. If the system is to arrive at a new steady state (following, for example, asymptotically constant set-point changes or disturbances) it is reasonable at least to include the models corresponding to the old and the new steady-state conditions.[2]

Consider for simplicity the single-input single-output (SISO) case. The same remarks that follow apply directly to each separate element of the transfer matrices in the multivariable case. The family Π of plants is defined in the frequency domain. The frequency response

$$\tilde{p}_k(j\omega) = C_k (j\omega I - A_k)^{-1} B_k + D_k \quad , \tag{19}$$

corresponding to each state-space model k of π, is first computed at a reasonably large number of frequencies in a relevant frequency range. The full-order state-space models obtained directly from the linearization are employed in this computation. At this stage, therefore, no model reduction procedure is yet applied, and all the dynamic characteristics of the models are intact.

At each frequency a set of points in the complex plane is defined. Each point corresponds to each model in π. The points determine a region in the complex plane, on the basis of which a new region defining the set Π is obtained. In general, the original region can have a complex shape and therefore a complex mathematical description that is difficult to deal with in the context of control system design. An example of such a region is shown in Fig. 8.

---

2. An alternative, entirely different procedure for characterizing the dynamic behavior of the nonlinear system in terms of linear models involves conducting appropriate transfer function identification "experiments" on the nonlinear *model*. From an appropriate analysis of the data, transfer functions and uncertainty regions can be directly obtained (see Section 6). Initial steps were undertaken for the application of this procedure to the reactor model (Appendix B).

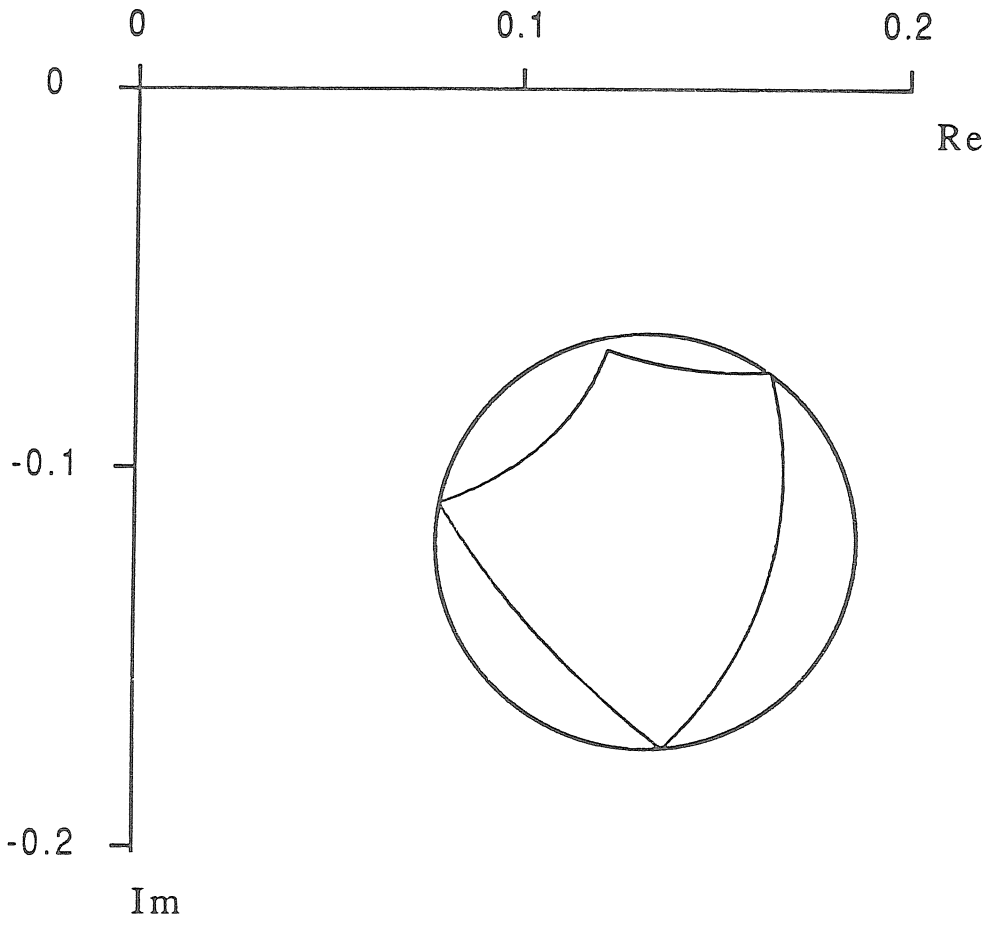

Figure 8 Uncertainty region in the complex plane, characteristic of cases in which both gain and phase uncertainty are present, and evaluated at one particular frequency. Approximation by the smallest disk that includes the entire region.

The analysis and synthesis techniques employed by us require the uncertainty to be described by disk-shaped regions (Chapter III). Any complex region can be approximated by a disk with more or less conservatism. Refer again to Fig. 8. The disk-shaped region includes more plants than the original region. The conservatism arises from the fact that the robustness tests will have to hold for a set of plants larger than what the set of possible plants is originally expected to be. On the other hand, since for the case of uncertainty resulting from the system nonlinearity it is difficult to predict boundaries for the set of possible plants, the approximation of the original region by a disk may in many cases be actually helpful because of the extra safety margin added.

On the basis of the set π, the set Π of all possible plants to which the actual plant belongs is defined as

$$\Pi = \left\{ p: \frac{|p(j\omega) - \tilde{p}(j\omega)|}{|\tilde{p}(j\omega)|} < \bar{l}_m(\omega) \right\} , \qquad (20)$$

where $\tilde{p}$, known as the nominal plant or simply as "the model," is chosen to correspond to the center, at each frequency, of the smallest circle enclosing all models of the original set π. $|\tilde{p}(j\omega)|\bar{l}_m(\omega)$ is the radius of that circle. Eq. (20) is known as a multiplicative uncertainty description (Chapter III). $\bar{l}_m(\omega)$ is a bound on the multiplicative uncertainty. The implications of the use of such an uncertainty description are explained in detail in the control system design Chapters III and IV.

The result of the above approach is a non-parametric description of the (full, nominal) model in the frequency domain, together with the corresponding bound on the multiplicative uncertainty. The non-parametric description consists simply of a table of the real and imaginary parts of $\tilde{p}(j\omega)$ as a function of frequency. This description can be utilized directly in most of the analysis techniques we employ. However, for the controller synthesis, a parametric description in the form of a transfer matrix or the equivalent state-space model (preferably of a reduced

order) is needed.

Reduced-order parametric descriptions are obtained from the frequency domain descriptions by means of a frequency-domain, control-relevant model reduction software package (Rivera and Morari, 1985). In essence, the technique finds out the parameters of a reduced-order rational transfer function which best fit the non-parametric description according to different optimality criteria. As the goal of the model reduction is the control system design, the control objectives are considered in the reduction process and are incorporated into the objective functions through appropriate frequency-dependent weights. As a result, the procedures give reduced-order models that best approximate the full models in the frequency interval that is most relevant to the control problem. The basis of this model reduction technique is explained in Section 4.4 of Chapter III, because it is strongly related to the theoretical concepts presented in that chapter. In all cases the validity of the model reduction is tested by analyzing the multiplicative error between the full and the reduced-order model and its effect in the context of the control problem under study (Rivera and Morari, 1985).

In some cases a state-space description may be directly available for the full, nominal model. This is the case, for example, if the nominal model is selected to be the one corresponding to the nominal operating conditions. In these cases either the above model reduction technique or other techniques requiring the state-space descriptions such as balanced realizations (Moore, 1981; Enns, 1984) may be applied. With the reduced state-space models on hand, the final step of the model development work is completed, and the control system design can be finally addressed.

5.2 Model Linearization for the Reactor System

The procedure described in the previous section for dealing with the nonlinear system requires not one but a number of linearizations before one can address the

control system design for a particular case-study. For a large-order model such as the one for the reactor, a straightforward numerical linearization based on finite-difference approximations of the Jacobian is very slow and may lead to inaccurate results. On the other hand, an analytic linearization, once the analytic expressions for the elements of the Jacobian have been determined, results in much more rapid and exact evaluation of the state-space matrices. If explicit analytic expressions for each element of the Jacobian are obtained, then the effect of different system parameters on each one of these elements can also be directly investigated.

Khanna (1984) performed an entirely analytic linearization of the reactor bed model. The procedure, although conceptually simple, required extremely lengthy algebraic manipulations. The model was linearized in three stages: 1) linearization of the reaction rates; 2) analytic linearization of the algebraic equations and substitution of the explicit, linearized analytic expressions for the corresponding variables into the differential equations, and 3) linearization of the resulting ODE's. The procedure had to be carried out with extreme care because of the complexity of the model and without the help, at that time, of appropriate algebraic manipulation software.

The need for redoing this entire procedure in several instances, due to modifications to the model, prompted us to reconsider the need for having explicit analytic expressions for each element of the Jacobian. It was realized that the step introducing the greatest complications in the case of the reactor model[3] was step 2) above. The procedure was replaced by a simple, semi-analytic approach (Appendix A). This latter procedure is easier to implement and less prone to mistakes, while retaining the accuracy of the complete analytic linearization. On the basis of this simple procedure, general software was later written, which, starting from any non-linear differential/algebraic model and with the help of symbolic manipulation

3. The previous version that included the nonlinear algebraic equations resulting from the continuity equation.

software, carries out the linearization and provides the state-space matrices ready for further use in FORTRAN subroutines (Lewin, 1986).

By means of the linearization procedure the nonlinear differential/algebraic equation models are converted into standard state-space models of order equal to the original number of ODE's. For the reactor model the order is 4N+1, where N is the number of interior axial collocation points. The state vector is given by

$$x = \left[\Theta_{s_1}, \cdots, \Theta_{s_N}, \Theta_{g_1}, \cdots, \Theta_{g_N}, \Theta_{t_1}, \cdots, \Theta_{t_N}, y_{1_1}, \cdots, y_{1_{N+1}}\right]^T , \qquad (21)$$

respectively, the temperatures of the catalyst phase, gas phase and thermal well at each interior collocation point, and the CO concentration at each interior collocation point and at the reactor exit. All variables are dimensionless, deviation variables. The reference temperature and concentration values are chosen to provide reasonable scalings. The entire procedure that leads from the set of dimensional partial differential equations to the state-space models is presented in detail in Appendix A.

The code that carries out the steady-state solution of the models and the calculation of the full state-space matrices (REACTORSS) is described shortly in Appendix B. Great flexibility has been achieved by separating the overall solution task into two programs, REACTORSS carrying out all steady-state related calculations, and the second program (REACSUBS) being a set of subroutines linked to SNTEG for the dynamic simulations. The results of REACTORSS are stored in appropriate files for use by REACSUBS or for direct use with the two different computer-aided control system design packages available to us (Chapter V).

For the case of the reactor model, if the number of interior axial collocation points N is 12 (as in most simulation studies carried out in this work), then a full linearized model of order 49 is obtained. Although the order is much smaller than what would result from the use of other discretization procedures (i.e., finite

differences) and although simulation times have been reduced considerably, further model reduction is very convenient. By means of the model reduction procedure mentioned in Section 5.1, reduced-order models of orders 5 to 8 have been obtained that adequately preserve the most relevant dynamic features of the full model.

6. PARAMETER ESTIMATION AND MODEL VALIDATION

The model parameters employed in the simulation studies presented in this thesis are in part easily measurable geometric parameters of the system, in part kinetic parameters obtained from experiments carried out in our laboratory, and in part values taken from the literature. Before control studies can be actually performed on the experimental reactor system, further parameter estimation is necessary together with a validation of the models. The model validation should be carried out by trying to reproduce on the experimental system the steady-state and dynamic behaviors obtained with the model. Also, as pointed out previously, transfer function identification experiments should be carried out to validate directly the transfer functions and the uncertainty descriptions.

Because of the relatively large number of reactor model parameters that need to be estimated, the parameter estimation needs to be carried out in several stages. The first stage involves the separate estimation of kinetic parameters of the reactions (Chiang, 1983; Webb, 1986). This parameter estimation is done on the basis of results from steady-state experiments carried out in an external recycle reactor built in our laboratory for this special purpose (Strand, 1984). This is an almost isothermal and gradientless reactor, certainly safer and allowing a more accurate evaluation of the reaction rates than if the experiments were to be conducted directly on the main reactor. The parameter estimation itself is carried out by means of standard nonlinear regression techniques. If global rate expressions based

on bulk gas conditions are to be employed, it is important to assure that the interphase and intraphase concentration and temperature gradients around the particles be negligible in both reactors. (If they are negligible only for the kinetic reactor, then the diffusion effects have to be incorporated into the rate expressions in the form of effectiveness factors.) If the gradients are not negligible it is necessary to assure that the kinetic experiments are carried out under flow conditions around the particles similar to the expected ones for the main reactor.

The second set of parameters to be estimated consists mainly of the heat transfer coefficients of the reactor model. These parameters have to be estimated from experiments carried out directly on the fixed-bed reactor, although these experiments need not be carried out under reaction conditions. By carrying out the experiments under conditions of zero reaction, we can better isolate the heat transfer effects and conduct safer experiments. The experiments should involve measuring the open-loop dynamic system response to a change in one or more of the input variables. One dynamic run is expected to yield the same amount of information that only many steady-state experiments would give, in a very small fraction of the time that the latter would require. The experiments should be carefully designed. For example, in order to estimate radial Biot numbers, a disturbance in the reactor wall temperature is more appropriate than one in the inlet temperature. In order to carry out the parameter estimation, a special routine for parameter estimation from dynamic experiments is required (Appendix B), together with a dynamic model of the system.

After the second stage of experiments, and after careful evaluation of the reactor model with the new set of heat and mass transfer parameters, the validation of the whole model should be carried out by means of experiments under reaction conditions. A list of model parameters that need to be estimated from experiments in the reactor is presented in Appendix A. It is important to estimate carefully those

parameters to which the model is most sensitive. The analysis should benefit from new techniques available in the literature for sensitivity analysis of nonlinear differential/algebraic equation systems (Caracotsios and Stewart, 1985).

The updated version of the model should be subsequently employed in reevaluating the system transfer functions. In addition, it should be employed for carefully designing transfer function identification experiments that should serve for a final validation of the model. These experiments also involve measuring the system response to an input test signal. Pseudorandom binary sequences (PRBS) have been shown to be most adequate as input signals for these identification experiments (Eykhoff, 1974). Following these experiments the frequency responses can be directly determined by techniques like spectral smoothing, which involve smoothing and Fourier-transformation of the data (Jenkins and Watts, 1968; Rivera, 1986).

REFERENCES

Bilous, O. and N.R. Amundson, 1956, Chemical reactor stability and sensitivity - II. Effect of parameters on sensitivity of empty tubular reactors. *A.I.Ch.E. Journal* **2**, 117-126.

Bird, R.B., W.E. Stewart and E.N. Lightfoot, 1960, *Transport Phenomena*, John Wiley and Sons, New York.

Bonvin, D., 1980, Dynamic modeling and control structures for a tubular autothermal reactor at an unstable state. Ph.D. Thesis, University of California, Santa Barbara, CA.

Bonvin, D., R.G. Rinker and D.A. Mellichamp, 1983, On controlling an autothermal fixed-bed reactor at an unstable state - I. Steady-state and dynamic modeling. *Chem. Engng Sci.* **38** , 233-244.

Caracotsios, M. and W.E. Stewart, 1985, Sensitivity analysis of initial value problems with mixed ODE's and algebraic equations. *Comput. and Chem. Engng* **9** , 359-365.

Carey, G.F. and B.A. Finlayson, 1975, Orthogonal collocation on finite elements. *Chem. Engng Sci.* **30** , 587-596.

Chiang, D.N., 1983, CO methanation over a nickel catalyst. M.Sc. Thesis, Calif. Inst. of Technology, Pasadena, CA.

Enns, D., 1984, Model reduction for control system design. Ph.D. Thesis, Stanford University, CA.

Eykhoff, P., 1974, *System Identification* , John Wiley and Sons, London, pp. 386-392.

Finlayson, B.A., 1972, *The Method of Weighted Residuals and Variational Principles*, Academic Press, New York.

Friedly, J.C., 1972, *Dynamic Behavior of Processes*, Prentice-Hall, Englewood Cliffs,

NJ, 345-346.

Froment, G.F. and K.B. Bischoff, 1979, *Chemical Reactor Analysis and Design*, John Wiley and Sons, New York, Ch. 11.

Gardini, L., A. Servida, M. Morbidelli and S. Carra, 1985, Use of orthogonal collocation on finite elements with moving boundaries for fixed-bed catalytic reactor simulation. *Comput. and Chem. Engng* **9** , 1-17.

Garza-Garza, O. and M.P. Dudukovic, 1982, Solution of models for gas-solid noncatalytic reactions by orthogonal collocation on finite elements with moving boundary. *Comput. and Chem. Engng* **6** , 131-139.

Georgakis, C., R. Aris and N.A. Amundson, 1977, Studies in the control of tubular reactors - I. General considerations. *Chem. Engng Sci.* **32** , 1359-1369.

Jenkins, G.M. and D.G. Watts, 1968, *Spectral Analysis and its Applications*, Holden-Day, San Francisco, CA.

Jensen, O.K. and B.A. Finlayson, 1980, Solution of the transport equations using a moving coordinate system. *Adv. Water Resources* **3** , 9-18.

Jutan, A., J.D. Wright and J.F. MacGregor, 1977, Multivariable computer control of a butane hydrogenolysis reactor: Part I. State space reactor modeling. *A.I.Ch.E. Journal* **23** , 732-742.

Keller, H.B., 1977, Numerical solution of bifurcation and nonlinear eigenvalue problems, in *Applications of Bifurcation Theory* , Academic Press, New York.

Khanna, R., 1984, Control model development for packed-bed chemical reactors. Ph.D. Thesis, Calif. Inst. of Technology, Pasadena, CA.

Khanna, R. and J.H. Seinfeld, 1982, Model development of a non-adiabatic packed-bed reactor. Paper 9d, 1982 Annual Meeting, A.I.Ch.E., Los Angeles, CA.

Khanna, R. and J.H. Seinfeld, 1986, Mathematical modeling of packed-bed reactors -

Numerical solutions and control model development. *Advances in Chemical Engineering*, in press.

Kubicek, M., 1976, Dependence of solution of nonlinear systems on a parameter (Algorithm 502). *ACM Trans. on Mathematical Software* **2** , pp. 98-107.

Lewin, D.R., 1986, Personal communication. Calif. Inst. of Technology, Pasadena, CA.

Moore, B.C., 1981, Principal component analysis in linear systems: controllability, observability and model reduction. *IEEE Trans. Automat. Contr.* **AC-26** , 17-32.

Morari, M., 1983, Design of resilient processing plants - III. A general framework for the assessment of dynamic resilience. *Chem. Engng Sci.* **38** , 1881-1891.

Petzold, L.R., 1982, A description of DASSL: a differential/algebraic system solver. *Sandia Tech. Rep.* 82-8637.

Powell, M.J.D., 1970, A hybrid method for nonlinear equations, in *Numerical Methods for Nonlinear Algebraic Equations*, P. Rabinowitz (ed), Gordon and Breach, New York.

Puszynski, J., D. Snita, V. Hlavacek and H. Hofmann, 1981, A revision of multiplicity and parametric sensitivity concepts in nonisothermal nonadiabatic packed bed chemical reactors. *Chem. Engng Sci.* **36** , 1605-1609.

Rivera, D.E., 1986, Modeling requirements for process control. Ph.D. Thesis, Calif. Inst. of Technology, Pasadena, CA, in preparation.

Rivera, D.E. and M. Morari, 1985, Internal Model Control perspectives on model reduction. Proceedings of the 1985 American Control Conference, Boston, MA, pp. 1293-1298.

Rivera, D.E., M. Morari and S. Skogestad, 1986, Internal Model Control - 4. PID controller design. *Ind. Engng Chem. Proc. Des. Dev.* **25** , 252-265.

Strand, D.M., 1984, Personal communication. Calif. Inst. of Technology, Pasadena,

CA.

Strand, D.M. and J.H. Seinfeld, 1982, Construction of a laboratory-scale fixed-bed methanation reactor for multivariable control studies. Paper 92d, 1982 Annual Meeting, A.I.Ch.E., Los Angeles, CA.

Vatcha, S.R., 1976, Analysis and design of methanation processes in the production of substitute natural gas from coal. Ph.D. Thesis, Calif. Inst. of Technology, Pasadena, CA.

Villadsen, J.V. and M.L. Michelsen, 1978, *Solution of Differential Equation Models by Polynomial Approximation* , Prentice-Hall, Englewood Cliffs, New Jersey.

Villadsen, J.V. and W.E. Stewart, 1967, Solution of boundary-value problems by orthogonal collocation. *Chem. Engng Sci.* **22** , 1483-1501.

Webb, C., 1986, Personal communication. Calif. Inst. of Technology, Pasadena, CA.

III. CONTROL SYSTEM DESIGN FOR A FIXED-BED METHANATION REACTOR

Accepted for Publication in

Chemical Engineering Science

(1986)

CONTROL SYSTEM DESIGN FOR A FIXED-BED METHANATION REACTOR

Jorge A. Mandler, Manfred Morari and John H. Seinfeld

Chemical Engineering, 206-41

California Institute of Technology

Pasadena, CA 91125

ABSTRACT

A systematic approach is applied to the design of robust controllers for a fixed-bed, non-adiabatic, laboratory methanation reactor, a unit inherently difficult to control. The fundamental limitations to the achievable closed-loop performance are established by both physical arguments and dynamic resilience considerations. The Internal Model Control (IMC) structure provides a suitable framework for this analysis. IMC controllers are designed and their performance in the face of model uncertainty tested both by simulation and by means of the Structured Singular Value (μ) analysis technique. The paper provides basic insight into the characterization and solution of control problems that are particular to fixed-bed reactor systems and constitutes the first account of the application of several recent advances in control theory to a complex chemical process.

1. INTRODUCTION

The systematic analysis of the control of chemical reactors can be considered to date from three pioneering papers by Aris and Amundson (1958a,b,c), in which the authors laid the foundation for the now standard linearized treatment and exposed for the first time some of the complexities of stirred reactor behavior. The subject of the current work is control of the fixed-bed reactor, the mathematical description of which is virtually synonymous with the name of Amundson. Indeed, not only the control analysis that we will develop but also the reactor model that we employ can be firmly traced to roots in the work of Amundson and his students. It is our sincere pleasure to dedicate this paper to the seventieth birthday of Professor Neal R. Amundson.

The basic steps in a systematic approach to the design of advanced control schemes are:

1. Modeling and identification, to obtain an understanding of the system under consideration and to provide the tools for the design of the controllers.
2. Selection of the control objectives.
3. Selection of the control configuration, i.e., of the sets of measured, controlled and manipulated variables.
4. The application of a systematic procedure for the design of the controller (the control law).

Recent advances in control theory, coupled to advances in modeling and numerical methods and the availability of better computational resources, have significantly improved the methods by which the above approach can be implemented. As a result, a clearer understanding of some longstanding issues in chemical process control has been gained. For example, through the Internal Model Control (IMC) structure, new results have been obtained that establish a quantitative

relationship between the design characteristics of a process and the best achievable closed-loop performance (so-called "dynamic resilience" (Morari, 1983a)). Also new directions have been suggested for the problems of control in the presence of constraints and nonlinear control system design (Morari, 1983b). The issue of "robustness" of the control system, namely, that stability and acceptable performance be maintained in the face of plant-model mismatch, has received a great deal of attention from the part of control theoreticians. Necessary and sufficient conditions for guaranteeing robustness of *both* stability and performance have only recently been derived (Doyle, 1984). The robustness issue is crucial in chemical process control, where accurate dynamic models of the processes are rarely available. No accounts exist in the process control literature of applications of these recent theoretical advances to practical control problems.

In order for new advances in control theory to be implemented in an industrial environment, it is essential that they be evaluated first in a research environment; this creates a need for the construction of flexible laboratory-scale or pilot plant-scale units that, in spite of their smaller size relative to plant scale, preserve much of the complexity of the industrial setting. The fixed-bed, non-adiabatic methanation reaction unit shown in Fig. 1 has been constructed as a system to evaluate advanced control schemes (Strand and Seinfeld, 1982). This experimental unit allows implementation of a variety of configurations, including operation under conditions of heat and/or product recycle.

The objectives of this paper are twofold: on the one hand, we want to address the design of control systems for the fixed-bed methanation reactor; on the second hand, we want to present a systematic approach to control system design through its application to this particular case-study. The approach is based on some of the recent theoretical developments mentioned above. Dynamic resilience considerations are employed in the selection of the control configuration (step 3 above). A

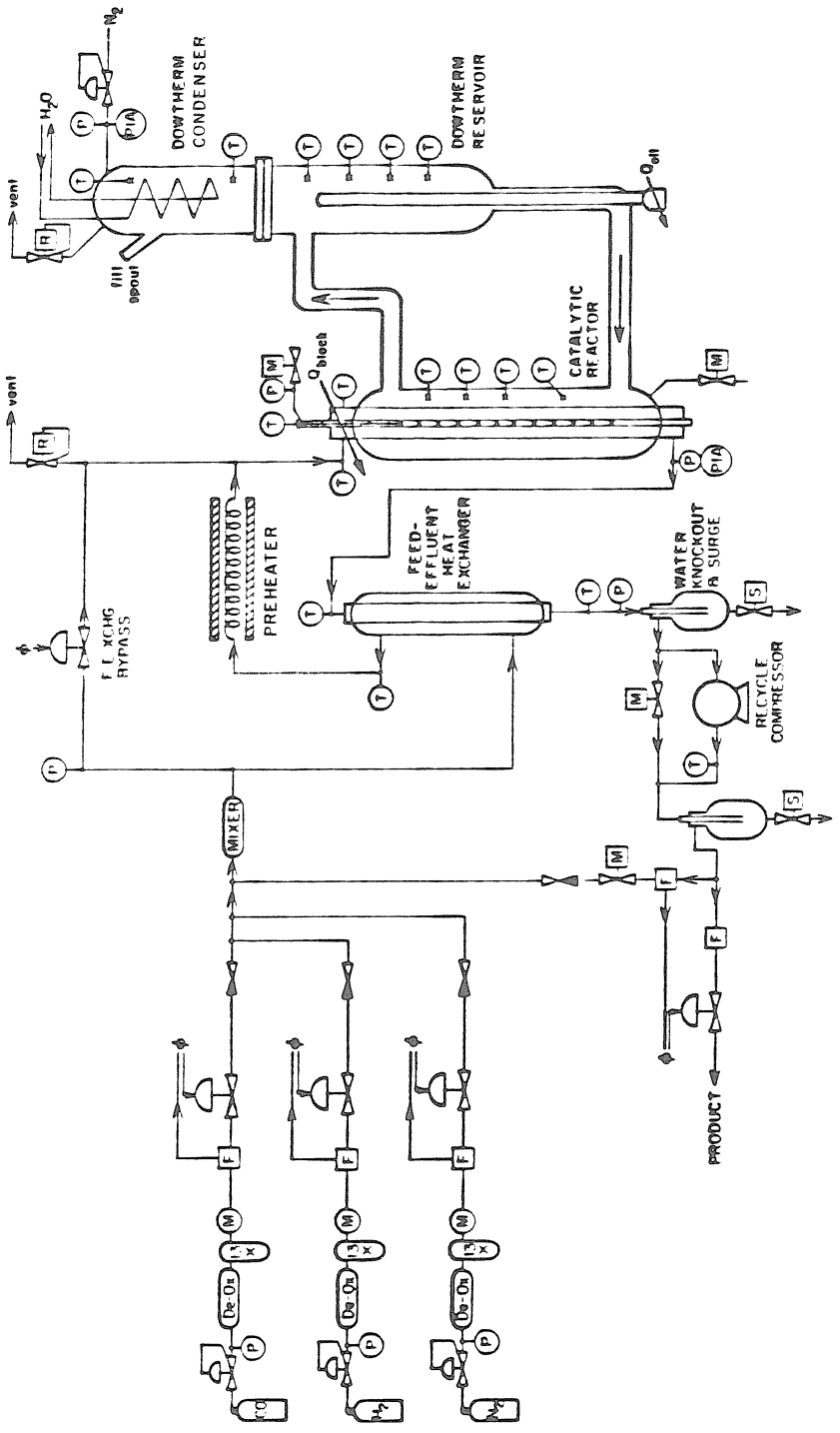

Figure 1 Process diagram of the experimental methanation reactor.

systematic procedure for the design of robust controllers is presented and applied (step 4). A recently developed control objective-related model reduction procedure is also utilized.

The discussion in the paper closely follows steps 1-4 above. Section 2.1 presents a short description of the mathematical model of the reactor and subsequently addresses the development of models appropriate for the control studies. The selected system configuration and operating conditions are given in Section 2.2. In Section 3.1, steady-state results are presented that help in the identification and selection of the control objectives. In Section 3.2, dynamic simulation results are combined with basic resilience studies for the selection of the control configuration. Section 4 presents a logical framework for the design of the control laws, concentrating on the single-input single-output (SISO) case and addressing the robustness issue. Finally, the theory of Section 4 is applied in Section 5 to the design of robust SISO controllers for the reactor system.

2. THE METHANATION REACTOR SYSTEM

2.1 Mathematical Model

The mathematical model of the fixed-bed methanation reactor is described in detail by Khanna (1984) and Khanna and Seinfeld (1982,1986). In particular, it:

— incorporates axial and radial dispersion of mass and energy;

— considers multiple reactions;

— involves a two-dimensional heterogeneous analysis;

— accounts for temperature, pressure and mole dependencies of gas velocity, density, average molecular weight and heat capacity, reaction rate constants and heats of reaction;

— incorporates the effects of axial pressure gradients;

— includes the analysis of an axial thermal well.

The model is described by the coupled set of mass and energy conservation equations. Radial gradients are important in this system, since heat is removed continuously from the catalytic bed into an outer jacket filled with a cooling fluid. The reactor is designed to simulate one tube of a type of non-adiabatic reactor employed for highly exothermic reactions; these reactors consist of a large number of tubes inside a cooling oil shell.

The methanation reaction

$$CO + 3H_2 \rightarrow CH_4 + H_2O \qquad (1)$$

is taken for the present purpose as the only significant reaction; the rate of the methanation reaction was found experimentally to be much greater than that corresponding to the steam-shift reaction on the nickel-over-alumina catalyst employed. The following global reaction rate expression, based on bulk gas conditions, was determined at 513 K (Chiang, 1983):

$$R_M = \frac{0.0217\ p_{CO}\ p_{H_2}\ t_d^{-0.3}}{(1 + 110\ p_{CO} + 2.32\ p_{H_2})^2} \quad \left(\frac{\text{moles}}{\text{sec gcat}}\right), \qquad (2)$$

where t_d, measured in hours, accounts for a long term deactivation effect. The activation energy was measured at 37 kcal/mol. This rate expression is used throughout the simulations presented here. This reaction kinetics and the operating conditions selected (see Section 2.2) correspond to the actual ones for the laboratory experimental system, and differ from those employed by Khanna (1984; Khanna and Seinfeld, 1982,1986). The latter give rise to profiles significantly milder than the profiles obtained in our case. The rate expression shows that the CO is a strong inhibitor in almost the whole range of concentrations. This has an

important effect on the behavior of the reactor. The values of some of the other parameters of the model, such as heat transfer coefficients in the reactor, are selected for the present purposes from the literature.

The basic numerical solution procedure employed on the reactor model is orthogonal collocation. The discretization of the reactor equations is first done in the radial direction by means of collocation, based on one interior point and a quadratic representation for the radial temperature profiles. Orthogonal collocation is then used for the discretization in the axial direction. Because of steep profiles for some conditions, simulations have been performed generally with 12 interior axial collocation points. The resulting system consists of 4N+1 nonlinear ODE's together with N+5 nonlinear algebraic equations (a nonlinear differential-algebraic equation system), where N is the number of interior axial collocation points.

Linearized models are employed for the control system design. These are obtained by means of an analytic evaluation of the corresponding partial derivatives at a desired nominal point. The resulting state vector consists of 4N+1 elements, i.e., for 12 collocation points, 49 elements. The importance of model reduction for the control system design is evident. However, as opposed to most previous accounts of the application of model reduction schemes to comprehensive reactor models, in this work the model reduction is not done in an "open-loop" manner; i.e., the model reduction problem is *not* separated from the control problem itself. The model reduction is therefore conveniently presented in Sections 4 and 5 together with the description of the controller design.

The computational implementation of the reactor model differs from the one reported by Khanna (1984). The model has been incorporated into the framework of a computer-aided control system design package, making it very convenient for the control studies. Simulations are carried out employing a special code that allows closed-loop simulations of nonlinear systems together with linear, nonlinear

or discrete controllers. This special code and its application to the reactor model will be presented elsewhere (Mandler and Morari, 1986).

2.2 System Configuration and Operating Conditions

For the purposes of this paper, the operating conditions are selected to correspond closely to those expected for the single-pass operation of the laboratory experimental reactor shown in Fig. 1. In this configuration only CO, H_2 and N_2 are fed to the reactor. Flow rates are low due to the limited availability of reactant gases. Operation is to be maintained in the low-to-mild conversion regime, because otherwise very high temperatures may develop (see Section 3.1). Typical settings for the different variables are given in Section 3.2.

The system configuration and operating conditions treated in this particular case-study do not follow the typical operation of industrial methanators. In most cases, methanation reactors serve to remove small traces of CO from H_2 streams employed in the production of ammonia. Complete conversion is then desired. The second use of methanation is in the production of synthetic natural gas (SNG). In this case higher CO concentrations are involved and high conversions are also desired. Product recycle is sometimes used to reduce the temperatures in the bed and still obtain high conversions (Harms *et al.*, 1980). Product recycle is allowed in our experimental system. The reactor model has also been extended to include the elements of the recycle line. However, product recycle introduces special complications and control problems, and their study is left as a subject of future work. The study of the single-pass reactor operated under low conversions is addressed first, as it serves as the basis for a study of more complicated configurations and because several conclusions can be drawn from it that are of general relevance to the control of fixed-bed reactors.[1] More importantly, this configuration gives rise to

1. The reactor and system configuration are similar to what would be a small-scale version of those employed for the synthesis of phthalic anhydride by o-xylene oxidation, an exothermic reaction with equivalent control problems (Froment and Bischoff, 1979).

interesting control problems and constitutes an excellent example of a complex chemical process full of system-inherent difficulties for the control system design.

3. OPEN-LOOP STUDIES

3.1 Steady-State Results; Definition of the Control Objectives

Steady-state relationships are helpful for an understanding of the control problems that may be encountered, and in our case they help in the definition of the control objectives. At steady state, the discretized model equations resulting from the collocation procedure become a system of nonlinear algebraic equations that can be solved by a number of techniques. Fig. 2 shows the steady-state relationships between the reactor outlet temperature (T_{out}) and the reactor inlet temperature (T_{in}) for different values of the inlet CO concentration. Each point on these curves corresponds to a steady-state solution of the reactor model.

As a result of the exothermicity of the methanation reaction and of the autocatalytic nature of the reaction rate for all CO concentrations (except very close to zero), temperature profiles increase monotonically along the reactor and a "hot spot" is unlikely to occur except at or after a point of complete conversion.[2] Therefore, T_{out} is for this particular case (and provided conversion is not complete) a very good indicator of the partial conversion achieved. The same conclusion can be reached by looking at the steady-state relationships of Fig. 3, where the outlet methane mole fraction is shown as a function of T_{out} for different values of the inlet CO concentration (x_{CO}). The curves correspond to low-to-mild conversions. Note the strong correlation between the outlet methane mole fraction and the reactor outlet temperature. Typically, the main control objective for the reactor would be the regulation of the product concentration around a desired set-point value. The close relationship between the methane concentration and the tempera-

2. Complete conversion, meaning the conversion at equilibrium.

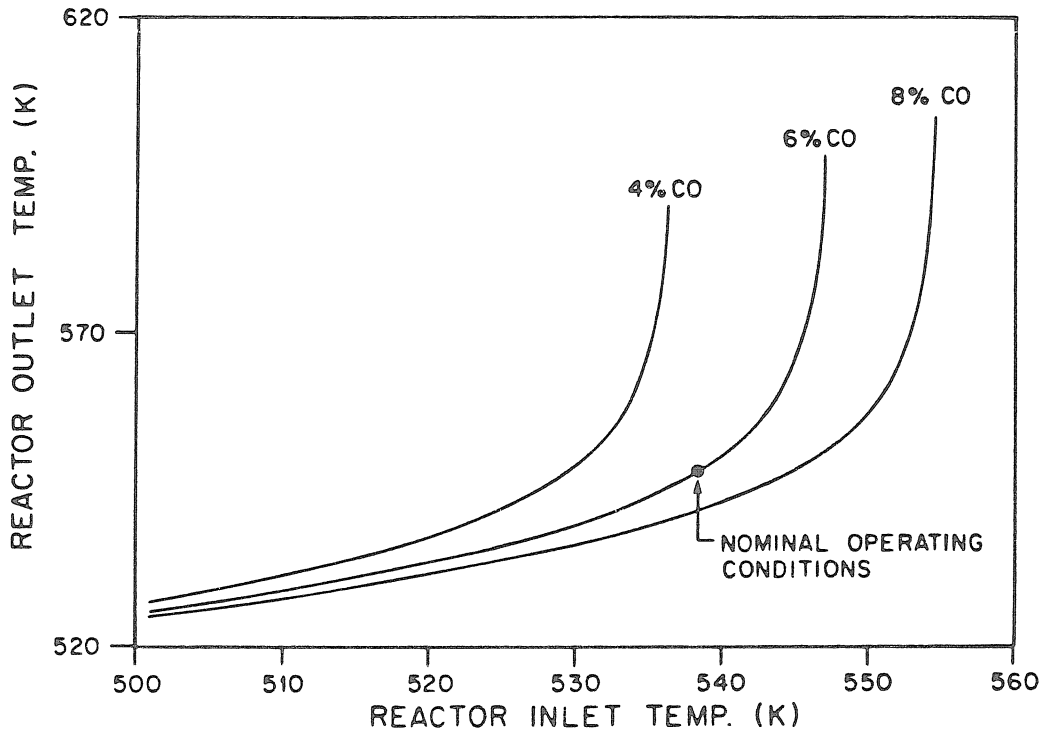

Figure 2 Steady-state relationships between the reactor outlet and inlet temperatures for different inlet CO concentrations. Total molar flow rate, F_P = 0.0223 gmol/sec; reactor wall temperature, T_w = 530 K.

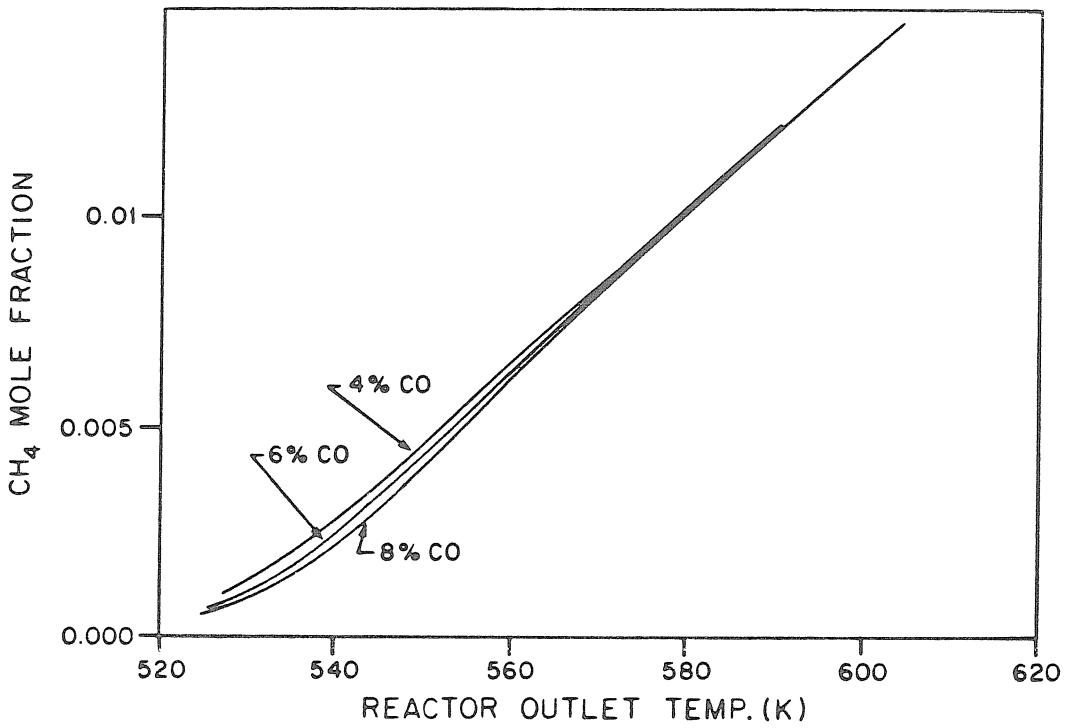

Figure 3 CH_4 outlet mole fraction vs reactor outlet temperature for different inlet CO concentrations.

ture justifies choosing, as the control objective, the regulation of the reactor outlet temperature about a corresponding set-point value. State estimation or inferential control techniques can, of course, be applied to improve the regulation of the product concentration; this is not, however, the main concern in this paper.

The points of maximum conversion shown in Fig. 2 correspond to a conversion of slightly less than 20 %, above which the curves "jump" to steady states of complete conversion. Close to these points the reactor is extremely sensitive in the following sense: sustained small changes in the inlet CO concentration or in the inlet temperature can result in very large changes in the profiles and therefore in very large changes in the conversion and reactor outlet temperature. The reactor is said then to "run away" (Froment and Bischoff, 1979). The main disturbances considered here are sudden changes in the inlet CO concentration, a type of upset that is encountered in industrial practice. For the single-pass configuration of the reactor the inlet temperature is, on the other hand, assumed to be well known and is taken as a manipulated variable.

Fig. 2 suggests that an upset causing a decrease in the inlet CO concentration (remember that the CO is an inhibitor here) will drive the reactor to a steady state of complete conversion unless some action is taken such as a reduction in the reactor inlet temperature. Steady states of complete conversion involve very high temperatures for the conditions presented here and have to be avoided. The control problem that we address is to regulate the outlet gas temperature around a set-point value located in the region close to the bend in the curves of Fig. 2, where, even though the conversion is mild, the sensitivity of the reactor is very high, and the danger of a reactor runaway clearly exists. A very reliable control system is required for this region of operation.

The available measurements in the reactor are temperatures along a central axial thermal well and the outlet gas temperature. Available as manipulated

variables are the reactor inlet temperature T_{in}, the total molar flow rate F_P and the reactor wall temperature T_w. The selection of the control configuration, i.e., of the subsets of measured and manipulated variables that actually enter in the control scheme, is done on the basis of the considerations of Section 3.2.

3.2 Dynamic Simulation and Resilience Studies; Control Configuration

Prior to the design of the control laws, a decision on the control configuration to be adopted is required. The satisfaction of the control objectives constitutes the main factor in this decision. However, in general, more than one control configuration may seem appropriate to satisfy the control objectives, and further discrimination is then necessary. When this is the case, an important factor in the selection among different control configurations is the relative quality of control achievable for the system resulting in each case. In the framework of the Internal Model Control structure, Morari (1983a) has shown that such an assessment can be made purely on the basis of properties of the open-loop system, with no, or minimal, assumptions about the particular controllers to be employed.

Morari introduced the term "dynamic resilience" to indicate the best closed-loop control performance achievable for a plant for all possible constant parameter linear controllers. Thus, control configurations or designs yielding plants with a better dynamic resilience are preferred. A methodology for the quantitative assessment of dynamic resilience was proposed (Morari, 1983a, Holt and Morari, 1985, Morari and Skogestad, 1985). The main *system-inherent* limitations to the achievable closed-loop performance, or, in other words, to the dynamic resilience, were shown to be imposed by:

— non-minimum phase elements (right-half-plane (RHP) zeros and time delays),

— constraints on the manipulated variables, and

— model uncertainty.

The reader is referred to the just-mentioned sources for further details on these topics.

Different combinations of measured and manipulated variables yield different control configurations for the reactor, several of which would seem appropriate for satisfying the control objectives. The assessment of the relative convenience of each configuration is now carried out on the basis of studies of the open-loop system dynamics and with the help of basic resilience considerations. Questions such as whether to use one or more measurements, or which and how many of the three possible manipulated variables to employ are addressed in what follows.

The nominal operating conditions are selected as (see Fig. 2): gas temperature at the reactor inlet, $T_{in} = 537$ K; CO mole fraction at the inlet, $x_{CO} = 0.06$; total molar flow rate, $F_P = 0.0223$ gmol/sec; reactor wall temperature, $T_w = 530$ K. They correspond to an outlet gas temperature (T_{out}) of 546 K and to a product CH_4 mole fraction of 0.0035. The steady state is stable. The disturbance variable selected is x_{CO}. The open-loop system response to a step-change in x_{CO} from 0.06 to 0.045 (−25 %) as computed from the full nonlinear model is shown in Figs. 4 and 5. We note from Fig. 4 that T_{out} rises immediately after the concentration wave has left the reactor (residence time of 1.4 sec) because of the immediate increase in the reaction rate. The product concentration curve shows first a sudden increase after the concentration wave has passed and subsequently a slower increase linked to that of the reactor temperatures. Fig. 5 shows the evolution of the gas temperature profile along the reactor. Notice that the profile at all times increases monotonically with length. The new steady state is reached after about 220 sec. Both figures show that because of the very short residence time and of the long time-constants of the thermal processes, the changes in temperatures caused by changes in x_{CO} occur essentially simultaneously at all points along the reactor. Therefore, for this type of disturbance, and also for disturbances in the flow rate, no additional advan-

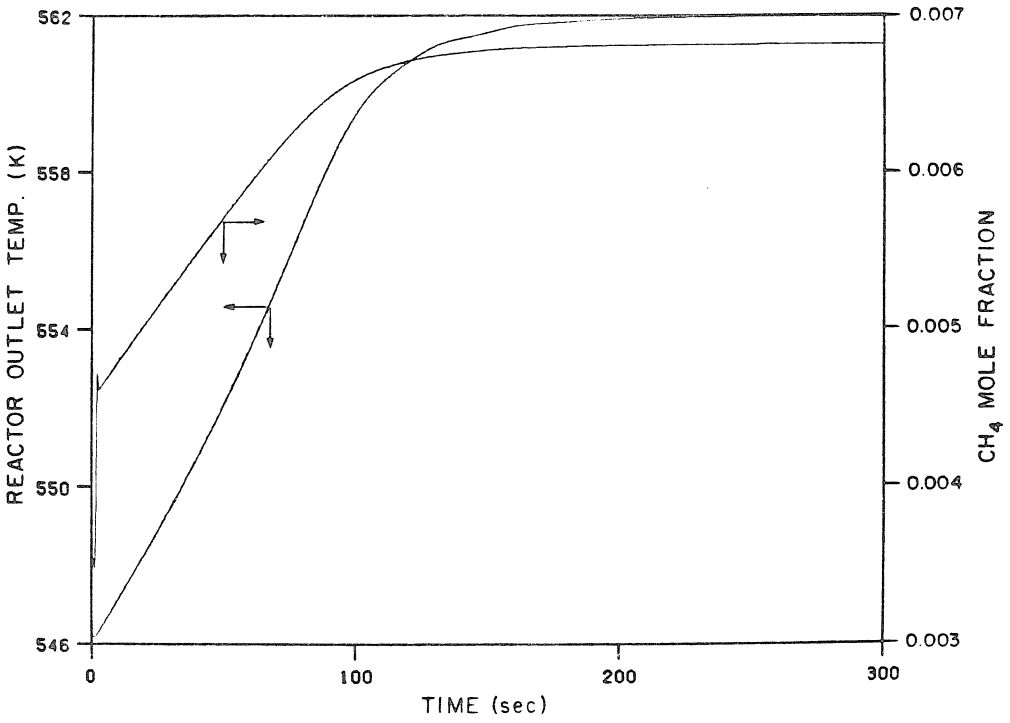

Figure 4 Open-loop system response to a −25% step-change in the inlet CO concentration (nonlinear model).

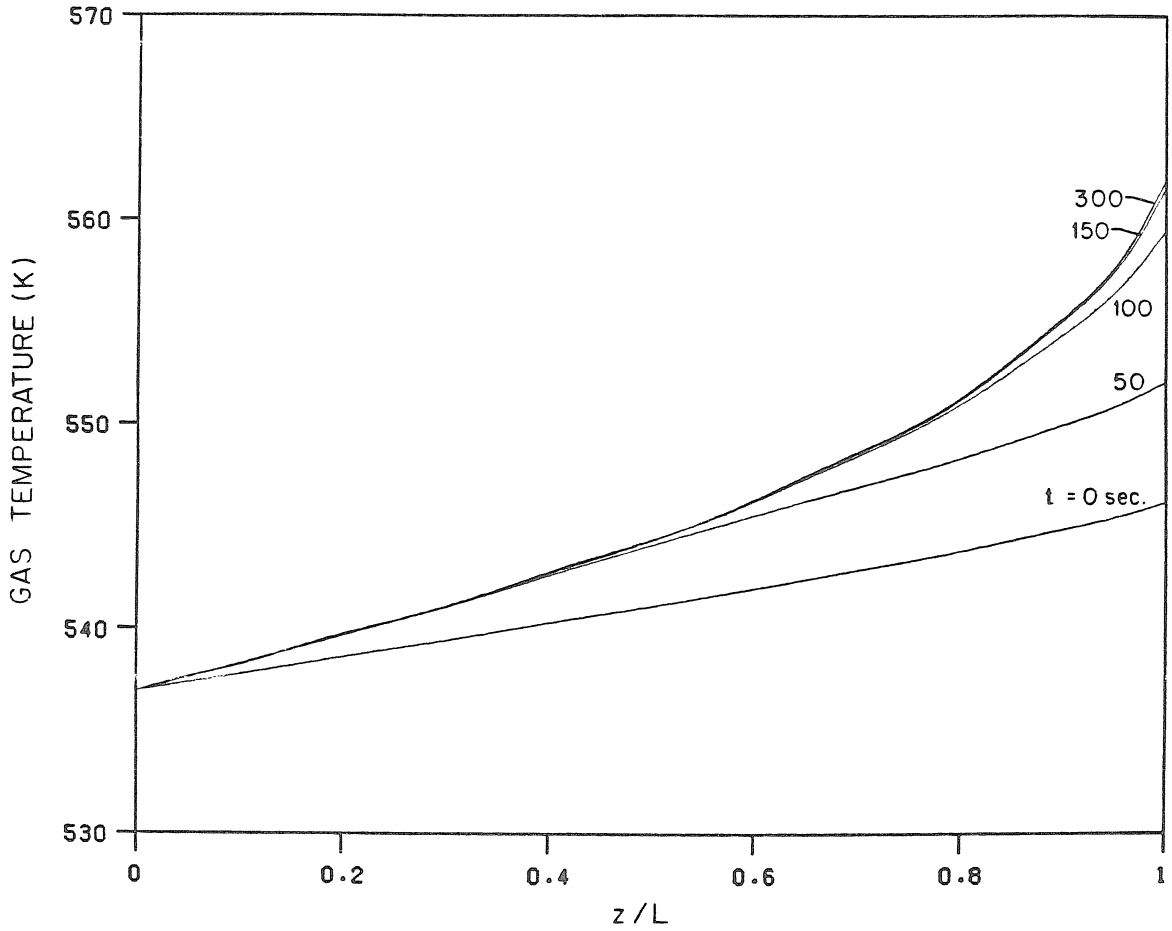

Figure 5 Open-loop time evolution of the gas temperature profile following a −25% step-change in the inlet CO concentration (nonlinear model).

tage can be obtained from the use of extra temperature measurements in early portions of the bed for the purpose of informing the control system that a disturbance is coming towards the reactor end.

For disturbances larger than that in Figs. 4-5 the reactor "jumps" to steady states of complete conversion. Fig. 6 shows the CO concentration profiles following a decrease of 50 % in its inlet concentration. As shown, the front first moves along the reactor, leaving it in 1.4 sec., after which the reaction starts accelerating. At just 45 sec., the reaction runs to complete conversion at the reactor exit. After this, although not shown, the point of complete conversion (and therefore the hot spot) moves towards the reactor inlet. It is clear then that the reactor exit is the first point at which the reactor runaway may be sensed, and therefore the reactor outlet temperature is the most logical measurement to select. In the actual experimental system shown in Fig. 1, temperature measurements are possible at different points along a central axial thermal well; even when selecting the reactor outlet temperature as the measured variable, these extra measurements can be utilized for the prevention of any unexpected (unmodeled) problems. The moving concentration front corresponding to $t < 1.4$ sec. shown in Fig. 6 is actually a step; the smoother curve obtained is a result of the orthogonal collocation procedure employed.

The relative convenience of each manipulated variable is now investigated. T_w, the reactor wall temperature, is discarded because of the small range over which it can be changed and the large time-constant of the actual process of changing the reactor wall temperature in the system. The remaining two variables are the gas temperature at the reactor inlet T_{in}, actually set by means of an electrical preheater and a bypass stream, and the total molar flow rate to the system F_P.

Let us first consider T_{in} as the manipulated variable, and let p(s) be the transfer function between T_{in} and T_{out}. This system has a relatively large steady-state gain. This is desirable from resilience considerations (Morari, 1983a). However, there is

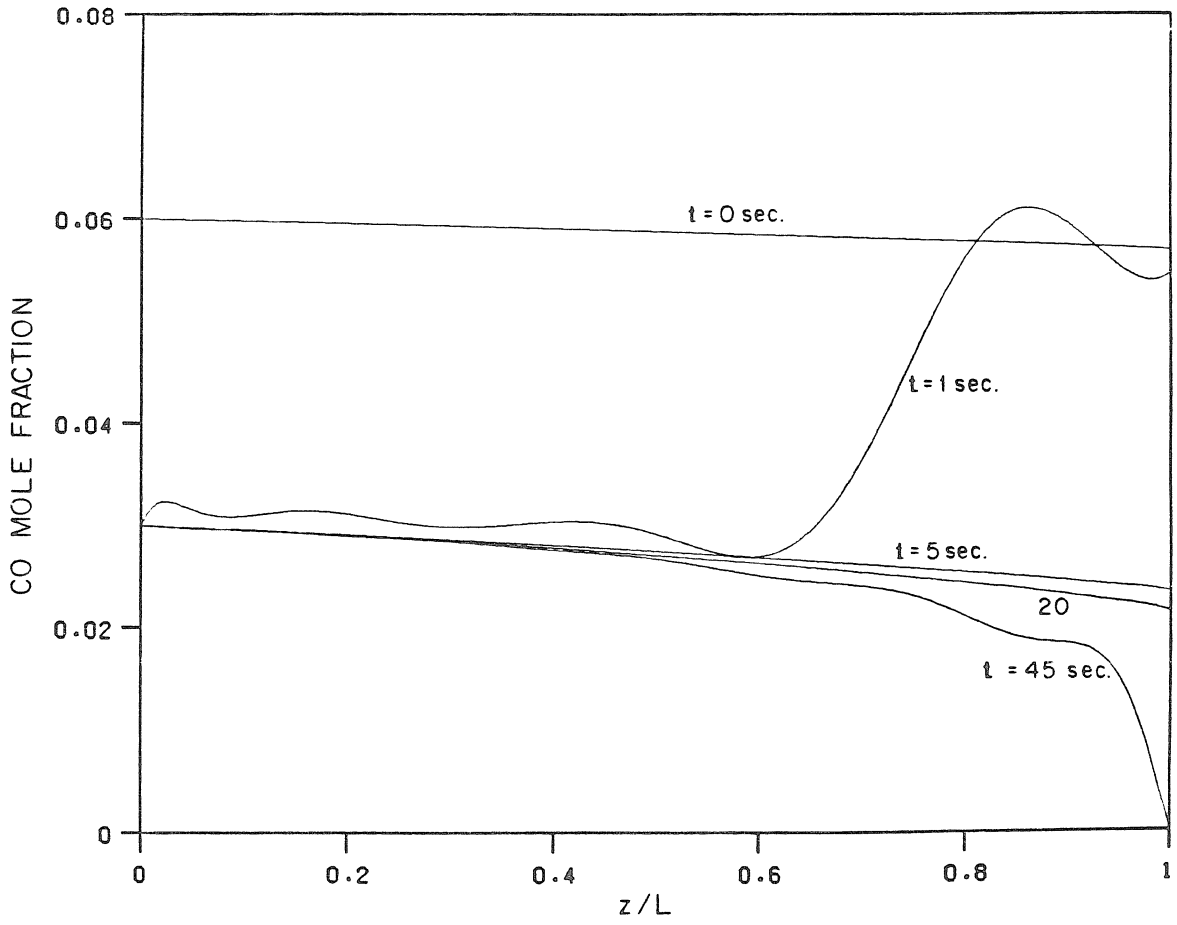

Figure 6 Open-loop time evolution of the CO concentration profile following a -50% step-change in the inlet CO concentration (nonlinear model).

a fundamental limitation to the achievable control quality for this system, resulting from the fact that the thermal wave is much slower than the concentration wave. For an infinite value of the heat transfer coefficient between the solid phase and the gas phase and zero axial dispersion, the ratio r between the speeds of the concentration wave and the thermal wave is given by $r = 1 + (1/B)$ where B is the ratio between the heat capacities of the gas phase and the solid phase (Friedly, 1972); r is 61 for our system. Actually, the thermal-wave speed is somewhat higher than 1/61 times the speed of the concentration wave because the heat transfer coefficient, although high, is finite. Still, while it takes about 1.4 sec for a concentration disturbance to arrive at the reactor end, it takes about 60 sec. for a temperature front resulting from a change in T_{in} to reach the exit; i.e., for our system the concentration wave is 43 times faster than the thermal wave. This is clearly seen in Fig. 7, where the response of T_{out} to a step-change in T_{in} is plotted. Then, assume that the inlet CO concentration suddenly decreases. After 1.4 secs., the temperature at the reactor exit starts increasing, and the control system changes T_{in}. Even if T_{in} is driven immediately to its desired value, the corrective action will arrive at the reactor end only after 60 sec.. (In fact, no control scheme would be able, *for this control configuration* , to prevent the reactor runaway if, as in the example of Fig. 6, the disturbance were such as to cause a runaway in 45 sec. at the reactor exit, because it takes 60 sec. for the correcting temperature wave to reach it.)

The observed dead-time-like response manifests itself, in our orthogonal collocation-based ODE model, through right-half-plane zeros of p(s). RHP zeros, as well as dead-time, impose, as noted, fundamental limitations on the achievable closed-loop performance, or in other words, on the dynamic resilience of the process (Holt and Morari, 1985). In our case it is found that, if z_i is the location of the ith RHP zero, $\sum_i (\frac{1}{|z_i|})$ roughly approximates the time-delay observed in the simulation. The pair of RHP zeros closest to the origin occurs at 0.114 rad/sec.

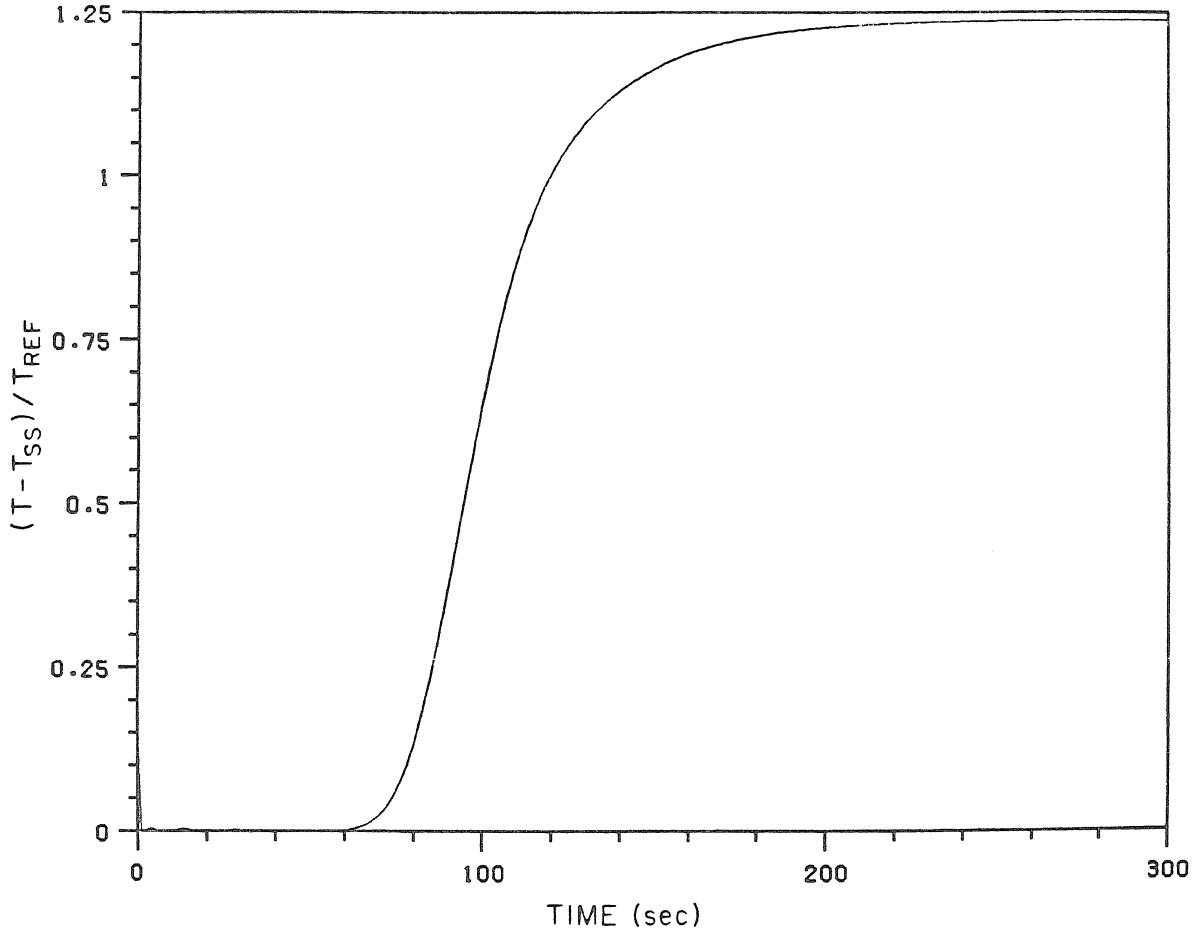

Figure 7 Open-loop outlet temperature response to a unit step-change in the inlet temperature. (T_{SS} = 546 K; T_{REF} = 40 K; Linearized Model).

Although the location of the RHP zeros can be shifted away from the imaginary axis (and their detrimental effect reduced) by changes in the set of operating conditions chosen, it is assumed for this paper that the operating conditions are fixed; then one can attempt to deal with these system-inherent limitations only by changes in the control configuration. Since no improvement can be obtained (for the type of disturbances considered) from the use of extra measurements, the only alternative to improve the response is the use of different manipulated variables.

Let us then consider the total molar flow rate F_P as a manipulated variable. Changes in F_P affect simultaneously all points in the reactor, and no RHP zeros are found for the transfer function between F_P and T_{out}. However, this transfer function has a small steady-state gain, which implies that large values of F_P would be required to compensate for a sustained concentration disturbance. This might not be implementable because of equipment constraints. More importantly, in actual operation of a reactor, the total flow rate is frequently fixed by the process requirements, and therefore it cannot be moved away from its nominal value for long periods of time. Let us assume first that this were not the case. To address the problem of the low steady-state gain for F_P one can take advantage of the best properties of T_{in} and F_P, namely, the large steady-state gain for T_{in} and the large initial effect of F_P, and use both manipulated variables in a coordinated way for the regulation of T_{out}. Formulated in this way the system is non-square, with 2 inputs and 1 output. Non-square systems generically do not have any transmission zeros (Holt and Morari, 1985), which means that the fundamental limitations on the performance can be alleviated by the use of two manipulated variables to satisfy *one* objective.

For the case in which F_P is fixed by the process, maintaining F_P around its nominal value becomes a second control objective. Thus, the system is actually MIMO, with the triangular structure shown in Fig. 8. F_P is considered both as an input to

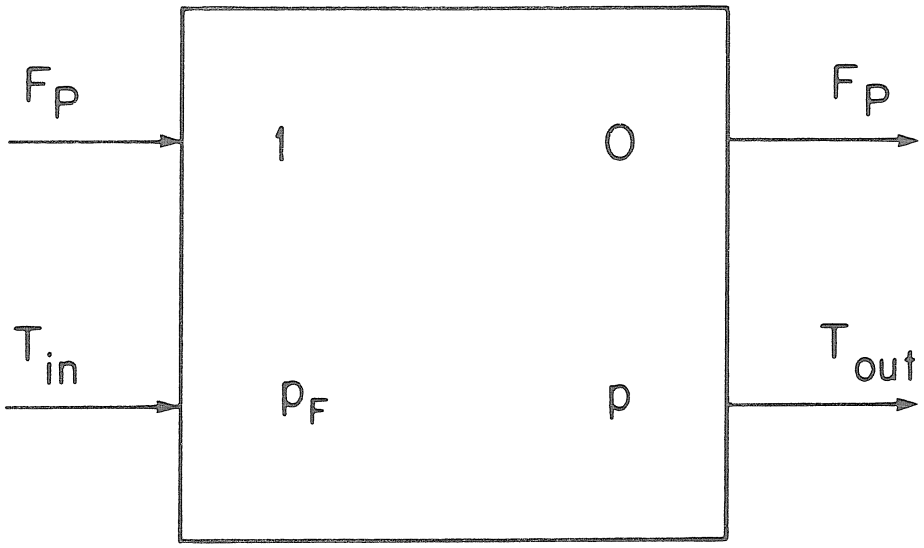

Figure 8 System transfer matrix P when F_P is considered both as an input to and an output from the process.

and an output from the process. A similar setting was suggested previously in the context of a different system configuration (Mandler *et al.*, 1984). The zeros of the transfer matrix P are the same as the zeros of the transfer function p between T_{in} and T_{out}. This means that, because of the fixed zero element, the fundamental limitation imposed by the RHP zeros has not been removed; however, the performance in terms of T_{out} *can* actually be improved, although at the expense of having to move F_P away from its nominal value *for a while* . If this is acceptable, then the MIMO configuration is appropriate; otherwise the only appropriate configuration for the single-pass reactor is the SISO one employing T_{in} as the manipulated variable. A detailed account of the controller design for the SISO case is presented in the remainder of the paper. The design of the control laws for the MIMO configuration presented above will be addressed in a subsequent paper.

4. CONTROLLER DESIGN; SISO CASE – THEORY

A systematic approach to the design of optimal and near-optimal controllers involves:

1. A system characterization step, in which a mathematical abstraction of the problem is obtained, which includes:
   a. the performance specifications;
   b. a characterization of the system inputs;
   c. the model to be employed for the design together with a characterization of the model uncertainty.
2. A selection of analysis and synthesis tools appropriate to the particular mathematical abstraction obtained in step 1.
3. The application of the tools obtained in step 2 to the design of the control laws.

Important recent advances in control theory have resulted in the development of new analysis and synthesis tools. Section 4 provides a detailed summary of the theory behind these new techniques, concentrating on the single-input single-output case. Several of the new techniques are later applied in Section 5 to our particular case-study. The treatment closely follows the guidelines of the approach stated above.

4.1 H_2– and H_∞– Optimal Control

The closed-loop system in Fig. 9a can be described by the input-output relationship

$$e(s) = \epsilon(s)\, v(s) \quad , \tag{3}$$

(Fig. 9b), where v=r-d , e=r-y , and where the sensitivity function $\epsilon(s)$, an important indicator of feedback controller performance, is given by

$$\epsilon(s) = \frac{1}{1 + p(s)\, c(s)} \quad . \tag{4}$$

The "set-point tracking" (or servo) problem (d=0) and the disturbance rejection problem (r=0) follow as special cases.

In Section 4.1 we assume that the plant p is accurately described by a model $\tilde{p}$; i.e., $p = \tilde{p}$. The sensitivity function *on the basis of a model* is defined in general, and for later use, as

$$\tilde{\epsilon}\,(s) = \frac{1}{1 + \tilde{p}(s)\, c(s)} \quad . \tag{5}$$

In this case of a perfect model, $\tilde{\epsilon}$ equals the sensitivity function $\epsilon = \frac{r-y}{r-d}$.

The objective of the control system in all cases is to make the error e small

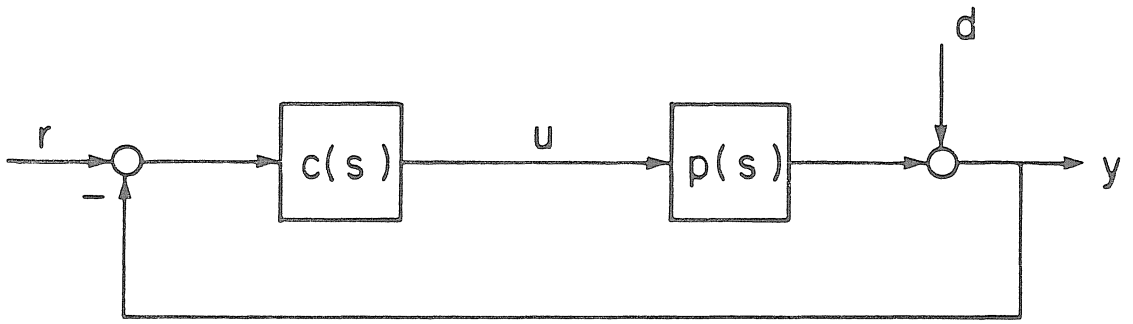

(a)

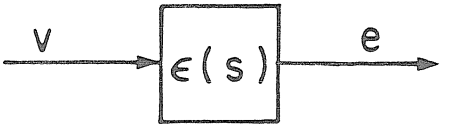

(b)

Figure 9 General feedback problem.

and ideally zero for all times. Performance specifications are therefore given in terms of some norm of e, and the optimal controller depends on the particular norm selected. A convenient norm is the 2-norm, equal to the square root of the integral square error (ISE):[3]

$$\|e\|_2 = \left(\int_0^\infty e(t)^2 dt \right)^{\frac{1}{2}} = \left(\frac{1}{\pi} \int_0^\infty |e(j\omega)|^2 d\omega \right)^{\frac{1}{2}} \quad . \tag{6}$$

The 2-norm of the error or equivalently the ISE will be employed throughout the rest of this paper as the basis for the performance specifications.

As the next step the inputs for which the error is to be made small have to be characterized. Two cases are considered here:

A. specific signals;

B. signals belonging to an equivalence class (i.e., a "family" of signals).

Each case gives rise to a different optimization problem.

In the case where performance is specified in terms of the 2-norm and the inputs are specific signals (case A), the Linear Quadratic (H_2-) optimization problem results. For several decades this was the only optimal control problem for which an effective solution technique was available. In this formulation the controller c(s) is determined such that the 2-norm of the error is minimized for one specific input change. As examples, the optimal tracking of step changes in the set-point might be desired, or the rejection of disturbances described by a step-change going through a first-order lag.

The performance objectives expressed in terms of the error can be translated into requirements on the sensitivity function $\tilde{\epsilon}$. In case A one can simply substitute Eq. (3) into Eq. (6) with v being the known input (r-d):

---

3. Other norms may be more appropriate for some problems. The 2-norm is mathematically convenient (Doyle, 1985).

$$\|e\|_2 = \|\tilde{\epsilon}\ v\|_2 = \left(\frac{1}{\pi} \int_0^{\infty} |\tilde{\epsilon}\ (j\omega)\ (r-d)(j\omega)|^2 d\omega \right)^{\frac{1}{2}} \quad . \tag{7}$$

For the case of a specific input signal, the optimal controller minimizes the 2-norm of the sensitivity function weighted by the inputs. Clearly, it is desirable to keep $\tilde{\epsilon}$ small over as wide a frequency range as possible.

For disturbance rejection problems where the disturbances are not known very well or vary unpredictably with time, assumption B for the inputs may be more appropriate. One example is to assume that the disturbances d, although themselves unknown, are known to belong to the class of all possible square-integrable (L_2) functions v' with bounded norm $\|v'(t)\|_2 \leq 1$, and weighted by appropriate frequency-dependent weights w_i; i.e., $d = w_i v'$. The weights are important to define the particular subset of L_2 to which the inputs belong (Doyle, 1984). For this family of L_2-signals, an appropriate performance objective is to minimize the 2-norm of the *largest* weighted error $e' = \frac{1}{w_o}\ e$ resulting from the disturbances. The output weights $\frac{1}{w_o}$ are specified in accordance with the performance objectives and such as to write the performance specifications as

$$\|e'(t)\|_2 \leq 1 \quad . \tag{8}$$

The optimal controller for case B minimizes

$$\sup_{\|v'\|_2 \leq 1} \|e'(t)\|_2 \quad . \tag{9}$$

The expression in Eq. (9) corresponds exactly to the definition of the operator norm induced by the 2-norm on input/output time functions (Doyle, 1984, Desoer and Vidyasagar, 1975); i.e., in this case:

$$\sup_{\|v'\|_2 \le 1} \|e'(t)\|_2 = \sup_{\|v'\|_2 \le 1} \|\frac{1}{w_o}\, \tilde{\epsilon}\,(\tilde{p},c)\, w_i\, v'(t)\|_2 \triangleq \|\frac{1}{w_o}\, \tilde{\epsilon}\,(\tilde{p},c)\, w_i\|_{i2} \ . \qquad (10)$$

It can be shown that the operator norm induced by the 2-norm equals the so-called ∞-norm of the corresponding transfer function (Desoer and Vidyasagar, 1975). For the SISO case, and in terms of the weighted sensitivity function:

$$\|\frac{1}{w_o}\, \tilde{\epsilon}\,(\tilde{p},c)\, w_i\|_{i2} = \sup_{\omega} |\tilde{\epsilon}\,(j\omega)\, w(j\omega)| \triangleq \|\tilde{\epsilon}\,(j\omega)\, w(j\omega)\|_\infty \ , \qquad (11)$$

where $w = w_i/w_o$. Therefore, the performance specification (8) will be met if and only if

$$\|\tilde{\epsilon}\,(j\omega)\, w(j\omega)\|_\infty \le 1 \ . \qquad (12)$$

Condition (12) is the basic analysis test for the performance of the nominal plant in this formulation. The controller design objective is

$$\min_c \|\tilde{\epsilon}\,(j\omega)\, w(j\omega)\|_\infty = \min_c \sup_{\omega} |\tilde{\epsilon}\ w\,(j\omega)| \ , \qquad (13)$$

namely, the minimization of the ∞-norm of the sensitivity function $\tilde{\epsilon}$ weighted by w, and to make it at least less than unity. This is a so-called "H_∞-optimization problem." The H_∞-Optimal Control formulation emerged in the 1970s. In addition to addressing specifically the case in which the input signals are not exactly known, this new formalism serves as the basis for the treatment of the robust controller design problem in a consistent framework.

4.2 Robust Controller Design

In the discussion so far it has been assumed that the plant is perfectly described by a linear time-invariant model. The fact that a model is never a perfect representation of the actual plant complicates the picture considerably. It is essential that our knowledge about the model uncertainty be incorporated into the con-

troller design procedure in order for the controllers to succeed in the real world. To account for model uncertainty we assume that the dynamic behavior of a plant is described not by a single linear time-invariant model but by a family Π of linear time-invariant models. We refer to this "set of possible plants" as the "uncertainty set." This is a somewhat primitive uncertainty description, especially when the effect of nonlinearities is to be captured, but it is the only feasible approach at present.

Model uncertainty brings about several important problems. The essential issue is to guarantee stability in the face of plant/model mismatch, i.e., that the closed-loop system be stable for *all* plants in the uncertainty set ("robust stability"). A second issue is to guarantee certain performance specifications for all plants in Π ("robust performance"). A third issue is to design the best controller for the set of possible plants, namely, to design for optimal robust performance. The particular analysis and synthesis techniques to be employed in addressing these issues depend on the assumptions on the model uncertainty.

Characterization of Model Uncertainty. Throughout this paper the uncertainty set Π will be defined on the basis of the so-called multiplicative uncertainty description: the regions in the Nyquist plane within which the true plant lies are approximated at each frequency by disks centered at a "nominal" plant $\tilde{p}(j\omega)$ and with frequency-dependent radius $|\tilde{p}(j\omega)|\bar{l}_m(\omega)$; i.e.,

$$\Pi = \left\{ p: \frac{|p(j\omega) - \tilde{p}(j\omega)|}{|\tilde{p}(j\omega)|} < \bar{l}_m(\omega) \right\} \quad . \tag{14}$$

Thus any member of the family Π satisfies

$$p(j\omega) = \tilde{p}(j\omega)\,(1 + l_m(j\omega)) \tag{15}$$

with

$$|l_m(j\omega)| < \bar{l}_m(\omega) \quad . \tag{16}$$

Clearly, $\bar{l}_m(\omega)$ is an upper bound on the multiplicative uncertainty and is the type of information sought in the uncertainty characterization process. This type of uncertainty description may in cases be somewhat conservative, as smaller regions with shapes other than disks may be enough to include all possible plants. However, regions of a more general shape have complex mathematical descriptions and are very difficult to deal with in the context of control system design. A general discussion of alternate ways to characterize uncertainty and the techniques for dealing with them is beyond the scope of this paper.

Robust Stability. We now present analysis techniques appropriate to the uncertainty description (14), starting with the robust stability conditions. First, we define the complementary sensitivity function based on the nominal plant as

$$\tilde{\eta} = 1 - \tilde{\epsilon} \quad . \tag{17}$$

Clearly,

$$\tilde{\eta} = 1 - \frac{1}{1+\tilde{p}(s)c(s)} = \frac{\tilde{p}(s)c(s)}{1+\tilde{p}(s)c(s)} \quad . \tag{18}$$

For the case of a perfect model, $\tilde{\eta}$ equals the closed-loop transfer function between the reference r and the output y, which for good control should be made as close to unity as possible. $\tilde{\eta}$ is important for the analysis of robust stability.

For the family of plants defined by Eq. (14), the following is required for robust stability (Doyle and Stein, 1981): given that p, $\tilde{p}$ and c have no poles in the open right-half plane, and given that the closed-loop system with the nominal plant $\tilde{p}$ and the controller c is stable, then the closed-loop system is stable for all plants in the family Π defined by Eq. (14) if and only if

$$\|\tilde{\eta}\ \bar{l}_m\|_\infty \triangleq \sup_\omega |\tilde{\eta}\ \bar{l}_m(\omega)| \leq 1 \quad . \tag{19}$$

Robust stability imposes a bound on the ∞- norm of the complementary sensitivity function $\tilde{\eta}$ weighted by $\bar{l}_m$. This provides a further justification for the use of the ∞-norm.

We note that, in the H_∞-Optimal Control framework, we want to minimize $\|\tilde{\epsilon}\ w\|_\infty$ for performance (see Eq. (13)) and $\|\tilde{\eta}\ \bar{l}_m\|_\infty$ for robustness. A trade-off between performance and robustness arises from the fact that $\tilde{\epsilon}$ and $\tilde{\eta}$ are not independent (see Eq. (17)), and making one small automatically makes the other large. This problem is inherent in feedback control and cannot be removed by clever controller design.

Robust Performance – The Structured Singular Value Analysis and Synthesis Techniques. In the H_∞-framework, as seen, both uncertain inputs and uncertain plants can be handled with the same analysis tool. It should be noted, however, that the analysis based on the ∞-norm provides necessary and sufficient conditions only when uncertain inputs and uncertain plants are considered individually but not for both together. The ∞-norm can be used to test robust stability and separately to analyze the performance of the nominal plant.

Robust stability is the minimum requirement a control system has to satisfy to be useful in an environment where model uncertainty is important. However, robust stability alone is not enough. Even if Eq. (19) is satisfied for the set Π, there may be plants $p \epsilon \Pi$ for which the performance is arbitrarily poor in relation to the specifications. Thus, it is also important to guarantee robust performance, namely, that the performance specifications be met for all plants in the set Π.[4] If the performance specifications are stated in the H_∞-framework, then, for robust

4. Robust stability can be viewed as a special case of robust performance in which the performance specifications are just stated (in the framework presented here) as the requirement that $\|e\|_2 < \infty \quad \forall\ p \epsilon \Pi$.

performance, condition (12) has to be met for the worst plant; i.e.,

$$\underset{p\epsilon\Pi}{\text{Max}} \; \|\epsilon \; w\|_\infty \leq 1 \tag{20}$$

or

$$\|\epsilon \; w\|_\infty \leq 1 \quad \forall \; p\epsilon\Pi \quad . \tag{21}$$

Necessary and sufficient conditions for guaranteeing robustness of stability and of performance have been derived recently by Doyle (1984). Doyle's analysis theorem is based on a new function called the structured singular value (μ) (Doyle, 1982). The theorem applies to assumption B of Section 4.1 for the inputs and holds for uncertainty described as disks in the complex plane, therefore holding for Eq. (14). The mathematical details will be avoided, and only a SISO disturbance rejection problem will be considered.

Doyle's theorem states that, given nominal stability, the closed-loop system is stable *for all plants* in the uncertainty set Π *and*

$$\|e'\|_2 \leq 1 \quad \forall \quad \|v'\|_2 \leq 1$$

if and only if

$$\sup_\omega \mu(P(j\omega)) \leq 1 \quad . \tag{22}$$

$\mu(P)$ is called the structured singular value of P. $\mu(P)$ for our case of a SISO disturbance rejection problem can be shown (Doyle, 1985) to be given by:

$$\mu(P) = |\tilde{\eta} \; \bar{T}_m| + |\tilde{\epsilon} \; w| \tag{23}$$

and therefore for robustness of stability and performance

$$|\tilde{\eta}\ \bar{T}_m| + |\tilde{\epsilon}\ w| \leq 1 \quad \forall\, \omega\ , \tag{24}$$

where w is in this case related to the type and size of disturbances the control system is expected to reject.

Clearly, robust performance (24) implies robust stability (19) and nominal performance (12). Condition (24) reflects the fundamental trade-off in feedback control mentioned above; the interdependence between $\tilde{\epsilon}$ and $\tilde{\eta}$ makes it a challenge to meet this condition. It may occur that, for some fixed $\bar{T}_m$ and w, the condition is not met by any value of $\tilde{\epsilon}$ and $\tilde{\eta}$. In this case the only way to satisfy condition (24) and guarantee that all plants in Π meet the performance specifications is to improve the knowledge about the system (by reducing $\bar{T}_m$), or to relax the performance specifications (by reducing w).

So far we have discussed analysis tools. The synthesis of an optimal controller for the case of plant/model mismatch is a complicated problem, and it involves finding the controller that optimizes the worst performance for the set Π, namely, the controller that optimizes robust performance. If the same assumptions hold as for the μ-analysis theorem, clearly from condition (22) the problem involves finding the controller that solves

$$\underset{C}{\text{Min}}\ \sup_{\omega}\ \mu(P(j\omega))\ . \tag{25}$$

Doyle proposed (25) as the basis of a synthesis method for optimal robust performance and also proposed a first solution strategy (Doyle, 1984). Unfortunately, this problem is a very complex one to solve; computational difficulties exist, and finding an efficient numerical technique for the solution of (25) is still a subject of active research. For the SISO disturbance rejection problem, (25) can be written as

$$\underset{c}{\text{Min}} \ \underset{\omega}{\sup} \ (|\tilde{\eta}\ \bar{I}_m| + |\tilde{\epsilon}\ w|) \ . \tag{26}$$

Clearly, the optimal controller in this case reaches the best compromise between the conflicting objectives of performance and robustness.

Doyle's μ-synthesis method is essentially the only one that has been proposed for solving the optimal robust performance problem. Although solving this problem is desirable, resorting to a near-optimal technique for robust controller synthesis is more appropriate at this stage of the theoretical developments. In Section 4.3 the IMC design technique is summarized. IMC yields near-optimal controllers in the face of plant/model mismatch. The IMC design technique is simple and systematic in itself and fits perfectly within the lines of an overall systematic approach.

4.3 The IMC Design Technique

The Internal Model Control structure (Fig. 10) was introduced by Garcia and Morari (1982), although a similar concept has been used previously and independently by a number of other researchers. Through its use, a clear insight can be gained on the fundamental limitations to control performance, and the robustness issue can be addressed in a direct manner.

The IMC design procedure consists of two steps:

1. H_2-optimal design of the controller $\tilde{q}$ for the nominal plant $\tilde{p}$ and the specific input under consideration.

2. Adjustment of the ideal controller $\tilde{q}$ found in step 1 to account for constraints on the manipulated variables and to guarantee robust stability and performance. (The controller is not designed for *optimal* robust performance, but results in near-optimal performance.)

The particular controller obtained via IMC depends on:

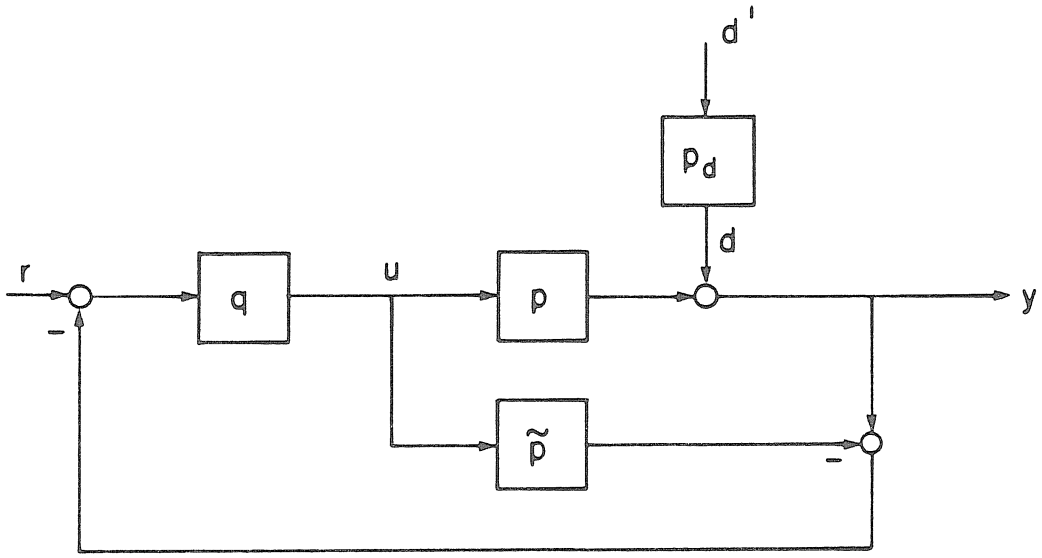

Figure 10 The IMC structure.

a. the performance specifications;

b. the input signal;

c. the model uncertainty.

Step 1 is addressed first. Referring to Fig. 10, if the model $\tilde{p}$ is perfect ($p = \tilde{p}$), then

$$e = r-y = (1 - \tilde{p}\tilde{q})(r-d) \tag{27}$$

$$u = \tilde{q}\,(r-d) \quad .$$

The requirement for internal stability is that the controller $\tilde{q}$ and the plant $\tilde{p}$ be stable.

For SISO systems $\tilde{q}$ is generally chosen such that it is H_2-optimal for the particular input (r-d). Thus, $\tilde{q}$ has to solve

$$\underset{\tilde{q}}{\text{Min}} \|e\|_2 = \underset{\tilde{q}}{\text{Min}} \|(1 - \tilde{p}\tilde{q})(r-d)\|_2 \quad , \tag{28}$$

subject to the constraint that $\tilde{q}$ be stable and causal. The absolute minimum (zero) is reached for

$$\tilde{q} = \frac{1}{\tilde{p}} \quad . \tag{29}$$

However, the model inverse is an acceptable solution only for minimum-phase (MP) systems. In this case perfect control is achieved (i.e., $y(t) = r(t)$ for all $t > 0$ and all $d(t)$). For non-minimum phase systems (NMP), the exact inverse (29) is unstable and/or noncausal. The objective function cannot be made zero, and an "approximate inverse" of $\tilde{p}$ has to be found such that the weighted 2-norm of the sensitivity function is minimized. For NMP systems the optimal solution depends on the weight (the input (r-d)), while for MP systems the controller given by Eq. (29) is

optimal independent of the weight. NMP elements clearly impose a fundamental limitation to the closed-loop performance, as perfect control cannot be achieved in their presence even with perfect models.

The model $\tilde{p}$ is factored into an all-pass part $\tilde{p}_A$ and a minimum-phase part $\tilde{p}_M$

$$\tilde{p} = \tilde{p}_A \, \tilde{p}_M \quad . \tag{30}$$

For the case of RHP zeros at $s=z_i$, $\tilde{p}_A$ selected as

$$\tilde{p}_A = \prod_i \frac{-s + z_i}{s + z_i} \tag{31}$$

and

$$\tilde{q} = \frac{1}{\tilde{p}_M} \tag{32}$$

solve the optimization problem (28) for *step inputs* in r and d. The sensitivity function in this case is given by

$$\tilde{\epsilon} \;=\; 1 - \tilde{p}_A \;=\; 1 - \prod_i \frac{-s + z_i}{s + z_i} \quad . \tag{33}$$

The limitation on performance imposed by the RHP zeros is clearly reflected in Eq. (33): $\tilde{\epsilon}$ is fixed by $\tilde{p}_A$.

If the input is of the form $\frac{1}{s(\tau_d s+1)}$, i.e., a step followed by a first-order lag, the optimal controller is instead

$$\tilde{q} = \frac{1}{\tilde{p}_M} \left[1 + \left(1 - \tilde{p}_A^{-1} \Big|_{s=-\frac{1}{\tau_d}} \right) \tau_d s)\right] \quad , \tag{34}$$

where $\tilde{p}_A(s)$ and $\tilde{p}_M(s)$ are again given by Eqs (30) and (31). We can write Eq. (34) as

$$\tilde{q} = \frac{\tau_d s \alpha + 1}{\tilde{p}_M} \tag{35}$$

$$\alpha = \left(1 - \tilde{p}_A^{-1} \Big|_{s=-\frac{1}{\tau_d}} \right) .$$

Controller (35) is like controller (32) but is augmented by an extra lead element.

A general and fairly simple analytic procedure for solving the H_2-optimization problem (28) for the case of stable systems was proposed by Newton *et al.* (1957).

Step 2 is now considered. For the IMC structure $\tilde{\epsilon}$ and $\tilde{\eta}$, the sensitivity and complementary sensitivity functions on the basis of the nominal plant, are

$$\tilde{\epsilon} = 1 - \tilde{p}q \tag{36}$$

$$\tilde{\eta} = \tilde{p}q ,$$

where, in general, $q \neq \tilde{q}$. As before, $\tilde{\epsilon}$ equals the sensitivity function $\epsilon = \frac{r-y}{r-d}$ only in the case of a perfect model.

For robustness, $\tilde{q}$ found in step 1 is augmented by a low-pass filter f:

$$q = \tilde{q}f . \tag{37}$$

In principle, both the structure and the parameters of f should be determined such that an optimal compromise between performance and robustness is reached. To simplify the design task, the filter structure is fixed, and a search is made over a small number of filter parameters (usually just one) to obtain desired robustness characteristics. Because of this simple filter structure, the resulting controller is, as said, nearly although not strictly optimal in the face of model uncertainty.

The filter f is always chosen such that the closed-loop system retains its asymptotic tracking properties (system type (Wiberg, 1971)). It can be shown

that the optimal controllers (32) and (35) are type 1. Therefore, the filter has to satisfy

$$\lim_{s\to 0} p\tilde{q}f = \lim_{s\to 0} p\tilde{q} \tag{38}$$

or

$$f(0) = 1 \ . \tag{39}$$

A typical filter satisfying condition (39) is the one-parameter filter

$$f(s) = \frac{1}{(\lambda s + 1)^n} \ . \tag{40}$$

Here λ is the adjustable filter parameter and n is selected large enough to guarantee a proper q. This is required because, for an improper controller, infinitely small high-frequency disturbances would give rise to infinitely large excursions of the manipulated variables, which are physically unrealizable.

The "filter time-constant" λ affects the speed of the closed-loop response. When $\lambda = 0$, the system response is H_2-optimal. In the case of a perfect model, how small λ can be is restricted only by the physical constraints on the manipulated variables.

In the face of model uncertainty the performance objective remains the same as in the case of a perfect model, but now the choice of the controller is constrained by the need to guarantee stability for all plants in the uncertainty set Π. Model uncertainty imposes another fundamental limitation to the achievable closed-loop performance. Referring again to Fig. 10, if the actual plant is not equal to the model ($p \neq \tilde{p}$), then

$$e = r - y = \left(1 - \frac{pq}{1 + (p-\tilde{p})q}\right)(r-d) \ , \tag{41}$$

and the stability of q and p is not sufficient for closed-loop stability. For *robust stability* it is necessary and sufficient that q be chosen such that $1 + (p-\tilde{p})q$ does

not encircle the origin as s traverses the Nyquist D contour for any plant p within the family Π of possible plants. This restricts the choice of q and therefore, even in the case where the system is minimum phase, perfect control cannot be achieved by the choice $q = \tilde{p}^{-1}$.

In order to obtain a controller q satisfying robust stability, appropriate values for the filter parameters have to be selected. This selection depends on the uncertainty description employed. As seen, for the multiplicative uncertainty description given by (14), the robust stability condition is (19). For IMC

$$\tilde{\eta} = \tilde{p}q = \tilde{p}\tilde{q}f \tag{42}$$

and condition (19) becomes

$$\sup_{\omega} |\tilde{p}\tilde{q}f\, \bar{l}_m(\omega)| \leq 1 \quad . \tag{43}$$

Therefore, the closed-loop system is robustly stable if and only if

$$|f| \leq \frac{1}{|\tilde{p}\tilde{q}\bar{l}_m|} \quad \forall\, \omega \ . \tag{44}$$

f can always be found such that (44) is satisfied. Condition (44) restricts the choice of f: the filter magnitude |f| has to be small wherever the plant/model mismatch is large. Clearly, |f| small implies $|\tilde{\eta}|$ small and thus poor performance. Generally $\bar{l}_m$ approaches or exceeds 1 for high frequencies. For a filter of the form given by (40), the filter time-constant λ is sufficiently *increased* until condition (44) is satisfied. This corresponds to decreasing the speed of response, namely, to a "detuning" of the controller.

For IMC the structured singular value condition (24) for robust performance becomes

$$|\tilde{p}\tilde{q}f\,\bar{l}_m| + |(1 - \tilde{p}\tilde{q}f)\,w| \leq 1 \quad \forall\,\omega\ . \tag{45}$$

In an IMC design procedure for robust performance, λ is selected to satisfy condition (45). As explained for the general case, depending on $\bar{l}_m$ and w there might be no λ for which (45) is satisfied. If condition (45) is not satisfied for any λ, then either the filter structure is too simplistic to meet the performance specifications, or the specifications are too tight for the uncertainty which is present.

4.4 Control Objective-Related Model Reduction

Although the analysis and synthesis techniques presented can be directly applied to linearized models of any order, the use of reduced-order models greatly facilitates the controller implementation and the computational tasks. As the goal of the model reduction is in this case control system design, the control objectives must be considered in the reduction process. In contrast to this, usual reduction methods are based on just obtaining a good "open-loop fit"; however, this fit by itself does not guarantee that a compensator q(s) designed on the basis of the reduced-order model will perform well when applied to the full-order model. Rivera and Morari (1985) have addressed this problem and developed frequency domain model reduction procedures that yield near-optimal models with respect to a user-designated closed-loop performance. These procedures result in reduced-order models that best approximate the full models in the frequency interval that is most relevant to the control problem. A short description of the method is presented here, and the reader is referred to Rivera and Morari (1985) for more details.

Let us assume, for simplicity, that the full-order model $\tilde{p}$ is an accurate description of the process without uncertainty. Refer now to Fig. 11, which is similar to Fig. 10, but in which $\tilde{p}$ represents the full model and $\hat{p}$ represents a reduced-order model, which is used to design the control system and which is to be determined. The IMC controller is defined in the context of this problem as

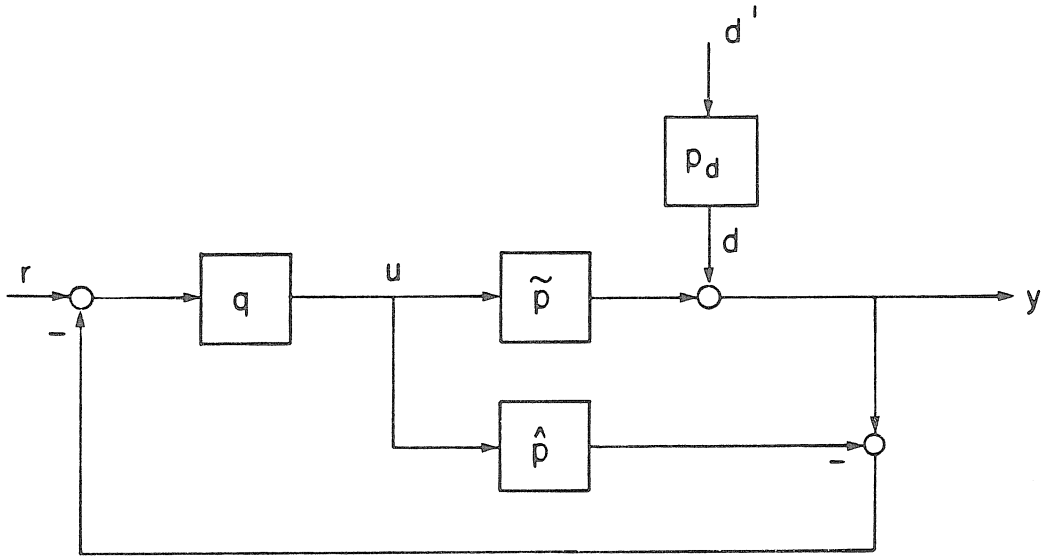

Figure 11 The model reduction problem.

$$q = \hat{p}^{-1}\hat{\eta} \ , \tag{46}$$

where $\hat{\eta}$ is the desired complementary sensitivity function. The choice of $\hat{\eta}$ determines indirectly the bandwidth over which the reduced-order model should approximate well the full model.

The closed-loop relationships for the system in Fig. 11 are

$$y = \frac{\hat{\eta}(1 + e_m)}{(1 + \hat{\eta}e_m)} (r - d) + d \tag{47}$$

$$e = r - y = \frac{(1 - \hat{\eta})}{(1 + \hat{\eta}e_m)} (r - d) \ , \tag{48}$$

where e_m is the multiplicative error

$$e_m = (\tilde{p} - \hat{p})/\hat{p} \tag{49}$$

between the full and reduced-order models. The error results in a degradation of the desired performance specified through $\hat{\eta}$.

The objective of the model reduction procedure is to determine the parameters of the reduced-order model such that this degradation in performance is minimized. Rigorously speaking, control-optimal model reduction would require selecting $\hat{p}$ such that the 2-norm or the ∞-norm of the error is minimized; this requires a complicated nonlinear programming solution and may not be feasible. Rivera and Morari (1985) have derived upper bounds on these norms which lead to simpler reduction objectives and require only the solution of linear regression problems. Through their analysis the problem is reformulated as the minimization of a weighted multiplicative error, where the weights incorporate the characteristics of the control problem. For example, for H_2-optimal control $\hat{p}$ has to solve

$$\underset{\hat{p}}{\text{Min}} \int_0^{\infty} (1+\omega^2)\, |1-\hat{\eta}|^4\, |r-d|^4\, |\hat{\eta}|^2\, |e_m|^2\, d\omega \quad . \tag{50}$$

The reduced-order models obtained by this method can, of course, be employed with any control design technique. On the other hand, since this model reduction procedure incorporates all the same considerations as the IMC design technique, reduced-order IMC controllers are automatically defined by the reduced-order models obtained (see Eq. (46)).

For the case where a reduced-order model $\hat{p}$ is employed for the design, it follows from Eq. (47) that for closed-loop stability in the nominal case, the Nyquist plot of $\hat{\eta} e_m$ should not encircle (-1,0). For robust stability the following condition, equivalent to (19), has to be, in addition, satisfied:

$$\left| \frac{\hat{\eta}(1 + e_m)}{1 + \hat{\eta} e_m} \right| < \frac{1}{\bar{l}_m} \qquad \forall\ \omega. \tag{51}$$

Finally, the robust performance condition (24) is:

$$\left| \frac{\hat{\eta}(1 + e_m)}{1 + \hat{\eta} e_m} \right| \bar{l}_m + \left| \frac{(1 - \hat{\eta})\, w}{1 + \hat{\eta} e_m} \right| \leq 1 \qquad \forall\ \omega \quad . \tag{52}$$

5. DESIGN OF SISO CONTROLLERS FOR THE REACTOR SYSTEM

5.1 Selection of Analysis and Synthesis Tools

The theory of Section 4 is now applied to the design of robust SISO controllers for the reactor system, with T_{in} as the manipulated variable and T_{out} as the controlled variable. The rejection of step disturbances in the inlet CO concentration (x_{CO}) is addressed. In this way we directly design for one of the worst possible types of disturbances. The performance specifications are in terms of the 2-norm of the error. Since in this case-study the inputs are specific signals, an H_2-optimal

design would be the most appropriate if the reactor model were perfect.

To represent the model uncertainty we will employ the multiplicative uncertainty description (Eqs (14)-(16)). Since reduced-order models will be employed in the design of the robust controllers, condition (51) is the one to be tested for robust stability.

For the analysis of robust performance we will apply Doyle's μ-analysis theorem to the case of a specific input signal by interpreting the weight w (Sections 4.1 and 4.2) as the inverse of the magnitude of the worst possible sensitivity function for the set of plants at each frequency. By doing so we will be able to obtain an exact (worst-case) bound for the performance in the face of model uncertainty, on the basis of our uncertainty description and for the specific input signal under consideration.

As a synthesis method for the case in which model uncertainty is important, one solving the optimal robust performance problem would be desirable. The μ-synthesis method addresses this problem; however, as said, efficient numerical techniques to implement it are yet to be found. This, combined with the difference in the input assumptions, makes the application of this method to the reactor system inappropriate at this stage. We select instead the IMC design technique, which yields near-optimal controllers in the face of plant/model mismatch, but which in the case of a perfect model yields the optimal controller for our particular performance specifications and input assumptions. Moreover, IMC allows us to address the robustness issues in a simple and explicit manner.

5.2 Nominal Design; Best Possible Closed-Loop Performance

For illustrative purposes we first present ideal closed-loop responses for the full (49th order) linearized model. In Section 5.3, robust IMC controllers based on reduced-order models will be obtained and applied to the nonlinear plant.

A comparison between two controllers is presented. By means of our example we address the question of how relevant it is to consider disturbance models in the control system design. "Controller 2" is designed assuming (incorrectly) that the disturbances are simply steps occurring at the plant output; "controller 1" is designed based on a more accurate disturbance model.

The input of interest in our system is $d = p_d d'$ where d' is x_{CO} and d is the effect of x_{CO} on the output T_{out}. The transfer function p_d (the disturbance model) is approximated quite well by a first-order lag, and therefore the input d is essentially of the form $\frac{1}{s(\tau_d s+1)}$ with $\tau_d \approx 58$sec.. The model $\tilde{p}$ has 12 RHP zeros for the selected nominal operating conditions. The optimal controller is then defined by Eq. (35).

The presence of the lead term in Eq. (35) results in high values of $|\tilde{\eta}| = |\tilde{p}q|$ for $\omega > \frac{1}{\tau_d \alpha}$. Therefore, controller 1 tends to give rise to robustness problems. If instead we neglect p_d and design for step inputs, we obtain a controller (given by Eq. (32)), whose performance is non-optimal for our actual input signal, but which is more robust since $|\tilde{\eta}|$ equals unity until rolled-off by a filter. Controller 1 is expected to require more "detuning" in order to guarantee robust stability.

Fig. 12 presents the nominal sensitivity functions for both controllers. Both controllers clearly have integral action, which is guaranteed automatically by the design procedure. Fig. 12 shows that the frequency range for which effective disturbance rejection is obtained (i.e., small $|\epsilon|$) is essentially limited by the RHP zeros in $\tilde{p}$, as can be expected from Eq. (33). For controller 2 the bandwidth ω_b, defined as the frequency at which $|\epsilon|$ first reaches $1/\sqrt{2}$, equals 0.0105 rad/sec. For a process with a pure delay $e^{-s\theta}$, Rivera *et al.* (1986) state, for the closed-loop bandwidth with controller 2, the exact expression,

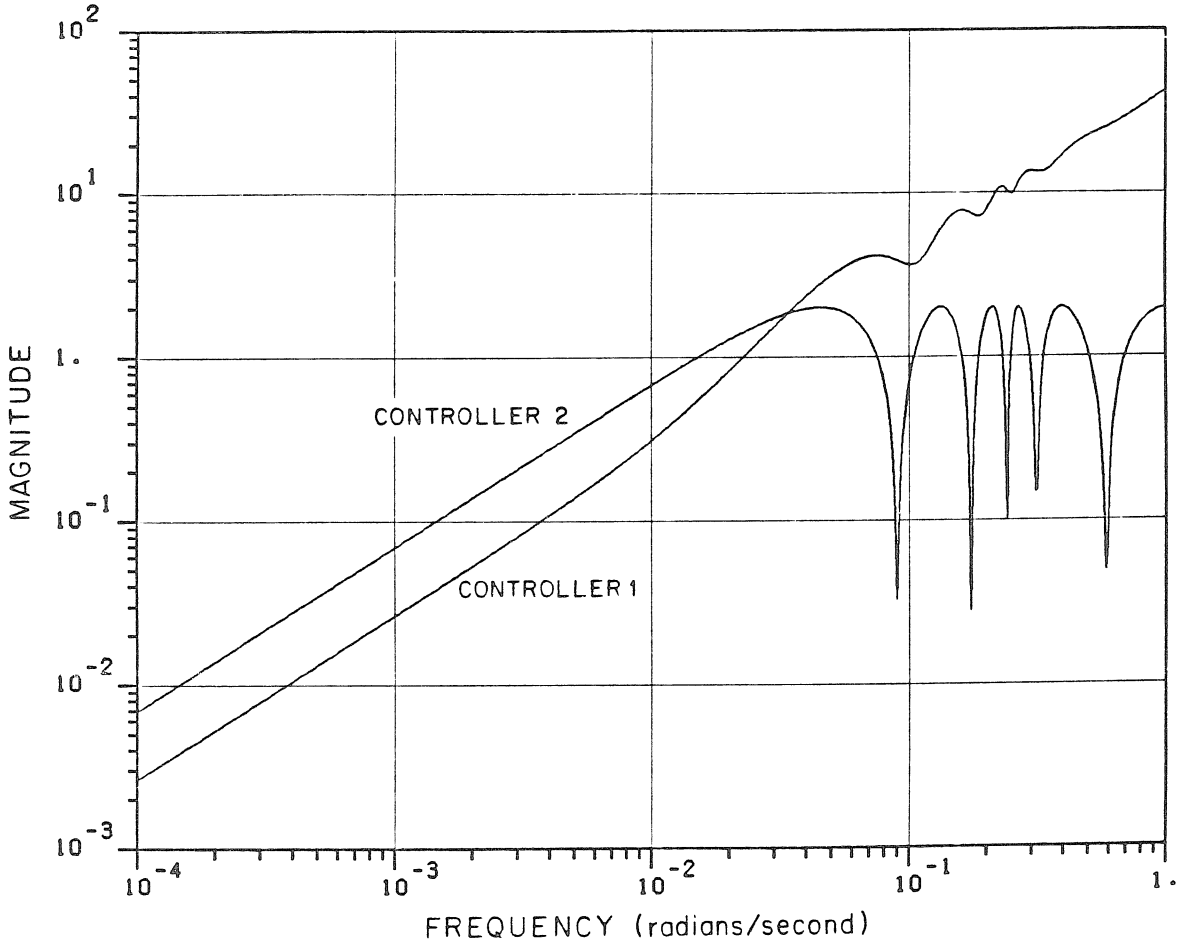

Figure 12 Sensitivity functions ($\tilde{\epsilon}$). Ideal closed-loop performance.

$$\omega_{b_D} = \frac{0.724}{\theta} \quad . \tag{53}$$

By substituting the value of θ observed in the simulation (60 sec.) in Eq. (53), the result is 0.012 rad/sec, which approximates quite closely the value obtained for ω_b. For the optimal controller 1, ω_b=0.018 rad/sec. The bandwidth decreases for increasing values of λ, but this effect is not felt until $1/\lambda$ is of an order of magnitude comparable to the RHP zeros.

Fig. 13 shows the open-loop response of T_{out} (based on the assumption that the full linearized model is a perfect model for the plant) to a step-change of −25% in x_{CO} and the closed-loop responses obtained employing each controller. For a unit step-change, $\|e\|_2 = 1.27$ for controller 1 and 1.95 for controller 2. Controller 1 is therefore significantly better than controller 2 ($\|e\|_2$ for controller 2 is 50% worse than for controller 1). The disturbance spectrum in this case falls within the bandwidth of the closed-loop system, and this results in a significant benefit from the use of optimal disturbance rejection in the nominal case. Of interest is to compare the performance of the two controllers *after* both are detuned to satisfy robust stability (condition (51)) to find out if the "optimal" controller 1 still results in significantly better performance. The two robust designs are compared in Section 5.3.

The solid line in Fig. 13, which corresponds to controller 1, is the best closed-loop response in terms of the 2-norm that can be obtained for this control configuration and disturbance. The small peaks appearing in the figure before the maximum at 60 sec. are not unexpected. They are a result of the amplification of the effect of the RHP zeros by the lead term. Moreover, they are devoid of physical meaning and come from the use of the orthogonal collocation to approximate the PDE model.

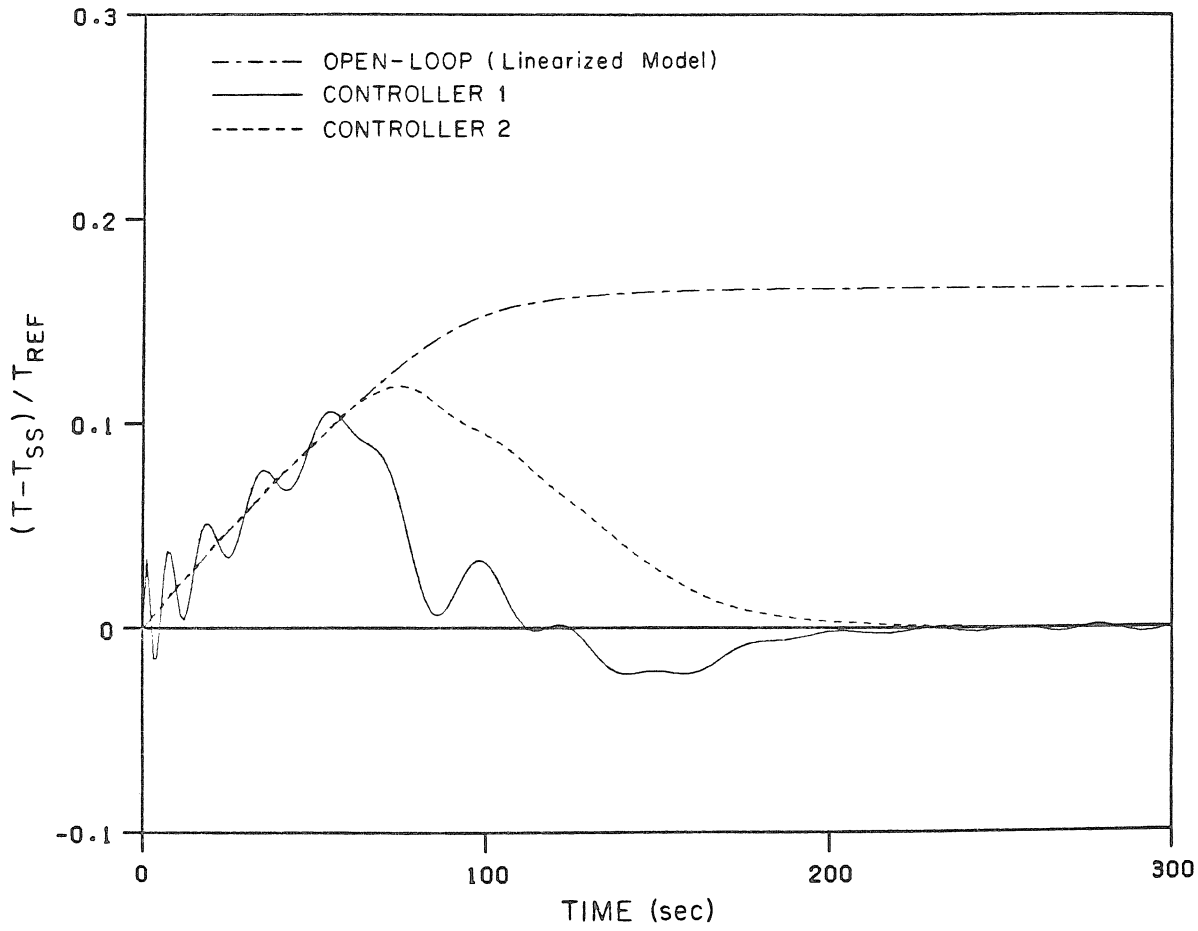

Figure 13 Open- and closed-loop outlet temperature responses to a −25% step-change in the inlet CO concentration. (T_{SS} = 546 K; T_{REF} = 40 K; Linearized Model).

5.3 Design in the Face of Model Uncertainty

The first step required in the design of robust control schemes is a characterization of model uncertainty.

The main sources of uncertainty in the reactor model are:

— the effects of the "discretization" technique employed for handling the PDE's;

— uncertainty resulting from the fact that the plant is nonlinear, whereas linearized models are employed for the control system design;

— uncertainty in model parameters, especially in those related to the reaction kinetics, for example, activation energy;

— modeling assumptions and neglected dynamics.

The first three sources are considered to be the most important and are those addressed here.

Let us consider first the uncertainty resulting from the use of a discretization technique for the approximation of the PDE's. An approximate description of the multiplicative uncertainty resulting from the discretization can be obtained in terms of the relative error between a model based on a large number of discretization points and the actual model employed. In Fig. 14, $\bar{l}_{m\,D}$ corresponds to the magnitude of the relative error between a model based on 20 collocation points ($\tilde{p}_{20}$), taken here to be the "exact" model, and the model based on 12 collocation points ($\tilde{p}_{12}$) employed for the control system design. The description by the model $\tilde{p}_{12}$ is seen to "break down" abruptly at a frequency of 0.22 rad/sec, with the relative error approaching 100% at 0.3 rad/sec. A similar comparison for a pure convective process with the same wave velocity and the same number of discretization points, but employing finite differences for the discretization, shows a steady, rather than an abrupt, degradation at about the same frequency range.

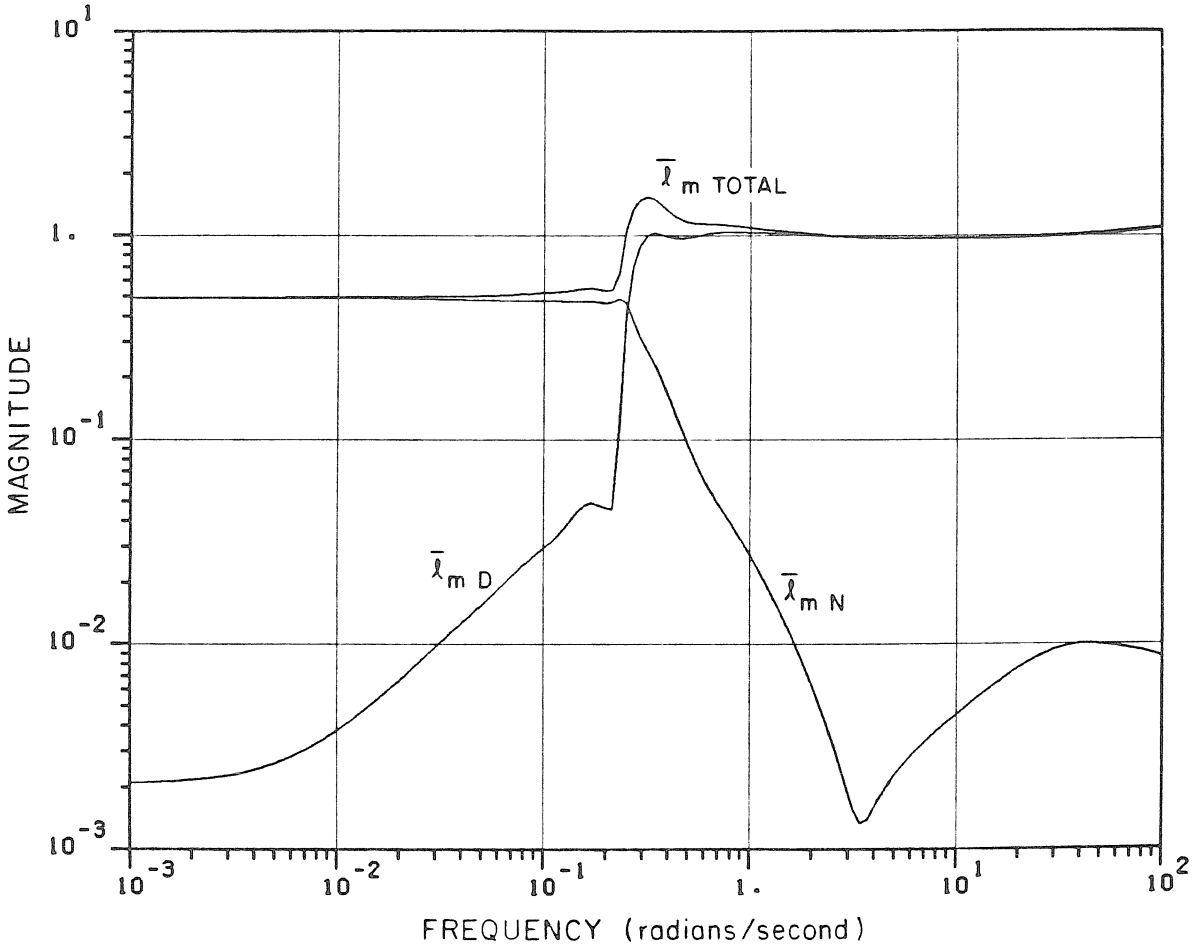

Figure 14 Upper bound $\bar{l}_m$ on the multiplicative uncertainty. $\bar{l}_{m\,D}$: discretization (relative error between a 20 collocation points-based model, and the model based on 12 points : $|\frac{\tilde{p}_{20}-\tilde{p}_{12}}{\tilde{p}_{12}}|$). $\bar{l}_{m\,N}$: nonlinearity. $\bar{l}_{m\,TOTAL} = \bar{l}_{m\,D} + \bar{l}_{m\,N} + \bar{l}_{m\,D}\bar{l}_{m\,N}$.

Frequencies that are much higher than the ratio of the distance between collocation points divided by the wave velocity cannot be described well by the model, and this determines the frequency range at which model validity breaks down. This occurs for the transfer function between T_{in} and T_{out} because of the finite time it takes for the temperature changes to travel along the bed, and it does not occur when changes are felt "immediately" along the entire bed. For example, for the transfer function between F_P and T_{out}, the frequency responses for 12 and 20 points are almost identical over the whole frequency range. The uncertainty resulting from the discretization ($\bar{l}_{m\,D}$ in Fig. 14) becomes large at significantly larger frequencies than the optimal closed-loop bandwidth of the nominal system.

Next, we attempt to characterize the uncertainty resulting from the system nonlinearity as parameter variations of the linearized model. For this purpose the nonlinear model is linearized at different points of the operating region so that a family Π of plants is obtained. The points are selected along the expected trajectory of the closed-loop system following a step-change in x_{CO}. At each frequency the frequency response of the nominal model for use in the control system design is selected to be the center of the smallest circle in the complex plane containing all plants of the family Π. $\bar{l}_{m\,N}$ is obtained from the radius of these circles (Fig. 14). $\bar{l}_{m\,N}$ is almost constant and relatively large at low frequencies and starts dropping at about the same frequency range in which the uncertainty from the discretization starts rising, i.e., where no linearized model is valid. The fact that the uncertainty resulting from the nonlinearity is important at the low frequencies is not unexpected, since the strongest nonlinearities in the model are associated with the exponential temperature dependence of the reaction rate. The temperature changes are associated with the slowest modes of the system.

Although, in the controller design examples that follow, it is assumed that all physical parameters are known exactly, an initial characterization of the uncertainty

resulting from uncertainty in a specific parameter, namely, the activation energy, has also been carried out. A similar procedure as for the uncertainty resulting from nonlinearity has been used. A plot of $\bar{l}_m$ obtained in this way is very similar to that of $\bar{l}_{m\,N}$ given in Fig. 14. The activation energy does, in fact, appear in those same terms that are most strongly nonlinear.

Both sources of uncertainty (discretization and nonlinearity) are combined on the assumption that they are independent. It can be shown that, for this assumption, the combined bound $\bar{l}_{m\,TOTAL}$ from both sources has to be calculated by

$$\bar{l}_{m\,TOTAL} = \bar{l}_{m\,D} + \bar{l}_{m\,N} + \bar{l}_{m\,D}\bar{l}_{m\,N} \quad . \tag{54}$$

$\bar{l}_{m\,TOTAL}$ calculated in this way is plotted in Fig. 14. $\bar{l}_{m\,TOTAL}$ will be denoted simply by $\bar{l}_m$ throughout the rest of the article. At the low frequency range, $\bar{l}_m$, although relatively large, is significantly less than 1. It is important that $\bar{l}_m$ is less than 1 at zero frequency because this guarantees that a robust controller with integral action exists for the family of plants (Morari, 1985).

Reduced-order models are employed in the design of the robust IMC controllers. The model reduction procedure developed by Rivera and Morari (Section 4.4) is applied. The procedure requires the selection of a structure for the reduced-order model (e.g., the order of the model) and the specification of d, $\bar{l}_m$ and an initial choice for $\hat{\eta}$.

For controller 2, for example, $\hat{\eta} = \hat{p}_A f$, where $\hat{p}_A$ is the allpass that, in the reduced-order model, accounts for the NMP behavior. The initial selection of $\hat{\eta}$ involves the choice of the filter time-constant λ. λ is selected on the basis of our knowledge about the system, namely, an idea of the closed-loop bandwidth (recall Eq. (53)) and the robust stability considerations. In an iterative fashion the procedure updates $\hat{p}_A$ and thus $\hat{\eta}$ with the RHP zeros found for the reduced-order model, until convergence.

Fig. 15 shows a comparison between the frequency responses for the full 49th order model and for a 6th order model obtained by this procedure. The reduced-order model closely approximates the full-order model in the frequency interval that is most relevant to the control problem and neglects the higher frequencies that are irrelevant because of the bandwidth limitations arising from the RHP zeros.

Condition (51) is used as the criterion in the design of robust SISO IMC controllers for the reactor system. Both controller 1 and controller 2 are detuned from the ideal controllers found for the nominal case by increasing the filter time-constant λ until robust stability is guaranteed. More precisely, the following considerations are taken into account. From a comparison of conditions (19) and (24), it is clear that if for some frequency ω, $|\tilde{\eta}\ \bar{l}_m|$ equals unity, then in order to satisfy the robust performance condition (24) the weight w has to equal zero at that particular frequency. As will be clear from the discussion later on, this means that no guarantees on robust performance can then be obtained. It turns out that only a slightly stronger detuning beyond the exact limit for robust stability (a small extra sacrifice in nominal performance) is required in our system in order to obtain reasonably good robust performance. Both controllers are therefore detuned so as to

make $\sup_{\omega} \left|\frac{\hat{\eta}(1 + e_m)}{1 + \hat{\eta} e_m} \bar{l}_m\right| \approx 0.95$ instead of 1.

The uncertainty, non-minimum phase and disturbance characteristics of the process are such that they require a much stronger detuning for controller 1 than for controller 2 in order to satisfy the robust stability condition. λ= 11.7 sec. is needed for controller 2 and instead λ= 23.7 sec. is needed for controller 1. The main reason for this is that the uncertainty is significant over the whole frequency range, including the frequencies that are close to the corner frequency of the lead element, at which the complementary sensitivity function for controller 1 starts increasing beyond unity. As a result, not much advantage can be obtained from the

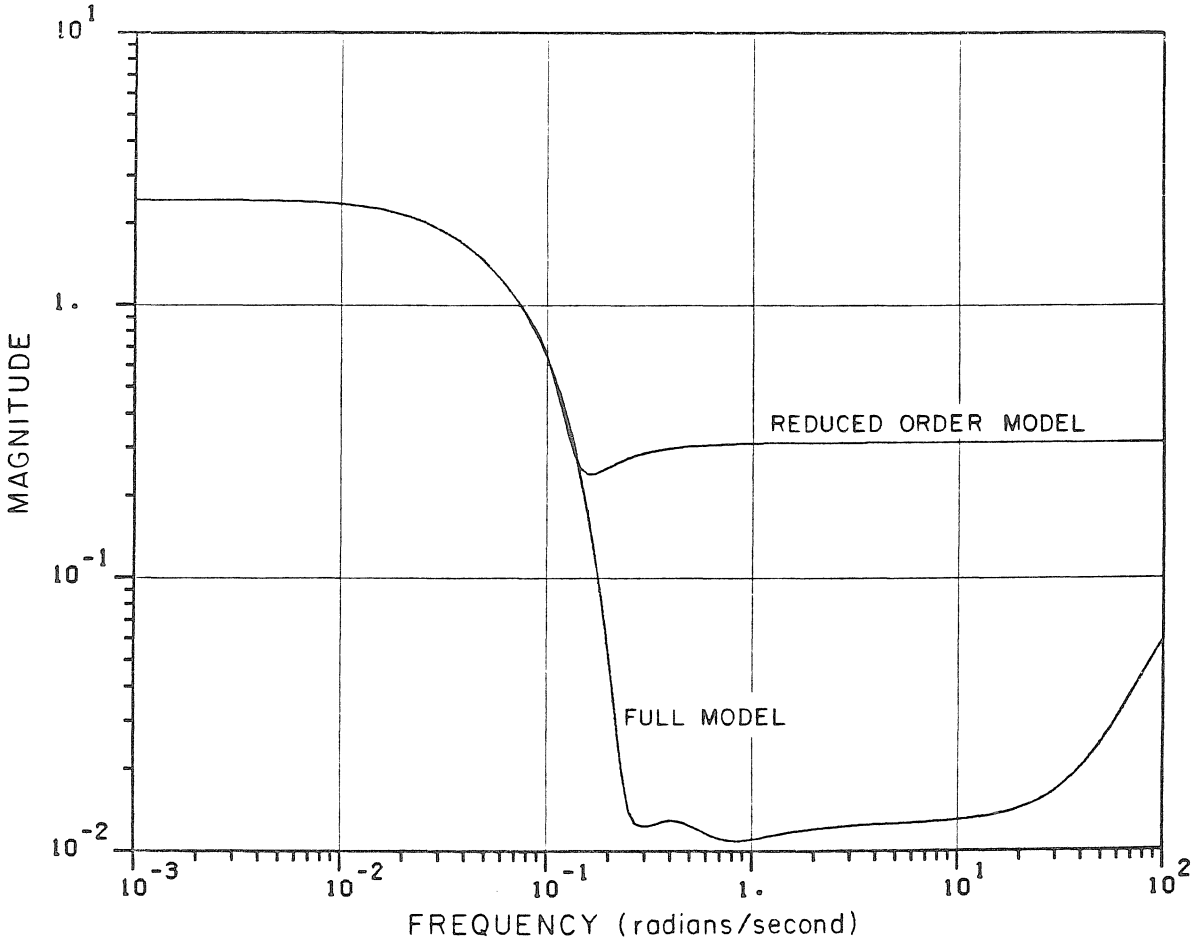

Figure 15 Comparison between the frequency responses of the full 49th order model and the 6th order model ($|\tilde{p}|$ vs $|\hat{p}|$).

beneficial effect of the lead element on the performance, because the robustness constraints require an immediate roll-off by means of the filter.

Fig. 16 presents the results of the implementation of both robust, reduced-order IMC controllers on the full nonlinear plant. While $\|e\|_2$ for controller 1 equals in this case 4.85, $\|e\|_2$ for controller 2 equals 4.95, namely, only 2% worse. No significant benefit is therefore obtained in our case from optimal disturbance rejection when model uncertainty enters into the picture. It is found that, for the employed values of λ, the manipulated variable lies always in the permitted range.

The degradation in performance with respect to the ideal case is mainly a result of: 1) the detuning required to satisfy robust stability; 2) the fact that the actual plant is not equal to the nominal plant. Compare the following results for the 2-norm of the error for controller 2, following a unit step-change in x_{CO}. As said, for the ideal case without detuning, $\|e\|_2 = 1.95$. After the controller is detuned to satisfy robust stability, and when implemented on the *nominal* plant, $\|e\|_2 = 2.4$. The NMP characteristics of the process cause the error, even with an ideal controller, to be already significantly high, and the degradation caused by the detuning is comparatively less important. When the robust controller is implemented on the actual nonlinear plant, $\|e\|_2 = 4.95$; the plant-model mismatch does cause a significant degradation in performance.

While the 2-norm of the error can be calculated exactly for the case of the nominal plant, it is clearly not possible to calculate it *a priori* for the actual plant, because the actual plant is unknown. (The value of $\|e\|_2 = 4.95$ listed above for the nonlinear plant was found *a posteriori*, from the simulation results. This is equivalent to looking at the value of the error after the controller is implemented on a real system.) The actual plant, as said, is only known to be a member of a set of possible plants. It is important then to determine, beforehand, a bound on the error applying to all plants in this set, i.e., a worst-case bound. In this way one can

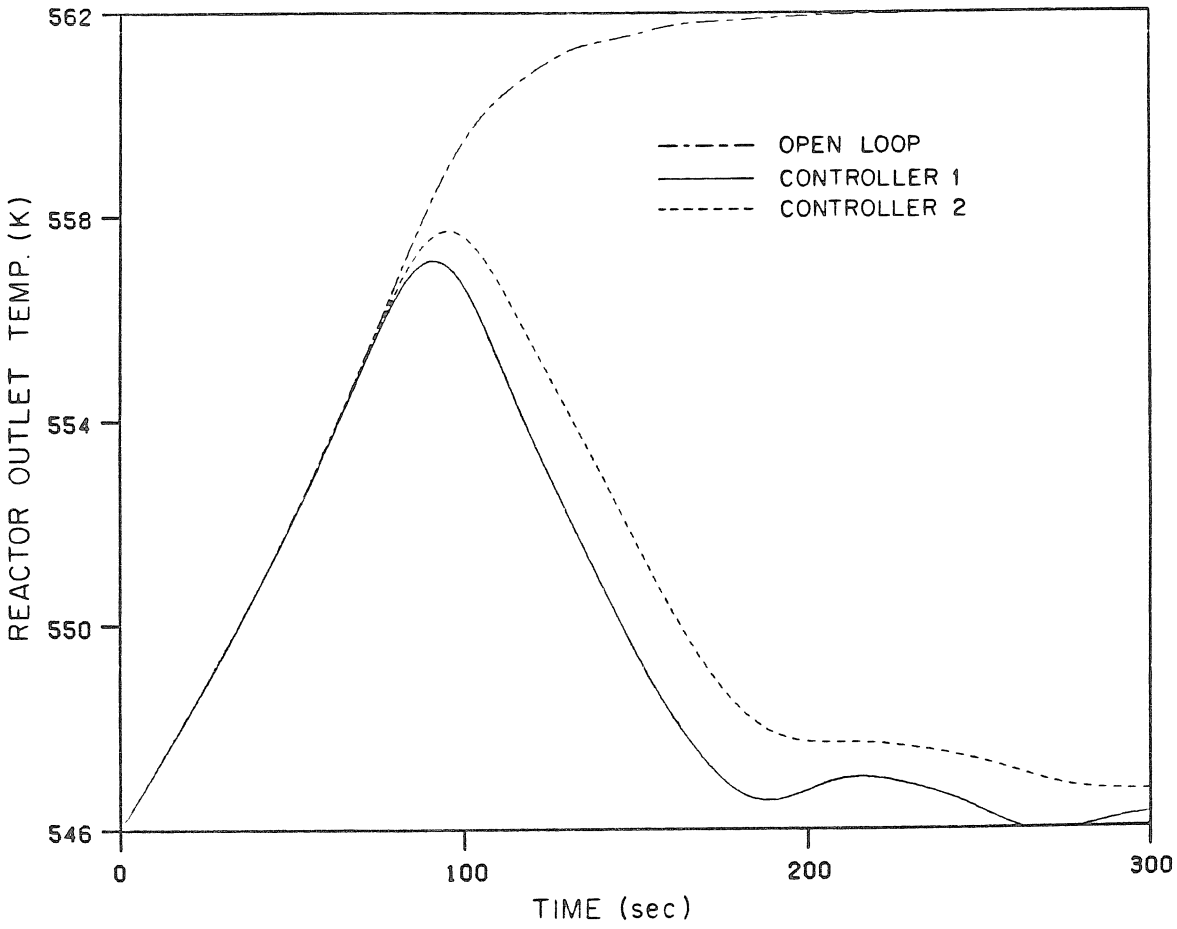

Figure 16 Open- and closed-loop outlet temperature responses to a −25% step-change in the inlet CO concentration. Nonlinear model.

then be assured, *a priori*, that the error for the actual plant will not exceed that bound.

The truth of the last statement, and the closeness of the bound to the actual error, will, of course, depend on how well the model uncertainty has been characterized. If the uncertainty description is too conservative, then the actual error may be much lower than the bound, and under such circumstances the bound will not provide useful information. On the other hand, it should be clear that, since the treatment of the system nonlinearity as uncertainty resulting from parameter variations of the linearized model is certainly not a rigorous approach (but one of the few practical approaches at present), it may occur that the bound obtained will be less than the actual error observed for the nonlinear plant. No absolute guarantees exist even if the set Π represents the behavior of the nonlinear plant properly.

In order to obtain *a priori* bounds on $\|e\|_2$ in the face of model uncertainty, we make use of Doyle's μ-analysis theorem (the robust performance condition (24) or (52)). While the condition could have been used to synthesize controllers meeting certain robust performance specifications (namely, by finding the value of λ satisfying (52) for a specified w and $\bar{l}_m$), we apply the theorem instead as an analysis tool, essentially to find w that satisfies condition (52) with λ and $\bar{l}_m$ fixed. The theorem employs information on the nominal plant and the uncertainty description and gives, as explained in Section 4.2, stability and performance guarantees for all plants in the uncertainty set.

Recall the discussion in Sections 4.1 and 4.2. From Doyle's theorem it follows that if $\mu(P(j\omega)) \leq 1 \ \forall \ \omega$, then $\|\epsilon\, w\|_\infty \leq 1 \ \forall \ p\epsilon\Pi$. From the definition of the structured singular value μ (Doyle, 1982), it follows that when at any particular frequency ω_0, $\mu(P(j\omega_0)) = 1$, then there exists some plant $p_0\epsilon\Pi$ that achieves the bound given above, namely, for this particular plant $|\epsilon_0\, w| = 1$ at that particular frequency. This plant is the one corresponding to the worst sensitivity function

(there exists no plant in Π for which $\epsilon(\omega_0) > \epsilon_0(\omega_0)$).

For the SISO case, under those circumstances,

$$|\epsilon_0| = \frac{1}{w} \quad ; \tag{55}$$

namely, the magnitude of the worst sensitivity function at each frequency can be found directly from the value of w that makes the equality in the robust performance condition (24) or (52) hold. From (24), when the equality holds, then

$$\frac{1}{w} = \frac{|\tilde{\epsilon}|}{1 - |\tilde{\eta}\ \bar{T}_m|} = |\epsilon_0| \ . \tag{56}$$

An explicit expression is therefore obtained for the magnitude of the worst possible sensitivity function of the uncertainty set at each frequency, in terms of the *nominal* sensitivity function and of the bound on the multiplicative uncertainty.

Having obtained the above, we now calculate the value of the worst possible 2-norm of the error for the specific input signal considered, by simply replacing the expression for $|\epsilon_0|$ in Eq. (7) and performing the integration. Since in our case the input signal is a step going through p_d, and since we actually employ condition (52) for the μ-analysis theorem, then

$$\|e_0\|_2 = \left(\frac{1}{\pi} \int_0^{\infty} |\epsilon_0(j\omega)\ p_d(j\omega)\ \frac{1}{j\omega}|^2\ d\omega \right)^{\frac{1}{2}}, \tag{57}$$

where

$$|\epsilon_0| = \frac{|1 - \hat{\eta}|}{|1 + \hat{\eta} e_m| - |\hat{\eta}\ (1 + e_m)\ \bar{T}_m|} \ . \tag{58}$$

For controller 1 we obtain

$$\|e_0\|_2 = 4.81$$

or

$$\|e\|_2 \leq 4.81 \quad \forall \ p \epsilon \Pi \ .$$

The theorem guarantees that the 2-norm of the error following a unit step-change in x_{CO} will not be greater than 4.81 for any plant in the uncertainty set. The bound obtained is almost equal to the actual error observed in the simulation for the non-linear plant (4.85). For controller 2 a somewhat lower value is obtained (4.64) and the bound is within 7% of the actual error observed in the simulation (4.95). The results are excellent, taking into account the simple approach employed for the characterization of model uncertainty and the difficulties mentioned above in properly dealing with nonlinear systems.

6. CONCLUSIONS

A systematic approach to control system design has been presented and applied to the control of a fixed-bed methanation reactor. The theoretical limits on the closed-loop performance and the causes for these limits were established. The limitations on performance imposed by the non-minimum phase characteristics of the plant were found to be the most important ones for the SISO control configuration studied. Alternative configurations were proposed to alleviate these limitations while still satisfying the same control objectives.

Primary importance was given to the crucial issue of controller design in the face of model uncertainty. Uncertainty was described in terms of norm bounds. Although conservatism may be introduced by accounting for model uncertainty through simple uncertainty descriptions, this conservatism is counterbalanced by the convenience of these descriptions for the analysis and synthesis tasks. It is

particularly difficult to characterize appropriately the uncertainty resulting from the system nonlinearity.

A near-optimal design for specific input signals was carried out employing the IMC design technique. Two IMC controllers, incorporating and not incorporating a disturbance model for the controller design, were compared. The benefits of optimal disturbance rejection, although important for the nominal case, were found to be less significant in the face of model uncertainty as a result of the particular non-minimum phase, uncertainty and disturbance characteristics of the process.

Tight bounds were obtained for the 2-norm of the error in the face of model uncertainty through the application of the μ-analysis theorem. Although for the SISO case and the multiplicative uncertainty description the same robust performance condition could have been obtained on the basis of geometric arguments, only through the μ-analysis theorem can necessary and sufficient conditions for robust stability and robust performance be obtained for structured uncertainty descriptions or for multivariable systems.

Acknowledgments

We are thankful to D.E. Rivera, E. Zafiriou, S. Skogestad and J.C. Doyle for many useful discussions. Acknowledgment is made to the Donors of The Petroleum Research Fund, administered by the American Chemical Society, to the National Science Foundation (CBT-8315228) and to the Department of Energy for the support of this research.

REFERENCES

Aris, R. and N.R. Amundson, 1958a, An analysis of chemical reactor stability and control - I. The possibility of local control, with perfect or imperfect control mechanisms. *Chem. Engng Sci.* **7**, 121-131.

Aris, R. and N.R. Amundson, 1958b, An analysis of chemical reactor stability and control - II. The evolution of proportional control. *Chem. Engng Sci.* **7**, 132-147.

Aris, R. and N.R. Amundson, 1958c, An analysis of chemical reactor stability and control - III. The principles of programming reactor calculations. Some extensions. *Chem. Engng Sci.* **7**, 148-155.

Chiang, D.N., 1983, CO methanation over a nickel catalyst. M.Sc. Thesis, Calif. Inst. of Technology, Pasadena, CA.

Desoer, C.A. and M. Vidyasagar, 1975, *Feedback Systems: Input-Output Properties*, Academic Press, New York, Ch. 2.

Doyle, J.C., 1982, Analysis of feedback systems with structured uncertainties. *IEE Proc.* **129**, D(6), pp. 242-250.

Doyle, J.C., 1984, Lecture notes, ONR/Honeywell Workshop on Advances in Multivariable Control, Minneapolis, MN.

Doyle, J.C., 1985, Lecture notes, Calif. Inst. of Technology, Pasadena, CA.

Doyle, J.C. and G. Stein, 1981, Multivariable feedback design: concepts for a classical/ modern synthesis. *IEEE Trans. Automat. Contr.* **AC-26**, 4-16.

Friedly, J.C., 1972, *Dynamic Behavior of Processes*, Prentice-Hall, Englewood Cliffs, NJ, pp. 345-346.

Froment, G.F. and K.B. Bischoff, 1979, *Chemical Reactor Analysis and Design*, John Wiley and Sons, New York, Ch. 11.

Garcia, C.E. and M. Morari, 1982, Internal Model Control - 1. A unifying review and some new results. *Ind. Engng Chem. Proc. Des. Dev.* **21** , 308-323.

Harms, H.G., B. Höhlein, E. Jorn, and A. Skov, 1980, High-temp methanation tests run. *Oil and Gas Journal* **78** , 120-124.

Holt, B.R. and M. Morari, 1985, Design of resilient processing plants - VI. The effect of right-half-plane zeros on dynamic resilience. *Chem. Engng Sci.* **40** , 59-74.

Khanna, R., 1984, Control model development for packed-bed chemical reactors. Ph.D. Thesis, Calif. Inst. of Technology, Pasadena, CA.

Khanna, R. and J.H. Seinfeld, 1982, Model development of a non-adiabatic packed-bed reactor. Paper 9d, 1982 Annual Meeting, A.I.Ch.E., Los Angeles, CA.

Khanna, R. and J.H. Seinfeld, 1986, Mathematical modeling of packed-bed reactors - Numerical solutions and control model development. *Advances in Chemical Engineering*, in press.

Mandler, J.A. and M. Morari, 1986, SNTEG: A dynamic simulation program for closed-loop systems. New Orleans Meeting, A.I.Ch.E. (Chapter V of this thesis).

Mandler, J.A., D.M. Strand, R. Khanna and J.H. Seinfeld, 1984, Control of a packed-bed reactor with feed-effluent heat exchange. Proceedings of the 1984 American Control Conference, San Diego, CA, pp. 1608-1613. (Appendix D of this thesis).

Morari, M., 1983a, Design of resilient processing plants - III. A general framework for the assessment of dynamic resilience. *Chem. Engng Sci.* **38** , 1881-1891.

Morari, M., 1983b, Internal Model Control - Theory and applications. P.R.P.- Automation 5, 5th International IFAC/IMEKO Conference on Instrumentation and Automation in the Paper, Rubber, Plastics and Polymerization Industries, Antwerp, Belgium.

Morari, M., 1985, Robust stability of systems with integral control. *IEEE Trans.*

Automat. Contr. **AC-30** , pp. 574-577.

Morari, M. and S. Skogestad, 1985, Effect of model uncertainty on dynamic resilience. Proc. PSE 85, Cambridge, April 1985, IChE Symp. Ser. No. 92.

Newton, G.C., L.A. Gould and J.F. Kaiser, 1957, *Analytical Design of Linear Feedback Controls*, John Wiley and Sons, New York.

Rivera, D.E. and M. Morari, 1985, Internal Model Control perspectives on model reduction. Proceedings of the 1985 American Control Conference, Boston, MA, pp. 1293-1298.

Rivera, D.E., M. Morari and S. Skogestad, 1986, Internal Model Control: PID controller design. *Ind. Engng Chem. Proc. Des. Dev.* **25** , 252-265.

Strand, D.M. and J.H. Seinfeld, 1982, Construction of a laboratory-scale fixed-bed methanation reactor for multivariable control studies. Paper 92d, 1982 Annual Meeting, A.I.Ch.E., Los Angeles, CA.

Wiberg, D.M., 1971, *State Space and Linear Systems*, McGraw-Hill, New York, pp. 167-169.

IV. ROBUST MULTIVARIABLE CONTROL SYSTEM DESIGN FOR A FIXED-BED REACTOR

Accepted for Publication in

Condensed Form in

Industrial & Engineering Chemistry

Fundamentals

(1986)

ROBUST MULTIVARIABLE CONTROL SYSTEM DESIGN FOR A FIXED-BED REACTOR

Jorge A. Mandler, Manfred Morari and John H. Seinfeld

Chemical Engineering, 206-41

California Institute of Technology

Pasadena, CA 91125

ABSTRACT

The design of multivariable controllers in the face of model uncertainty is addressed. Recently developed Structured Singular Value (μ)-based analysis techniques allow one to assess robust stability and robust performance of multivariable systems in a non-conservative manner. On the basis of these techniques a methodology for the design of robust multivariable controllers is outlined. This methodology is applied to the design of control systems for a fixed-bed, laboratory methanation reactor. In one configuration the inlet temperature and the flow rate are optimally combined as manipulated variables for the regulation of the outlet temperature in the face of inlet concentration disturbances. In a second configuration, the optimal regulation of the product concentration is investigated when only temperature measurements are available. First, H_2-optimal controllers are designed for the nominal cases. Next, knowledge about the model uncertainty is incorporated explicitly into the design procedure, and robust controllers are designed on the basis of either H_2- or H_∞-performance criteria.

1. INTRODUCTION

Process control is often characterized by a lack of complete and accurate mathematical models. It is particularly difficult to obtain accurate mathematical descriptions for distributed chemical reaction systems. The issue of robustness of the control system, namely, that stability and acceptable performance be maintained in the face of plant-model mismatch, is therefore of paramount importance for these reactor systems. Nevertheless, robustness considerations are generally not incorporated explicitly into the controller design procedure.

Mandler *et al.* (1986) presented the basis for a systematic treatment of the single-input single-output (SISO) control system design problem in the face of model uncertainty, in the context of the control system design for a fixed-bed methanation reactor. In that work the fundamental limitations to the achievable closed-loop performance were pinpointed, and on the basis of a characterization of the model uncertainty, *a priori* bounds for the performance in the face of plant-model mismatch were determined. The model uncertainty was considered in that case-study to result mainly from the system's nonlinearity. Simulations of the linear controller applied to the full nonlinear plant showed the closed-loop performance to correspond very closely to that predicted by the analysis. This paper extends the concepts and the treatment of Mandler *et al.* (1986) to the multivariable situation, by presenting a general methodology for multivariable controller design in the face of model uncertainty and its application in two case-studies of control of the fixed-bed methanation reactor. The techniques employed are motivated in Section 2 and detailed in Section 3. Sections 4 and 5 focus on the case-studies.

2. OVERVIEW OF THE MULTIVARIABLE CONTROL PROBLEM

2.1 Nominal Performance

The closed-loop multi-input multi-output system in Fig. 1 can be described by the input-output relationships

$$e = (I + PC)^{-1}(r-d) = S(r-d) \tag{1}$$

and

$$y = (I + PC)^{-1}PCr = Hr \ , \tag{2}$$

where r,d,y, and e are vectors, e = r−y, S is the sensitivity operator and H is the complementary sensitivity operator. S is an important indicator of feedback controller performance. $\tilde{S}$ and $\tilde{H}$ will denote the sensitivity and complementary sensitivity operators calculated on the basis of a model $\tilde{P}$. For the case of a perfect model (nominal design case, $\tilde{P} = P$), $\tilde{S} = S$, and $\tilde{H} = H$.

The definition of the norms for signals is extended from the scalar case to the case of vector-valued functions of time or frequency by the use of an appropriate spatial norm, in general, the Euclidean norm. For example, the 2-norm of the vector-valued error signal e is given by

$$\|e\|_2 = \left(\int_0^\infty |e(t)|^2 \, dt\right)^{\frac{1}{2}} = \left(\int_0^\infty e^T e \, dt\right)^{\frac{1}{2}} \ , \tag{3}$$

where |.| denotes the Euclidean norm.

The Linear Quadratic (H_2-) optimization problem, which applies to the case of specific input signals and to the 2-norm of the (weighted) error as the basis for the performance specifications, can be expressed as

$$\min_C \|\bar{e}'\|_2 = \min_C \|W_o \tilde{S} W_i\|_2 = \min_C \left(\frac{1}{\pi}\int_0^\infty tr\,(W_o \tilde{S} W_i)^*(W_o \tilde{S} W_i)\, d\omega\right)^{\frac{1}{2}} \ . \tag{4}$$

In arriving at Eq. (4) we have made use of Parseval's theorem, and we have included

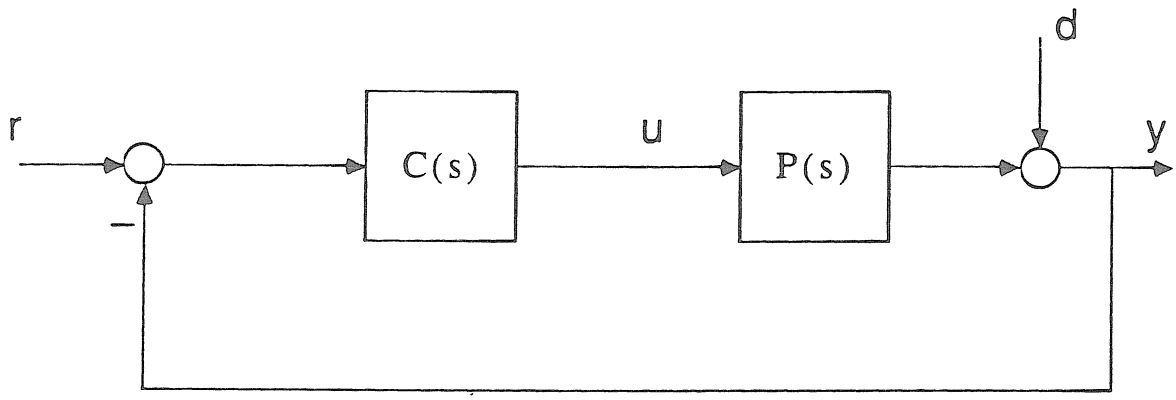

Figure 1 General feedback problem.

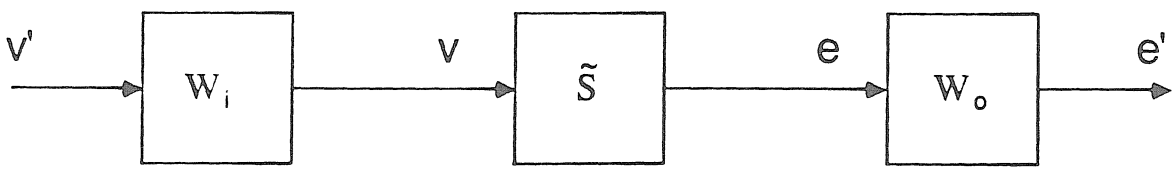

Figure 2 Weighted sensitivity operator.

input and output frequency-dependent weights, W_i and W_o, respectively, on the sensitivity operator $\tilde{S}$ (Fig. 2). The specific input signals v are given by $v = W_i v'$, where v' is an array of unit impulses separately applied to each channel. The weighted output error vector e' is given by $e' = W_o e$. $\|\bar{e}'\|_2$ is an average error 2-norm over all input channels, defined by

$$\|\bar{e}'\|_2 \triangleq \Big(\sum_{\substack{\text{input} \\ v'_j}} (\|e'\|_2^2)_j \Big)^{\frac{1}{2}} \quad , \tag{5}$$

where $(\|e'\|_2)_j$ is the 2-norm of the error resulting from an impulse applied only to input channel j. From now on, for the case of specific input signals, $\|\bar{e}'\|_2$ will be denoted as $\|e'\|_2$, and the averaging process of Eq. (5) will be implied. Note that the weights W_i and W_o in Eq. (4) are transfer matrices. Therefore, they shape not only the frequency content of the signals but also their spatial directions. For example, through W_o the designer can specify the relative importance of one output or another.

A second type of optimization problem is the H_∞-optimization problem. In Mandler *et al.* (1986) we showed that this formulation is appropriate for the case when the inputs, although themselves unknown, belong to a set of bounded signals such that $\|v'(t)\|_2 \leq 1$. The input matrix weight W_i is required to shape both the frequency content and the spatial direction of the inputs. As a performance specification, the designer requires the weighted error e' to be norm-bounded; i.e.,

$$\|e'(t)\|_2 \leq 1 \quad . \tag{6}$$

The optimal controller in this formulation is the one that minimizes the 2-norm of the largest weighted error over all input signals in the set:

$$\underset{C}{\text{Min}} \sup_{\|v'\|_2 \leq 1} \|e'(t)\|_2 \quad . \tag{7}$$

It can be shown (Desoer and Vidyasagar, 1975) that the operator norm

induced by the 2-norm on *vector-valued* input/output time functions, defined by

$$\sup_{\|v'\|_2 \le 1} \|e'(t)\|_2 = \sup_{\|v'\|_2 \le 1} \|W_o \tilde{S} W_i v'\|_2 \triangleq \|W_o \tilde{S} W_i\|_{i2} \tag{8}$$

is equal, if the Euclidean norm is used spatially, to

$$\|W_o \tilde{S} W_i\|_{i2} = \sup_{\omega} \bar{\sigma}(W_o \tilde{S} W_i) \triangleq \|W_o \tilde{S} W_i\|_\infty \quad , \tag{9}$$

where $\bar{\sigma}$ denotes maximum singular value and Eq. (9) defines the ∞-norm of the weighted sensitivity operator. Equation (9) is the natural extension of the scalar result, since the maximum singular value equals the maximum gain of the operator over all possible input directions. The performance requirement of Eq. (6) is satisfied if, and only if,

$$\|W_o \tilde{S} W_i\|_\infty \le 1 \quad . \tag{10}$$

The controller design objective is

$$\min_C \|W_o \tilde{S} W_i\|_\infty = \min_C \sup_\omega \bar{\sigma}(W_o \tilde{S} W_i) \quad . \tag{11}$$

Alternatively, the H_∞-formulation allows the designer to obtain controllers that satisfy control objectives set directly in terms of bounds on the sensitivity operator. At times this may be more appealing than the use of the 2-norm of the error as the basis for the performance specifications. This approach is demonstrated in Section 5.

2.2 Unstructured and Structured Uncertainty. Robust Stability Conditions

Consider the system of Fig. 3. $\tilde{P}$ is a model of the actual plant P. The plant, although unknown, has been characterized to lie within a neighborhood of $\tilde{P}$, known only in terms of a magnitude bound; i.e.,

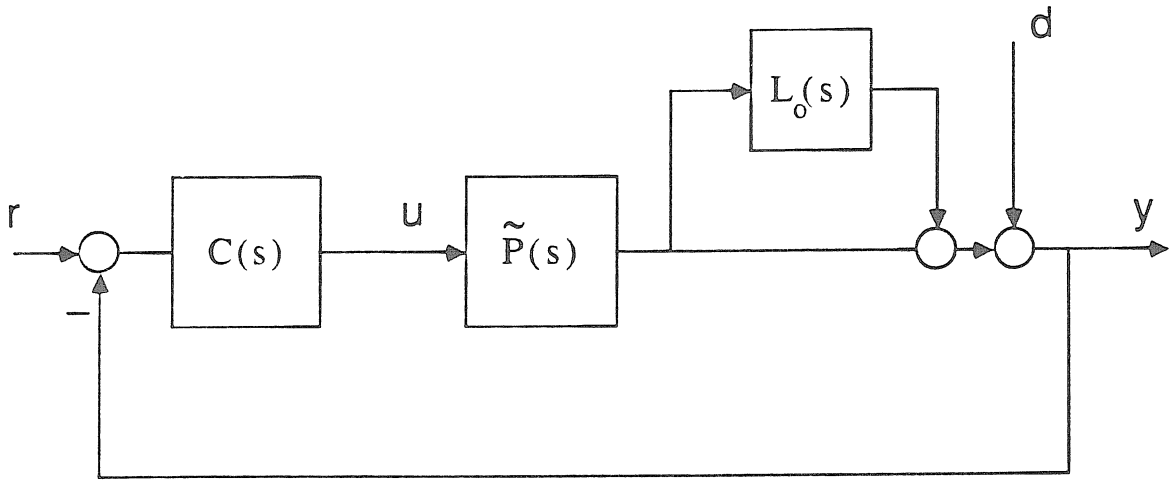

Figure 3 System with multiplicative output uncertainty.

$$P(j\omega) = (I + L_o(j\omega))\ \tilde{P}\ (j\omega) \tag{12}$$

with

$$L_o(j\omega) = \bar{l}_{m_o}(\omega)\ \Delta \tag{13}$$

and

$$\|\Delta\|_\infty = \sup_\omega \bar{\sigma}(\Delta(j\omega)) < 1 \quad . \tag{14}$$

In general, the set of possible plants that is used to describe the dynamic behavior of the actual plant is referred to as the uncertainty set Π.

Equations (12)-(14) correspond to the so-called *unstructured* multiplicative output uncertainty. The uncertainty is represented by one full perturbation block Δ and a scalar weight $\bar{l}_{m_o}$. This scalar weight shapes only the frequency content of the uncertainty. No mechanism or structure for the uncertainty is implied. For this type of uncertainty description, robust stability is guaranteed by the following condition involving the maximum singular value of the complementary sensitivity operator (Doyle and Stein, 1981): Assume that all plants in the family defined by Eqs (12)-(14) have the same number of RHP poles and that a particular controller C stabilizes the nominal plant $\tilde{P}$. Then the system is robustly stable if, and only if,

$$\|\tilde{H}\ \bar{l}_{m_o}\|_\infty = \sup_\omega \bar{\sigma}(\tilde{H}\ \bar{l}_{m_o}) \leq 1 \quad . \tag{15}$$

The multiplicative output uncertainty description is representative, for example; of uncertainty about the sensors or of output errors at high frequencies resulting from unmodeled high frequency dynamics of the plant. The first disadvantage of employing an unstructured description with a scalar weight resides in the fact that this weight does not incorporate directionality. If the uncertainty in all channels is of the same order of magnitude, then this description may be appropriate. If, for example, the uncertainty in one sensor is much higher than that in another, only

conservative results can be obtained from the singular-value test of Eq. (15), since the bound assumes a single worst case uncertainty applicable to all channels. This problem can be addressed and singular value tests still be employed by allowing a "more structured" uncertainty description through the use of matrix weights instead of scalar weights. If the right-hand side in Eq. (13) is replaced by

$$L_o(j\omega) = W_L(j\omega)\Delta(j\omega)W_R(j\omega) \quad , \tag{16}$$

where Δ satisfies condition (14) and W_L and W_R are transfer matrices, then the spatial content of the perturbations can be taken into account with Δ still being a full matrix. The robust stability condition equivalent to condition (15) is in this case (Doyle *et al.* , 1982)

$$\sup_{\omega} \bar{\sigma}(W_R \tilde{H} W_L) \leq 1 \quad . \tag{17}$$

Consider, on the other hand, the case in which the uncertainty is a result only of uncertainty in the sensors, and the individual sensors are independent. In this case Δ should be diagonal and not full as assumed in Eq. (14). Uncertainty that is best represented by something other than just one full Δ-block is known as structured uncertainty. Singular value tests are based on the assumption of full Δ-blocks, and, for the case of structured uncertainty, they provide only sufficient but not necessary conditions for robust stability (i.e., the tests are conservative), since the set of true perturbations is only a subset of the set of modeled perturbations.

In most practical situations, uncertainty exists in different components of a system. For example, in addition to uncertainty about the model, uncertainty may exist about the manner in which the manipulated variables act on the system. The latter is better characterized through an input rather than an output uncertainty description. Because of the non-commutativity of the matrix product, structured uncertainty arises when there exist simultaneous uncertainties at different points of the loop in a multivariable system (Doyle *et al.* , 1982). Structured uncertainty

also arises naturally in the case in which the uncertainties in the plant itself are described in terms of uncertainties of the individual transfer matrix elements (cf. Sections 4 and 5). This corresponds to treating each element as an independent SISO plant and is appropriate for cases in which the uncertainties of the different elements are more or less uncorrelated. In Section 3 a tight stability test for general structures of model uncertainty is discussed.

2.3 The Robust Performance Problem in the Multivariable Case

Robust performance is the requirement that the performance specifications be met for all plants in the uncertainty set Π. If, for example, the performance specifications are stated in the H_∞- framework, then, for robust performance, condition (10) has to be met for the worst plant; i.e.,

$$\max_{P \in \Pi} \| W_o \, S \, W_i \|_\infty \leq 1 \quad . \tag{18}$$

For the SISO case, as shown in Mandler *et al.* (1986), a necessary and sufficient condition for robust performance (RP) is

$$| \tilde{\eta} \; \bar{l}_m | + | \tilde{\epsilon} \; w | \leq 1 \quad \forall \, \omega \tag{19}$$

where $\tilde{\eta}$ is the nominal complementary sensitivity function, $\bar{l}_m$ is the bound on the multiplicative uncertainty, $\tilde{\epsilon}$ is the nominal sensitivity function and w is a performance weight. Let us call RS the first term in Eq. (19) (standing for robust stability) and NP the second term (standing for nominal performance). If w (and therefore NP in Eq. (19)) is zero, then the resulting condition is a robust stability condition (cf. Eq. (15)). If, instead, $\bar{l}_m$ is zero, a nominal performance condition results. Clearly, in the SISO case "good" robust performance is a direct result of having both "good" robust stability and "good" nominal performance; i.e., RP = RS + NP.

On the other hand, the multivariable case is characterized by the fact that robust performance can be much worse than just the "sum" of nominal performance

and robust stability (namely, RP $\gg$ RS + NP may occur for some systems). In other words, even if robust stability is guaranteed and good nominal performance exists, and even if a condition equivalent to condition (19) is satisfied, there exist cases in which the robust performance can still be extremely poor and condition (18) not be satisfied (Stein, 1985).

Assume for simplicity that directional dependences are not important, namely, all performance and uncertainty weights are taken as scalars. The uncertainty bound is then denoted as in the SISO case by $\bar{l}_m$ and the performance weight by w. If the uncertainty is at the output, then a sufficient although not necessary condition for robust stability and robust performance is given by the direct equivalent of condition (19) (Stein, 1985):

$$\bar{\sigma}(\tilde{H})\,\bar{l}_{m_o} + \bar{\sigma}(\tilde{S})\,w \leq 1 \quad \forall\,\omega \quad . \tag{20}$$

On the other hand, if the uncertainty is located at the input, a sufficient condition for robust stability and robust performance is given by

$$\bar{\sigma}(\tilde{P}^{-1}\tilde{H}\,\tilde{P})\,\bar{l}_{m_i} + \kappa(\tilde{P})\bar{\sigma}(\tilde{S})\,w \leq 1 \quad \forall\,\omega \ , \tag{21}$$

where $\kappa(\tilde{P}) = \bar{\sigma}(\tilde{P})/\underline{\sigma}(\tilde{P})$ is known as the plant condition number and $\underline{\sigma}$ denotes minimum singular value. The presence of the condition number makes Eq. (21) fundamentally different and points to the fact that a large condition number may be detrimental to the robust performance and cause it to be much worse than what would be expected from just looking at nominal performance and robust stability. This shows that MIMO systems are inherently different from SISO systems. For ill-conditioned plants ($\kappa(\tilde{P})$ large), design techniques, like decoupling, that transform a MIMO system into a series of SISO systems, may fail.

Note, finally, that the above conditions based on $\bar{\sigma}$ are not a suitable starting point for a multivariable design methodology, since they are only sufficient and therefore may be arbitrarily conservative. The reasons for this will be

demonstrated in Section 3. From the discussion in the present section, the need is clear for having a formal design methodology for systematically treating these particular problems of the multivariable case, namely, the structured uncertainty issues and the peculiarities of the robust performance issue. Such a design methodology, based to a large extent on the work of Doyle, is presented in what follows.

3. ROBUST MULTIVARIABLE CONTROLLER DESIGN METHODOLOGY

3.1 Interconnection Structure

Of importance in the development and also for the application of the theoretical results exposed in this section is the representation of a system as shown in Fig. 4 (Doyle, 1982; Doyle, 1984). The nominal model M provides the basic interconnections among the signals, the perturbations, and the controller. M is simply referred to as the "interconnection structure." M includes not only information on the plant model $\tilde{P}$ but also weighting matrices associated with the uncertainty description and the performance specifications. v' is a vector of external inputs (set-points, disturbances, measurement noise) and e' is a (weighted) output-error vector, corresponding to the difference between the desired system outputs and the actual ones. In all cases the objective of the control system is to make e' small and ideally zero for all times. Δ in Fig. 4 is a block diagonal perturbation (uncertainty) matrix, of which only its block structure and the fact that it is norm-bounded are known:

$$\Delta = \underset{\text{diag}}{\overset{\text{block}}{}} (\Delta_1, \Delta_2, \cdots, \Delta_m) \ , \tag{22}$$

with Δ_k satisfying Eq. (14). M and Δ define a set Π of possible plants describing the dynamic behavior of the actual (unknown) plant. All known spatial and frequency content of the perturbations is represented in the form of weights that are imbedded in M. By means of this representation, uncertainties occurring at different locations in the feedback loop are treated as a single uncertainty occurring at one

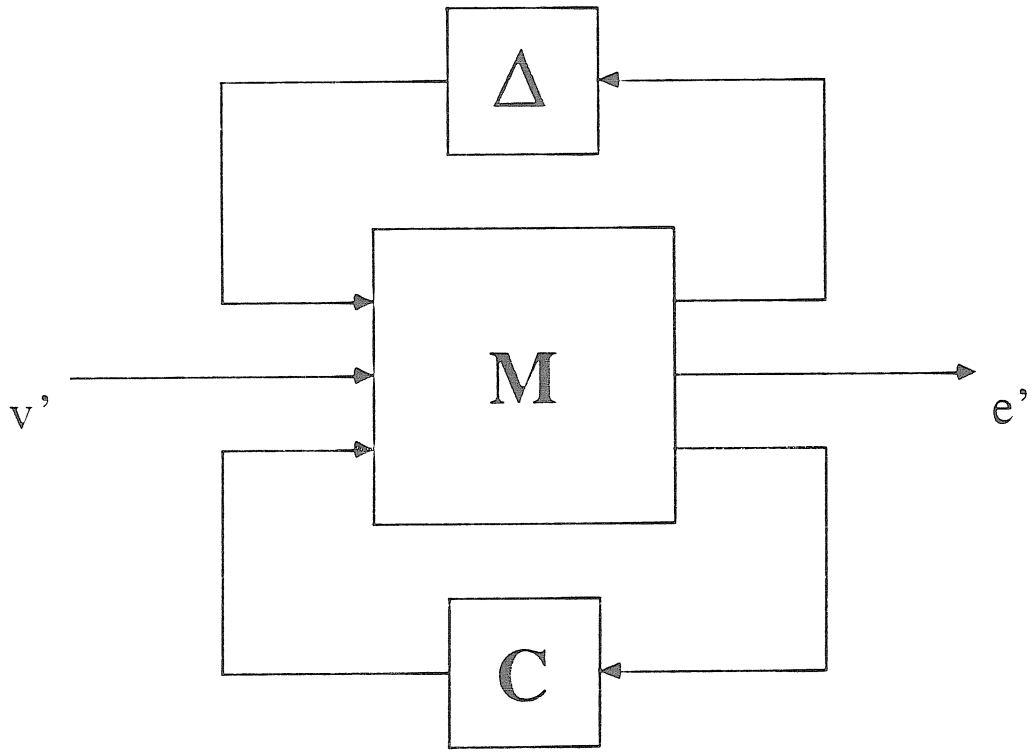

Figure 4 General interconnection structure.

location in a larger feedback loop. The representation turns out to be remarkably general and applies to a wide variety of practical problems.

3.2 Analysis

When the purpose is to *analyze* the performance and robustness characteristics of a particular closed-loop system, the controller C is known and can be imbedded into the interconnection structure. In this way a representation is obtained as in Fig. 5. M′ can be obtained directly from M and C as a linear fractional transformation on the controller

$$M' = F_L(M,C) \triangleq M^{11} + M^{12}C(I-M^{22}C)^{-1}M^{21} , \tag{23}$$

where M is partitioned according to the size of C. The total closed-loop system is given by

$$e' = F_U(M',\Delta)\, v' \triangleq (M'_{22} + M'_{21}\Delta(I-M'_{11}\Delta)^{-1}M'_{12})\, v' , \tag{24}$$

where M′ is partitioned according to the size of Δ.

Nominal Performance. If the purpose is to analyze nominal performance, then in Eq. (24), $\Delta = 0$, and only M'_{22} is of interest. For both the set-point-tracking and the disturbance-rejection problems, M'_{22} equals the weighted sensitivity operator of Section 2.1.

Robust Stability. Throughout this treatment nominal (closed-loop) stability is assumed, and also the perturbation Δ itself is assumed to be stable. Clearly, then, from Eq. (24), the only source of possible instability in the face of a perturbation Δ is in the factor $(I-M'_{11}\Delta)^{-1}$. As a result, only M'_{11} is of relevance in the analysis of robust stability.

Simultaneous uncertainties or uncertainty of any structure can always be put into the block-diagonal form of Eq. (22) by just constructing the associated matrix M (Doyle, 1982, Doyle *et al.*, 1982). Doyle (1982) has introduced the concept of a

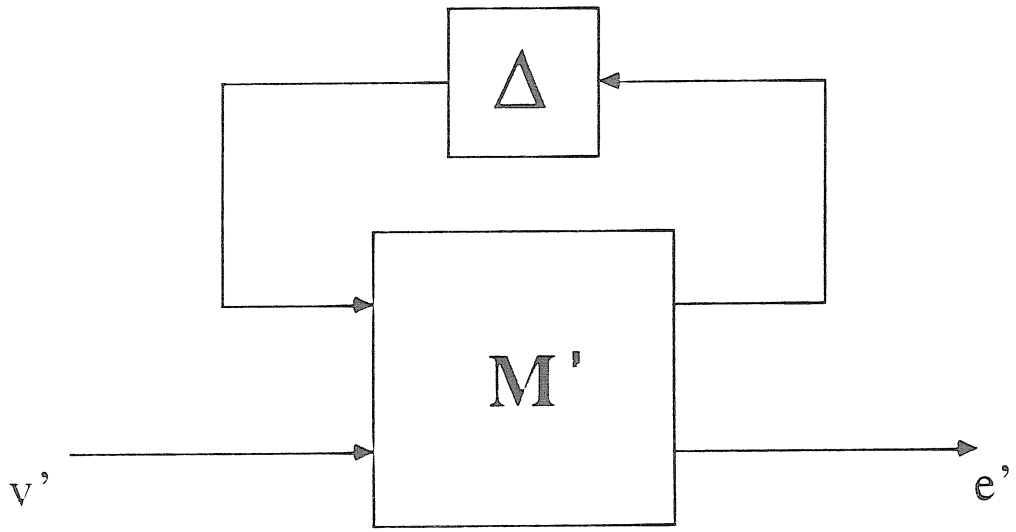

Figure 5 General interconnection structure for analysis (controller C imbedded in M').

structured singular value (SSV, μ) to analyze the robustness characteristics of systems with block-diagonal perturbations. The SSV is a generalization of the notion of maximum singular value for the case of block-diagonal structures. Suffice it to say here that μ depends not only on M as $\bar{\sigma}$ does, but also on the structure assumed for Δ. For the case when Δ is assumed to be full, μ reduces to $\bar{\sigma}$.

Consider now a system with uncertainty of block-diagonal structure. If the usual maximum singular value is employed, the block structure of Δ has to be ignored and a sufficient condition for robust stability is

$$\|M'_{11}\|_\infty \triangleq \sup_\omega \bar{\sigma}(M'_{11}(j\omega)) \leq 1 \quad . \tag{25}$$

Conservatism is introduced when we ignore the block structure, since more plants than necessary are then included in the uncertainty set Π. On the other hand, a necessary and sufficient condition for robust stability is given by

$$\sup_\omega \mu(M'_{11}(j\omega)) \leq 1 \quad . \tag{26}$$

The techniques to compute μ are based on several of its properties (discussed by Doyle (1982)).

Robust Performance. Probably a more important result of the Structured Singular Value theory is that it provides necessary and sufficient conditions for robust stability *and* robust performance (Doyle, 1984). This applies to the case in which the performance specifications are stated in the H_∞-framework. In this framework the robust performance specifications require the output e' to be unit-norm-bounded for all unit-norm-bounded inputs v' and all plant perturbations Δ, or, equivalently,

$$\|F_U(M',\Delta)\|_\infty \leq 1 \quad . \tag{27}$$

Condition (18) is a special case of condition (27).

Conditions for robust stability and robust performance are equivalent in the ∞-norm. Condition (27) is a necessary and sufficient condition for stability of the system $F_U(M',\Delta)$ in the face of (full) perturbations Δ_P norm-bounded as defined by Eq. (14) (Fig. 6a). Thus, robust performance of the system M' is equivalent to robust stability in the presence of the two simultaneous perturbations Δ and Δ_P. In other words, simultaneous stability and performance are guaranteed by a stability condition. In order to combine the two perturbations into one, they have to be put into block-diagonal form

$$\Delta' = \begin{bmatrix} \Delta & 0 \\ 0 & \Delta_P \end{bmatrix} \tag{28}$$

(Fig. 6b). Stability and performance robustness are clearly achieved simultaneously if, and only if,

$$\sup_\omega \mu(M'(j\omega)) \leq 1 \quad , \tag{29}$$

where μ is now calculated on the basis of the whole interconnection matrix. If $\overline{\sigma}$ is employed instead, only an arbitrarily conservative result can be obtained, because the block structure in the perturbation matrix of Eq. (28) is then ignored. Doyle's result is the first one ever reported that provides necessary and sufficient conditions for testing robust stability (with structured or unstructured perturbations) and robust performance.

As noted, condition (29) applies only to the case in which the performance specifications are stated in the H_∞-framework. For the case of specific input signals we are interested in finding the worst possible 2-norm of the error for the specific input vector v and uncertainty description considered. It can be shown (Zafiriou

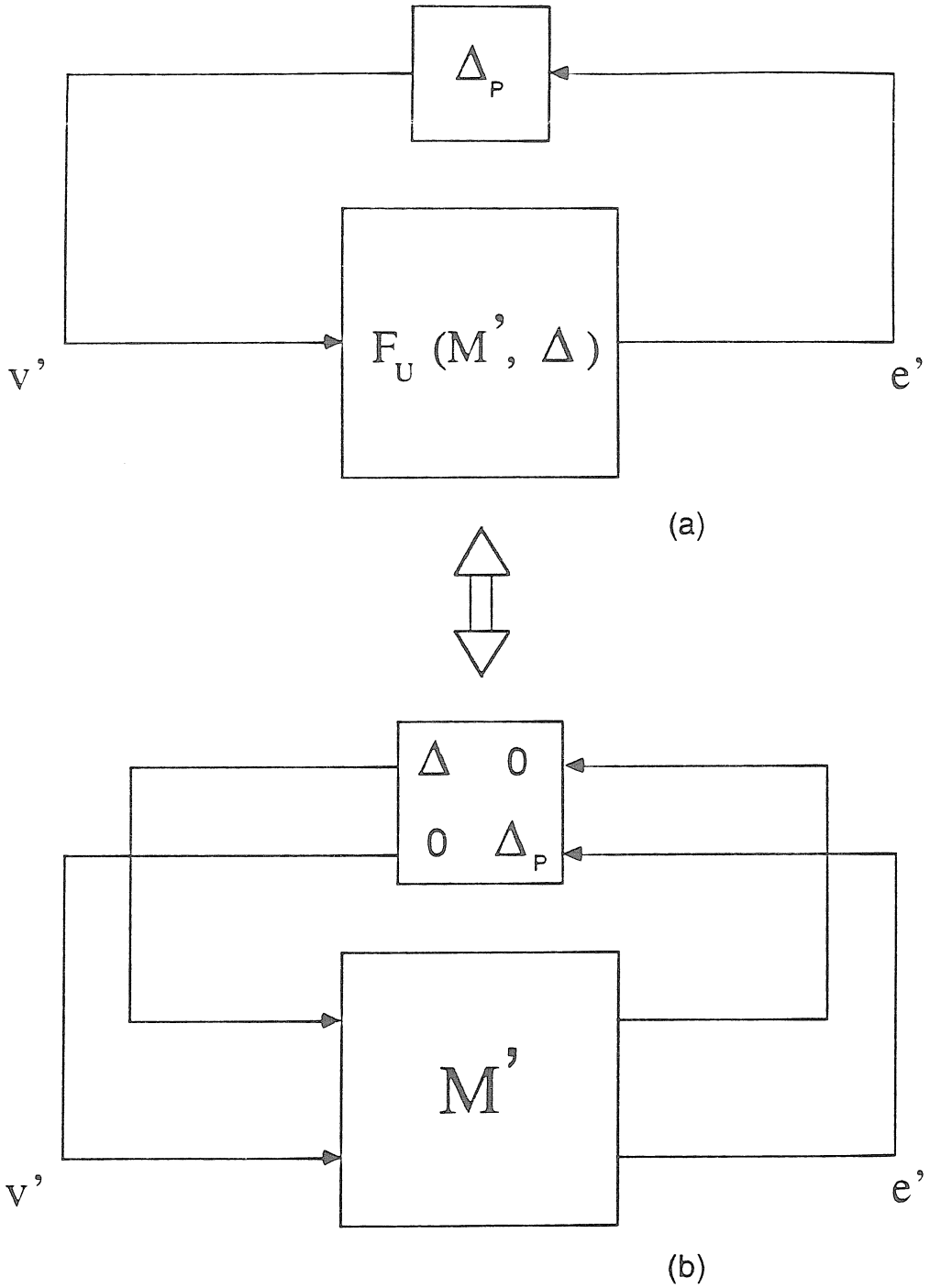

Figure 6 Equivalence of robust performance and robust stability with structured perturbations.

and Morari, 1986) (see also Mandler *et al.* (1986)) that the error 2-norm that would arise when taking the worst plant of Π at each frequency is given by

$$\max_{p \in \Pi} \|e'\|_2 = \|\hat{w}^{-1}\|_2 \quad , \tag{30}$$

where $\hat{w}$ is a scalar frequency-dependent weight, chosen such that

$$\mu(M'') = 1 \tag{31}$$

at each frequency. M'' equals

$$M'' = \begin{bmatrix} M'_{11} & M'_{12}v & 0 \\ \hat{w}M'_{21} & \hat{w}M'_{22}v & 0 \end{bmatrix} \quad . \tag{32}$$

The zero-blocks are appropriately dimensioned to make M'' square. Equation 30 is of considerable importance as a tool for evaluating, *a priori* , the closed-loop system performance in the face of model uncertainty for the case of specific input signals.

3.3 Synthesis

The performance specifications have been stated in terms of the error 2-norm. The synthesis of an optimal controller involves finding the controller that minimizes this norm. When the plant is perfectly known, either the H_2- or the H_∞-optimization problems apply, depending on how the input signals have been characterized (Section 2.1).

In the face of model uncertainty, the best controller is the one that optimizes robust performance. In making this statement we assume that the uncertainty has been appropriately characterized (i.e., non-conservatively, namely, all plants in Π may occur as the actual plant). For the case of performance specifications stated in the H_∞-framework, it follows from Eq. (29) that the controller that optimizes robust performance is the solution to the following optimization problem (Doyle, 1984):

$$\underset{C}{\text{Min}} \sup_{\omega} \mu(M'(j\omega)) = \underset{C}{\text{Min}} \sup_{\omega} \mu(F_L(M,C)(j\omega)) \quad . \tag{33}$$

Clearly, "all" that is needed to find the best controller in the face of model uncertainty is to set up the interconnection structure M (of course, this is not a trivial task since it involves characterizing the nominal plant, the uncertainty and the performance requirements) and to solve Eq. (33). Unfortunately, solving Eq. (33) is a problem of great complexity. Although initial solution strategies have been proposed (Doyle, 1984), finding an efficient numerical technique for the solution of Eq. (33) is a topic of active research, and the "μ-synthesis" approach has not progressed to a stage where it can be applied in a routine manner.

Our robust controller synthesis procedure, on the one hand, draws extensively from the new techniques and analysis tools presented in Sections 3.1 and 3.2. On the other hand, it is a direct extension of the Internal Model Control (IMC) design procedure (as outlined, for example, in our previous paper (Mandler *et al.* , 1986) and by Morari and Doyle (1986)) to the multivariable case. While relatively easy to implement, the procedure usually yields near-optimal controllers in the face of model uncertainty.

The IMC controller Q is related to the classical feedback structure controller C by

$$Q = C(I + \tilde{P}\, C)^{-1} \quad , \tag{34}$$

where $\tilde{P}$ is a model of the plant. $Q = \tilde{Q}F$ is obtained in two steps:

1. A nominal design step ($P = \tilde{P}$), yielding a controller $\tilde{Q}$ of good nominal performance (optimal if desired).

2. The design of the filter F to guarantee robust stability and performance. In general F is of a simple structure with as few adjustable parameters as possible. This simplifies the design procedure and reduces the optimization problem for

robust performance to a parameter search.

Nominal Design Step. In the case of specific input signals, an appropriate choice for $\tilde{Q}$ is in many cases the controller that solves the H_2-optimization problem for the specific input vector under consideration and selected output weights. The solution of this problem is well known. Details on the particular approach we employ to solve this problem are given in the application section.

For $P = \tilde{P}$, $\tilde{Q}$ can be written as

$$\tilde{Q} = \tilde{P}^{-1} \tilde{H} \quad . \tag{35}$$

The H_2-solution makes the complementary sensitivity operator $\tilde{H}$ as close to identity (perfect control) as is allowed by the non-minimum phase characteristics of the plant. $\tilde{H}$ has to include all the RHP zeros of $\tilde{P}$, if such exist, to cancel the resulting RHP poles of $\tilde{P}^{-1}$. This is automatically guaranteed when we solve the H_2-optimization problem.

In a few circumstances, mainly in the case of high-condition-number plants, choosing $\tilde{Q}$ to be as close to the plant inverse as possible (cf. Eq. (35)) may not be appropriate since it may have negative effects when it comes to robust performance considerations (Doyle, 1984). In these cases, if the H_2-solution procedure is used as the nominal design step, in general only full (instead of diagonal) filters F will be able to provide reasonably good robust performance, namely, small values of μ. Adjusting a small number of parameters of a full filter may, in general, suffice; in the most difficult cases the direct application of the μ-synthesis approach may be justified.

Alternative approaches to the design of $\tilde{Q}$ may be applied. These include methods involving the direct specification of $\tilde{H}$ (the closed-loop transfer matrix) according to the designer's own choice of desired properties for the closed-loop system, for example, a decoupled response, one output more important than

another, etc. (Holt and Morari, 1985). Zafiriou and Morari (1985) have formalized such a procedure for the case of sampled-data controllers. Finally, $\tilde{Q}$ can also be designed to satisfy an H_∞-optimality criterion.

Filter Design. The IMC filter that we consider has the general structure (shown for the case of a 2x2 system)

$$F(s) = \begin{bmatrix} \dfrac{1}{(\lambda_1 s^2+\lambda_2 s+1)^n} & \dfrac{\alpha\, s}{(\lambda_5 s^2+\lambda_6 s+1)^n} \\ \dfrac{\alpha\, s}{(\lambda_3 s^2+\lambda_4 s+1)^n} & \dfrac{1}{(\lambda_7 s^2+\lambda_8 s+1)^n} \end{bmatrix}, \tag{36}$$

where $\Lambda = (\lambda_1, \cdots, \lambda_n)^T$ is an array of adjustable filter parameters and α can be chosen as either zero (diagonal filter) or one (full filter). Of course, more complex filter structures can be specified, but this does not affect the considerations to follow for the selection of the filter parameters. Note that $F(0) = I$. This is required so that the closed-loop system will retain its asymptotic tracking properties, i.e., no steady-state offset in any channel.

For robust stability, Λ is specified to satisfy condition (26). For (near-optimal) robust performance, consider first the case in which the μ-analysis theorem can be directly applied (performance specifications stated in the H_∞-framework). F may be designed with an H_∞-type of objective, even in the case in which $\tilde{Q}$ is obtained as an H_2-optimal controller in the first step of the design procedure (Zafiriou and Morari, 1986). Because $\tilde{Q}$ is given, it can be imbedded into the interconnection structure. Let us now call M the interconnection structure that is obtained when F appears instead of C as the lower block in Fig. 4. Then the optimization problem is clearly given by

$$\min_{\Lambda} \sup_{\omega} \mu(F_L(M,F)(j\omega)) \quad . \tag{37}$$

A gradient search technique (Zafiriou and Morari, 1986) may be employed to find

the filter parameters that minimize μ. In this way the controller is obtained that results in the best robust performance for the class of controllers given by $Q = \tilde{Q}F$ and Eq. (36). Clearly, this is not the actual optimal robust performance, since the controller is restricted to be of a special structure. On the other hand, this structure is general enough that the actual optimum may be closely approached in many cases.

Consider, finally, the case of specific input signals and performance specifications in terms of $\|e'\|_2$. From Eq. (30) the optimization problem is now

$$\min_{\Lambda} \max_{p \in \Pi} \|e'\|_2 = \min_{\Lambda} \|\hat{w}^{-1}\|_2 \quad . \tag{38}$$

Details on how to compute the necessary gradients to solve this optimization problem are provided by Zafiriou and Morari (1986).

4. CONTROLLER DESIGN FOR THE REACTOR SYSTEM. CASE-STUDY I

4.1 Control Objectives and Control Configuration

The laboratory fixed-bed methanation reactor system under study is described in detail by Mandler *et al.* (1986). In short, in the reactor a CO/H_2 feed reacts catalytically to produce CH_4. As in that work, the operating conditions are selected to correspond closely to those expected for the single-pass operation of the laboratory experimental reactor. For the case-study considered here, the main control objective is, as before, the regulation of the reactor outlet temperature in the face of sustained disturbances in the inlet CO concentration. In this way it is expected to indirectly achieve regulation of the product (CH_4) concentration, which cannot be measured on-line, as well as to prevent the reactor from "running away" following a large disturbance in the inlet CO.

Mandler *et al.* (1986) showed that, for the SISO configuration with T_{in} as the manipulated variable, a fundamental limitation to the achievable control quality

results from the fact that the corrective action resulting from a change in the inlet temperature travels along the bed much more slowly than the concentration disturbance itself. With such a control configuration, it is therefore impossible to avert reactor runaway (independently of the controller employed), when the disturbance is so large as to cause the runaway to occur faster than it takes the thermal wave to reach the reactor outlet. To attack this problem the authors proposed the use of the total molar flow rate F_P as a second manipulated variable, in a coordinated fashion with T_{in} for the regulation of T_{out}. The design of the control laws for such a configuration was not addressed, however.

Because it is actually preferable not to have to change the total molar flow rate from the value prescribed by the process requirements, the specification of a second control objective becomes appropriate, this second objective being to return F_P to its nominal value as quickly as possible. The system considered is therefore a 2-input, 1-output system with certain extra performance requirements on one of the inputs. Alternatively, the system can be written as a multi-input multi-output (MIMO) system, with F_P considered both as an input to and an output from the process, namely:

$$\begin{bmatrix} F_P \\ T_{out} \end{bmatrix} = \begin{bmatrix} 1 & 0 \\ p_F & p_T \end{bmatrix} \begin{bmatrix} F_P \\ T_{in} \end{bmatrix}, \tag{39}$$

where p_F is the transfer function between F_P and T_{out} and p_T is that between T_{in} and T_{out}. Writing the system as in Eq. (39) allows us to specify the relative importance of maintaining T_{out} at its set-point or F_P at its nominal value by means of a ratio between two scalar output weights and to include the possibility of disturbances acting directly on the flow rate. By writing the system as in Eq. (39), it can be clearly seen that the fundamental limitation to the closed-loop performance is actually not removed by adding F_P as a manipulated variable, since the right-half-plane (RHP) zeros of the transfer matrix are identically those of the transfer function p_T.

However, the performance in terms of T_{out} *can* actually be improved, although at the expense of having to move F_P away from its nominal value for a while. Reactor runaway can be easily prevented as well.

Case-study I addresses the design of the control laws for the system given by Eq. (39), the control objectives being the regulation of T_{out} around its set-point value (by means of T_{in} and F_P) and driving F_P back to its nominal value as soon as allowed by the requirements on T_{out}. The general design procedure of Section 3 is applied and demonstrated. The closed-loop system under consideration is shown in Fig. 7 in the framework of the IMC structure. Only the disturbance-rejection problem and the case of specific input signals are addressed. Different elements of the block diagram are defined along the lines of the explanation that follows.

4.2 Nominal Design

For illustrative purposes we first present ideal closed-loop responses for the full (49th order) linearized reactor model, assumed momentarily to be a perfect model for the plant. In Fig. 7, for this case, Δ_F and Δ_T equal zero. The closed-loop system is given by

$$e' = \begin{bmatrix} e'_F \\ e'_T \end{bmatrix} = W_o \tilde{S} W_i v' = \begin{bmatrix} -w_1 & 0 \\ 0 & -w_2 \end{bmatrix} (I - \tilde{P}\tilde{Q}) \begin{bmatrix} c_F & 0 \\ 0 & \frac{p_d}{s} \end{bmatrix} \begin{bmatrix} v'_F \\ v'_c \end{bmatrix} . \qquad (40)$$

The input signal v'_c corresponds to a disturbance in the inlet CO concentration. p_d accounts for the effect of this disturbance on the output T_{out}. Since step-changes in x_{CO} will be be considered, $\frac{1}{s}$ is included in the input weight. $c_F v'_F$ is a disturbance in the flow rate due to some external source. For this case-study we assume such disturbances to be negligible and take c_F to be very small. The output weight $\begin{bmatrix} -w_1 & 0 \\ 0 & -w_2 \end{bmatrix}$ allows us to specify the relative importance of regulating one output or another.

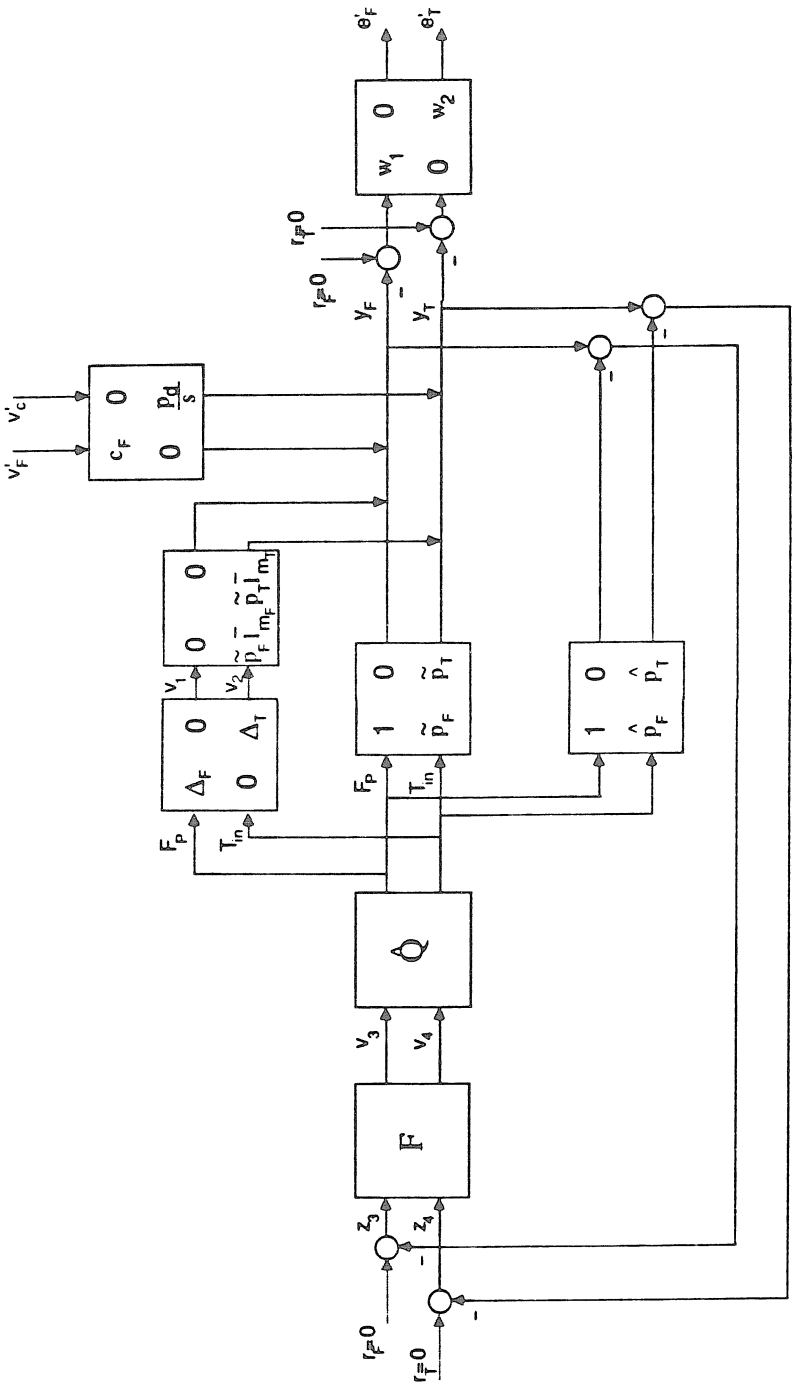

Figure 7 Block diagram for the reactor system. Case-study I. ~ : full models; ^ : reduced-order models.

The optimal controller is found by solving the H_2-optimization problem of Eq. (4) ($\tilde{Q}$ replaces C in the context of the IMC structure). We solve this problem by first setting up the appropriate interconnection structure M that arises when $\tilde{Q}$ is taken as the lower block in Fig. 4, F=I and $\Delta = 0$. A parameterization/unitary invariance/projection approach (Doyle, 1984) is then applied to solve

$$\min_{Q} \|M'_{22}\|_2 = \min_{Q} \|F_L(M_{22},\tilde{Q})\|_2 \quad . \tag{41}$$

The optimal controller obtained has its first column essentially equal to zero (non-square controller). This is expected because of the special structure of this system and the negligible disturbance on the flow rate. The closed-loop responses corresponding to a -0.5 step-change in the inlet CO concentration and to two different sets of output weights are shown in Fig. 8. Note that, when w_1 is set to be small (indicating that excursions in the flow rate are of no great concern), then perfect regulation of T_{out} can be achieved. The maximum excursion of F_P is in this case almost twice its nominal value. As expected, F_P returns to zero after the corrective action of the inlet temperature is felt at the reactor outlet (cf. Mandler *et al.* (1986)). If large excursions of F_P are not acceptable, w_1 has to be increased appropriately. It is shown that the maximum excursion of F_P can be reduced by half while still obtaining a very good regulation of T_{out}.

Fig. 9 shows a comparison between $|\tilde{\epsilon}|$ for the SISO case-study of Mandler *et al.* (1986) and $|\tilde{S}_{22}|$ for the present configuration and the first set of output weights ($\tilde{S}_{22}$ is the element of $\tilde{S}$ corresponding to the same input-output pair as the SISO case). Note the considerable improvement in the closed-loop system bandwidth achieved by employing the flow rate as a second manipulated variable.

4.3 Controller Design in the Face of Model Uncertainty

In order to fully compare the closed-loop performances for the present configuration and for the SISO configuration of Mandler *et al.* (1986), we penalize

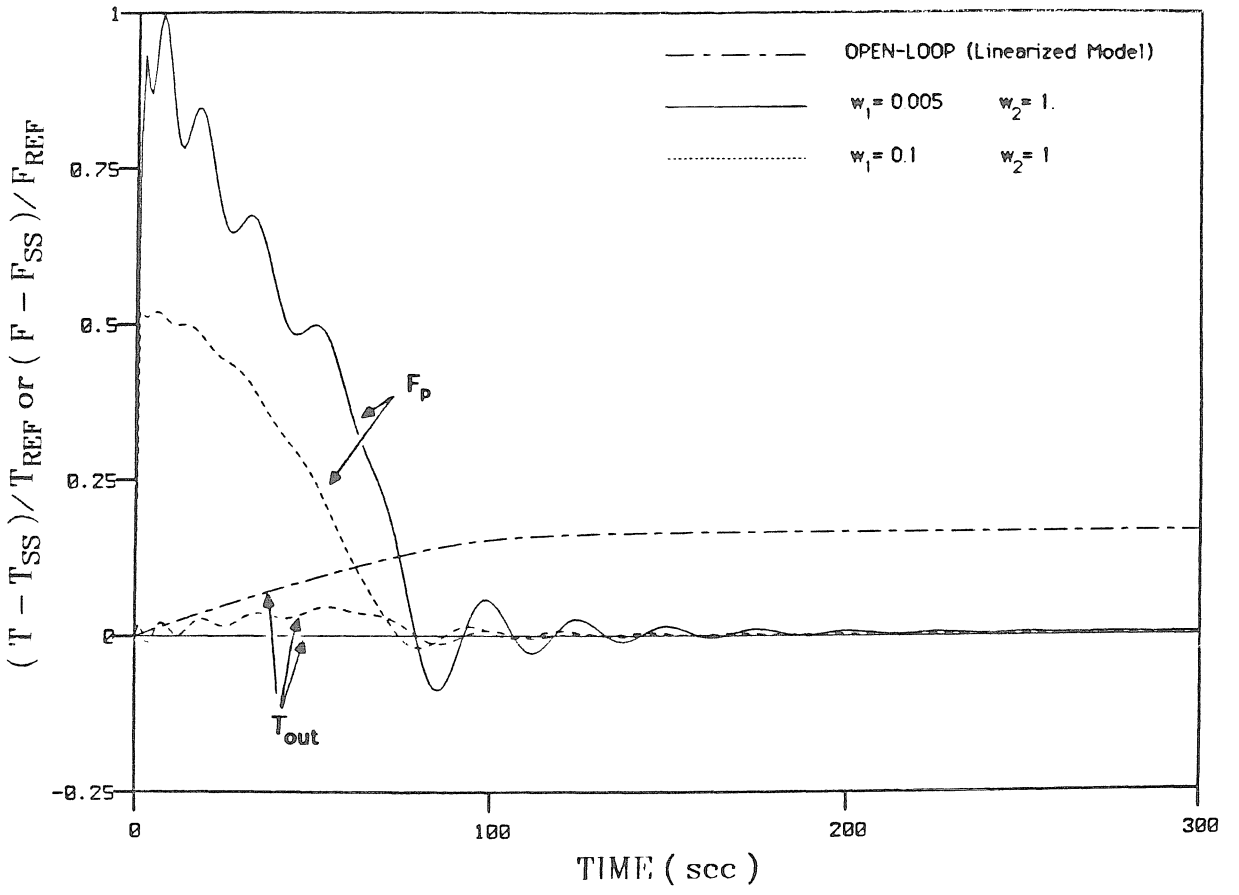

Figure 8 Case-study I. Open- and closed-loop responses to a -0.5 step change in the inlet CO concentration. H_2-optimal controller. (T_{SS} = 546 K; T_{REF} = 40 K; F_{SS} = F_{REF} = 0.022 gmol/sec; linearized model).

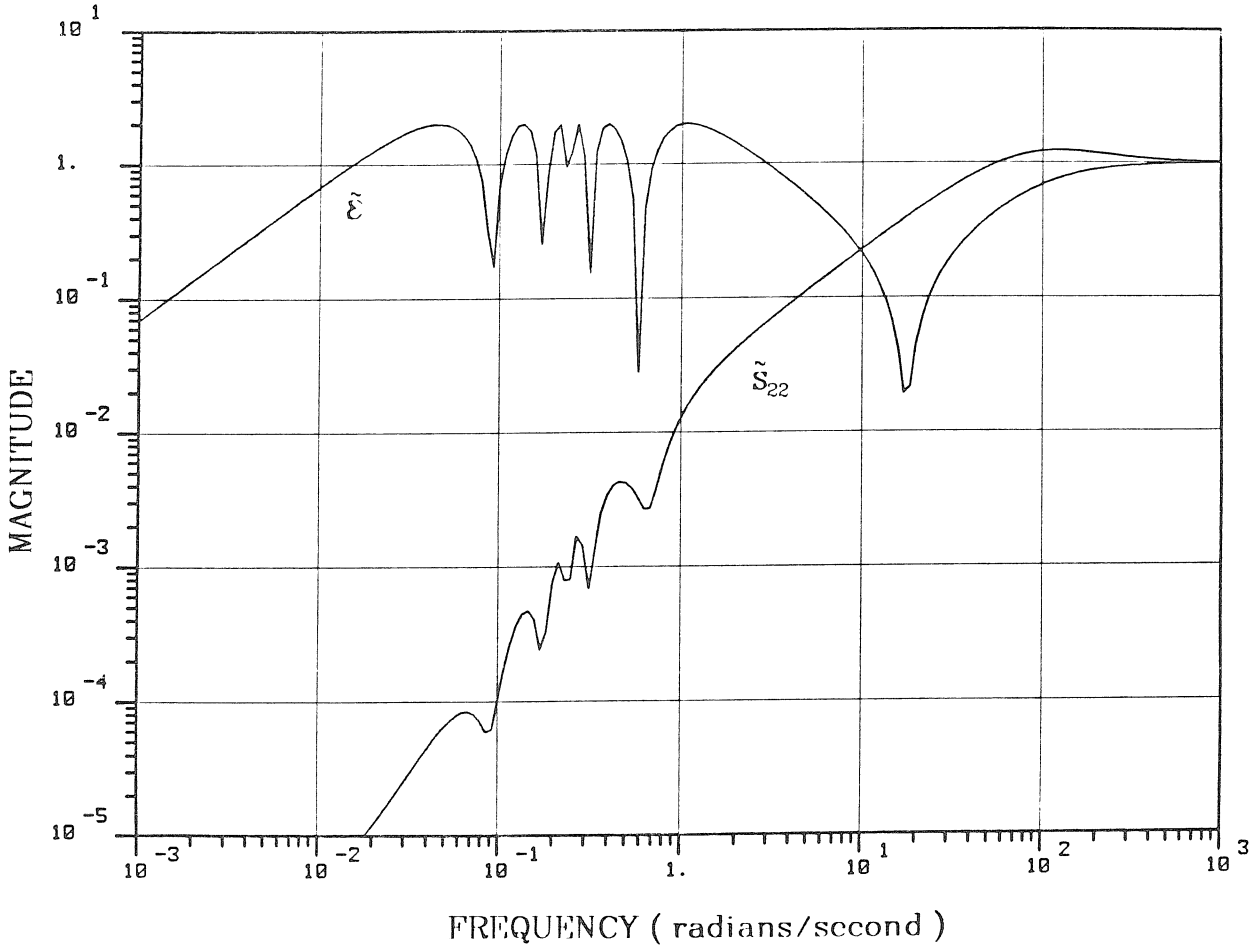

Figure 9 Sensitivity functions. Ideal closed-loop performance. $\tilde{\epsilon}$: sensitivity function for SISO temperature controller of Mandler *et al.* (1986); $\tilde{S}_{22}$: 2,2 element of the sensitivity function for the H_2-optimal controller of case-study I.

the flow-rate excursions very little (w_1 very small). As seen, for the case of a perfect model and for the resulting performance specifications, almost perfect control can be achieved. This was not possible for the SISO case because of the fundamental limitations imposed by the NMP elements. The gap between both cases is, however, reduced in the face of model uncertainty.

Characterization of the Uncertainty. The main source of uncertainty considered results from the fact that the plant is nonlinear, whereas linearized models are employed for the control system design. The procedure employed for the SISO case by Mandler *et al.* (1986) is essentially repeated and the uncertainty resulting from the nonlinearity characterized as parameter variations of the linearized model. The nonlinear model is linearized about different points along the expected trajectory of the closed-loop system, and a family Π of plants is obtained. At each frequency the frequency response of the nominal model is selected to be the center of the smallest circle in the complex plane containing all the plants of Π. The bound $\bar{l}_m$ on the multiplicative uncertainty is found from the radius of these circles. The procedure is carried out separately for each element of the transfer matrix. By finding separate bounds for each element, we are assuming that the uncertainties that apply to each of them are uncorrelated. It is found that assuming full correlation between the uncertainties ($\Delta_F = \Delta_T$ in Fig. 7), or no correlation ($\Delta_F \neq \Delta_T$), affects only slightly the conclusions regarding robust stability and robust performance for this system. Note that the perturbation matrix is diagonal. Also note that the elements 1,1 and 1,2 of the transfer matrix have zero uncertainty. This is reflected by the uncertainty weight (Fig. 7).

The bounds $\bar{l}_{m_F}$ and $\bar{l}_{m_T}$ on the multiplicative uncertainty for each element of the transfer matrix are shown in Fig. 10. Also shown is $\bar{l}_{m_S}$ for the transfer function between T_{in} and T_{out} for the SISO case of our previous paper. The larger uncertainty bound for the multivariable case arises from the fact that the flow-rate

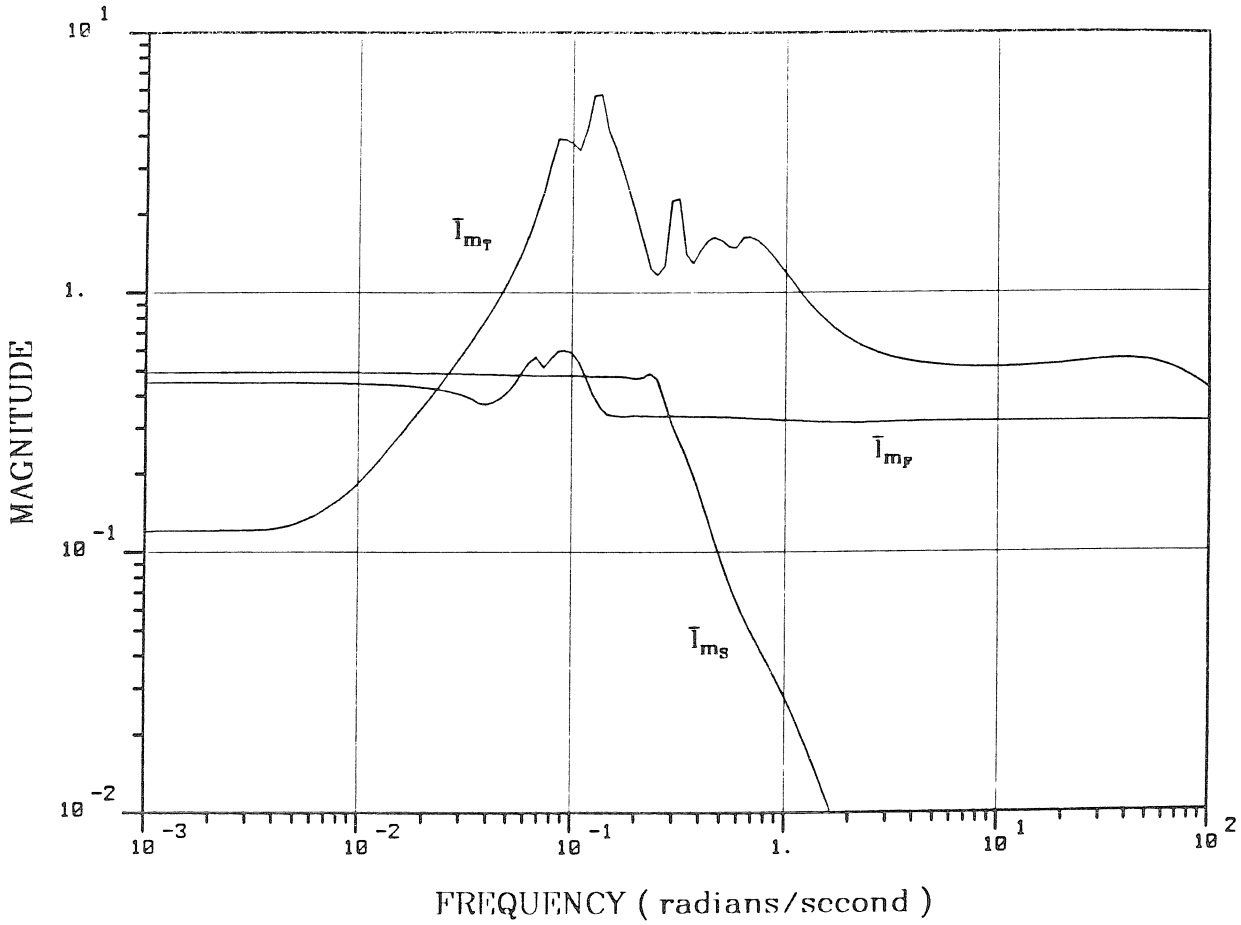

Figure 10 Upper bound $\bar{I}_m$ on the multiplicative uncertainty resulting from the system nonlinearity. $\bar{I}_{m_F}$: for transfer function between F_P and T_{out}. $\bar{I}_{m_T}$: for transfer function between T_{in} and T_{out}, multivariable configuration of case-study I. $\bar{I}_{m_S}$: for transfer function between T_{in} and T_{out}, SISO configuration (Mandler *et al.*, 1986).

variations cause extra uncertainty. The flow rate directly affects the velocity of the thermal wave. The fact that the value of the flow rate cannot be predicted *a priori* (except at steady state) introduces large phase uncertainty that was not present in the SISO case.

Robust Controller Design. In order to guarantee robust stability, it is required to detune the optimal controller $\tilde{Q}$. This is done by means of the filter F. Because $\tilde{Q}$ is fixed, it is imbedded in the interconnection structure, which in this case is the 6-by-6 transfer matrix M between the following inputs and outputs (Fig. 7),

$$\left[F_P, T_{in}, e'_F, e'_T, z_3, z_4\right]^T = M \left[v_1, v_2, v'_F, v'_c, v_3, v_4\right]^T \quad . \tag{42}$$

Because $\tilde{Q}$ has its first column equal to zero and because of the special structure of P, only the 2,2 element of F affects the response. This element is selected to be a first-order lag with time-constant λ. The controller is detuned by increasing λ until the robust stability condition (26) is satisfied. It is found that $\lambda = 30$ sec. is enough to satisfy condition (26).

Fig. 11 shows a comparison between $\mu(M'_{11}(j\omega))$ and $\bar{\sigma}(M'_{11}(j\omega))$ for $\lambda = 30$. $\bar{\sigma}(M'_{11}(j\omega))$ is calculated for two different representations of the uncertainty weights. The weights can be written as in Fig. 7, in which case W_R (cf. Eq. (16)) equals the identity matrix, or as

$$W_L = \begin{bmatrix} 0 & 0 \\ 1 & 1 \end{bmatrix} \; ; \; W_R = \begin{bmatrix} \tilde{p}_F \bar{l}_{mF} & 0 \\ 0 & \tilde{p}_T \bar{l}_{mT} \end{bmatrix} , \tag{43}$$

which is completely equivalent in the case of a diagonal perturbation matrix but leads to entirely different results if the perturbation matrix is assumed to be full. In the first case the values of $\bar{\sigma}$ are much higher than those of μ, and the results are very conservative since they indicate that much stronger detuning is needed to satisfy robust stability. In the case in which the weights are written as in Eq. (43),

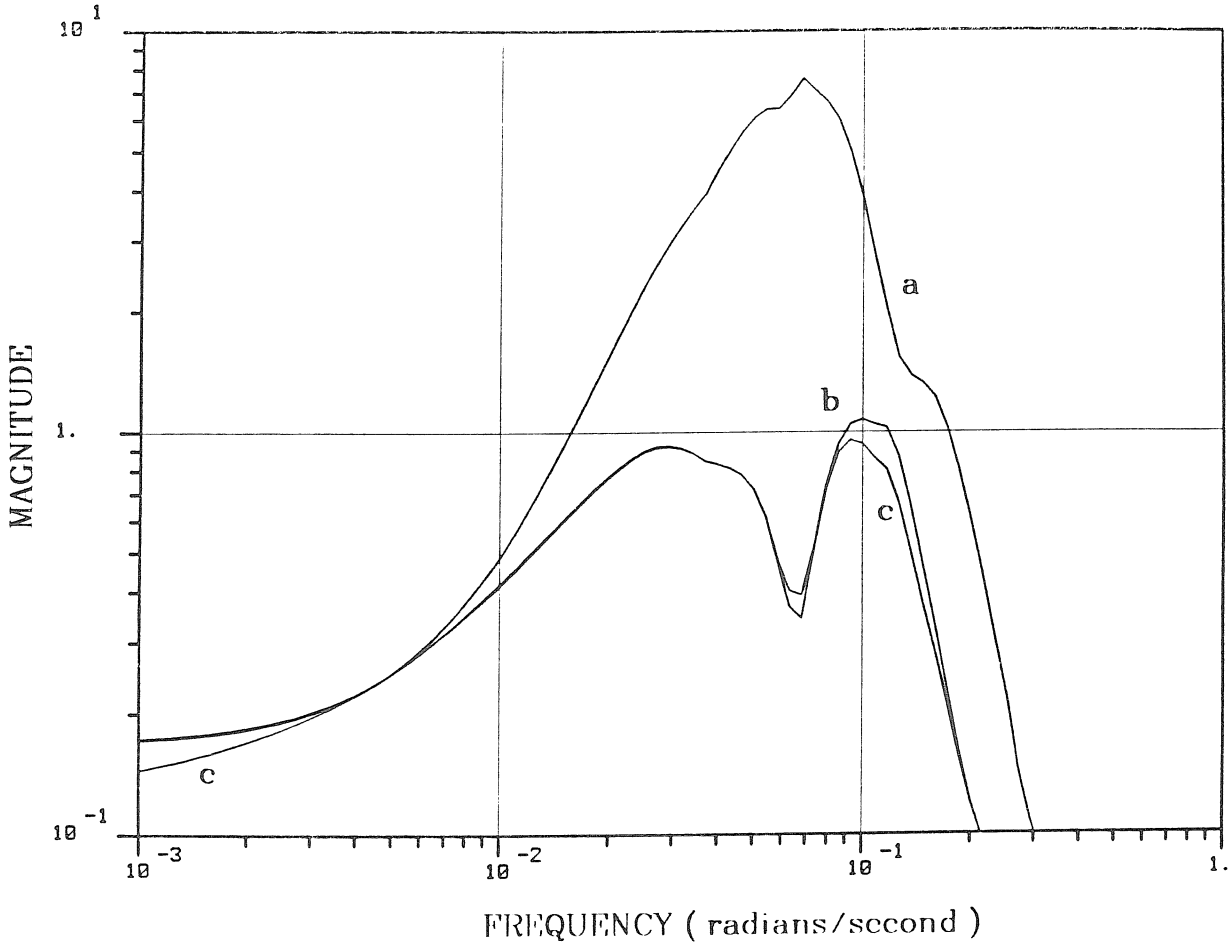

Figure 11 Case-study I. Robust stability analysis. a) $\bar{\sigma}(M'_{11}(j\omega))$ for uncertainty weights of Fig. 7. b) $\bar{\sigma}(M'_{11}(j\omega))$ for uncertainty weights of eq. (43). c) $\mu(M'_{11}(j\omega))$.

the results obtained with $\overline{\sigma}$ are, for this example, only slightly more conservative than those obtained with the SSV. In general, however, finding a correct way of writing the uncertainty weights to obtain non-conservative results after having assumed a full Δ-block, may not be trivial. The SSV, on the other hand, always and automatically provides the tightest bounds. This is a result of the very nature of the computation of μ, which involves essentially a search for the optimal scaling of the uncertainty weights.

As a final step in the design procedure, the search for the filter parameter that optimizes robust performance on the basis of an H_2-optimality criterion is carried out. The value of λ that solves the optimization problem of Eq. (38) is found to be 52 sec.

4.4 Nonlinear Simulation Results ; Discussion

Fig. 12 shows the results of implementing a robust controller with $\lambda = 35$ on the nonlinear plant. It is seen that the outlet-temperature response ceases to be perfect. An interesting situation arises: the increased uncertainty introduced by the use of the flow rate as a second manipulated variable requires relatively stronger detuning for robust stability than what is needed when only T_{in} is employed. This counteracts part of the benefits of using the extra variable. In spite of this, as is apparent from Fig. 12, the multivariable controller still results in a better response than the one obtained for the SISO case for a controller designed by an equivalent procedure. When both cases are compared on the basis of the same weights (w_1 very small and $w_2 = 1$) the error 2-norm for the present case equals 1.24, while in the SISO case 4.85 is obtained. The multivariable configuration proposed therefore offers definite advantages over the SISO configuration in spite of the larger uncertainty.

We now compare the error 2-norm obtained when implementing the linear robust controller on the nonlinear plant with the bounds obtained from the

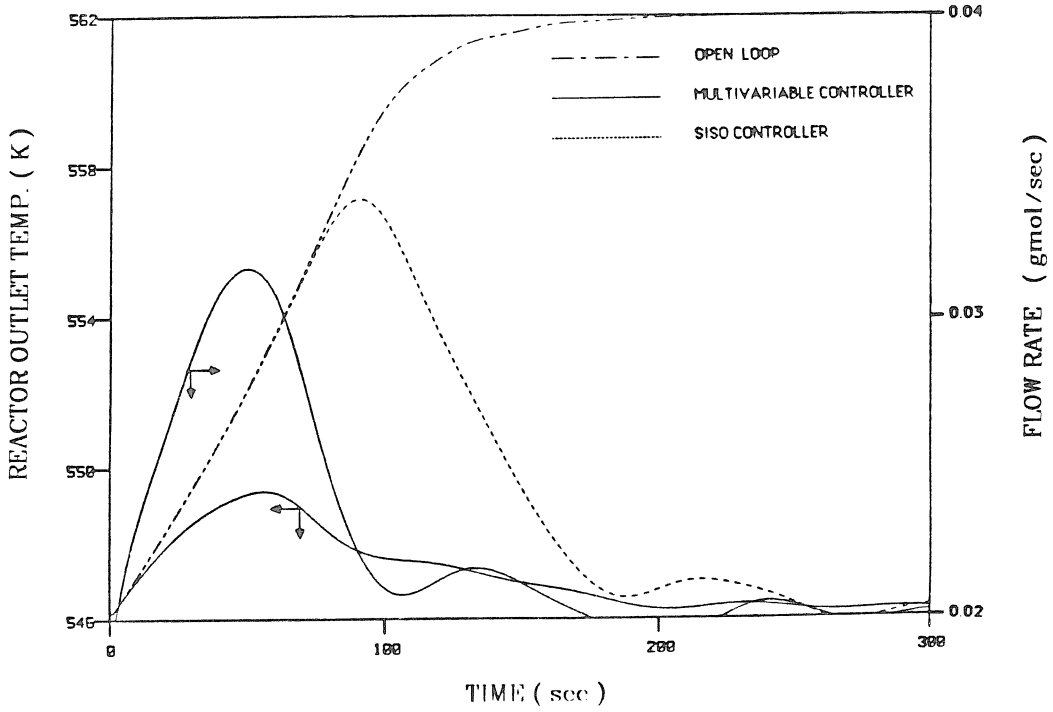

Figure 12 Case-study I. Open- and closed-loop responses to a -25% step change in the inlet CO concentration. Nonlinear model.

analysis. The worst possible error 2-norm predicted, *a priori*, by means of Eq. (30) for the IMC controller designed to have the best robust performance ($\lambda = 52$), equals 2.77. The observed value for this case is 1.7. For $\lambda = 35$ the predicted and observed values are 3.30 and 1.24, respectively. It can be seen that the prediction is relatively conservative. More significantly, controllers with $\lambda < 52$ are observed to have better performance than the one with $\lambda = 52$ when applied to the nonlinear system. Because the bounds obtained through Eq. (30) are tight, the source of conservatism must reside in the uncertainty characterization process.

The appropriate characterization of model uncertainty resulting from system nonlinearity is a challenging task. In spite of this, for the SISO case studied by Mandler *et al.* (1986), very tight bounds were obtained by the same basic methods as those employed here. In the SISO system the nature of the nonlinearity was amenable to treatment by linear methods. This is not the case, however, for the present multivariable system. The uncertainty in our system is time-varying, and this nature is not adequately captured by the methods employed. The methods are based on the definition of a set of possible plants whose elements may occur as the actual plant at all frequencies. (The perturbations are assumed to be time-invariant .) However, including plants corresponding to the expected highest flow rates at the low frequencies is a conservative step, since it is known that the flow-rate deviation drops to zero at steady state. Including plants corresponding to the low flow rates at the high frequency range also adds to the conservatism. An alternative approach for the selection of the nominal model and the uncertainty characterization is applied in the case-study of Section 5.

A second possible source of conservatism resides in the fact that, because of the large phase uncertainty, disk-shaped regions are not very adequate to cover the set of possible plants. Smaller regions of other shapes (sectors of annuli) may be enough to include all possible plants. However, regions of shapes more general than

disks have more complex mathematical descriptions and present theoretical/computational difficulties in the context of control system design. Techniques for analyzing robust stability and performance of multivariable systems for the case in which the uncertainty of the individual elements is described by regions other than disks have not been developed yet and present an open research problem.

5. CONTROLLER DESIGN FOR THE REACTOR SYSTEM. CASE-STUDY II

5.1 Control Objectives and Control Configuration

The second case-study is an extension of the SISO case-study of Mandler *et al.* (1986) in a different direction. The control system here is specifically designed for the regulation of the outlet methane concentration, y_{CH_4}, instead of the outlet temperature. The methane concentration is assumed not to be measurable. The inlet temperature T_{in} is the only manipulated variable; T_{out} is the only measured variable; as before, the rejection of step disturbances in x_{CO} is investigated.

Even though two outputs are involved (one measurable and one not), there exists only one control objective. As a result, SISO schemes may be successfully applied to this system. Robust performance problems that may exist in truly multivariable control systems do not arise in this particular case-study, as is demonstrated later. The extension of this case-study to include additional control objectives, besides the regulation of the methane concentration, is left as a subject for a subsequent paper.

The general procedure described in Section 3 is again applied to this system. In our approach, instead of explicitly designing an estimator or observer for inferring y_{CH_4} from T_{out}, we directly solve for the optimal controller that minimizes the 2-norm of the error in y_{CH_4} following the disturbance. This is accomplished by writ-

ing the appropriate interconnection structure and solving the standardized optimization problem given by Eq. (41). In the second step of the design procedure, as before, robust stability and robust performance considerations are explicitly incorporated.

The block diagram for this configuration is shown in Fig. 13a in the framework of the IMC structure, together with the interconnection structures employed for the design of the optimal controller $\tilde{Q}$ in the nominal case (Fig. 13b) and for the design of the filter F for robust stability and performance (Fig. 13c).

5.2 Nominal Design

From the interconnection structure of Fig. 13b it can be seen that the optimal controller $\tilde{Q}$ is independent of $\tilde{p}_T$. The closed-loop system is simply given by

$$e'_{y_{CH_4}} = (\tilde{p}_{dc} - \tilde{p}_c \tilde{Q} \tilde{p}_{dT})\frac{1}{s}v'_c \quad . \tag{44}$$

The H_2-optimal controller results in no steady-state offset ($\tilde{Q}(0) = \tilde{p}_c(0)^{-1}\tilde{p}_{dc}(0)\tilde{p}_d(0)^{-1}$).

The closed-loop performance is affected by the RHP zeros of $\tilde{p}_c$. Fig. 14 shows the H_2-optimal y_{CH_4} response to a -0.5 step-change in x_{CO} for the linearized model. Fig. 14 shows, in addition, the open-loop responses of y_{CH_4} to the same disturbance, and to a step-change in the manipulated variable T_{in}. $\tilde{p}_c$ has an even number of RHP zeros with one pair relatively close to the origin. Even though the RHP zeros don't manifest themselves in the open-loop response through an apparent time-delay or through wrong-way behavior, their presence affects the closed-loop performance and eliminates the possibility of perfect control, even for perfect models. The reason for the existence of a fundamental limitation on the closed-loop performance can be understood from the fact that, even though a change in T_{in} immediately changes the CH_4 concentration at the reactor inlet and this change almost immediately has an effect on the concentration at the outlet, the most important effect,

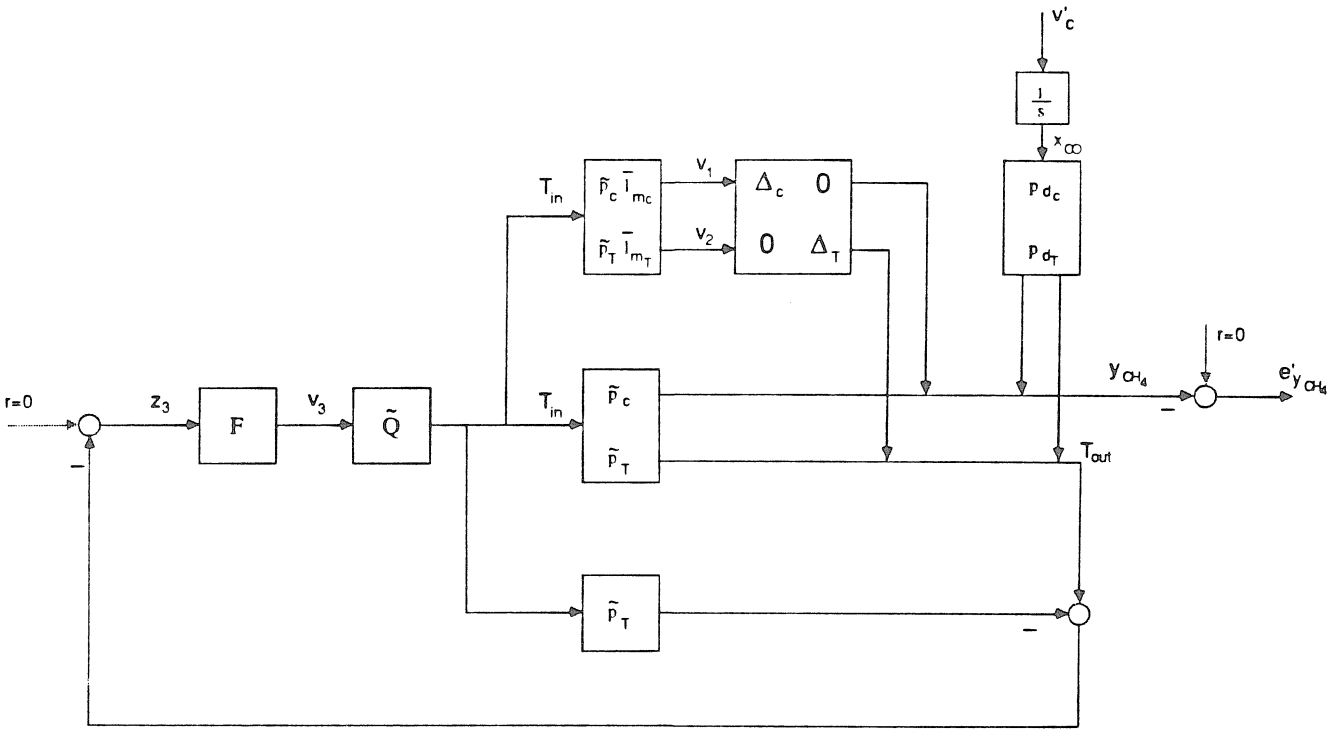

(a)

Figure 13 a) Case-study II. Block diagram for the reactor system.

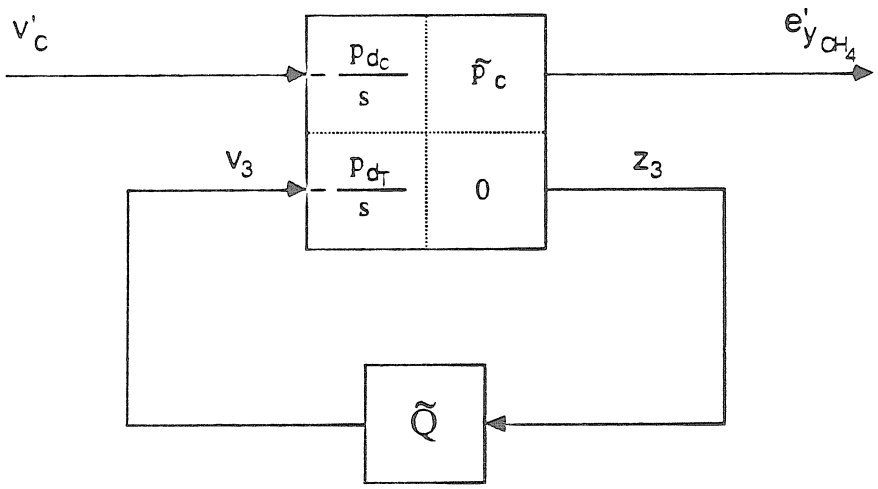

(b)

Figure 13 b) Case-study II. Interconnection structure for the nominal case.

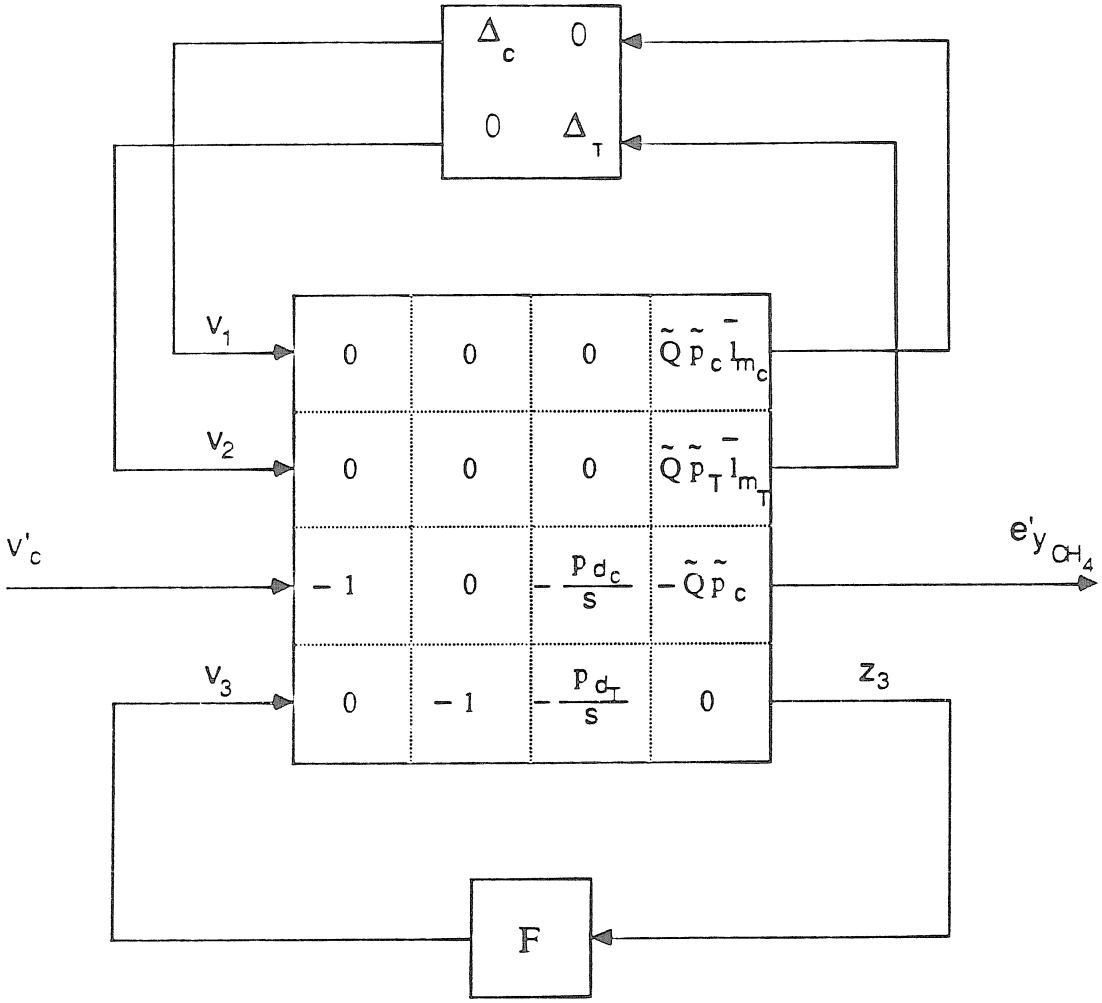

(c)

Figure 13 c) Case-study II. Interconnection structure employed in the design of F for robust stability and performance.

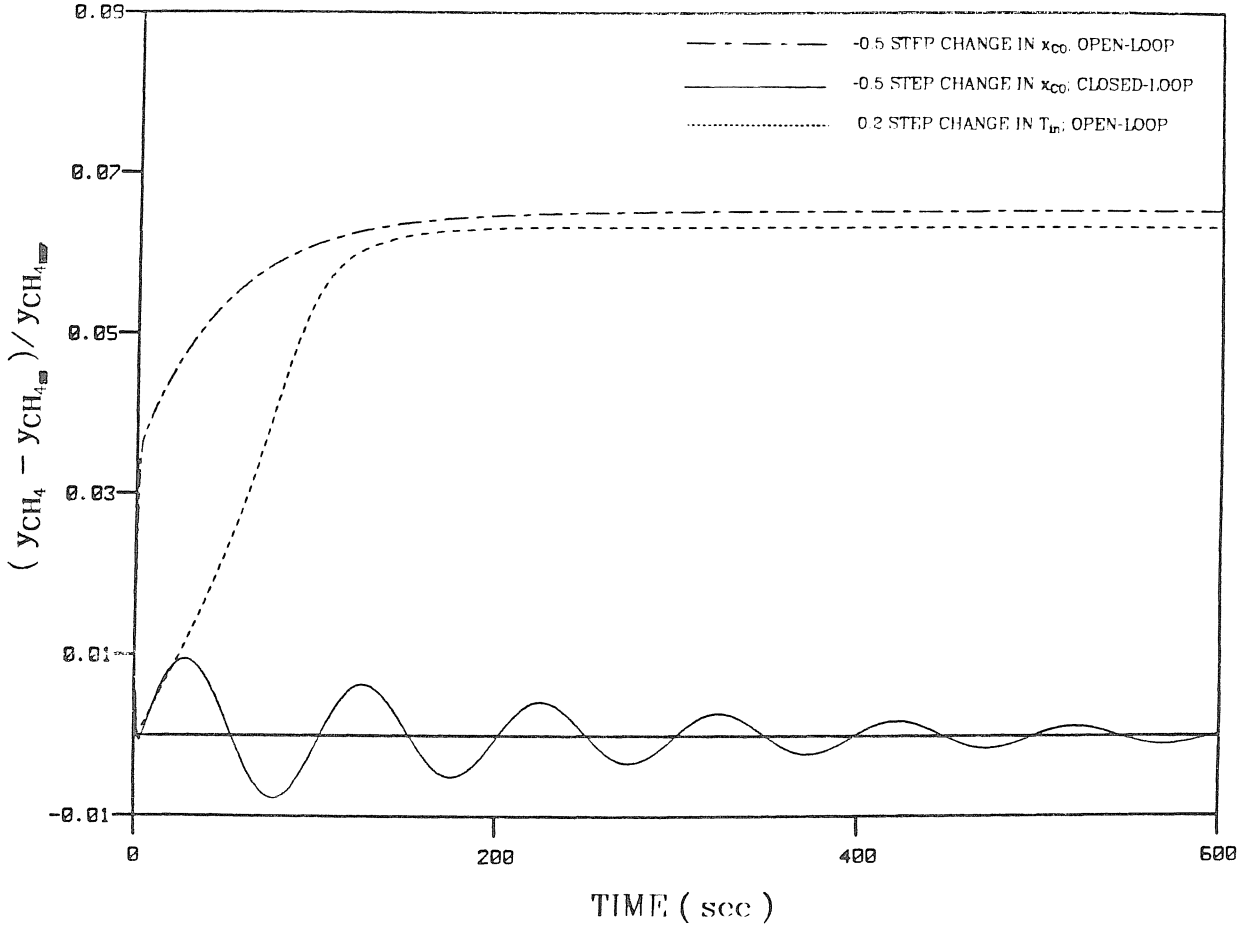

Figure 14 Case-study II. Open- and closed-loop responses of y_{CH_4}. Linearized model. H_2-optimal controller. ($y_{CH_{4SS}}$= 3.55e-03; $y_{CH_{4REF}}$= 0.03; $x_{CO_{SS}}$= 0.045; T_{in}= 529.8 K; T_{REF}= 40 K; F_{SS}= 0.022 gmol/sec.

namely, the accumulated change in y_{CH_4} due to temperature changes along the entire reactor, is still very much affected by the relatively slow movement of the thermal wave (cf. Mandier *et al.*, 1986).

5.3 Controller Design in the Face of Model Uncertainty

Characterization of the Uncertainty. Because there is no feedback of the product concentration, perfect asymptotic regulation of y_{CH_4} can be achieved only if all the steady-state gains of the relevant transfer functions of the actual plant are perfectly known.

The uncertainty considered is mainly a result of the system nonlinearity. If the main concern resides in obtaining little or no steady-state offset for the unmeasured output variable, and if step disturbances are expected, a reasonable nominal model to choose is one corresponding to a linearization about the new steady state at which the system will arrive following the expected average disturbance. For this particular nominal model, the multiplicative uncertainty in each element resulting from the system nonlinearity is expected to be low at the low frequencies.

The following procedure is carried out to obtain good uncertainty bounds for this particular case-study. Each element of the transfer matrix is studied separately as a SISO system. First, we assume a form for the uncertainty bounds. Simple expressions of the form $\frac{\beta s}{\beta s + 1}$ are selected for both $\bar{l}_{mT}$ and $\bar{l}_{mc}$. These expressions satisfy the requirement stated above of low uncertainty at the low frequencies. Next, we carry out closed-loop simulations of each nonlinear SISO system with an IMC controller (assuming for once that we can measure the outlet concentration), and we determine the value of the IMC-filter time-constant for which the system goes unstable. For the particular controller found in this way, we next investigate robust stability. Since for this controller the test should *not* predict stability, we adjust $\bar{l}_m$ by means of β until $\sup_{\omega} |\tilde{\eta}\, \bar{l}_m|$ is above 1. In this way, for a -25% x_{CO} step-

change as the expected average disturbance on which we base the nominal model, and for a -35% step-change as the worst expected disturbance, we determine

$$\bar{l}_{mT} = \frac{5s}{5s + 1} \tag{45}$$

and

$$\bar{l}_{mc} = \frac{11s}{11s + 1} \quad . \tag{46}$$

(Recall from Mandler *et al.* (1986) that the CO acts as an inhibitor and, therefore, a negative CO disturbance leads to an increase in the reaction rate, which may lead to reactor runaway. The controller design is carried out specifically for these worst-type disturbances. As will be observed in the simulations, the controller works appropriately, also, for disturbances of the opposite sign. These actually are easier to reject .)

Of course, the characterization of uncertainty has to be carried out *before* the design or application of a control scheme. The philosophy in our approach here is that, once obtained for a simple configuration, the uncertainty bounds for each element can be employed in more complex configurations, although with due caution. An alternative, more rigorous approach for the *a priori* characterization of the uncertainty resulting from the nonlinearity is currently under investigation. In this approach the uncertainty bounds are obtained from an analysis of data from identification experiments involving pseudorandom binary sequence (PRBS) pulsing of the open-loop, nonlinear system.

Robust Stability. Fig. 13c gives the overall interconnection structure employed in determining the values of the filter parameters for robust stability and robust performance. F is a scalar in this case. Because there is no feedback of y_{CH_4}, the uncertainty in p_c clearly does not affect stability. The values of λ that satisfy robust stability (Eq. (26)) are functions of $\bar{l}_{mT}$, $\tilde{p}$, $\tilde{p}_c$, $\tilde{p}_{dT}$ and $\tilde{p}_{dc}$. It is found that for a

first-order filter a very high value of the filter time-constant is required. On the other hand, if a third-order filter is used, $\lambda = 30$ sec. is just enough to satisfy robust stability. Third-order filters are employed throughout this case-study.

H_2-Optimal Filter Design. The search for the filter parameter that optimizes robust performance on the basis of an H_2-optimality criterion is carried out first. The value of λ that solves the optimization problem of Eq. (38) is 31.5, a value quite close to the one at the limit for robust stability. The bound on $\|e'\|_2$ predicted from Eq. (30) for the case of model uncertainty equals 1.05.

H_∞-Optimal Filter Design. We now demonstrate the design of F to satisfy an H_∞-type objective. Here the control objectives are set directly in terms of a bound, $b(\omega)$, on the sensitivity operator. This bound defines the worst closed-loop performance acceptable to us at each frequency. We choose first as an objective

$$b(s) = \frac{15\ s}{100s + 1} \quad . \tag{47}$$

The bound of Eq. (47) indicates that the error should be zero at steady state. In this case b(s) closely bounds above the *nominal* closed-loop transfer function, $\tilde{S}\ W_i = (\tilde{p}_{dc} - \tilde{p}_c\ \tilde{Q}\ \tilde{p}_{dT})$ (which relates x_{CO} and y_{CH_4}), for the controller with $\lambda = 31.5$. We want the performance specifications given through Eq. (47) to be met for the actual plant, or, in other words, for all plants in the uncertainty set. Therefore, for robust performance (cf. Eq. (18)):

$$\underset{P \in \Pi}{\text{Max}}\ \|b^{-1}\ S\ W_i\|_\infty \leq 1 \quad . \tag{48}$$

The optimal filter parameter is found by solving the optimization problem of Eq. (37), and robust performance is evaluated on the basis of condition (29). The optimal filter parameter is found to be $\lambda = 31$, but even for this best filter time-constant $\mu(M'(j\omega))$ lies above 1 at some frequencies with a maximum peak of 1.15. This means that at least one plant exists in the uncertainty set that will not meet

the performance specifications; robust performance cannot be guaranteed. The performance specifications had been selected to be very close to the nominal performance obtained with almost the same controller. It is therefore not surprising that these specifications cannot be met for all plants in the uncertainty set. We can now either improve the uncertainty characterization or relax the performance specifications. We opt for the latter. (We could also investigate different forms for the filter, or employ directly the μ-synthesis approach to find the controller with the optimal robust performance. This is not attempted, since, as demonstrated at the end of this section, the robust performance obtained with our scheme for this particular system is essentially as good as can be possibly obtained .)

The performance specifications are relaxed to

$$b(s) = \frac{18.5\ s}{100s + 1} \quad . \tag{49}$$

For b(s) of Eq. (49), the best filter time-constant is found to be $\lambda = 32$ (only slightly higher than the H_2-optimal filter time-constant), and robust performance is guaranteed since μ is less than 1 for all frequencies. Fig. 15 shows $\mu(M'(j\omega))$ for the optimal value $\lambda = 32$, for $\lambda = 31$, and for $\lambda = 36$. $\lambda = 31$ does not satisfy robust performance as a result of being too close to the robust stability limit, and $\lambda = 36$ as a result of the nominal performance being too degraded.

We now demonstrate that the system studied here is well behaved in the sense that no serious robust performance problem exists for the system and the controllers employed. To do so, we choose b(s) equal to $\tilde{S}\,W_i$ for the controller with $\lambda = 32$. Clearly now,

$$NP = b^{-1}\tilde{S}\,W_i = 1 \quad . \tag{50}$$

We also have $RS = \mu(M'_{11}(j\omega))$ and $RP = \mu(M'(j\omega))$ (cf. Sections 2.3 and 3.2). For SISO systems RP = RS + NP (Eq. (19)). For certain multivariable systems, as pointed out in Section 2.3, $RP \gg RS + NP$ can occur, this being very undesirable. If this occurs,

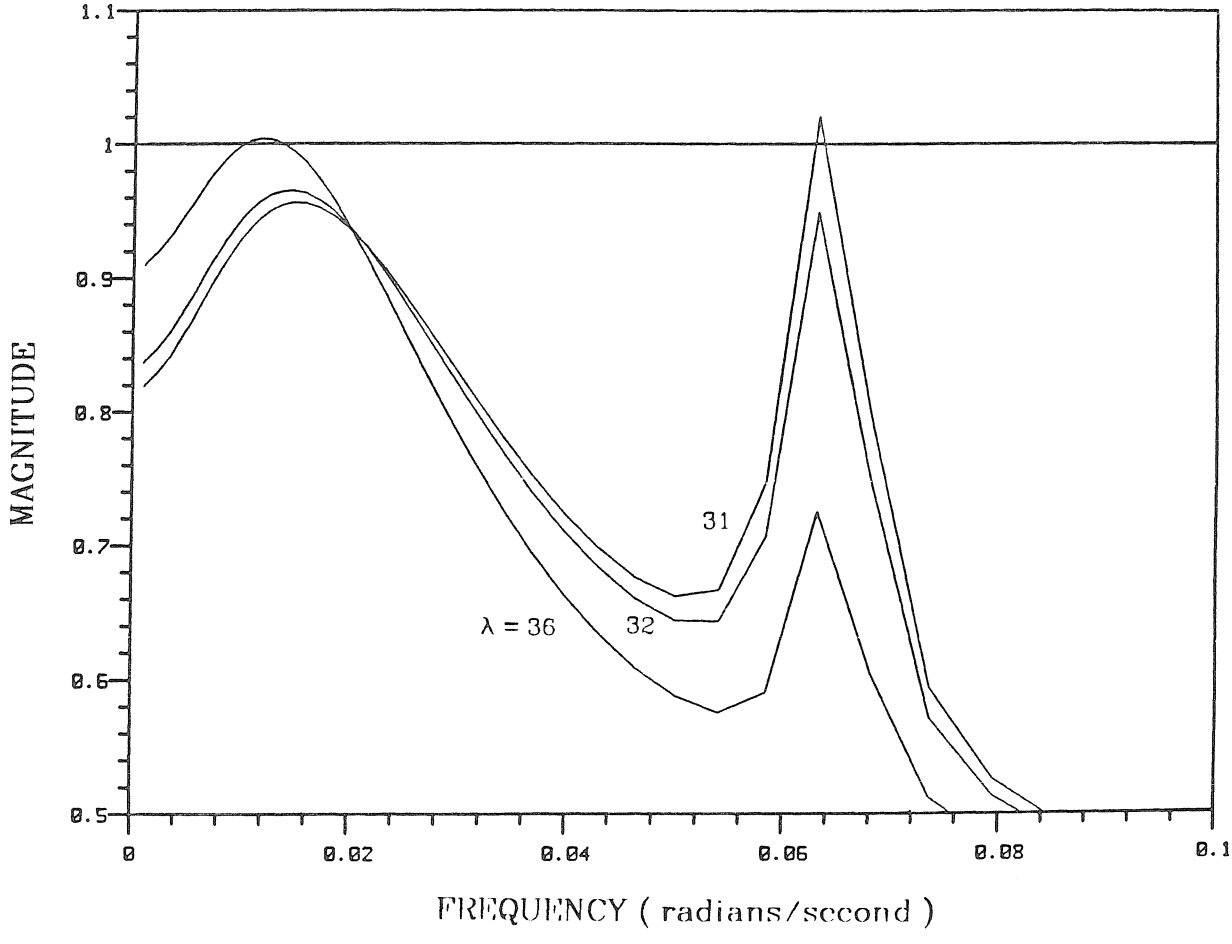

Figure 15 Case-study II. $\mu(M'(j\omega))$ for different values of the filter time constant λ.

the μ-synthesis approach is recommended for finding the controller that minimizes RP. In Fig. 16 it is shown that RP for the present case-study is close to and even less than RS + NP. This is in agreement with the "almost" SISO nature of the system. In this case the application of the μ-synthesis approach is not justified, since the robust performance cannot be radically improved beyond the results of our current design procedure.

5.4 Nonlinear Simulation Results

Fig. 17 shows the open-loop y_{CH_4} response, for the nonlinear plant, to a -25% x_{CO} step disturbance, and the closed-loop response obtained employing the controller with $\lambda = 31.5$, i.e., with the filter designed on the basis of an H_2-optimality criterion (Eq. (38)). The observed value of $\|e'\|_2$ equals 1.06, which is only 1% higher than the predicted worst bound of 1.05 found in Section 5.3. The fact that the prediction is so close to the observed $\|e'\|_2$-value indicates the tightness of the bound when the uncertainty is characterized appropriately. As a reference, Fig. 17 shows is the "best" closed-loop concentration response obtained employing a controller designed for the regulation of the outlet temperature (Mandler *et al.* , 1986). No significant offset in the product concentration is observed when the concentration controller designed here is employed, in spite of the fact that the system is nonlinear and the concentration is assumed not to be measurable.

The linearizations about the "new steady state" are based on expected step-changes of -25%. Therefore, for step-changes of this magnitude, no offset was expected. Fig. 18 shows closed-loop responses obtained with the controller with the H_∞-optimal filter. Responses are shown for disturbances of different magnitudes than the one on the basis of which the nominal controller was designed. It is shown that the offset continues to be negligible for the assumed worst disturbance of -35% and also for disturbances of the opposite sign, which indicates the adequacy of the nominal models employed.

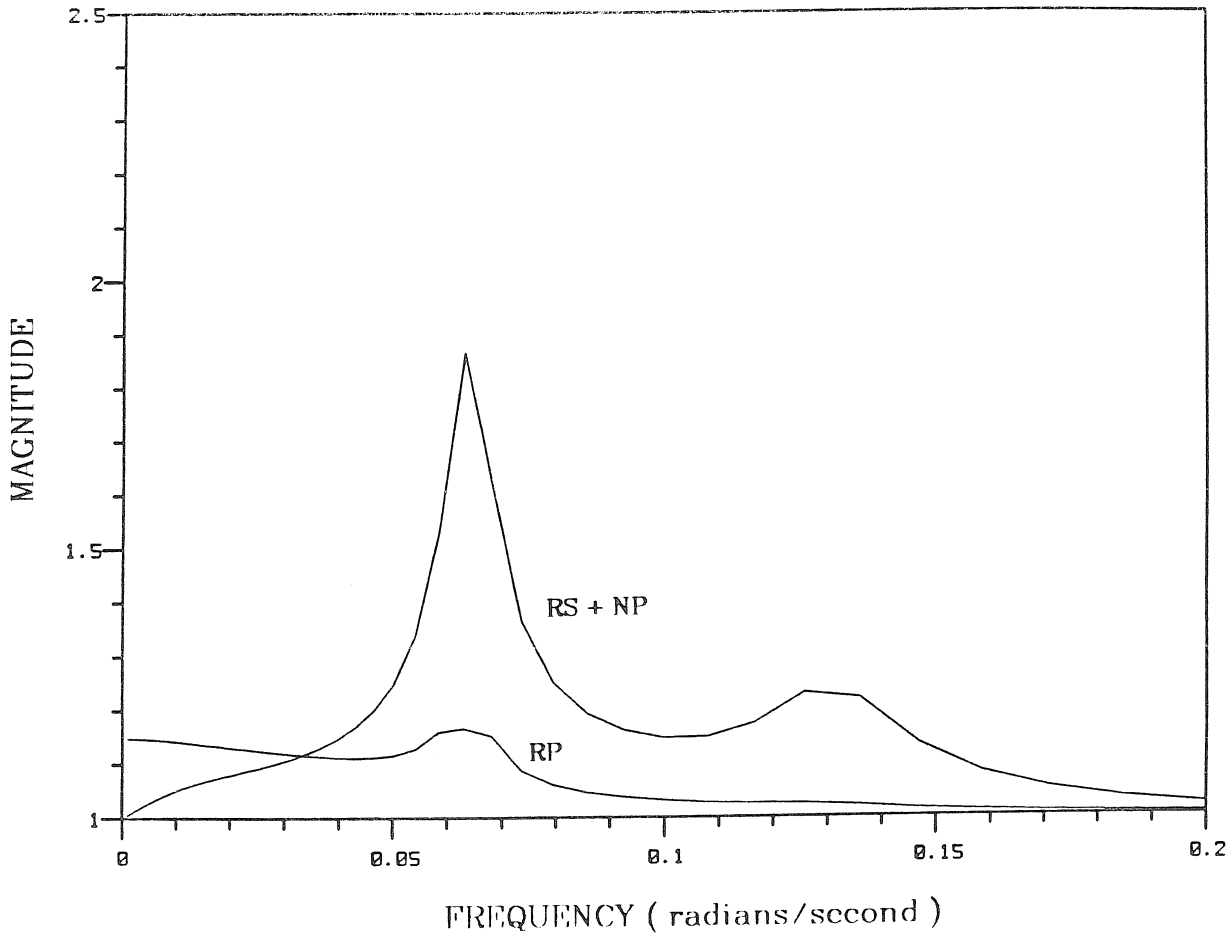

Figure 16 Comparison between the robust performance term and the sum of the robust stability and the nominal performance terms.

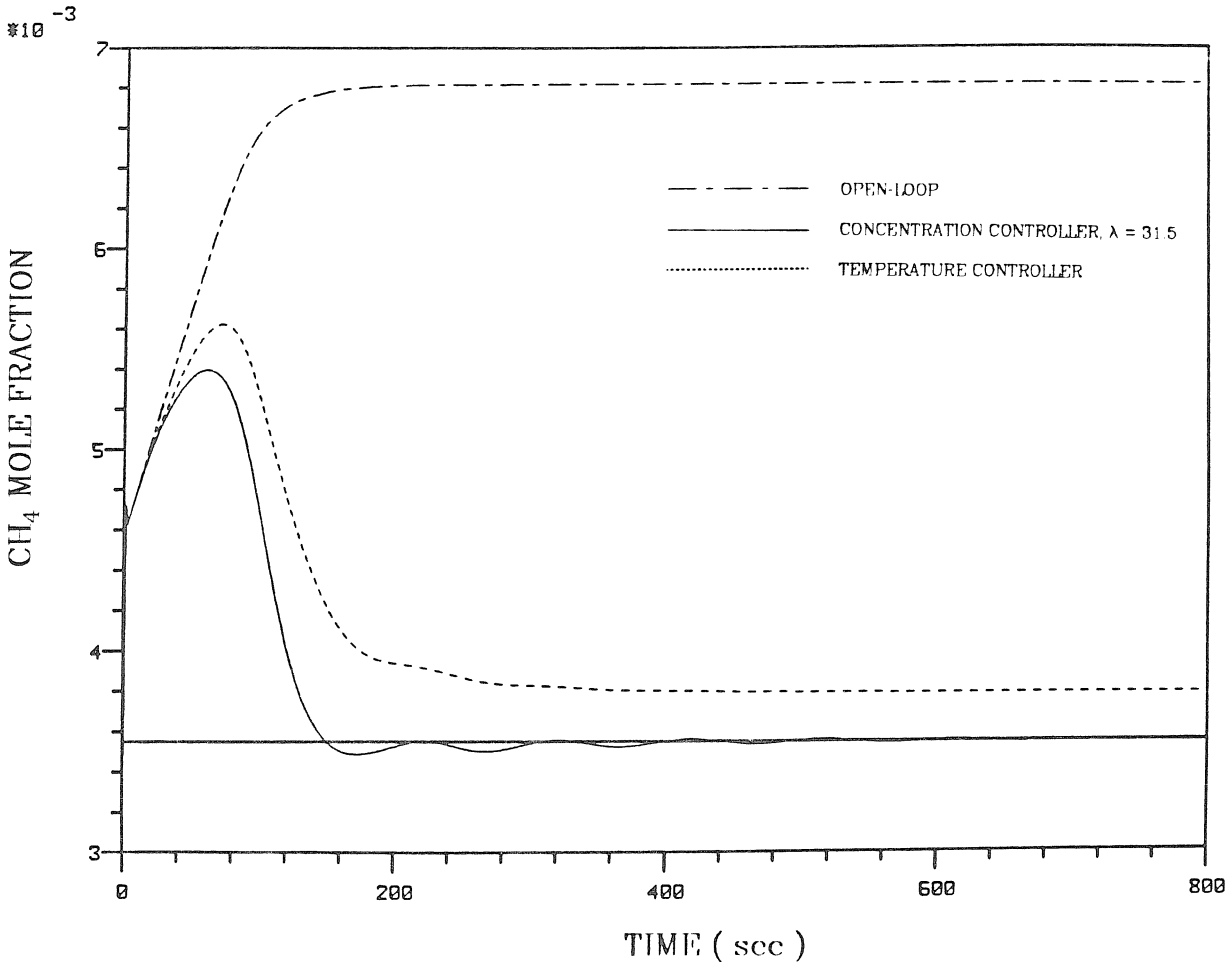

Figure 17 Case-study II. Open- and closed-loop y_{CH_4} responses to a -25% step change in the inlet CO concentration.

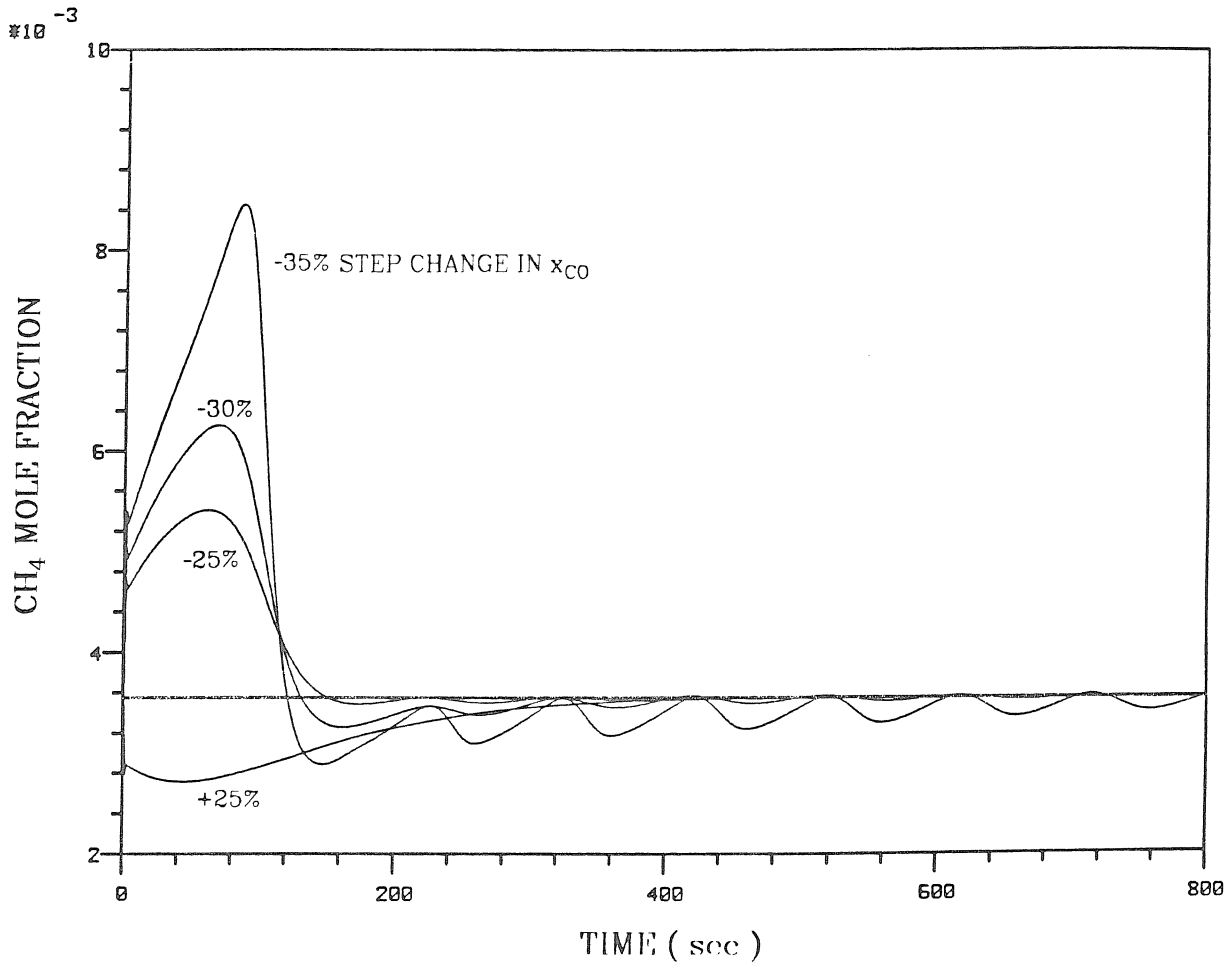

Figure 18 Case-study II. Closed-loop y_{CH_4} responses to x_{CO} step-changes of different magnitudes. $\lambda = 32$.

6. CONCLUDING REMARKS

In addition to addressing the control system design for a fixed-bed reactor, this paper has exposed recent important developments in control theory and has outlined and demonstrated a methodology for multivariable controller design in the face of model uncertainty that is based on these developments. The paper describes one of the first applications of the Structured Singular Value-based analysis and synthesis techniques to a complex chemical process.

In each case-study presented, the controller design procedure was divided into four steps: first, the definition of the control objectives, which not only leads to the selection of the appropriate control configuration but also determines the most adequate design techniques to employ; second, a nominal design step, in which the system-inherent limitations to the closed-loop performance are highlighted; third, a characterization of the uncertainty and the use of this information in the design of robust controllers; and, fourth, the evaluation of the designs through nonlinear simulations.

The power of the new mathematical theory for robust control system design was demonstrated. It was clearly shown, however, that success in applying any robust control design methodology is ultimately dependent on the ability of the engineer to understand and appropriately characterize the system under study.

Acknowledgments

We are thankful to S. Skogestad, J.C. Doyle, E. Zafiriou and D.E. Rivera for many useful discussions. Acknowledgment is made to the National Science Foundation (CBT-8315228) and the Department of Energy for the support of this research.

REFERENCES

Desoer, C.A. and M. Vidyasagar, 1975, *Feedback Systems: Input-Output Properties*, Academic Press, New York, Ch. 2.

Doyle, J.C., 1982, Analysis of feedback systems with structured uncertainties. *IEE Proc.* **129**, D(6), 242-250.

Doyle, J.C., 1984, Lecture notes, ONR/Honeywell Workshop on Advances in Multivariable Control, Minneapolis, MN.

Doyle, J.C. and G. Stein, 1981, Multivariable feedback design: concepts for a classical/ modern synthesis. *IEEE Trans. Automat. Contr.* **AC-26**, 4-16.

Doyle, J.C., J.E. Wall and G. Stein, 1982, Performance and robustness analysis for structured uncertainty. Proceedings of the IEEE Conference on Decision and Control, Orlando, FL, 629-636.

Holt, B.R. and M. Morari, 1985, Design of resilient processing plants - VI. The effect of right-half-plane zeros on dynamic resilience. *Chem. Engng Sci.* **40**, 59-74.

Mandler, J.A., M. Morari and J.H. Seinfeld, 1986, Control system design for a fixed-bed methanation reactor. *Chem. Engng Sci.*, in press. (Chapter III of this thesis).

Morari, M. and J.C. Doyle, 1986, A unifying framework for control system design under uncertainty and its implications for chemical process control. Proceedings of the Third International Conference on Chemical Process Control, Asilomar, CA.

Stein, G., 1985, Beyond singular values and loop shapes. Proceedings of the 1985 American Control Conference, Boston, MA.

Zafiriou, E. and M. Morari, 1985, Robust digital controller design for multivariable systems. Paper 103f, 1985 Annual Meeting, A.I.Ch.E., Chicago, IL.

Zafiriou, E. and M. Morari, 1986, Design of the IMC filter by using the structured singular value approach. Proceedings of the 1986 American Control Conference, Seattle, WA.

V. SOFTWARE TOOLS FOR CONTROL SYSTEM DESIGN

The control system design studies carried out during the course of this work benefited from the use of two computer-aided control system analysis and design packages:

— CONSYD (Morari and Ray, 1986; Holt *et al.*, 1986), developed jointly at the University of Wisconsin and at Caltech. This is an interactive, menu-driven package designed to deal with problems important to chemical process control. The package has extensive capabilities to analyze systems and design controllers for processes with time-delays and non-linear processes, and an emphasis on analysis and design for control system robustness.

— HONEY-X, a state-space oriented control system analysis and design package developed at Honeywell in the framework of the UNIX operating system. An extension of this package includes experimental software for analysis and synthesis of control systems subject to structured uncertainties, based on the use of the structured singular value, μ, as an analysis tool and H_∞ as a synthesis tool. This software is based on the results by Doyle (1984) discussed in the previous chapters, and on more recent developments by Doyle and Chu (1986), and uses only standard matrix operations and linear algebra.

The use of these packages in the context of the control system design for the methanation reactor is shortly summarized in Appendix C.

In addition to, although motivated by, the control studies on the fixed-bed reactor, the research reported in this thesis includes the development of a number of general software tools. Most significant of all is the development of code for the open- or closed-loop simulation of general dynamic systems described by systems of ODE's and algebraic equations. This code, SNTEG, is now the standard nonlinear simulation program of the CONSYD package. SNTEG was written to meet the needs posed by complex, large-order, nonlinear systems such as the methanation reactor. The remainder of this chapter describes this code.

SNTEG: A DYNAMIC SIMULATION PROGRAM FOR CLOSED-LOOP SYSTEMS[1]

Jorge A. Mandler and Manfred Morari

Chemical Engineering, 206-41

California Institute of Technology

Pasadena, CA 91125

ABSTRACT

Interactive software for the dynamic simulation of MIMO closed-loop systems has been written taking full advantage of existing software for the solution of systems of mixed nonlinear ODE's and nonlinear algebraic equations.

The main features of the code and its application to the study of the control of a fixed-bed methanation reactor are presented.

1. (AIChE New Orleans National Meeting, 1986)

1. INTRODUCTION

Dynamic simulation of the closed-loop system is an important tool in the analysis and design of advanced control schemes. Although stability and performance guarantees can be rigorously obtained, *a priori*, for linear systems, most processes are nonlinear. Since in general it is not possible to obtain exact guarantees for the nonlinear case, simulations of the closed-loop system consisting of the nonlinear plant and a linear or nonlinear controller constitute the ultimate method by which the controller can be tested before implementing it in the real world. The importance of closed-loop simulation software designed so as to efficiently handle the nonlinear case is then evident.

In this paper we describe SNTEG, a FORTRAN-written, interactive program for the open-loop or closed-loop dynamic simulation of linear or nonlinear systems. The following are some of the features discussed in the paper, which combined make SNTEG an unique tool for implementing advanced controllers on complex dynamical systems:

— Both the classical feedback structure as well as the Internal Model Control (IMC) structure (Garcia and Morari, 1982, Morari, 1983) are allowed.

— The program allows any combination of linear or nonlinear plants or models with linear or nonlinear, continuous or discrete controllers. SISO, MIMO and non-square systems are allowed.

— The code solves simultaneously the systems of nonlinear ODE's and possible nonlinear algebraic equations of the plant, model or controller. Very complex systems can then be implemented and efficiently solved.

— The last feature combined with the generality of the controller subroutine accepted by SNTEG, allow for practically any type of control structure to be implemented.

— The closed-loop is solved simultaneously at every point without the need to employ some kind of iterative procedure or introduce a time-delay.

— Arbitrary types of set-point or disturbance changes are allowed. Constraints on the manipulated variables can be specified.

The program has been written in the framework of CONSYD, a computer-aided control system design package developed jointly at the University of Wisconsin and Caltech (Morari and Ray, 1986; Holt *et al.*, 1986). The file handling capabilities, standard plotting routines and several input-output features are those of the general package.

A description of the code is given in Section 2. Section 3 presents several application examples, including an example corresponding to the control of a fixed-bed methanation reactor.

2. PROGRAM DESCRIPTION

The basic control structures that SNTEG can handle are shown in Fig. 1. For linear systems the Internal Model Control (IMC) structure, shown in Fig. 1d, is equivalent to the classical feedback structure (Fig. 1c) through the relationships

$$Q = (I + K\tilde{P})^{-1} K \tag{1}$$

$$K = (I - Q\tilde{P})^{-1} Q \ , \tag{2}$$

where $\tilde{P}$ indicates a model of the plant P. The IMC structure has definite advantages over the classical feedback structure, resulting mainly from the fact that, for the case of a perfect model ($P = \tilde{P}$), the closed-loop transfer functions are linear functions of the controller Q (Morari, 1983, Mandler *et al.* , 1986).

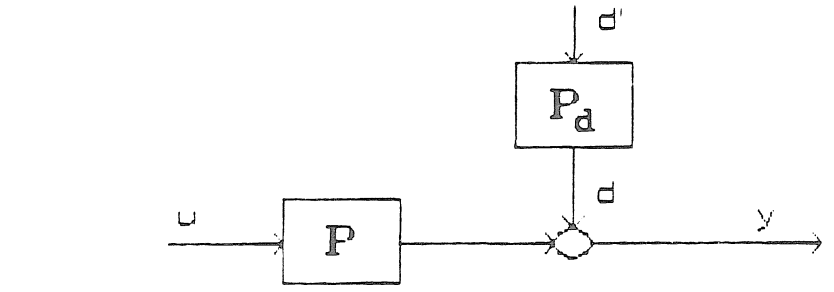

(a)

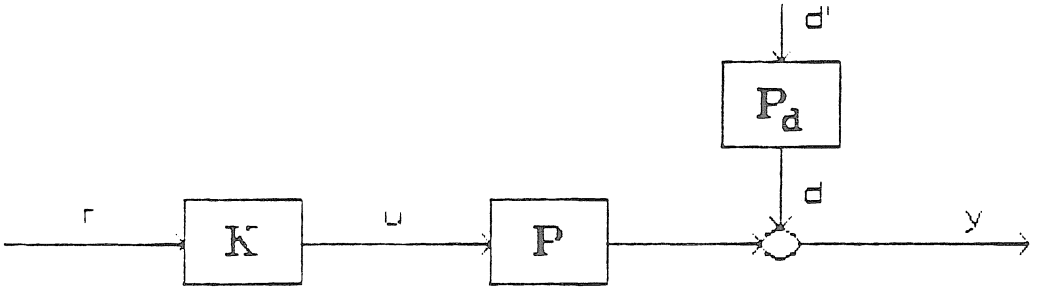

(b)

Figure 1 Basic control structures handled by SNTEG: (a) open-loop; (b) open-loop with controller (also feedforward controller).

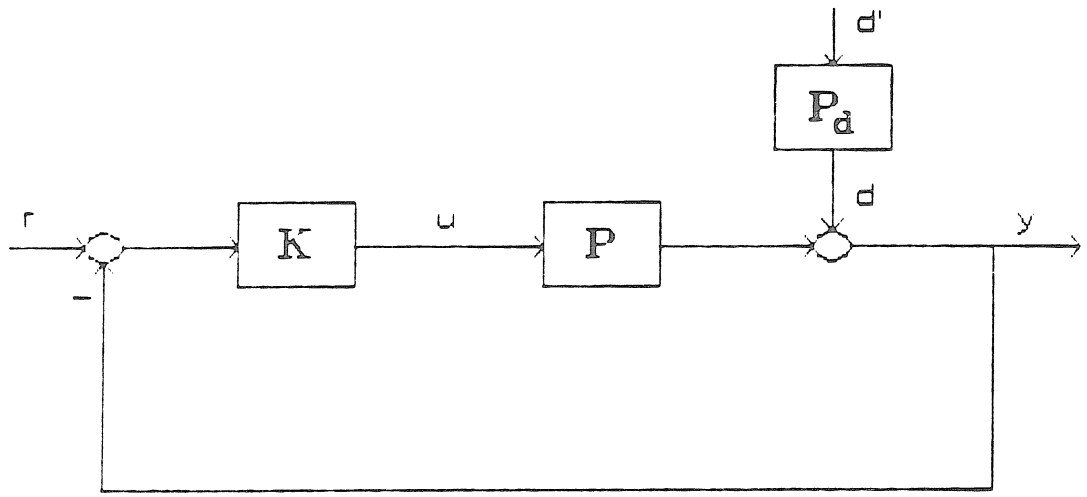

(c)

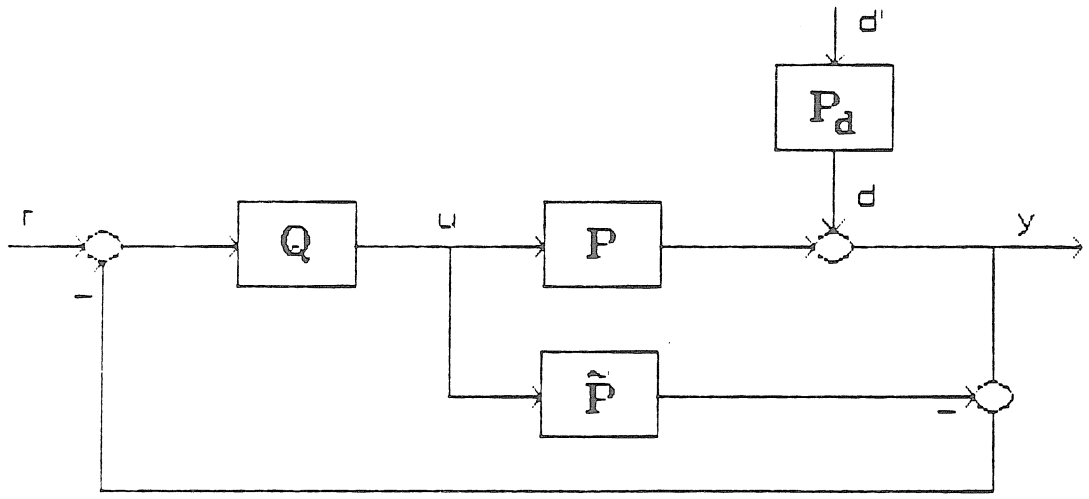

(d)

Figure 1 Basic control structures handled by SNTEG: (c) classical feedback structure; (d) IMC structure.

SNTEG is structured as shown in Fig. 2: following the initialization and data entry parts, the program separates into sixteen subprograms, each one carrying out the solution of the system of equations for a different combination of linear or nonlinear elements within the four basic structures of Fig. 1. At the end of the simulation, the results may be saved and/or displayed in the form of tables or graphs, and the user is given a choice of options for restarting.

The method used for solution is time-domain integration of the state-space representations. Basically, SNTEG combines the systems of ordinary differential equations (and possible linear or nonlinear algebraic equations) of plant, controller and model into one system of coupled differential/algebraic equations (DAE) of the form

$$\begin{aligned} F(t,y,\dot{y}) &= 0 \\ y(t_0) &= y_0 \\ \dot{y}(t_0) &= \dot{y}_0 \,, \end{aligned} \tag{3}$$

where F, y and $\dot{y}$ are N dimensional vectors. This representation can include systems that are substantially more complex than standard ODE systems of the form

$$\dot{y} = f(t,y) \quad . \tag{4}$$

The code DASSL, developed by Petzold (1982) at Sandia National Laboratories for the solution of implicit systems of differential/algebraic equations, is used in SNTEG for the solution of Eq. (3). Gear first pointed out (1971a,b) that numerical methods for solving stiff differential systems could be adapted to solve some DAE systems. DASSL is based on such a "stiff ODE method" for solving DAE's. These methods are based on replacing the derivative in Eq. (3) by a difference approximation and then solving the resulting equation for the solution at the current time t_n, using Newton's method. DASSL approximates the derivative using backward differentiation formulae of order one to five. DASSL is robust and has been reported

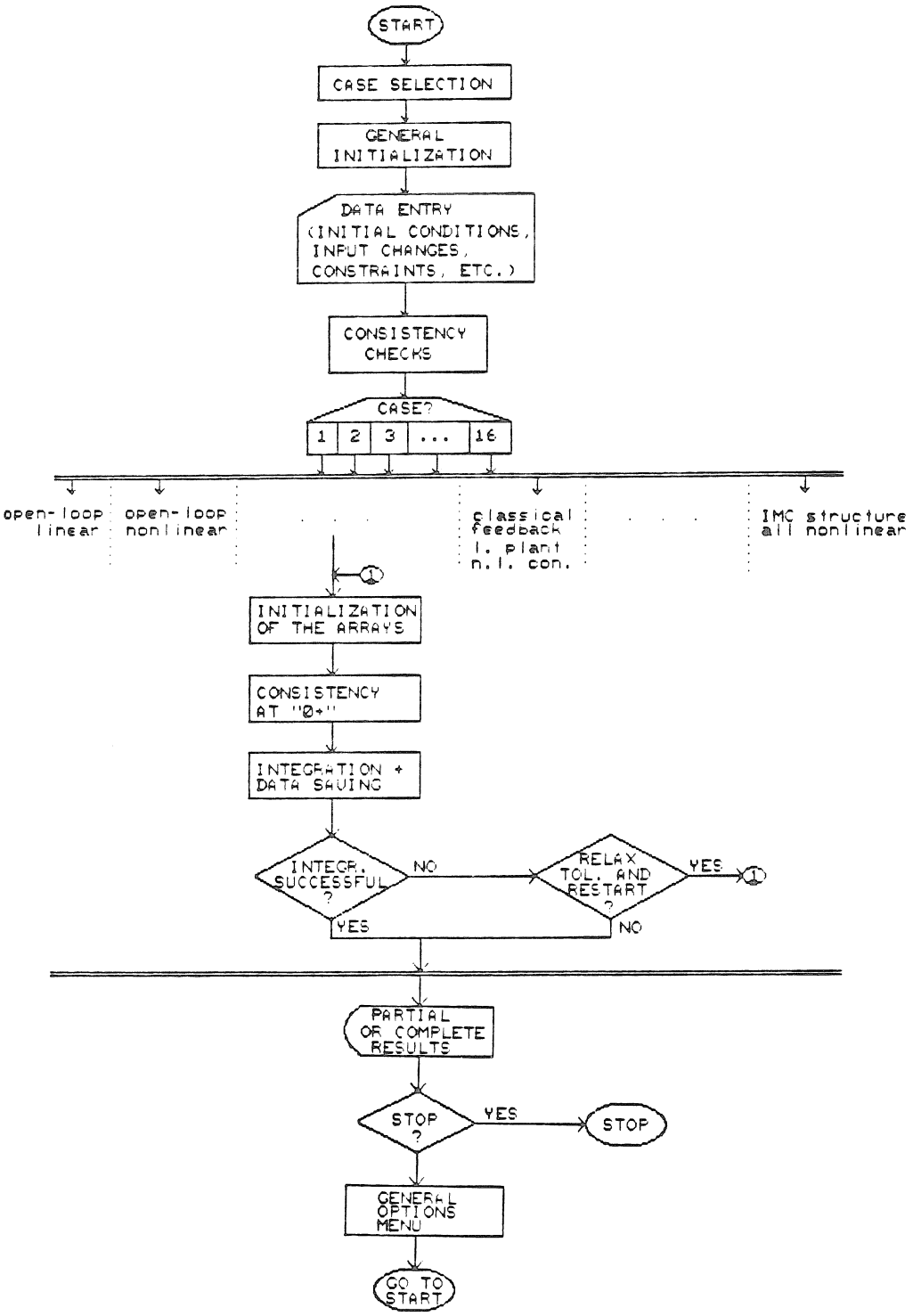

Figure 2 General block diagram of the SNTEG code.

to be successful in a wide variety of stiff problems, both differential and mixed (Caracotsios and Stewart, 1985).

SNTEG was written taking full advantage of the possibilities resulting from being capable of directly solving DAE systems by means of codes such as DASSL. This is reflected in several of the special features of our code.

First, as mentioned, very complex systems of mixed differential and algebraic equations can be implemented and efficiently solved. This is of particular importance, for instance, for the dynamic simulation of systems with recycles, since the interconnection between different system elements is generally expressed in the form of linear or nonlinear algebraic equations. Differential/algebraic equations also arise in the analysis of reaction schemes, where equilibrium considerations may impose algebraic constraints on the concentrations. Finally, the methanation reactor model described in Section 3 constitutes another good example of a complex DAE system.

We should note that, for the examples above and in general for the most common chemical engineering applications, Eq. (3) can actually be written as

$$\begin{aligned} 0 &= -\dot{x} + f(t,x,z) \\ x(t_0) &= x_0 \end{aligned} \tag{5a}$$

$$0 = g(t,x,\dot{x},z) \ , \tag{5b}$$

where $y = \begin{bmatrix} x \\ --- \\ z \end{bmatrix}$, and z are the variables corresponding to the algebraic equations (5b). The system given by Eq. (5) can actually be solved in a two-step fashion, employing a separate nonlinear algebraic equation method to solve Eq. (5b) for z, and carrying out this solution at the beginning of each function evaluation of a standard ODE solution method applied to Eq. (5a). However, any implementation of

this two-step approach will in general be less convenient and in many cases less efficient than the direct use of a DAE solver, especially if the ODE part already possesses stiffness characteristics as it occurs in a large number of chemical engineering applications.

In addition to its convenience for the simulation of complex plants, a second feature of SNTEG which results from formulating the system of equations as in Eq. (3) and solving it through DASSL, is the ease with which control structures more complex than the four basic structures shown in Fig. 1 can be implemented. The four basic structures are those corresponding to the standard linear controller options of SNTEG. More complicated control structures can be specified employing the option of a user-written controller subroutine. This subroutine accepts as inputs to the controller algorithm not only the plant or model outputs or the error but also the current value of the disturbances, of the plant and model states and their derivatives, and of the states, state derivatives and even outputs of the controller itself. Since the whole system of differential/algebraic equations of plant, model and controller is solved simultaneously, all the inputs to the controller algorithm can be employed for conveniently implementing virtually any complex control structure, including feedback-feedforward controllers, full state-feedback controllers, adaptive controllers, etc.. Linear or nonlinear, continuous or discrete controllers are equally acceptable. Section 3 presents a few examples of different controller implementations. Finally, we have included the controller output equations among the set solved by DASSL, allowing us to solve simultaneously for all points in the closed-loop even for the case of both plant and controller being semiproper, without the need to introduce a time-delay or to employ some type of iterative procedure.

At the beginning of the interactive session the user needs to select one of the four basic structures of Fig. 1 and to specify the elements as linear or nonlinear. For

the linear elements the user has to provide a file in standard CONSYD format with the state-space matrices; such a file can be obtained for example by specifying the transfer matrices in Laplace domain through the CONSYD program ENTER and then employing the CONSYD REALization program (Morari and Ray, 1986; Holt *et al.* , 1986). The gain and time-constants of PID controllers can be specified directly, and SNTEG determines their state-space realizations. For the linear elements the initial conditions are taken as zero (deviation variables).

The nonlinear elements are specified through user-written subroutines that need to be linked to SNTEG. The initial conditions can be specified either interactively or be read from a file. In general, the initial conditions are taken to correspond to "old steady-state" conditions, namely, steady-state conditions prevailing before any change in the inputs (set-points or disturbances) occurs. SNTEG does appropriate checkings for the consistency of these "old steady-state" conditions. Proper care is taken of all special cases of mixed linear and nonlinear elements.

Simple set-point or disturbance changes (steps, ramps) can be specified interactively. Arbitrary set-point or disturbance changes (sine-waves, random noise, an arbitrary sequence of step-changes, etc.) can be read from another type of CONSYD file, basically, a table with the values of the variables at different time points. This table can be obtained as output from another CONSYD program, named INCIC. DASSL requires that the system given by Eq. (3) be consistent at time zero; i.e., it requires correct values of y and $\dot{y}$ satisfying the equality in Eq. (3) for the conditions just after the input change is made (at time "0+"). SNTEG takes the necessary steps to insure that this requirement is met.

At each function evaluation k by DASSL, the new values v_k of inputs and disturbances to the system are calculated, if necessary and when appropriate, by interpolation between tabulated values. This allows an accurate simulation even in

the face of very rapidly changing inputs or disturbances. Next, constraints on the manipulated variables are checked, and finally the residual δ_k of the differential/algebraic system

$$\delta_k = F_k(t_k, y_k, \dot{y}_k, v_k) \tag{6}$$

is calculated and returned to DASSL. For the case of a discrete controller an extra function evaluation is carried out (outside DASSL) at the sampling point. By using an appropriate flag, the user has to specify that the output from the controller be maintained constant between samples. More detailed information on the use of SNTEG can be found in the CONSYD documentation (Morari and Ray, 1986).

3. APPLICATION EXAMPLES

3.1 Discrete Controller

We reproduce with SNTEG an example presented by Zafiriou and Morari (1985). A discrete controller is implemented with the IMC structure for the plant

$$G(s) = \frac{2}{(s^2+1.2s+1)(s+2)} \quad . \tag{7}$$

A perfect model for the plant is assumed. The sampling time is 1.65 sec. The z-transform model, for a zero-order hold is

$$G(z) = 0.4168 \frac{(z+0.0708)\,(z+1.058)}{(z^2-0.184z+0.138)\,(z-0.0369)} \quad . \tag{8}$$

A controller that minimizes the sum of squared errors of the discrete output is found by using the inverse of the zero outside the unit circle as a pole for the controller (Kucera, 1972). The controller is given by

$$Q(z) = 2.268\ \frac{z^3-0.221z^2+0.145z-0.0051}{z^3+1.016z^2+0.067z} \quad . \qquad (9)$$

The controller is implemented by means of a user-written subroutine as detailed in Appendix 1. Note that the discrete controller has no states as such. All that is required is a calculation of the controller output at the current sampling point on the basis of the previous values of the controller input and output and the current value of the input (as results from the difference equation directly obtained from Eq. (9)) and the specification that the controller output be maintained constant between samples. For the plant and the model, the state-space realizations are obtained from Eq. (7) employing the REAL program of CONSYD. The closed-loop response to a unit step-change in the set-point is shown in Fig. 3.

Note that the output is equal to the set-point at the sampling points. Although the controller clearly minimizes the sum of squared errors of the discrete output, no attention is paid by this control algorithm to the intersample behavior of the system output. Ringing of the manipulated variable and rippling of the system output between the samples occur as a result of the existence of zeros with negative real part near the unit circle. This simulation with SNTEG reproduces exactly the results obtained by Zafiriou and Morari (1985), employing code designed for linear system simulation with discrete controllers, based on the use of the convolution integral and also available in CONSYD. No problems are encountered with SNTEG in the convergence of the integration, in spite of the strong test imposed by the sudden changes in the controller output.

3.2 Implementing More Complex Control Structures

Assume that the control structure of Fig. 4a needs to be implemented starting from the basic classical feedback structure of Fig. 1c. Assume that for some reason it is not desired or it is not possible to do the necessary manipulations in state-space, or Laplace or frequency domain, to reduce the three blocks C, E_1 and E_2 of

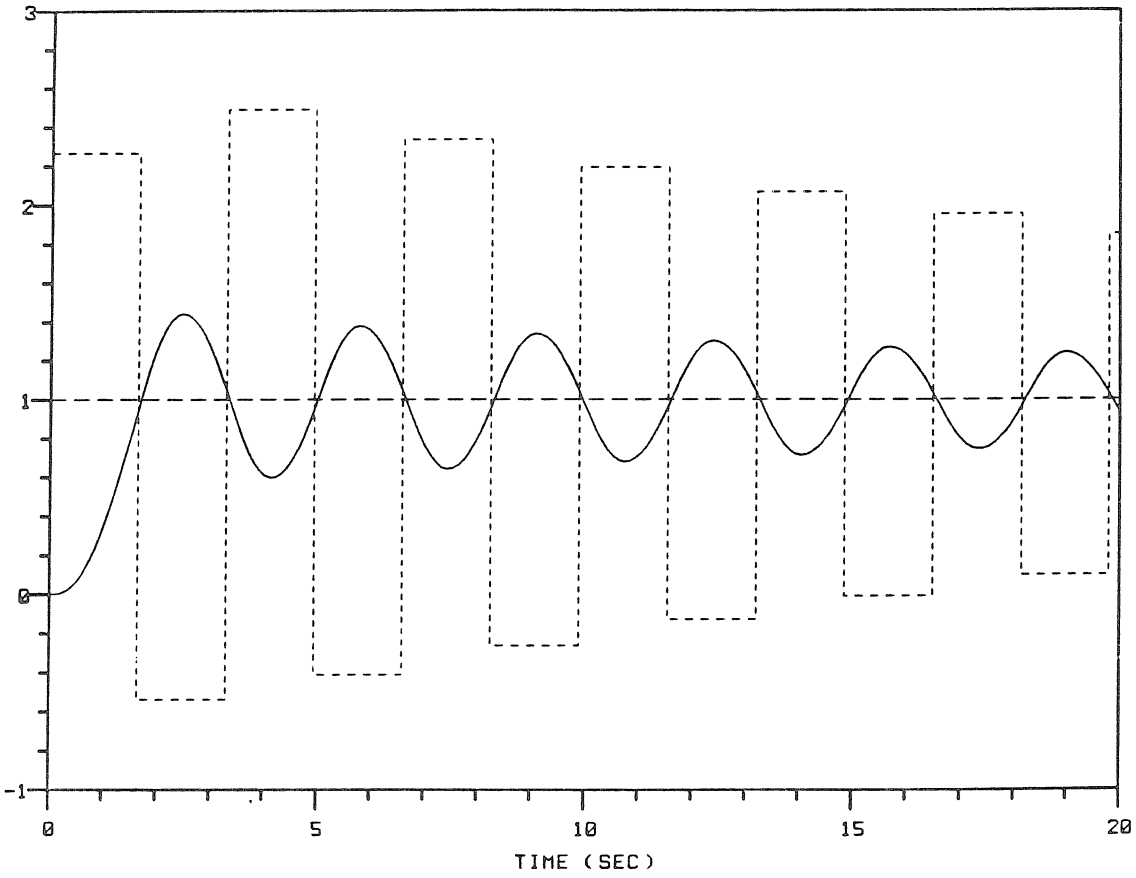

Figure 3 Discrete controller example. $G(s) = 2/(s^2+1.2s+1)(s+2)$; sampling time = 1.65 sec. Closed-loop response to a unit step-change in the set-point for the controller that minimizes the sum of squared errors. Dashed line: set-point; solid line: output; dotted line: manipulated variable.

Fig. 4a to one block implementable as in Fig. 1c (for example, one or more of the blocks might correspond to nonlinear elements). The structure of Fig. 4a may correspond to an inferential control scheme (Stephanopoulos, 1984).

In order to implement in SNTEG the structure of Fig. 4a and solve simultaneously at all points in the closed-loop system, the state-space descriptions of the 3 blocks C, E_1 and E_2 need to be defined in a user-specified controller subroutine. Note from Figs. 4b and 4c that there are two ways of defining the "controller boundaries" to include the three blocks; both can be implemented in SNTEG starting from the classical feedback structure.

Fig. 4b corresponds to what would be the "usual way" of implementing the controller. For this case the vector u of manipulated variables is as usual just an output from the controller block and correspondingly from the controller subroutine. However, implementing the controller as in Fig. 4b would require an iteration on u inside the controller subroutine, and this, clearly, is undesirable. Since in SNTEG we have included the controller output equations among the DAE set solved by DASSL (making DASSL *solve* for u), u can be selected to be not only an input to the controller subroutine, but also an output of it, through the corresponding elements of the residual vector δ. The "controller boundaries" can therefore be defined as in Fig. 4c. No iterations are required inside the controller subroutine corresponding to Fig. 4c (given in Appendix 2), and, still, a simultaneous solution can be obtained for all points in the closed-loop.

3.3 Closed-Loop Simulation of a Fixed-Bed Methanation Reactor

The design of SISO IMC controllers for the rejection of inlet concentration disturbances in a fixed-bed non-adiabatic methanation reactor is described by Mandler *et al.* (1986). The closed-loop simulations are conveniently and efficiently carried out by means of SNTEG. The full nonlinear methanation reactor model is employed to simulate the actual plant. A linearized reduced-order model,

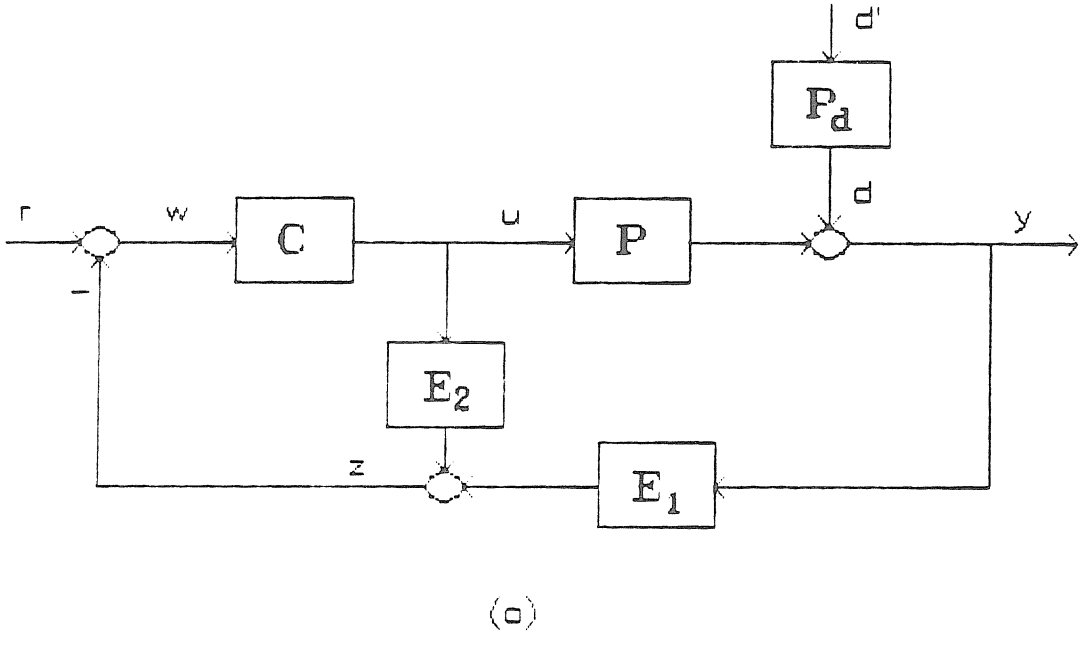

Figure 4 (a) Example 2. "Inferential" control structure to be implemented starting from the classical feedback structure of Figure 1c.

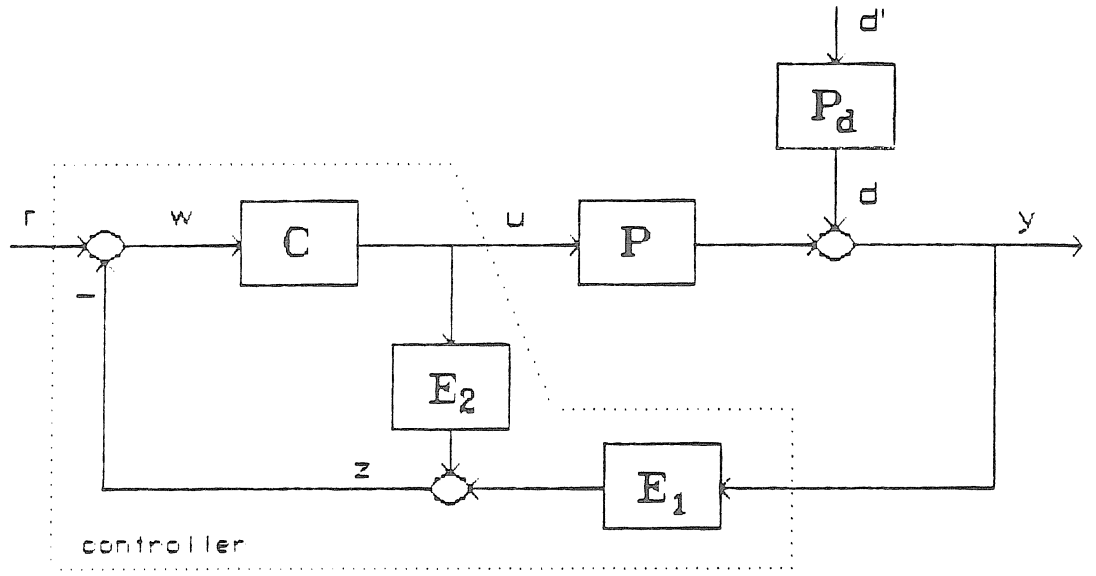

(b)

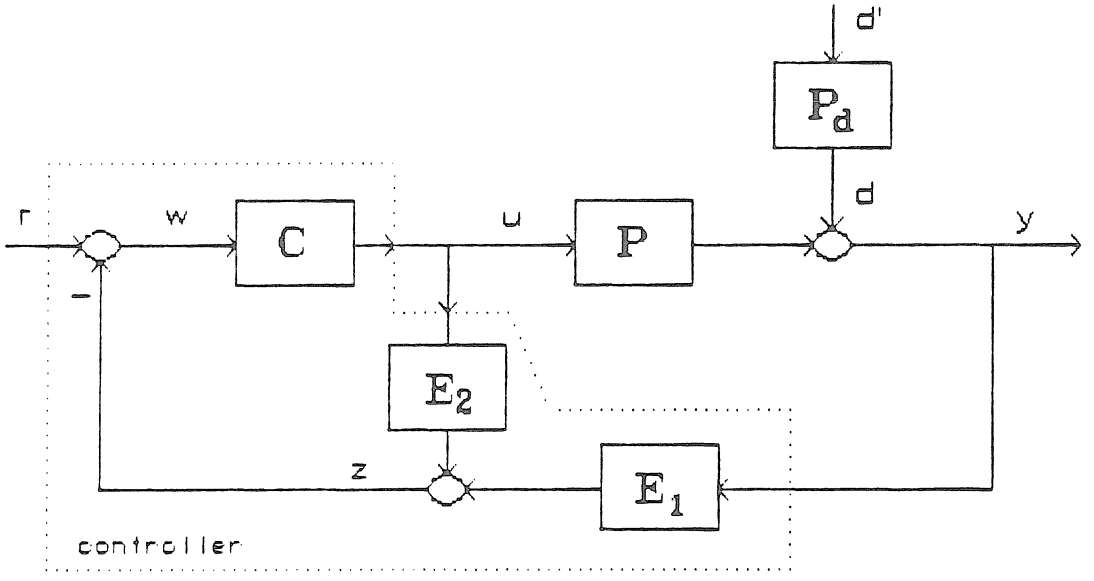

(c)

Figure 4 Example 2. (b) u taken as just an output from the controller subroutine; (c) u taken as both an input to and an output from the controller subroutine.

obtained by means of control-relevant model reduction techniques (Rivera and Morari, 1985), is used as the model in the IMC structure, and serves as the basis for the design of the IMC controller.

The methanation reactor model (Khanna, 1984; Mandler, 1986) is described by the coupled set of mass and energy conservation equations. These include energy balances for the catalyst phase, the gas phase and a central axial thermal well used for temperature measurements, the CO species balance and the continuity equation; the latter is employed for the evaluation of the linear gas velocity, required, for example, in some heat transfer correlations.[2]

The nonlinear PDE's are first discretized in the radial direction by means of collocation employing one interior collocation point and a quadratic representation for the radial temperature profiles, and then in the axial direction by means of orthogonal collocation. Because of steep profiles for some conditions and for the kinetics employed, 12 interior axial collocation points are used. For each PDE corresponding to an energy balance, there results a set of 12 nonlinear ODE's. The CO species balance is translated into a set of 13 ODE's, including one for $z=1$, and the continuity equation similarly into a set of 13 algebraic equations. These equations, together with 4 heat-flux boundary conditions, constitute a coupled system of 49 nonlinear ODE's and 17 linear and nonlinear algebraic equations. This nonlinear model represents the plant in the simulation with SNTEG.

The ODE system is stiff as a result of widely differing time-constants. The system modes are almost equally divided into slow and fast ones. The slow modes correspond to the catalyst-phase and thermal-well energy balance equations. The fast modes correspond to the CO species balance equations, and even faster ones to the gas phase energy balance equations (this resulting from the almost negligible accumulation of energy in the gas phase compared to the solid phase). Fig. 5 gives

2. As noted in Chapter II, the model was later simplified and explicit references to the continuity equation eliminated.

the open-loop system poles for the 49th order linearized model and shows this clear separation into slow and fast modes. Because of the stiffness and the relatively large number of algebraic equations in the nonlinear model, DAE solvers like DASSL provide the most efficient way of integrating the system of equations.

In addition to the system poles, Fig. 5 shows the system zeros for the SISO configuration with the inlet temperature as the manipulated variable and the outlet temperature as the controlled variable. Notice in Fig. 5b that 12 zeros lie in the right-half plane. The fact that there exist right-half-plane zeros reflects a fundamental limitation to the achievable closed-loop performance for this control configuration, a limitation that results from the fact that the thermal wave (and therefore the corrective action caused by a change in the inlet temperature) is much slower than the concentration wave (and the effect of inlet concentration disturbances on the outlet temperature). Unless a change in the control configuration or in the system design is made, this limitation cannot be removed by the use of a more sophisticated control algorithm (Mandler *et al.* , 1986).

The closed-loop simulation with SNTEG is carried out with the IMC structure. The nonlinear plant is implemented through a user-written subroutine, detailed elsewhere (Mandler, 1986). The linearized reduced-order model (6th order) and the 8th order robust IMC controller designed on its basis are entered through standard CONSYD state-space files. The total number of equations to be solved by DASSL is 81. The CPU time for the integration, corresponding to a -25% step-change in the inlet concentration, a local error tolerance of 10^{-5} and a simulation-time of 300 sec., is 200 sec. on a VAX 11/780. The open and closed-loop responses are shown in Fig. 6. For the open-loop simulation (66 equations) the CPU-time is 143 sec.. This represents an improvement by more than a factor of 10 over an equivalent simulation carried out on the basis of a two-step approach employed in the previous version of the reactor model (Khanna, 1984).

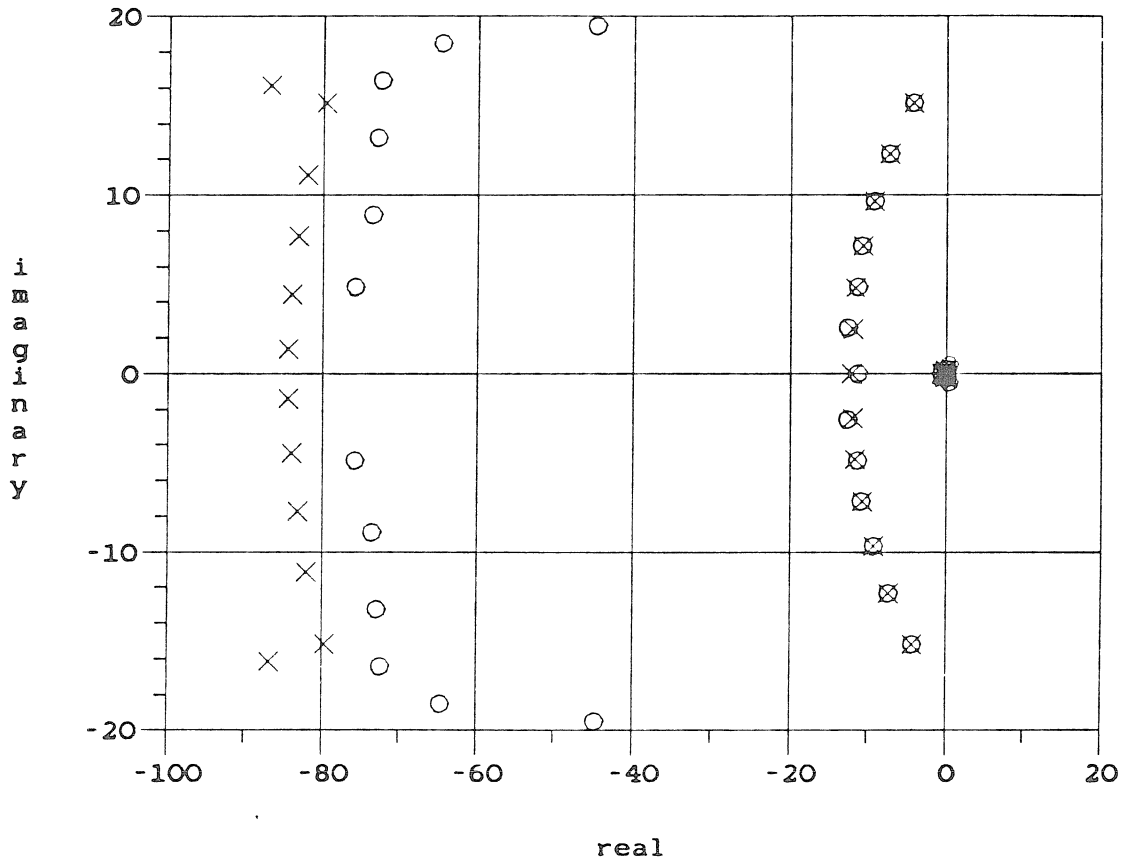

Figure 5 (a) Example 3. Open-loop system poles and zeros for the 49th order linearized reactor model. ×: poles; ○: zeros.

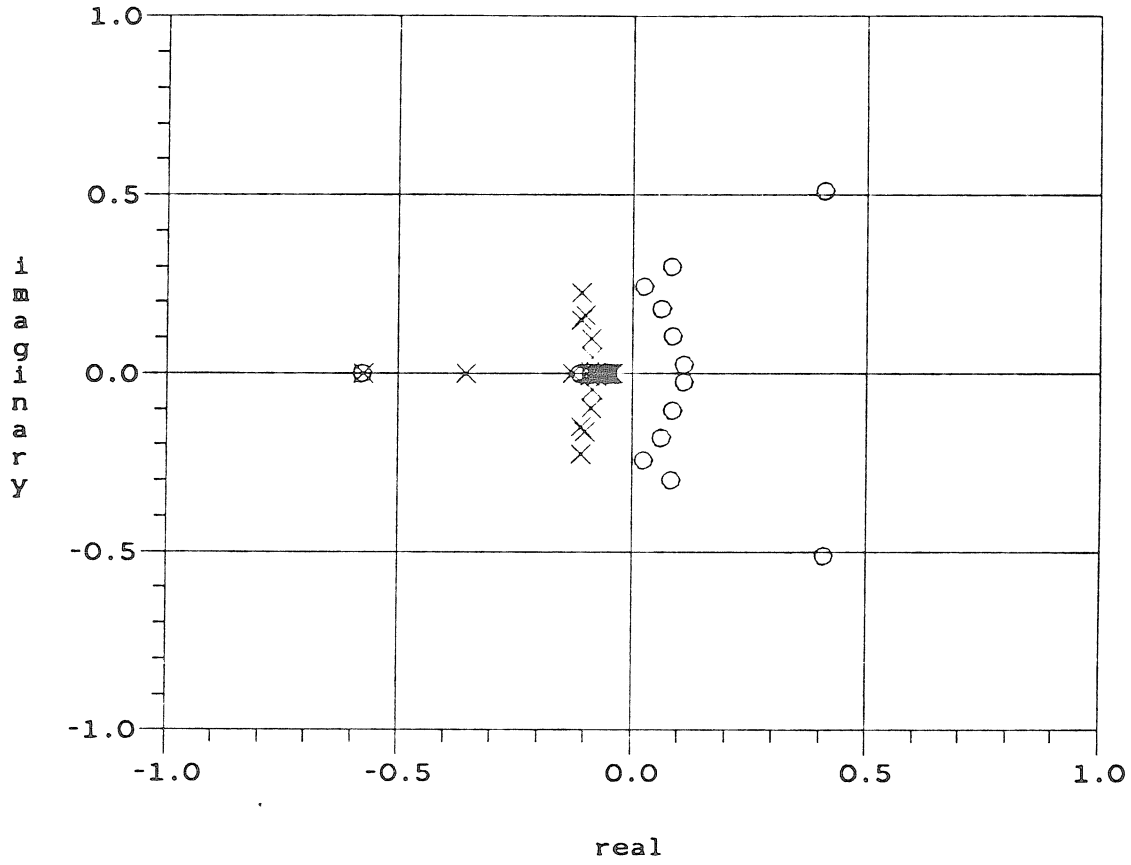

Figure 5 (b) Example 3. Augmented view of the poles and zeros near the origin. ×: poles; ○: zeros.

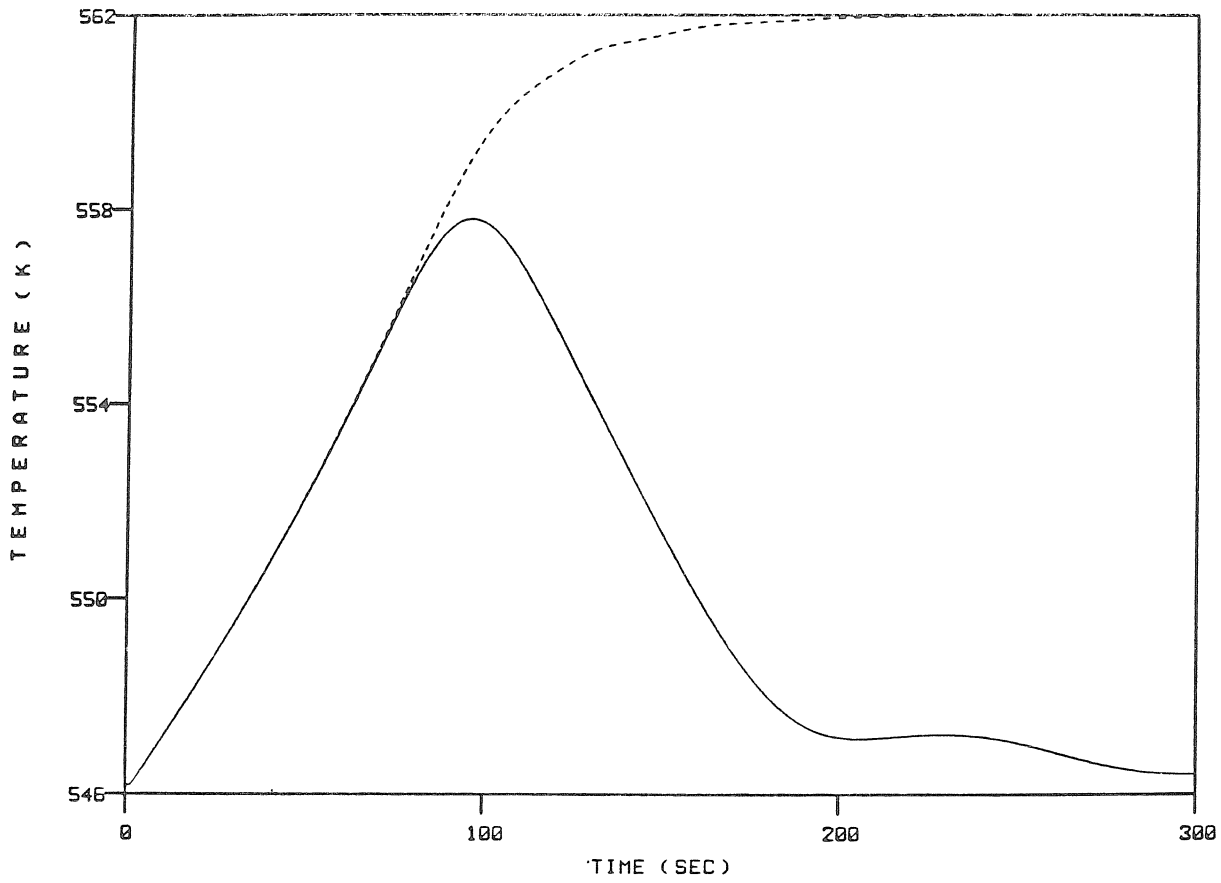

Figure 6 Example 3. Open- and closed-loop outlet temperature responses to a -25% step change in the inlet CO concentration. Nonlinear reactor model. Dashed line: open-loop response; solid line: closed-loop response.

4. CONCLUDING REMARKS

A versatile and efficient code for the open- and closed-loop simulation of general dynamic systems has been presented. This code has been integrated into the framework of a computer-aided control system design package, making it a powerful tool for the evaluation of advanced control schemes.

The code was written taking into account the complexities of systems like the fixed-bed methanation reactor model described. This system, like many others in chemical engineering applications, is highly nonlinear, stiff, of large dimensionality and described by a system of mixed ODE's and algebraic equations. The control studies for this reactor system were greatly facilitated by the use of SNTEG.

Acknowledgments

We are thankful to E. Zafiriou and S. Skogestad for many useful discussions during the writing of the code and of this paper. Acknowledgment is made to the Donors of The Petroleum Research Fund, administered by the American Chemical Society, to the National Science Foundation (CBT-8315228) and to the Department of Energy for the support of this research.

REFERENCES

Caracotsios, M. and W.E. Stewart, 1985, Sensitivity analysis of initial value problems with mixed ODE's and algebraic equations. *Comput. and Chem. Engng* **9**, 359-365.

Doyle, J.C., 1984, Lecture notes, ONR/Honeywell Workshop on Advances in Multivariable Control, Minneapolis, MN.

Doyle, J.C. and C. C. Chu, 1986, Robust control of multivariable and large scale systems. Technical report to A.F.O.S.R. for period July 1984/ October 1985.

Garcia, C.E. and M. Morari, 1982, Internal Model Control - 1. A unifying review and some new results. *Ind. Engng Chem. Proc. Des. Dev.* **21** , 308-323.

Gear, C.W., 1971a, *Numerical Initial Value Problems in Ordinary Differential Equations*, Prentice-Hall, Englewood Cliffs, NJ, Ch. 11.

Gear, C.W., 1971b, Simultaneous numerical solution of differential-algebraic equations. *IEEE Trans. on Circuit Theory* **CT-18**, 89-95.

Holt, B.R. *et al.*, 1986, CONSYD - Integrated software for computer-aided control system design and analysis. *Comput. and Chem. Engng*, in press.

Khanna, R., 1984, Control model development for packed-bed chemical reactors. Ph.D. Thesis, Calif. Inst. of Technology, Pasadena, CA.

Kucera, V., 1972, State-space approach to discrete linear control. *Kybernetika* **8**, 233-257.

Mandler, J.A., 1986, (Appendices A and B of this thesis).

Mandler, J.A., M. Morari and J.H. Seinfeld, 1986, Control system design for a fixed-bed methanation reactor. *Chem. Engng Sci.*, in press (Chapter III of this thesis).

Morari, M., 1983, Internal Model Control - Theory and applications. P.R.P.- Automation 5, 5th International IFAC/IMEKO Conference on Instrumentation and

Automation in the Paper, Rubber, Plastics and Polymerization Industries, Antwerp, Belgium.

Morari, M. and W.H. Ray, 1986, CONSYD - Control System Design Software. Version 3.0. California Inst. of Technology, Pasadena, CA and University of Wisconsin, Madison, WI.

Petzold, L.R., 1982, A description of DASSL: a differential/algebraic system solver. *Sandia Tech. Rep.* 82-8637.

Rivera, D.E. and M. Morari, 1985, Internal Model Control perspectives on model reduction. Proceedings of the 1985 American Control Conference, Boston, MA.

Stephanopoulos, G., 1984, *Chemical Process Control - An Introduction to Theory and Practice*, Prentice-Hall, Englewood Cliffs, NJ, p. 441.

Zafiriou, E. and M. Morari, 1985, Digital controllers for SISO systems: a review and a new algorithm. *Int. J. Control* **42**, 855-876.

APPENDIX 1

Subroutines for the discrete controller example.

```
      SUBROUTINE DCPAR(...,IFLAG,...)

C
C     (ONLY THE PARAMETER LIST ELEMENTS RELEVANT TO THIS CASE ARE INCLUDED)
C
C     THIS SUBROUTINE, CALLED BY SNTEG AT THE BEGINNING OF THE
C     SIMULATION, ALLOWS THE USER TO SPECIFY PARAMETERS OF THE CONTROLLER;
C     THESE ARE TRANSFERRED TO THE MAIN CONTROLLER SUBROUTINE (DCONTR)
C     THROUGH THE USER-SPECIFIED COMMON BLOCK
C
C     INPUTS:
C             IFLAG, =.TRUE. IF AT THE BEGINNING OF THE PROGRAM
C                      (ONE CALL, FOR ASSIGNING VALUES TO CONSTANT
C                      PARAMETERS)
C                    =.FALSE., WHEN CALLED AT THE BEGINNING OF EACH
C                      SIMULATION; USED FOR INITIALIZING OR
C                      REINITIALIZING THE VARIABLES ENTERING IN THE
C                      CONTROLLER CALCULATION
C
C

      IMPLICIT DOUBLE PRECISION (A-H,O-Z)
      LOGICAL IFLAG


      COMMON /CONTR/AK,A0,A1,A2,A3,B0,B1,B2,B3,E1,E2,E3,
     *              U1,U2,U3,UCURR

C
C     AK,...,B3 ARE THE PARAMETERS OF THIS DISCRETE CONTROLLER (cf. Eq. (9));
C     E1,E2 AND E3 ARE INITIALIZED HERE, AND IN DCONTR THEY WILL BE
C     USED TO STORE THE LAST THREE VALUES OF THE INPUT TO THE CONTROLLER;
C     THE SAME FOR U1,U2 AND U3, WHICH WILL STORE THE LAST THREE
C     VALUES OF THE CONTROLLER OUTPUT (THE MANIPULATED VARIABLE);
C     UCURR WILL STORE THE CURRENT VALUE OF THE CONTROLLER OUTPUT
C     FOR USE BETWEEN THE SAMPLES
C

      IF (IFLAG) THEN
C
C     SPECIFY ALL THE CONSTANT PARAMETERS
C
      AK=2.268
      A3=1.
      A2=-0.221
      A1=0.145
      A0=-0.0051
      B3=1.
      B2=1.016
      B1=0.067
      B0=0.

      ELSE
C
C     INITIALIZE OR REINITIALIZE ALL THE VARIABLES NEEDED IN THE
C     CONTROL ALGORITHM
C
      E1=0.
      E2=0.
      E3=0.
      U1=0.
      U2=0.
      U3=0.
      UCURR=0.

      END IF


      RETURN
      END
```

```
      SUBROUTINE DCONTR(...,DELTA,...,E,U,...,ISAMPL,...)
C
C     (THE ELEMENTS OF THE PARAMETER LIST RELEVANT TO THIS EXAMPLE
C      ARE THE ONLY ONES INCLUDED; FOR A COMPLETE LISTING REFER TO
C      APPENDIX 2)
C
C
C     INPUTS:
C             E, CURRENT VALUE OF THE INPUT TO THE CONTROLLER
C             U, CURRENT VALUE OF THE CONTROLLER OUTPUT
C             ISAMPL, =.TRUE., IF AT A SAMPLING POINT
C                     =.FALSE., IF NOT AT A SAMPLING POINT
C
C     OUTPUTS:
C             U, CURRENT VALUE OF THE CONTROLLER OUTPUT
C                ( AN OUTPUT ONLY FOR THE SAMPLING POINT CALL )
C             DELTA, RESIDUAL OF THE DAE SYSTEM;
C                    RECALL THAT THE CONTROLLER OUTPUT EQUATIONS HAVE
C                    BEEN INCLUDED AMONG THE SET SOLVED BY DASSL;
C                    IF THESE EQUATIONS ARE GIVEN BY
C                    u = h(...)
C                    THEN
C                    delta = -u + h(...)

      IMPLICIT DOUBLE PRECISION (A-H,O-Z)
      LOGICAL ISAMPL
      DIMENSION ...,DELTA(1),...,E(1),U(1),...


      COMMON /CONTR/AK,A0,A1,A2,A3,B0,B1,B2,B3,E1,E2,E3,
     *              U1,U2,U3,UCURR


      IF (ISAMPL) THEN
C
C     SAMPLING POINT CALL; THE CURRENT VALUE OF THE CONTROLLER OUTPUT
C     IS COMPUTED, EMPLOYING THE CURRENT VALUE OF THE CONTROLLER INPUT
C     AND PREVIOUS VALUES (STORED IN THE COMMON) OF INPUT AND OUTPUT;
C     NOTICE THAT THIS IS NOT A CALL BY DASSL, AND THEREFORE IT DOESN'T
C     INVOLVE THE RESIDUAL DELTA; FOR THIS CALL, U IS CONSIDERED AN
C     OUTPUT FROM THE SUBROUTINE
C
      S1=AK*(A3*E(1)+A2*E1+A1*E2+A0*E3)
      S2=B2*U1+B1*U2+B0*U3
      U(1)=(S1-S2)/B3
C
C     THE VARIABLES E1,E2,E3 AND U1,U2,U3 ARE UPDATED
C
      E3=E2
      E2=E1
      E1=E(1)
      U3=U2
      U2=U1
      U1=U(1)
C
C     UCURR STORES THE CURRENT VALUE OF THE CONTROLLER OUTPUT
C     FOR USE BETWEEN THE SAMPLES
C
      UCURR=U(1)


      ELSE
C
C     NOT A SAMPLING POINT (DASSL CALL); THE CONTROLLER OUTPUT IS FIXED
C     AT THE VALUE CALCULATED AT THE LAST SAMPLE
C
      DELTA(1)=-U(1)+UCURR

      END IF

      RETURN
      END
```

APPENDIX 2

Controller subroutine for Example 2.

```
      SUBROUTINE DCONTR(T,ST,DT,
     *  XC,XCALG,XCDOT,DELTA,XP,XPALG,XPDOT,XM,XMALG,XMDOT,
     *  SETP,DIST,E,U,YP,YM,YF,
     *  SETPSS,DISTSS,ESS,USS,YPSS,YMSS,DUMMY,
     *  NC,NCALG,NP,NPALG,NM,NMALG,
     *  MDIS,MIP,MOP,ISAMPL,ISM)

C
C       (ALL THE ELEMENTS OF THE PARAMETER LIST OF DCONTR HAVE BEEN
C        INCLUDED)
C
C       INPUTS:
C               T,  CURRENT TIME
C               ST, SAMPLING TIME
C               DT, TIME DIFFERENCE BETWEEN TWO POINTS FOR WHICH AN
C                   OUTPUT OF THE SOLUTION IS DESIRED
C               XC, CONTROLLER STATE VECTOR
C               XCALG, CONTROLLER VARIABLES GIVEN BY ALG. EQNS.
C               XCDOT, DERIVATIVE OF THE CONTROLLER STATE VECTOR
C               XP, XPALG, XPDOT, XM, XMALG, XMDOT, SAME AS FOR
C                   THE CONTROLLER, BUT CORRESPONDING TO PLANT AND MODEL
C               SETP, SET-POINTS
C               DIST, DISTURBANCES TO THE SYSTEM
C               E , VECTOR OF INPUTS TO THE CONTROLLER AS CALCULATED FOR
C                   THE CLASSICAL FEEDBACK STRUCTURE ( SETP - YP )
C               U , VECTOR OF CONTROLLER OUTPUTS (MANIPULATED VARIABLES)
C               YP, PLANT OUTPUTS
C               YM, MODEL OUTPUTS
C               YF  (NOT USED IN SNTEG)
C               SETPSS, DISTSS, ESS, USS, YPSS, YMSS ARE AS BEFORE BUT
C                   CORRESPONDING TO THE "OLD STEADY-STATE" VALUES
C               NC, NUMBER OF CONTROLLER STATES
C               NCALG, NUMBER OF CONTROLLER VARIABLES GIVEN BY ALG. EQNS.
C               NP, NPALG, NM, NMALG, SAME FOR PLANT AND MODEL
C               MDIS, NUMBER OF DISTURBANCES
C               MIP, NUMBER OF PLANT INPUTS
C               MOP, NUMBER OF PLANT OUTPUTS
C               ISAMPL, =.TRUE., IF A SAMPLING POINT
C                       =.FALSE., IF NOT A SAMPLING POINT
C               ISM, =2, CALLING PROGRAM IS SNTEG
C
C
C       OUTPUTS:
C               DELTA, VECTOR OF RESIDUALS REQUIRED BY DASSL
C
C


C
C       THE CONTROLLER BLOCKS CAN OF COURSE BE FUNCTIONS OF ANY OF THE
C       INPUTS TO THIS SUBROUTINE; WE JUST SPECIFY THE DEPENDENCES
C       THAT ARE CLEAR FROM THE BLOCK DIAGRAM OF FIG. 4C;
C       FOR SIMPLICITY WE WRITE THE VECTOR EQUATIONS
C
C

      IMPLICIT DOUBLE PRECISION (A-H,O-Z)
      LOGICAL ISAMPL
      DIMENSION XC(1),XCALG(1),XCDOT(1),DELTA(1),XP(1),XPALG(1),
     *  XPDOT(1),XM(1),XMALG(1),XMDOT(1),SETP(1),DIST(1),E(1),U(1),
     *  YP(1),YM(1),YF(1),SETPSS(1),DISTSS(1),ESS(1),USS(1),YPSS(1),
     *  YMSS(1),DUMMY(1)

C
C       PARAMETERS DEFINED IN DCPAR ARE PASSED BY MEANS OF THE
C       USER-DEFINED COMMON
C
      COMMON /USER_CONTR/ ...
```

```
C
C       DAE'S CORRESPONDING TO THE BLOCK E1
C
        DELTA()=FE1(...,YP,...)

C
C       OUTPUT EQUATIONS FOR THE BLOCK E1
C
        YE1()=HE1(...,YP,...)

C
C       DAE'S CORRESPONDING TO E2
C
        DELTA()=FE2(...,U,...)

C
C       OUTPUT EQUATIONS FOR E2
C
        YE2()=HE2(...,U,...)

C
C       SUM OF YE1 AND YE2
C
        Z=YE1+YE2

C
C       INPUT TO THE BLOCK C
C
        W=SETP-Z

C
C       DAE'S CORRESPONDING TO BLOCK C
C
        DELTA()=FC(...,W,...)

C
C       OUTPUT EQUATIONS FOR BLOCK C, ALSO THE OUTPUT EQUATIONS FOR
C       THE WHOLE CONTROLLER; THIS SET IS INCLUDED AMONG THE EQNS.
C       SOLVED BY DASSL
C
        DELTA()=-U + HC(...,W,...)

        RETURN
        END
```

VI. CONCLUSIONS AND SUGGESTIONS FOR FUTURE RESEARCH

The design of robust control systems for a fixed-bed catalytic methanation reactor has been approached employing the Structured Singular Value (μ) as an analysis tool and Internal Model Control (IMC) as the synthesis framework. The design procedure allowed a clear insight on the fundamental limits to the closed-loop performance and provided controllers with explicit stability and performance guarantees for the case of plant-model mismatch.

Modeling and simulation. The overall controller design effort was initiated with a careful mathematical modeling of the system. Based on a previous version by Khanna (1984), the reactor model was modified to better meet the needs of the control studies, and was simplified to delete unnecessary features of the previous version. A new computer implementation allowed significant reductions in solution times over the previous implementation and facilitated closed-loop simulations in which the nonlinear reactor model serves as the actual plant.

The deficiencies of orthogonal collocation in describing steep profiles were indicated and alternative techniques suggested. Because the linearizations were carried out around steady states of relatively mild profiles, these deficiencies should not have a significant effect on the results of the control studies. The importance of mechanistic modeling, in contrast to empirical modeling involving, for example, time series analysis of input/output data, was stressed. The latter techniques are important, but they should be used in conjunction with and as a means to corroborate, rather than to completely replace, the mathematical models.

System configuration. Control configurations. Dynamic resilience. Non-minimum phase behavior. Three control case-studies were investigated corresponding to different control configurations, although all involving single-pass operation and a fixed set of operating conditions. The effect of design considerations on the control of fixed-bed reactors, and therefore the implications of process control on deci-

sions at the design level, a topic not addressed in these studies, is an interesting, important and open subject for research, which should benefit from the models and the techniques developed or applied in this thesis.

For the three different control configurations investigated, the fundamental limitations to the achievable closed-loop performance were established by both physical arguments and dynamic resilience considerations. When the inlet reactor temperature is employed as the only manipulated variable for the regulation of the outlet temperature or product concentration, fundamental limitations arise as a result of the slow propagation of temperature changes along the bed as compared to the propagation of concentration disturbances. The slowness of the thermal wave is due to the thermal coupling between the gas and the stationary masses and hinders a rapid correction of the effect of the concentration disturbances.

It was shown that the above limitations manifest themselves in the discretized model through right-half-plane zeros of the transfer functions, i.e., non-minimum phase behavior, which precludes the possibility of perfect control even in the case of perfect models. Through IMC these performance limitations were easily quantified. The best possible closed-loop performance for the case of a perfect model was directly determined as a function of the right-half-plane zeros. It was also shown, in one of the case-studies, that right-half-plane zeros may exist without being noticeable in the open-loop response, but, of course, still affecting the closed-loop performance. The investigation of the presence of right-half-plane zeros, therefore, should always be carried out even if no apparent indications exist.

A control configuration based on the combined use of the total flow rate and the inlet temperature as manipulated variables for the case in which fast disturbance rejection is necessary was proposed and investigated. Although with this configuration the fundamental limitations to closed-loop performance are in essence not removed, much faster regulation of, for example, the outlet

temperature can be achieved. This involves, however, having to move the flow rate away from its nominal value until the corrective action of the inlet temperature changes reaches the reactor outlet. Although this is feasible to do in single-pass operation of the laboratory reactor, the feasibility of implementing this control configuration in an industrial setting will depend on the characteristics of each particular process.

In a system configuration involving product recycle, the recycle ratio could be employed as the manipulated variable instead of the inlet flow rate to the system, as a means to change the velocity-per-pass through the bed without affecting the flow rate specifications imposed by the process requirements. In spite of the importance of recycle in industry, and in spite of the extensive literature on fixed-bed reactor control, no accounts seem to exist of the use of the recycle ratio as a manipulated variable in a control configuration. How effective, if at all, recycle ratio changes will be in the rejection of, for example, inlet concentration disturbances, is certainly a subject that deserves investigation, and another study that may directly benefit from the present work and in particular from the case-study of Chapter IV mentioned in the last paragraph. In a reactor/recycle configuration, challenging control problems are predicted to arise as a result of the positive feedback of mass, and of the complications typical of any realistic recycle line (e.g., capacitances, compressor performance, product separation, etc.).

Controller design. Uncertainty characterization and the design of robust controllers. One major contribution of this thesis was to show that the design of control systems for complex, distributed systems such as the methanation reactor can be addressed in a practical way, and low-order controllers be adequately obtained, which possess near-optimal characteristics when applied in a realistic environment of uncertainty and unavailability of measurements. The thesis presented a design methodology that achieves this objectives. This methodology is based on

input/output, i.e., frequency domain methods. The strong advantages of these methods over state-variable oriented methods, so frequently employed in previous fixed-bed reactor control studies, were detailed in Chapter I. The reactor control case-studies further demonstrated the adequacy of the input/output methods. Although the methods reported are based, and the "thinking" is done, in the frequency domain, in many cases the computations employ the state-space representations and involve only the use of standard matrix operations and linear algebra. In what concerns to the particular advantages of Structured Singular Value analysis or of Internal Model Control, these were largely stressed throughout the thesis and will not be repeated here.

Both the single-input single-output and the multivariable case were treated. The multivariable framework employed facilitated a direct and clear formulation and solution of the optimal control of an unmeasured variable. Whereas a simple scheme involving only one measurement was investigated, extra measurements, measurement noise, input constraints, etc. could have been incorporated with the same ease. Adequately formulated, the approach in essence leads to equivalent results as those obtained by the standard procedures involving the separate design of a state estimator or observer; it has, however, an important advantage – that considerations such as robustness can be explicitly incorporated. Moreover, the performance objectives might be stated in terms of H_∞ rather than H_2 optimality criteria. The new framework allows the solution of both these optimization problems.

In two of the three case-studies very tight bounds were obtained for the closed-loop performance of the nonlinear plant. In a third case-study, however, conservative results were obtained. The new mathematical theory for robust control system design is powerful in the sense that it has solved a number of issues that in the past could not be adequately addressed, including the derivation of

exact (non-conservative) conditions for robust stability and robust performance in the face of unstructured or structured perturbations (Doyle, 1984). The new techniques and computational methods have helped to reduce the gap between reality and the mathematical representations of reality which can actually be solved. It is still important, however, for the application of the techniques to be successful, that the selected mathematical representation of the real problem be adequate. Some situations still exist, of course, in which how to find an adequate representation of reality is not yet sufficiently well known and deserves further investigation. The problem of how to characterize uncertainty resulting from system nonlinearities is one example of such a situation. This particular problem will continue to remain an important problem to solve for as long as linear methods are employed for the control of nonlinear systems.

Some suggestions for future research on the control of the reactor system. This thesis has presented the first in a long series of control studies that are expected to arise in the context of the fixed-bed methanation reactor system. Studies will generate other studies. This is inherent in research. Some initial suggestions for future studies follow. Some others were presented in the discussion above. This thesis is offered as a basis for the studies that will come.

— Study of a configuration involving single-pass reactor operation, and the use of the total flow rate and inlet temperature as manipulated variables for the regulation of both the outlet temperature and outlet methane concentration (initial calculations showed the condition number at steady state to be 15). Evaluation of the robust performance of controllers designed through IMC as detailed in this thesis. Application of μ-synthesis if serious robust performance problems exist for the controllers designed by the above procedure.

— Characterization of the uncertainty resulting from the system nonlinearity through pseudorandom binary sequence pulsing of the nonlinear reactor

model and spectral smoothing analysis (Chapter II).

— Study of uncertainty resulting from uncertain real parameters of the system (activation energy, kinetic constants, etc.). Combination of this and other sources of uncertainty (nonlinearity, discretization). Design of robust controllers for this case.

— Study of configurations with product recycle (see discussion above).

— Study of configurations with heat recycle. Initial investigations in this direction are summarized in Appendix D.

— Experimental studies on the actual reactor unit. Because of the potentially dangerous conditions (Chapter II) the experimental studies should be preceded by a careful parameter estimation and model validation.

REFERENCES

Doyle, J.C., 1984, Lecture notes, ONR/Honeywell Workshop on Advances in Multivariable Control, Minneapolis, MN.

Khanna, R., 1984, Control model development for packed-bed chemical reactors. Ph.D. Thesis, Calif. Inst. of Technology, Pasadena, CA.

APPENDICES

A. FIXED-BED REACTOR: MATHEMATICAL MODEL AND NUMERICAL SOLUTION

A.1 Mathematical Relationships

For convenience, the original mathematical relationships for the reactor model, in terms of dimensional quantities, are reproduced from Chapter II.

Energy balance for the catalyst phase:

$$(1-\epsilon)\rho_s c_{p_s}\frac{\partial T_s}{\partial t} = k_{zs}\frac{\partial^2 T_s}{\partial z^2} + \frac{k_{rs}}{r}\frac{\partial}{\partial r}\left[r\frac{\partial T_s}{\partial r}\right] - h_{sg}a_{sg}(T_s-T_g) + (-\Delta H_M)\tilde{R}_M \qquad (A1)$$

$$\begin{aligned}
r = R_0 \qquad & k_{rs}\frac{\partial T_s}{\partial r} = h_{ts}(T_s-T_t)\\
r = R_1 \qquad & -k_{rs}\frac{\partial T_s}{\partial r} = h_{ws}(T_s-T_w)\\
z = 0 \qquad & k_{zs}\frac{\partial T_s}{\partial z} = h_{sg}(T_s-T_g)\\
z = L \qquad & -k_{zs}\frac{\partial T_s}{\partial z} = h_{sg}(T_s-T_g) \quad .
\end{aligned}$$

Energy balance for the gas phase:

$$\epsilon\rho_g c_{p_g}\frac{\partial T_g}{\partial t} = -\epsilon G c_{p_g}\frac{\partial T_g}{\partial z} + k_{zg}\frac{\partial^2 T_g}{\partial z^2} + \frac{k_{rg}}{r}\frac{\partial}{\partial r}\left[r\frac{\partial T_g}{\partial r}\right] - h_{sg}a_{sg}(T_g-T_s) \qquad (A2)$$

$$\begin{aligned}
r = R_0 \qquad & k_{rg}\frac{\partial T_g}{\partial r} = h_{tg}(T_g-T_t)\\
r = R_1 \qquad & -k_{rg}\frac{\partial T_g}{\partial r} = h_{wg}(T_g-T_w)\\
z = 0 \qquad & k_{zg}\frac{\partial T_g}{\partial z} = h_{sg}(T_g-T_s) - G c_{p_g}\epsilon(T_{in}-T_g)\\
z = L \qquad & -k_{zg}\frac{\partial T_g}{\partial z} = h_{sg}(T_g-T_s) \quad .
\end{aligned}$$

Energy balance for the thermal well:

$$\rho_t c_{p_t} \frac{\partial T_t}{\partial t} = k_{zt} \frac{\partial^2 T_t}{\partial z^2} + h_{ts} a_{ts} (T_{s_{r=R_0}} - T_t) + h_{tg} a_{tg} (T_{g_{r=R_0}} - T_t) \qquad \text{(A3)}$$

$$z = 0 \qquad T_t = T_{in}$$
$$z = L \qquad \frac{\partial T_t}{\partial z} = 0 \quad .$$

Species balance for the CO:

$$\rho_g \frac{\partial \hat{x}_1}{\partial t} = -G \frac{\partial \hat{x}_1}{\partial z} + \frac{D_r}{r} \frac{\partial}{\partial r} \left[r \rho_g \frac{\partial \hat{x}_1}{\partial r} + \frac{2 \rho_g \hat{x}_1 r}{1-2\delta} \frac{\partial \delta}{\partial r} \right] - \frac{\bar{R}_M \hat{M}_g}{\epsilon} \qquad \text{(A4)}$$

$$r = R_0 R_1 \qquad D_r \frac{\partial \hat{x}_1}{\partial r} = 0$$
$$z = 0 \qquad \hat{x}_1 = \hat{x}_{1_{in}} \quad .$$

Reaction rate:

$$\bar{R}_m = R_m \rho_s \psi (1-\epsilon) \qquad \text{(A5)}$$

$$R_M = \frac{0.0217\ p_{CO}\ p_{H_2}\ t_d^{-0.3} (1-\upsilon)}{(1 + 110\ p_{CO} + 2.32\ p_{H_2})^2} \quad \left(\frac{\text{moles}}{\text{sec gcat}} \right) \qquad \text{(A6)}$$

$$\upsilon = \frac{p_{CH_4} p_{H_2O}}{p_{CO} (p_{H_2})^3} \frac{1}{K_{p_M}} \qquad \text{(A7)}$$

Additional relationships:

$$\delta = \frac{x_{1_0} - x_1}{1 - 2x_1} \qquad \text{(A8)}$$

$$\hat{x}_1 = x_1 (1-2\delta) \qquad \text{(A9)}$$

$$\rho_g = \frac{M_g P}{RT_g} = \frac{\hat{M}_g \hat{P}}{RT_g} \tag{A10}$$

$$\hat{M}_g = M_g(1 - 2\delta) \tag{A11}$$

$$\hat{P} = P(1 - 2\delta)^{-1} \tag{A12}$$

$$\hat{P} = \left[\frac{\hat{P}_{z=L} - \hat{P}_{z=0}}{L}\right] z + \hat{P}_{z=0} \tag{A13}$$

A.2 Parameters of the Reactor Model

Table A1 defines the parameters of the reactor model. The table includes the names of the different parameters as they appear in the reactor code, the numerical values employed in the case-studies and their sources, and indications regarding the need for further direct measurement on the experimental system, or for parameter estimation, prior to the experimental control studies. The parameters are divided into groups. The group names are those of the corresponding COMMON blocks in the reactor code.

TABLE A1: REACTOR PARAMETERS

Parameter		*Code*	*Value*	*Notes†*
REACTOR DIMENSIONS (/REACP/)				
L	length of reactor bed, cm	L	30	K
R_0	radius of thermal well, cm	R0	0.158	K
R_1	radius of reactor bed, cm	R1	1.194	K
CATALYST BED (/CATLS/)				
d_p	characteristic particle diameter, cm	DC	0.27	K,M
ϵ	void fraction, cm^3 void/cm^3 bed	EPS	0.57	K,M
ψ	dilution factor, cm^3 cat/cm^3 pellets	DIL	0.25	S,M
ρ_s	catalyst density, g/cm^3 cat	RHOS	1.041	K
c_{p_s}	heat capacity, cal/g K	CPS	0.25	K
k_{zs},k_{rs}	thermal conductivity of the solid phase, cal/sec cm K	TC	0.0005	K,C
k_{zg},k_{rg}	effective thermal conductivity of the fluid, cal/sec cm K	TCGAS	0.0001	P,C
THERMAL WELL (/THWEL/)				
ρ_t	density, g/cm^3	RHOT	8.02	K
c_{p_t}	heat capacity, cal/g K	CPT	0.12	K
k_{zt}	thermal conductivity, cal/sec cm K	KT	0.039	K
HEAT TRANSFER PARAMETERS (/HEATT/)				
$U_{sg} = h_{sg}a_{sg}V_{bed}$	overall heat transfer coefficient (solid/gas), cal/sec K	OHSG	17.02	K,E
$U_{ts} = h_{ts}a_{ts}V_{thw}$	overall heat transfer coefficient (th.well/solid), cal/sec K	OHTS	0.0179	K,E
$U_{tg} = h_{tg}a_{tg}V_{thw}$	overall heat transfer coefficient (th.well/gas), cal/sec K	OHTG	0.1436	K,E

TABLE A1: CONTINUED

Parameter		*Code*	*Value*	*Notes†*
$Bi_{gzs} = \frac{h_{sg}L}{k_{zs}}$	Biot number (solid-gas)	BGS	600	K,E
$Bi_{szg} = \frac{h_{sg}L}{k_{zg}}$	Biot number (gas-solid)	BSG	13.09	K,E; 3000
$Bi_{trs} = \frac{h_{ts}R_1}{k_{rs}}$	Biot number (th.well-solid)	BTS	7.163	K,E
$Bi_{trg} = \frac{h_{tg}R_1}{k_{rg}}$	Biot number (th.well-gas)	BTG	1.25	K,E; 64.7
REACTION PARAMETERS (/REAC1/)				
$\Delta H_M = \Delta H_a T + \Delta H_b$	constants for heat of reaction, cal/mole	DH1A DH1B	-6.144 -48350.3	K K
$\ln K_{p_M} = K_{pA} + K_{p_B}/T$	equilibrium constant	KP1A KP1B	-29.437 26341.6	K K
METHANATION REACTION RATE (/REAC2/)				
$k_0' = k_0 \exp(\frac{E_a}{RT_{exp}})$	pre-exponential factor, moles/sec gcat atm^2	K0P	0.0217	Ch,Ek
E_a	activation energy, cal/gmole	EA1	37000	Ch,Ek
T_{exp}	reference temp. for evaluation of k_0', K	TEXPR	513	Ch
t_d	time spent by catalyst on stream (for deactivation factor), hr	TDEAC	400	Ch
	exponent of CO in rate expression	EXA	1	Ch,Ek
	exponent of H_2 in rate expression	EXB	1	Ch,Ek
	exponent of adsorption group in rate expression	EXC	1	Ch,Ek
K_1	reaction rate constant, atm^{-1}	K1	110.05	Ch,Ek

TABLE A1: CONTINUED

Parameter		*Code*	*Value*	*Notes†*
K_2	reaction rate constant, atm^{-1}	K2	2.317	Ch,Ek
OPERATING CONDITIONS (/INPUTV/)				
T_w	reactor wall temperature, K	TW	530	S
F_P	total molar flow rate, gmol/sec	FLOW	0.0223	S
T_{in}	reactor inlet temperature, K	TF	537	S
$x_{1_{in}}$	CO inlet mole fraction	XCO0	0.06	S
	CO_2 inlet mole fraction	XCO20	0.	S
	H_2O inlet mole fraction	XH2O0	0.	S
	H_2 inlet mole fraction	XH20	0.18	S
	CH_4 inlet mole fraction	XCH40	0.	S
$P_{z=0}$	total inlet pressure, atm	PT0	20.	S
$P_{z=L}$	total outlet pressure, atm	PT1	19.	S
REFERENCE CONDITIONS (/REFCON/)				
c_{REF}	reference concentration	SCO	0.03	R
T_{REF}	reference temperature, K	ST0	40	R
F_{REF}	reference flow rate, gmol/sec	FLOWRF	0.0223	R

TABLE A1: CONTINUED

†NOTES

C Correlations are available (e.g., Pereira-Duarte *et al.* (1984)) for further verification for the conditions of the experimental system.

Ch Source: Chiang (1983).

E Should be determined from parameter estimation based on results of dynamic experiments under conditions of zero reaction (Chapter II).

Ek Estimated from results of steady-state kinetic experiments.

K Source : Khanna (1984).

M Should be measured or determined for the particular conditions of each catalyst batch.

P Source: Pereira-Duarte *et al.* (1984).

R The reference values were selected for adequate input/output scaling in the control studies.

S Source: Strand (1984).

Realistic values for the ratio between the thermal conductivities of the solid and gas phases suggest a different set of values for Bi_{szg} and Bi_{trg}. The new values, shown under this heading, are the ones appearing in the latest version of the data file. Simulations run with these new values showed a relatively minor change in the results, considering the large differences between the old and new values. These and all other parameters should be further verified for the final conditions under which the experiments will be run.

A.3 Normalized Reactor Model

For convenience in the control studies, the balance equations of Section A1 are normalized *to leave all terms in units of 1/sec*, rather than in entirely dimensionless form. The normalization is based on the definition of the following dimensionless variables:

$$\zeta = \frac{z}{L} \qquad r = \frac{r}{R_1}$$

$$\Theta = \frac{T}{T_{REF}} \qquad y_1 = \frac{\hat{x}_1}{c_{REF}} \qquad \hat{P}^* = \frac{\hat{P}}{\hat{P}_{z=0}}$$

$$\rho_g^* = \frac{\rho_g}{\rho_{g_{REF}}} \qquad c_{p_g}^* = \frac{c_{p_g}}{c_{p_{gREF}}} \qquad \hat{M}_g^* = \frac{\hat{M}_g}{M_{g_{REF}}} \quad .$$

Note also the following definitions and relationships:

$$\phi_0 = \frac{R_0}{R_1}$$

$$\Delta H_M = \Delta H_1 T_s + \Delta H_2$$

$$\phi_1 = \frac{\Delta H_1 T_{REF}}{\Delta H_2}$$

$$\rho_g^* = \frac{\hat{M}_g^* \hat{P}^*}{\Theta_g} \quad .$$

In the normalized balance equations that follow, the $(^*)$ is dropped from ρ_g^*, $c_{p_g}^*$, $\hat{M}_g^*$ and $\hat{P}^*$.

Energy balance for the catalyst phase:

$$\frac{\partial \Theta_s}{\partial t} = \alpha_s \frac{\partial^2 \Theta_s}{\partial \zeta^2} + \frac{\beta_s}{r}\frac{\partial}{\partial r}\left[r\frac{\partial \Theta_s}{\partial r}\right] - \gamma_s(\Theta_s - \Theta_g) + \delta_1(1 + \phi_1\Theta_s)R'_M \qquad \text{(A14)}$$

$$\begin{aligned}
r &= \phi_0 \qquad \frac{\partial \Theta_s}{\partial r} = Bi_{trs}(\Theta_s - \Theta_t) \\
r &= 1 \qquad -\frac{\partial \Theta_s}{\partial r} = Bi_{wrs}(\Theta_s - \Theta_w) \\
\zeta &= 0 \qquad \frac{\partial \Theta_s}{\partial \zeta} = Bi_{gzs}(\Theta_s - \Theta_g) \\
\zeta &= 1 \qquad -\frac{\partial \Theta_s}{\partial \zeta} = Bi_{gzs}(\Theta_s - \Theta_g) \quad .
\end{aligned}$$

Energy balance for the gas phase:

$$\rho_g C_{p_g}\frac{\partial \Theta_g}{\partial t} = -\kappa C_{p_g}\frac{\partial \Theta_g}{\partial \zeta} + \alpha_g\frac{\partial^2 \Theta_g}{\partial \zeta^2} + \frac{\beta_g}{r}\frac{\partial}{\partial r}\left[r\frac{\partial \Theta_g}{\partial r}\right] - \gamma_g(\Theta_g - \Theta_s) \qquad \text{(A15)}$$

$$\begin{aligned}
r &= \phi_0 \qquad \frac{\partial \Theta_g}{\partial r} = Bi_{trg}(\Theta_g - \Theta_t) \\
r &= 1 \qquad -\frac{\partial \Theta_g}{\partial r} = Bi_{wrg}(\Theta_g - \Theta_w) \\
\zeta &= 0 \qquad \frac{\partial \Theta_g}{\partial \zeta} = Bi_{szg}(\Theta_g - \Theta_s) - \Gamma C_{p_g}(\Theta_{in} - \Theta_g) \\
\zeta &= 1 \qquad -\frac{\partial \Theta_g}{\partial \zeta} = Bi_{szg}(\Theta_g - \Theta_s) \quad .
\end{aligned}$$

Energy balance for the thermal well:

$$\frac{\partial \Theta_t}{\partial t} = \alpha_t\frac{\partial^2 \Theta_t}{\partial \zeta^2} + \gamma_{ts}(\Theta_{s_{r=\phi_0}} - \Theta_t) + \gamma_{tg}(\Theta_{g_{r=\phi_0}} - \Theta_t) \qquad \text{(A16)}$$

$$\zeta = 0 \qquad \Theta_t = \Theta_{in}$$
$$\zeta = 1 \qquad \frac{\partial \Theta_t}{\partial \zeta} = 0 \quad .$$

Species balance for the CO:

$$\frac{\partial y_1}{\partial t} = -\frac{\kappa}{\rho_g}\frac{\partial y_1}{\partial \zeta} + \frac{\beta_m}{\rho_g r}\frac{\partial}{\partial r}\left[r\rho_g \frac{\partial y_1}{\partial r} + \frac{2\rho_g y_1 r}{1-2\delta}\frac{\partial \delta}{\partial r}\right] - \sigma_1 \frac{\Theta_g}{\hat{P}} R'_M \qquad \text{(A17)}$$

$$r = \phi_0 \, , \, 1 \qquad \frac{\partial y_1}{\partial r} = 0$$
$$\zeta = 0 \qquad y_1 = y_{1_{in}} \quad .$$

The normalized parameters of the reactor model are listed below.

Convection

$$\kappa = \frac{G}{\rho_{g_{REF}} L} \qquad \Gamma = \frac{G c_{p_{gREF}} \epsilon L}{k_{zg}}$$

Axial dispersion

$$\alpha_s = \frac{k_{zs}}{(1-\epsilon)\rho_s c_{p_s} L^2} \qquad \alpha_g = \frac{k_{zg}}{\epsilon \rho_{g_{REF}} c_{p_{gREF}} L^2} \qquad \alpha_t = \frac{k_{zt}}{\rho_t c_{p_t} L^2}$$

Radial dispersion of heat

$$\beta_s = \frac{k_{rs}}{(1-\epsilon)\rho_s c_{p_s} R_1^2} \qquad \beta_g = \frac{k_{rg}}{\epsilon \rho_{g_{REF}} c_{p_{gREF}} R_1^2}$$

Radial dispersion of mass

$$\beta_m = \frac{D_r}{R_1^2}$$

Heat transfer

$$\gamma_s = \frac{h_{sg} a_{sg}}{(1-\epsilon)\rho_s c_{p_s}} \qquad \gamma_g = \frac{h_{sg} a_{sg}}{\epsilon \rho_{g_{REF}} c_{p_{gREF}}}$$

$$\gamma_{ts} = \frac{h_{ts} a_{ts}}{\rho_t c_{p_t}} \qquad \gamma_{tg} = \frac{h_{tg} a_{tg}}{\rho_t c_{p_t}}$$

Heat of reaction

$$\delta_1 = \frac{(-\Delta H_2)\, k'_0\, P^2_{z=0}\, c^2_{REF}\, t_d^{-0.3} \psi}{c_{p_s} T_{REF}}$$

Reaction coefficient

$$\sigma_1 = \frac{k'_0\, P^2_{z=0}\, c^2_{REF}\, t_d^{-0.3} \rho_s \psi (1-\epsilon)\, M_{g_{REF}}}{\rho_{g_{REF}} \epsilon}$$

Reaction rate

$$R'_M = \exp\left(-\frac{E_a}{R}\left(\frac{1}{T} - \frac{1}{T_{exp}}\right)\right) \quad \frac{x'_{CO} x'_{H_2} P'^2}{(1+K'_1 x'_{CO} P' + K'_2 x'_{H_2} P')^2}\,(1-\upsilon) \qquad \text{(A18)}$$

where

$$P' = \frac{P}{P_{z=0}}$$

$$x'_{CO} = \frac{x_{CO}}{C_{REF}} = \frac{y_1}{1-2\delta}$$

$$x'_{H_2} = \frac{x_{H_2}}{C_{REF}}$$

$$K'_1 = K_1 P_{z=0} C_{REF}$$

and

$$K'_2 = K_2 P_{z=0} C_{REF} \quad .$$

The Biot numbers are defined in Table A1. Bi_{wrs} and Bi_{wrg} are assumed equal, respectively, to Bi_{trs} and Bi_{trg}.

A.4 Radial Collocation

The collocation in the radial direction is carried out employing the same procedure as the one detailed in Appendix 3 of the thesis by Khanna (1984). Therefore, only the final equations are presented here. For convenience, the same names are kept as those employed by Khanna to indicate the coefficients of the radially discretized model.[1]

In the following equations Θ_s and Θ_g indicate, respectively, the catalyst and gas temperatures *at the radial collocation point.* As discussed in Chapter II, because of the zero-flux radial boundary conditions for the concentration equation, the quadratic representation of the radial concentration profiles (inherent when employing one interior collocation point) reduces to an assumption of constant concentrations along the radial direction. In the CO species balance, therefore, y_1 indicates this radially uniform concentration. Indications as to how to discretize the model employing multiple interior collocation points for the concentration profiles are given in the thesis by Khanna (p. 235).

1. The Biot numbers, here indicated by Bi, are indicated by Khanna with λ's.

Energy balance for the catalyst phase:

$$\frac{\partial \Theta_s}{\partial t} = \alpha_s \frac{\partial^2 \Theta_s}{\partial \zeta^2} + \omega_1 \Theta_s + \omega_2 \Theta_t + \gamma_s \Theta_g + \delta_1 (1 + \phi_1 \Theta_s) R'_M + \omega_3 \Theta_w \qquad \text{(A19)}$$

$$\zeta = 0 \qquad \frac{\partial \Theta_s}{\partial \zeta} = Bi_{gzs}(\Theta_s - \Theta_g)$$

$$\zeta = 1 \qquad -\frac{\partial \Theta_s}{\partial \zeta} = Bi_{gzs}(\Theta_s - \Theta_g) \quad .$$

Energy balance for the gas phase:

$$\rho_g C_{p_g} \frac{\partial \Theta_g}{\partial t} = -\kappa C_{p_g} \frac{\partial \Theta_g}{\partial \zeta} + \alpha_g \frac{\partial^2 \Theta_g}{\partial \zeta^2} + \omega_4 \Theta_g + \omega_5 \Theta_t + \gamma_g \Theta_s + \omega_6 \Theta_w \qquad \text{(A20)}$$

$$\zeta = 0 \qquad \frac{\partial \Theta_g}{\partial \zeta} = Bi_{szg}(\Theta_g - \Theta_s) - \Gamma C_{p_g}(\Theta_{in} - \Theta_g)$$

$$\zeta = 1 \qquad -\frac{\partial \Theta_g}{\partial \zeta} = Bi_{szg}(\Theta_g - \Theta_s) \quad .$$

Energy balance for the thermal well:

$$\frac{\partial \Theta_t}{\partial t} = \alpha_t \frac{\partial^2 \Theta_t}{\partial \zeta^2} + \omega_7 \Theta_s + \omega_8 \Theta_g + \omega_9 \Theta_t + \omega_{10} \Theta_w \qquad \text{(A21)}$$

$$\zeta = 0 \qquad \Theta_t = \Theta_{in}$$

$$\zeta = 1 \qquad \frac{\partial \Theta_t}{\partial \zeta} = 0 \quad .$$

Species balance for the CO:

$$\frac{\partial y_1}{\partial t} = -\frac{\kappa}{\rho_g} \frac{\partial y_1}{\partial \zeta} - \sigma_1 \frac{\Theta_g}{\hat{P}} R'_M \qquad \text{(A22)}$$

$$\varsigma = 0 \qquad y_1 = y_{1_{in}} \quad .$$

In the equations above, $\omega_1, \cdots, \omega_{10}$ equal those defined by Khanna (1984, pp. 393-395) with the exception that ω_3, ω_6 and ω_{10} are as those defined by Khanna, but divided by Θ_w.

A.5 Orthogonal Collocation in the Axial Direction

The radially discretized model given by Eqs (A19)-(A22) is still too complex for direct mathematical solution, and further discretization is carried out by orthogonal collocation in the axial direction. This results in a significant increase in the number of differential equations, but these equations are of the ordinary type and well posed for direct solution in time, i.e., for dynamic simulation.

The procedure developed by Villadsen and Michelsen (1978), summarized in Section 3 of Chapter II, is applied. The N interior collocation points are selected to be the roots of an Nth degree Legendre polynomial ($\alpha = \beta = 0$ in the general expression for the Jacobi polynomials in Villadsen and Michelsen (1978)). The collocation points are calculated using programs provided by Villadsen and Michelsen in their book. The assumed axial profiles (Eq. (12) of Chapter II) are replaced in the differential equations (A19)-(A22), and the residuals set equal to zero at the collocation points. The assumed profiles and their derivatives, evaluated at each collocation point, are given by Eqs (14)-(16) of Chapter II. The boundary conditions need also be satisfied by the assumed profiles. For each PDE, then, one equation results for each collocation point and one for each boundary condition involving an unknown dependent variable. In our case, both ς=0 and ς=1 are included as interpolation points and the interpolation polynomial is, therefore, of degree N+2, as indicated in Chapter II.

The Lagrange polynomials l_i and their derivatives

$$A_{ij} = \frac{dl_j}{d\zeta}(\zeta_i) \tag{A23}$$

$$B_{ij} = \frac{d^2 l_j}{d\zeta^2}(\zeta_i) \tag{A24}$$

are functions only of the collocation points, and are evaluated *a priori* , also by means of a program provided by Villadsen and Michelsen (1978). By replacing Eqs (14)-(16) of Chapter II into the radially discretized model (A19)-(A22), the following equations result in terms of conditions at the collocation points ζ_i.

Energy balance for the catalyst phase:

$$\frac{d\Theta_{s_i}}{dt} = \alpha_s \sum_{j=0}^{N+1} B_{ij}\Theta_{s_j} + \omega_1\Theta_{s_i} + \omega_2\Theta_{t_i} + \gamma_s\Theta_{g_i} + \delta_1(1 + \phi_1\Theta_{s_i})R'_{M_i} + \omega_3\Theta_w \tag{A25}$$

$$\zeta = 0 \qquad \sum_{j=0}^{N+1} A_{0j}\Theta_{s_j} = Bi_{gzs}(\Theta_{s_0} - \Theta_{g_0})$$

$$\zeta = 1 \qquad -\sum_{j=0}^{N+1} A_{N+1,j}\Theta_{s_j} = Bi_{gzs}(\Theta_{s_{N+1}} - \Theta_{g_{N+1}}) \quad .$$

Energy balance for the gas phase:

$$\frac{\hat{M}_g \hat{P}_i}{\Theta_{g_i}} c_{p_{gi}} \frac{d\Theta_{g_i}}{dt} = -\kappa c_{p_{gi}} \sum_{j=0}^{N+1} A_{ij}\Theta_{g_j} + \alpha_g \sum_{j=0}^{N+1} B_{ij}\Theta_{g_j} + \omega_4\Theta_{g_i} + \omega_5\Theta_{t_i} + \gamma_g\Theta_{s_i} + \omega_6\Theta_w \tag{A26}$$

$$\zeta = 0 \qquad \sum_{j=0}^{N+1} A_{0j}\Theta_{g_j} = Bi_{szg}(\Theta_{g_0} - \Theta_{s_0}) - \Gamma c_{p_{g0}}(\Theta_{in} - \Theta_{g_0})$$

$$\zeta = 1 \qquad -\sum_{j=0}^{N+1} A_{N+1,j}\Theta_{g_j} = Bi_{szg}(\Theta_{g_{N+1}} - \Theta_{s_{N+1}}) \quad .$$

Energy balance for the thermal well:

$$\frac{d\Theta_{t_i}}{dt} = \alpha_t \sum_{j=0}^{N+1} B_{ij}\Theta_{t_j} + \omega_7\Theta_{s_i} + \omega_8\Theta_{g_i} + \omega_9\Theta_{t_i} + \omega_{10}\Theta_w \qquad \text{(A27)}$$

$$\zeta = 0 \qquad \Theta_{t_0} = \Theta_{in}$$

$$\zeta = 1 \qquad \sum_{j=0}^{N+1} A_{N+1,j}\Theta_{t_j} = 0 \quad .$$

Species balance for the CO:

$$\frac{dy_{1_i}}{dt} = -\left(\frac{\kappa}{\hat{M}_g} \sum_{j=0}^{N+1} A_{ij}y_{1_j} + \sigma_1 R'_{M_i}\right) \frac{\Theta_{g_i}}{\hat{P}_i} \qquad \text{(A28)}$$

$$\zeta = 0 \qquad y_{1_0} = y_{1_{in}} \quad .$$

The index i ranges from 1 to N for all the differential equations, except for Eq. (A28), in which it ranges from 1 to N+1, since otherwise the concentration at $\zeta = 1$ would be unspecified. An index "0" indicates conditions at the reactor inlet ($\zeta = 0$), and "N+1", conditions at $\zeta = 1$.

A.6 Numerical Solution of the Nonlinear Discretized Model

The unknowns in Eqs (A25)-(A28) are Θ_{s_i}, i=0,...,N+1, Θ_{g_i}, i=0,...,N+1, Θ_{t_i}, i=1,...,N+1, and y_{1_i}, i=1,...,N+1. At each collocation point, the reaction rate, R'_{M_i}, and the heat capacity of the gas, $c_{p_{gi}}$, are calculated explicitly on the basis of the temperatures and CO mole fraction at the point. Stoichiometric relationships are employed to determine the concentrations of all the species. The molecular weight, $\hat{M}_g$, is based on the conditions at the reactor inlet. The pseudopressure, $\hat{P}$, is calculated as a function of axial position on the basis of Eq. (A13), which after nondimensionalization can be written as

$$\hat{P} = \tau_1 \varsigma + 1 \tag{A29}$$

where

$$\tau_1 = \frac{\hat{P}_{\varsigma=1}}{\hat{P}_{\varsigma=0}} - 1 \quad .$$

A simple algebraic manipulation on the second boundary condition of Eq. (A27) allows for explicit solution of the thermal well temperature at $\varsigma = 1$; i.e.,

$$\Theta_{t_{N+1}} = -\frac{\sum_{j=1}^{j=N} A_{N+1,j}\Theta_{t_j} + A_{N+1,0}\Theta_{in}}{A_{N+1,N+1}} \quad . \tag{A30}$$

After replacing Eq. (A30), the system (A25)-(A28) reduces to a coupled system of 4N+1 ODE's (only the N thermal-well equations being linear) and four algebraic equations corresponding to the boundary conditions in Eqs (A25) and (A26).[2] Of the algebraic equations, one is nonlinear because of the temperature dependence of the gas heat capacity. The 4N+5 equations constitute the nonlinear dynamic model of the reactor, which is solved numerically by the techniques described in Chapters II and V.

A.7 State, Input and Output Vectors of the Reactor Model

Although not actually necessary because of the treatment of the system as a nonlinear DAE system (Chapter V), in the program SNTEG, for convenience, the vector of unknowns is partitioned into two vectors: the state vector x and a vector z of variables corresponding to the algebraic equations. In the reactor code the state vector is defined as

2. The N+1 additional nonlinear algebraic equations included by Khanna (1984) for the overall continuity equation are eliminated in the present formulation.

$$XP \triangleq [\Theta_{s_1}, \cdots, \Theta_{s_N}, \Theta_{g_1}, \cdots, \Theta_{g_N}, \Theta_{t_1}, \cdots, \Theta_{t_N}, y_{1_1}, \cdots, y_{1_{N+1}}]^T \qquad (A31)$$

(i.e., 4N+1 variables), and the second vector as

$$XPALG \triangleq [\Theta_{s_0}, \Theta_{s_{N+1}}, \Theta_{g_0}, \Theta_{g_{N+1}}]^T \quad . \qquad (A32)$$

The (normalized) input vector in the reactor model is defined as

$$UR \triangleq [\Theta_w, F'_P, byp, \Theta_{in}, \Theta_{sys}, x'_{CO_{in}}, x'_{CO_{2_{in}}}, x'_{H_2O_{in}}, x'_{H_{2_{in}}}, x'_{CH_{4_{in}}}]^T. \qquad (A33)$$

$F'_P = \frac{F_P}{F_{REF}}$ is the normalized total molar flow rate to the system (The total mass flow rate G is readily calculated from F_P and the inlet composition .) Two of the elements of the input vector, byp and Θ_{sys}, are not used in the context of single-pass operation.

The output vector is defined to be equal to the state vector but is augmented with the CH_4 mole fraction at the outlet, the outlet gas temperature, and the total molar flow rate to the system, in this particular order. Temperatures or concentrations at any location other than the collocation points can be obtained through Lagrange interpolation (Villadsen and Michelsen, (1978), p. 132), and in this way they can be readily included as elements of the output vector.

A.8 Linearization; State-Space Model

The nonlinear discretized reactor model can be written as[3]

$$\dot{x} = F(x, z, u) \qquad x(0) = x_0 \qquad (A34)$$

$$0 = G(x, z, u) \qquad (A35)$$

3. In the following discussion, the letter z will indicate the vector of dependent variables corresponding to the algebraic equations and should not be confused with distance along the reactor bed.

$$y = H(x, z, u) \quad , \tag{A36}$$

where x is given by Eq. (A31), z by Eq. (A32) and u by Eq. (A33). The linearization of this model to arrive to the standard state-space description

$$\begin{aligned} \dot{x}(t) &= Ax(t) + Bu(t) \qquad x(0) = x_0 \\ y(t) &= Cx(t) + Du(t) \end{aligned} \tag{A37}$$

is carried out by a semi-analytic procedure. The procedure involves determining analytic expressions for the partial derivatives of F, G and H with respect to x, z and u. Finding these expressions is straightforward. A second step involves rearrangement and substitution to eliminate all explicit references to z. This is done numerically for the reasons noted in Chapter II.

For convenience, the rate expression of Eq. (A18) is first linearized separately. The linearized rate is of the form

$$R'_M \approx R'_{M_s} + \frac{\partial R'_M}{\partial \Theta_s}\Big|_s (\Theta_s - \Theta_{s_s}) + \frac{\partial R'_M}{\partial x'_{CO}}\Big|_s (x'_{CO} - x'_{CO_s}) + \frac{\partial R'_M}{\partial u}\Big|_s (u - u_s) \tag{A38}$$

where the last term indicates, in a compressed notation, terms corresponding to each one of the elements of the input vector. Note that the partial derivatives are with respect only to elements of the state or input vectors. Stoichiometric relationships are therefore employed to replace, for example, x'_{H_2} in terms of elements of x and u. Equation (A38) is replaced directly in Eqs (A25) and (A28). Then, the linearization of (A34)-(A36) is done in the usual fashion, to obtain

$$\dot{\hat{x}} \approx \frac{\partial F}{\partial x}\Big|_s \hat{x} + \frac{\partial F}{\partial z}\Big|_s \hat{z} + \frac{\partial F}{\partial u}\Big|_s \hat{u} \tag{A39}$$

$$\hat{y} \approx \frac{\partial H}{\partial x}\Big|_s \hat{x} + \frac{\partial H}{\partial z}\Big|_s \hat{z} + \frac{\partial H}{\partial u}\Big|_s \hat{u} \quad , \tag{A40}$$

where the hats denote deviation variables. The algebraic system of equations becomes

$$0 \approx \frac{\partial G}{\partial x}\Big|_s \hat{x} + \frac{\partial G}{\partial z}\Big|_s \hat{z} + \frac{\partial G}{\partial u}\Big|_s \hat{u} \quad . \tag{A41}$$

$\hat{z}$ is solved explicitly from Eq. (A41) and replaced in Eqs (A39)-(A40) to arrive at the final state-space model. For example, the A matrix in Eq. (A37) equals

$$A = \frac{\partial F}{\partial x}\Big|_s - \frac{\partial F}{\partial z}\Big|_s \left(\frac{\partial G}{\partial z}\Big|_s\right)^{-1} \frac{\partial G}{\partial x}\Big|_s \tag{A42}$$

The previous formulation of the nonlinear discretized reactor model included derivatives of the states inside the algebraic equations (Khanna, 1984). This case was handled with the same ease by means of this semi-analytic linearization.

B. PRINCIPAL COMPUTER PROGRAMS

The following list summarizes the main computer programs developed during the course of this work. Further details are provided within the internal documentation of each program. Most programs are set up for interactive sessions. Program usage (input/output), as well as the subroutine calls, are included only for the reactor programs. The reactor programs are ordered and numbered ((1),(2),...,etc.) in the *typical* sequence in which they are used. Several of these programs use the same subroutines and files. These are described only in their first appearance in the list.

SIMULATION

Name: SNTEG, DSNTEG (double precision)

Purpose: Open- and closed-loop simulation of general dynamic systems described by systems of differential and algebraic equations. Described in Chapter V, and documented internally and in Morari and Ray (1986).

REACTOR PROGRAMS

Name: REACTORSS (1)

Purpose: Steady-state solution of the reactor model, and computation of the state-space matrices corresponding to a linearization about this steady state.

Desc./Algor.:[1] The discretized reactor model (Eqs (A25)-(A28)) is implemented in a subroutine named DPLANT. This subroutine is set up to be used for the function evaluations both in the steady-state solution with REACTORSS

1. Description; Algorithm.

and in the dynamic simulations with RSNTEG (see below). The only difference resides in the way the subroutine is called. At steady state the discretized reactor model becomes a nonlinear system of algebraic equations. This system is solved either by Newton's method or by Powell's algorithm. The semi-analytic linearization procedure of Section A.8 is applied for the calculation of the state-space matrices.

Input: Files:[2]

".GEN": operating conditions of the reactor system

".REA": parameters of the reactor model

".SAV": initial guess for the steady-state profiles (result of a previous solution by REACTORSS)

Interactive

Output: Files:[3]

".SAV": new profiles are saved here for later use as initial guesses

".STE": saves the new profiles + additional data for use by SELECT

".MAT": saves the full state-space matrices (A,B,C,D) including all possible input/output pairs in the system; later used as input to SELECT

Tables

Plots

Calls:[4] GENDAT: reads operating conditions

REACDAT: reads reactor parameters; calculates dimensionless parameters; calls:

RADIAL: calculates the constants for the radially discretized model (written by Khanna (1984))

2. The three letters indicate the file-name extensions accepted by the program for each type of file. How to specify these files is described in the internal documentation of the programs. File-names are entered by the user in the interactive session.
3. Output files are saved only if desired by the user.
4. Only the main subroutine calls are listed. The list follows the logical sequence in the code.

COLLOC: calls JCOBI (Villadsen and Michelsen, 1978), which finds the collocation points as the roots of a Legendre polynomial, and DFOPR (same source), which finds the collocation matrices A and B (Section A.5)

STEADY: finds the steady-state solution; calls:

NLES: Newton's method, or

NSES1: Powell's method (CIT subroutine)

Both subroutines call:

FREAC: (declared external), a front end to

DPLANT: the reactor model subroutine; calls:

REAC: calculation of the dimensionless reaction rate

OUTPUT: displays the steady-state profiles in the form of tables or plots; calls:

JCOBI

INTRP: (Villadsen and Michelsen, 1978), evaluates the Lagrange interpolation coefficients for calculation of the solution at points other than the collocation points

MAPPLT: spawns the ZPLOT interactive graphics package (Morari and Ray, 1986)

REACMAT: calculates the state-space matrices and puts the data into ".MAT" files; calls:

LIREAC: linearization of the reaction-rate expressions

ANALIN: model linearization following the approach detailed in Section A.8; calls LINPACK subroutines for the matrix inversions (cf. Eq. (A42))

Location: XHMEIA::USER1:[JAM.REACTOR]

Name: SELECT (2)

Purpose: Selection of manipulated, disturbance and output variables.

Desc./Algor.: The output files ".STE" and ".MAT" from REACTORSS are "raw" files including entries corresponding to all possible input/output variables in the reactor system. (In the current implementation there are 10 possible inputs, and, for 12 collocation points, 56 possible outputs .) SELECT allows the user to choose the particular set needed for a control study. SELECT is convenient because one may need to carry control studies based on different control configurations, but always with the same steady-state data.

Input: Files:

".STE"

".MAT"

Interactive

Output: Files:

".INC": saves the initial conditions (old steady state) in the format required by SNTEG

".COD": saves an integer array indicating the selection of manipulated, disturbance and output variables

".CSC": the standard CONSYD state-space file (Morari and Ray, 1986)

".CSD": same as ".CSC", but in double precision

Calls: SELINP: selection of manipulated and disturbance variables

SELOUT: selection of output variables

Location: XHMEIA::USER1:[JAM.REACTOR]

Name: RSNTEG, REACSUBS (3)

Purpose: Dynamic simulation of the nonlinear reactor model.

Desc./Algor.: RSNTEG is the general program DSNTEG but compiled allowing a larger number of state variables than in the usual CONSYD implementation. In addition, the program can read directly double precision state-space files (".CSD" files). REACSUBS is a set of subroutines defining the non-linear reactor model, structured in the usual way required by SNTEG/DSNTEG for the dynamic simulation of nonlinear systems. REACSUBS is linked to RSNTEG to form the RSNTEG executable. RSNTEG can simulate the full nonlinear reactor model as the actual plant, full-order or reduced-order linearized state-space models for the reactor (specified through ".CSC" or ".CSD" files) as the plant or as the model in the IMC structure and can carry out either open-loop or closed-loop simulations with linear or nonlinear controllers.

Only the subroutines within REACSUBS are described. The names of these subroutines (DPPAR, DPLANT and DPOST) are the standard names required by SNTEG/DSNTEG.

Name: DPPAR (in REACSUBS)

Purpose: Initialization routine required by SNTEG. In this case it provides all the parameters needed for the simulation of the non-linear reactor model.

Desc./Algor.: DPPAR reads the reactor data in the same way as does REACTORSS, and reads and transfers the information contained in the ".COD" file. DPPAR also opens the ".PDY" file (see

DPLANT).

Input: Files:

".COD"

".GEN"

".REA"

".INC" (read directly by RSNTEG (not through DPPAR))

Interactive

Output: Data are sent through COMMON blocks to the subroutine DPLANT, and through the parameter list, to the main program RSNTEG

Name of the ".PDY" file (see DPLANT)

Calls: GENDAT

REACDAT

Name: DPLANT (in REACSUBS)

Purpose: Main subroutine called by SNTEG for the function evaluations corresponding to the nonlinear plant.

Desc./Algor.: DPLANT is in essence the same subroutine employed in REACTORSS. The discretized reactor model (Eqs (A25)-(A28)) is implemented in the standard form required by the non-linear differential/algebraic equation solver DASSL (Petzold, 1982). The current value of the time derivatives is an *input* to the subroutine, and the output from the subroutine is the residual DELTA of the differential/algebraic system (cf. Eq. (6) of Chapter V). SNTEG calls DASSL; DASSL calls one of 16 subroutines RES01-RES16 according to the particular case within SNTEG (Chapter V); these RESxx subroutines are front-end

subroutines declared external in SNTEG; the RESxx subroutines call DPLANT.

Input: Reactor data coming from DPPAR through COMMON blocks, plus current values for the state, state derivative, input and disturbance vectors coming from RSNTEG through the parameter list.

Output: Current values for the residual of the differential/algebraic system, and for the system outputs. At regular intervals (specified by the user at the beginning of the interactive session) the values of all the reactor outputs are stored into a ".PDY" file for later use in different types of plots.

Calls: REAC

Name: DPOST (in REACSUBS)

Purpose: "Custom-made" output subroutine accepted by SNTEG.

Desc./Algor.: DPOST of REACSUBS reads the data stored in the ".PDY" file by DPLANT and plots the results. Different types of plots may be selected by the user in the interactive session. These include plots of temperature or concentration vs. time responses, or the time evolution of the temperature or concentration profiles along the reactor bed (for example, the plots in Fig. 7 of Chapter II).

Input: Data from the ".PDY" file

Interactive

Output: Plots

Calls: SELOUT2: Similar to SELOUT

MAPPLT

JCOBI

INTRP

Location: XHMEIA::USER1:[JAM.REACTOR]

Name: DYPLOT (4)

Purpose: As DPOST of REACSUBS, but can be run independently starting from any ".PDY" file.

Desc./Algor.: Essentially the same program as DPOST of REACSUBS.

Input: Files:

".PDY"

Interactive

Output: Plots

Location: XHMEIA::USER1:[JAM.REACTOR]

CONTROL SYSTEM DESIGN

Name: IMC

Purpose: SISO IMC controller computation.

Desc./Algor.: This program reads the poles, zeros and steady-state gain of a SISO transfer function, the desired filter time-constant and the time-constant of a first-order disturbance model and computes a state-space realization of the IMC controller, for inputs of the form $\frac{1}{s}$ or $\frac{1}{s(\tau_d s+1)}$ (Eqs (29)-(35), (37) and (40) of Chapter III). It also computes a state-space realization of the complementary sensitivity function (Eq. (42), Chapter III). The program is specially designed to handle systems of very large

order (like the 49th-order linearized reactor model). The state-space realization is done on the basis of the Jordan canonical form. Handles HONEY-X-type files.

Location: tybalt.caltech.edu[5] (/grad/jam)

Name: LMCALC

Purpose: Nominal model and multiplicative uncertainty computation in the frequency domain, starting from frequency domain data for a set of plants.

Desc./Algor.: At each frequency, each plant in the set π (Chapter II, Section 5.1) is defined by a point in the complex plane. At each frequency, the "nominal plant" is computed at the center of the smallest circle enclosing all points of π. A bound $\bar{l}_m$ on the multiplicative uncertainty is computed from the radius of this circle.

Location: tybalt.caltech.edu (/grad/jam)

Name: FFILTER

Purpose: This program finds the parameters of the IMC filter that minimize the SSV for a given interconnection structure and filter structure. (Written by E. Zafiriou and J.A. Mandler).

Desc./Algor.: Zafiriou and Morari (1986)

Location: tybalt.caltech.edu (/grad/ezz)

PARAMETER ESTIMATION/ MODEL IDENTIFICATION

Name: NONLIN

5. UNIX operating system.

Purpose: Parameter estimation from steady-state experiments for the methanation reaction.

Desc./Algor.: Levenberg/Marquardt method (IMSL routine ZXSSQ).

Location: XHMEIA::USER1:[JAM.NL]

Name: PARAMS (old implementation)

Purpose: Parameter estimation based on results of dynamic experiments. (For estimation of heat transfer coefficients of the reactor.)

Desc./Algor.: Marquardt algorithm. For each guess of the parameter vector, the steady-state solution is recomputed together with the state-space matrices. Analytic integrations of the linearized model are carried out to obtain the state-vector and the sensitivity coefficients as a function of time. These are required for the gradient and Hessian calculations.

A different implementation is suggested that would involve incorporating the nonlinear dynamic reactor model directly in the framework of the GREG package, a general regression software package for nonlinear parameter estimation (Caracotsios *et al.* , 1985). The sensitivity coefficients as a function of time (together with the solution vector) can be computed directly on the basis of the nonlinear reactor model, employing DASAC (Caracotsios and Stewart, 1985), a program for sensitivity analysis of nonlinear differential/algebraic systems. Because DASAC is written as an extension of DASSL, it employs the same type of subroutines for the nonlinear model as utilized throughout this work; this fact should facilitate the new implementation.

Location: PARAMS: XHMEIA::USER1:[JAM.PAR]

GREG: recently received from its authors; stored in

XHMEIA::USER1:[JAM.GREG]

Name: PRBSIN

Purpose: This program generates a pseudorandom binary sequence and saves it in a standard CONSYD ".CIC" file. (Written by J.A. Mandler and D.E. Rivera).

Use: SNTEG accepts ".CIC" files for the specification of input changes to the system. A procedure to characterize the dynamic behavior of the non-linear system in terms of linear models and to obtain a characterization of the uncertainty resulting from the system nonlinearity would involve pulsing the nonlinear reactor model with a PRBS generated by PRBSIN (carrying out the simulation with RSNTEG) and analyzing the simulation results through time series spectral analysis (program SPECTRAL (Rivera, 1986)).

Location: PRBSIN: IMC::USER:[JAM]

SPECTRAL: IMC::USER:[DER.SPECT]

OTHER COMPUTER PROGRAMS

HEXCH: code for the steady-state and dynamic simulation of the feed-effluent heat exchanger in the methanation reactor system (the heat exchanger model is solved through orthogonal collocation)

REACON: code for the solution of the steady-state reactor model through continuation techniques

CONHX, VMSUX: utility routines for data transfer from CONSYD to HONEY-X files

C. COMPUTER IMPLEMENTATION OF THE CONTROLLER DESIGN PROCEDURE

Listed below are the main steps followed in the control system design for the fixed-bed methanation reactor. The main computer programs employed in each step are indicated. Programs developed in the course of this project that run under UNIX are indicated with big *ITALICS*; HONEY-X programs (developed at Honeywell Systems and Research Center, Minneapolis, MN) are indicated with small *italics*. Programs developed in this work that run under VMS, and programs that belong to CONSYD, are indicated with capital ROMAN letters.

SISO STUDIES (Chapter III)

NOMINAL DESIGN (FULL LINEARIZED MODEL)

1. Steady-state solution for the nominal operating conditions. Computation of full state-space matrices. (REACTORSS)
2. Selection of input/output variables. (SELECT)
3. File transfer to HONEY-X. (CONHX; *VMSUX*)
4. Computation of poles and zeros. (*poles; zeros*)
5. Computation of the SISO IMC controller and the complementary sensitivity function. (*IMC*)
6. Sensitivity function plots. (*sub; fresp*)
7. Nominal closed-loop transfer function computation. (various HONEY-X commands)
8. File transfer to CONSYD. (*UXVMS*; HXCON)
9. Simulation. (RSNTEG; also SFOURIER (CONSYD program) for frequency files)

ROBUST CONTROLLER DESIGN[6]

6. File transfers between CONSYD and HONEY-X are no longer indicated, and are implied.

1. Steady-state solution for "operating conditions" corresponding to different points along the expected trajectory of the closed-loop system. Computation of full state-space matrices. (REACTORSS)

2. Selection of input/output variables. (SELECT)

3. Frequency response for each plant in π (cf. Chapter II). (*fresp*)

4. Nominal model computation (non-parametric description). The nominal model is selected at the center of the smallest circle including all plants in π, and a bound on the multiplicative uncertainty resulting from the system nonlinearity is calculated. (*LMCALC*)

5. Control-relevant model reduction, starting from the non-parametric description and incorporating information such as uncertainty bounds, disturbance models, and an initial choice for $\hat{\eta}$ (Chapter III). (REDUCE, written by D.E. Rivera (Rivera and Morari, 1985))

6. IMC controller, and complementary sensitivity function computation (for the reduced-order model). Appropriate values for the filter time constant are selected to satisfy robust stability according to Eq. (51) of Chapter III. (*IMC*)
   The evaluation of Eq. (51) is done through manipulations of the frequency files by means of HONEY-X commands or with the CONSYD program FMANI.

7. Simulation (nonlinear plant, linear model and controller). (RSNTEG)

MULTIVARIABLE STUDIES (Chapter IV)

NOMINAL DESIGN (FULL LINEARIZED MODEL)

1. Steady-state solution for the nominal operating conditions. Computation of full state-space matrices. (REACTORSS)

2. Selection of input/output vectors. (SELECT)

3. Construction of the interconnection structure for the nominal case (like the one in Fig. 13b of Chapter IV). The state-space description of the interconnected system is obtained through various HONEY-X commands (*para; mpy*), or by using the HONEY-X program *sico*.

4. H_2-optimal controller computation. This is done through an affine-parametrization/unitary-invariance/projection approach, fully explained by Doyle (1984) and Doyle and Chu (1986). The program *qparmn*, located in the extension to the HONEY-X package developed by Doyle and Chu (1986), is employed.

5. Nominal closed-loop transfer function computation. (Various HONEY-X commands or *sico*)

6. Simulation. (RSNTEG: open-loop simulation of the previously constructed, full-order closed-loop system)

ROBUST CONTROLLER DESIGN

1. Nominal model selection. This is done either as in the SISO case (the procedure is applied separately to each element of the transfer matrix and the uncertainty expressed as additive uncertainty on each element), or through other approaches, such as the one detailed in Section 5.3 of Chapter IV. (REACTORSS, SELECT, LMCALC, etc.)

2. For non-parametric descriptions, "open-loop" model reduction for each element of the transfer matrix. (REDUCE) (A multivariable version of REDUCE was not available at the time of conducting these control studies)

   For nominal models obtained directly in state-space (as in case-study II of Chapter IV) model reduction through balanced, minimal realizations. (*minrel*)

3. H_2-optimal controller computation for the nominal model selected. (*qparmn*)

4. Construction of the interconnection structure for the filter design step (cf. Fig. 13c of Chapter IV). This is done either in the state-space through *sico* or in the frequency domain through various HONEY-X commands. (*fresp, mpy, aug*)

5. Robust stability and robust performance analysis. The frequency-domain representation of the above interconnection structure is first found. (*fresp*)

   The selected filter is imbedded in this interconnection structure to obtain M' (cf. Chapter IV). (*fgdfb*)

   For robust stability analysis, $\mu(M'_{11}(j\omega))$, and for robust performance analysis, $\mu(M'(j\omega))$ (cf. Section 3 of Chapter IV) are computed employing the programs *mu* or *fmu*.

6. IMC filter design for robust performance (Eqs (37) or (38), Chapter IV). (Program *FFILTER* applied to the interconnection structure of step 4))

7. Simulation (nonlinear plant, linear model and controller). (RSNTEG)

B. CONTROL OF A PACKED-BED REACTOR WITH FEED-EFFLUENT HEAT EXCHANGE

Preliminary studies were conducted on possible control configurations for the reactor/feed-effluent heat exchanger system. These are summarized by the following paper presented at the 1984 American Control Conference, San Diego, CA.

CONTROL OF A PACKED BED REACTOR WITH FEED EFFLUENT HEAT EXCHANGE

J.A. Mandler, D.M. Strand, R. Khanna and J.H. Seinfeld

Department of Chemical Engineering
California Institute of Technology
Pasadena, California 91125

Abstract

Feed-effluent heat exchange and product recycle are common features of many industrial reactors. Nevertheless, there are few available studies on the design of control systems for packed bed, catalytic reactors operated under conditions of heat and/or mass recycle. This research addresses the design of control systems for a laboratory fixed bed methanation reactor with feed-effluent heat exchange. Together with the mathematical models, steady state relationships are presented which give an insight into the control problems to be encountered and the control strategies needed for a satisfaction of the proposed objectives.

1. Introduction

Feed-effluent heat exchange and product recycle are common features of many industrial reactors. Recycle streams are often employed with packed bed reactors for temperature control, inhibition of undesired side reactions or efficient use of reactants. Many industrial reactors utilize a configuration in which the reactor effluent is used to preheat the incoming fresh feed, resulting in energy recycle and an overall reduction in energy consumption.

Processes with recycle may be considerably more complex than their counterparts in the absence of recycle. In the packed bed catalytic reactor, positive thermal or mass feedback can contribute to the occurrence of multiple steady states and unstable behavior. Species fractionation and heat exchange processes, as well as significant transportation lags may be present in the recycle stream, which may have a strong effect on the dynamics of the system. In spite of this importance, there are few available studies on the development and implementation of control systems for reactors with recycle, particularly the packed bed, catalytic reactor.

This research addresses the design of control systems for a laboratory packed bed methanation reactor with feed-effluent heat exchange. Detailed mathematical models are employed for both the reactor and the feed-effluent heat exchanger. For some regions of operation the system is found to be highly sensitive, this resulting in a need for reliable control strategies.

In Section 2 a short description of the mathematical model for the reactor/heat exchanger system is given. In Section 3, steady state relationships are presented; these give an insight into the types of control problems that can be encountered, and a first indication of the control strategies that might satisfy the proposed objectives.

2. Mathematical Models

The experimental system, shown in Figure 1, is described in detail elsewhere [1]. The product recycle section will not be included in the present discussion; in addition, the preheater will be considered as being located between the mixer and the heat exchanger, that is, before and not after the latter.

The mathematical model of the fixed bed methanation reactor

1. incorporates axial and radial dispersion of mass and energy;
2. considers multiple reactions with nonlinear rate expressions;
3. involves a two-dimensional heterogeneous analysis;
4. accounts for the mole changes that occur with the reactions;
5. accounts for temperature, pressure and mole dependencies of gas velocity, density, average molecular weight and heat capacity, reaction rate constants and heats of reaction;
6. incorporates the effects of axial pressure gradients;
7. includes the analysis of a central thermal well.

The model is described by a coupled set of nonlinear partial differential equations. The methanation reaction is taken for the present purpose as the only significant reaction; the rate of the methanation reaction was experimentally found to be much greater than that corresponding to the steam-shift reaction on the nickel over alumina catalyst employed [2]. The reaction rate expression is a global rate expression, based on bulk gas conditions. Other major assumptions underlying the model are:

1. reactor wall temperature is equal to the cooling fluid temperature and is independent of length along reactor;

2. gas properties are functions of temperature, pressure and total moles as dictated by the ideal gas law;
3. there is no radial velocity; the applicability of this assumption has been verified by Hoiberg et al. [3].

A reactor model of this level of complexity has seldom been used in control studies. A more detailed description of the model and its formulation is given elsewhere [4].

The mathematical model for the countercurrent feed-effluent heat exchanger contains energy balances for the shell and tube walls in addition to those for the feed and effluent sides; axial conduction in the walls is included, also are the heat capacities dependences on the temperature; density variations are accounted for through the ideal gas law. The design flow rates and the geometry of this heat exchanger are such that operation close to the laminar flow region (Nusselt number approximately constant) is expected. The model is nonlinear as a result of the temperature dependences of the gas density and heat capacities.

One interior point is employed for the discretization of the reactor equations in the radial direction by means of collocation, based on a quadratic representation for the radial profiles. Orthogonal collocation is used for the discretization in the axial direction. Due to the steep profiles for some conditions, simulations have been performed using generally 12 interior collocation points. The number of interior collocation points required, and therefore the resulting number of ODE's, may be reduced (as required for controller design purposes) through the use of collocation on finite elements instead of the usual technique, even with an increase in the accuracy. The profiles obtained using the orthogonal collocation were compared with those obtained from three-point finite difference approximations with a large number of grid points; the match was satisfactory.

The heat exchanger PDE's were also converted to a set of ODE's by means of orthogonal collocation. Nonlinearities and arbitrary flow forcing are easily accounted for by the numerical approach. Four interior collocation points have been usually employed for the simulations. The resulting system consists of $4n_{colr}+1$ nonlinear ODE's together with $n_{colr}+5$ nonlinear algebraic equations for the reactor, plus $4n_{colh}+2$ nonlinear ODE's for the heat exchanger.

3. Steady State Solution of the Reactor-Feed-Effluent Heat Exchanger System

At steady state, the discretized model equations resulting from the collocation procedure become a system of nonlinear algebraic equations, which can be solved by a number of techniques.

Steady state relationships are important for an understanding of the control problems that may be encountered. For the reactor-feed-effluent heat exchanger system of Figure 2, an important relationship is the one between the outlet (T_{out}) and inlet (T_{in}) reactor temperatures, which are respectively related to the inlet temperature of the heat exchanger's effluent side, and to the outlet temperature of the heat exchanger's feed side. This relationship is shown in Figure 3. Each point in the reactor curve corresponds to a solution of the reactor's system of algebraic equations, and similarly the heat exchanger line represents a solution for the heat exchanger. The steady states for the combined system are given by the intersections between the reactor and heat exchanger lines. Two such steady states are shown in that figure. The reactor curve corresponds to a 6 percent CO concentration at the reactor's inlet. The heat exchanger line corresponds to a bypass ratio of zero and a temperature of 534 deg. K at the feed side's inlet. The reactor and heat exchanger curves were here calculated separately and later superposed. The steady states predicted in this way were then found by means of the secant method based on iterating on T_{in}. The lower and here upper (middle) steady state profiles are respectively shown in Figures 4 and 5. The upper (middle) steady state is unstable. At the first stage of these control studies, only operation about stable steady states is sought.

Numerical difficulties were experienced in the solution of the reactor equations due to the strong nonlinearities caused by the very high value for the activation energy determined experimentally. The reactor curve for E_a = 37000 cal/mol in Fig. 6 shows that while the profiles change slowly with an increase in T_{in} from 450 deg. K to about 535 deg. K (almost negligible conversion in that range), they change abruptly around 545 deg. K. The last point (A) drawn on that curve corresponds to approximately 20% conversion. The points at the maxima of the two other curves shown (calculated for lower values of E_a) correspond to complete conversion. The curves were obtained employing a pseudo arc-length method for continuation around regular and normal limit points [5] based on either Newton's method or Powell's method [6]. The method is appropriate for cases in which folds might appear in a x vs λ curve, where x corresponds to a dependent variable (in this case T_{out}) and λ to a parameter (here T_{in}). No other points could be found on that branch beyond point (A), even with the continuation procedure. The E_a = 37000 curve resembles the lower branch in a multiplicity pattern reported by Puszyński et al. [7] for a similar reactor but with different kinetics. An upper branch of complete conversion (separated from the lower branch) is also shown by those authors. The lower branch (kinetic regime) is characterized by flat profiles while the upper branch (diffusion regime) presents instead a hot spot very close to the reactor entrance. No steady state solution in an upper branch of complete conversion could yet be found numerically for E_a = 37000; dynamic simulations and techniques like coordinate stretching have been also unsuccessful to date for the elucidation of this question.

Operation in a steady state of complete conversion is of little interest in the context of these

control studies, as not much is left for regulation when all the reactant is consumed at the very entrance of the reactor. A challenging control problem, and the one which we currently address, is instead to regulate the product concentration around a set point located in the region where the reactor sensitivity is high, i.e., close to the bend in the reactor curve, where the conversion is mild but the danger of the reactor literally "blowing up" is high. A very reliable control system is obviously required for that region of operation.

The main disturbances considered are fluctuations in the reactant (CO) feed concentration. Such upsets are common in practice. Figure 7 shows the steady state relationships between the CH_4 outlet concentration and the reactor outlet temperature, for different CO inlet concentrations. The curves suggest that the mole fraction of the product is not strongly dependent on that of the reactant for this low conversion region (up to around 20%) but instead it is strongly correlated and in an almost linear fashion to T_{out}. Therefore, in order to regulate the product concentration, an initial simplified control strategy based on the regulation of the reactor outlet temperature is justified.

Figure 8, in which outlet vs inlet reactor temperatures are plotted for different reactant concentrations, suggests the importance of a rapid and correct manipulation of the inlet temperature, to maintain the outlet temperature set point (and also prevent the reactor runaway), in the face of reactant fluctuations. (Here is convenient to note that the reaction rate vs CO concentration curve has a maximum at very low CO concentrations, and therefore the carbon monoxide acts as an inhibitor over almost the entire range of concentrations.)

Up to this point the presence of the feed-effluent heat exchanger has not been considered. The inlet temperature would be manipulated for example by means of an electrical preheater and a bypass stream around it, the bypass allowing fast control action. An obviously more difficult situation results from the inclusion of the feed-effluent heat exchanger. This inclusion is in general well justified by economic considerations, as one important objective is the minimization of the energy consumption from elements such as the electrical preheater. Of course, the heat exchanger's presence results in the following problem: disturbances, strongly amplified by the reactor because of the nonlinearities (Fig. 8), now also affect the inlet temperature; in other words, the positive feedback of heat introduces a destabilizing effect, which needs to be stabilized by the control system.

The first proposed control strategy is shown in Figure 9a. Regulation of the reactor outlet temperature around its set point (determined from the relationship of Figure 7), will be performed by means of a SISO control system including a cascade. Fast response is required from the actuator: the manipulative variable will be the ratio B of feed stream bypassed around the preheater and the heat exchanger. The cascade, introduced to eliminate the effects of minor disturbances, is (as shown by Figure 9b) equivalent to an inner loop in which an extra measurement and a controller are employed for trying to improve the characteristics of the open loop system. Steady state relationships like the ones given by Figure 10 will be utilized for a determination of the set point for the outlet temperature from the preheater (T_f). This temperature is especially important because its change shifts up or down the heat exchanger lines; an appropriate set point must be found for this temperature, such that there would always be a heat exchanger line (given by a certain value of B) that would intersect the reactor curve at the desired value of the reactor outlet temperature, for the whole range of expected disturbances; that is the case in Figure 10, where it is seen that for T_f = 537°K there always exists a heat exchanger line that crosses a reactor curve, if the only disturbances are in the CO concentration with minimum and maximum values respectively 4 and 6 percent; if instead the CO concentration were increased to 8 percent, then it would be impossible to obtain lower steady states having T_{out} greater than 540 deg. K; if disturbances as such were expected, the T_f set point would have to be fixed instead at a greater value (the dashed line corresponds to T_f = 555 deg. K, and B = 0). Having fixed T_f at a convenient value the SISO scheme with B as the manipulative variable would be sufficient for this "idealized" case. The bypass ratio value for the nominal set point would be in a middle range, therefore allowing control in the face of disturbances to both sides. As seen in Figure 10, operation in the steady states of low conversion requires high values of T_f; the heat exchanger is not a very effective device in this region, but this is not of great concern in the context of these control studies; the low bypass ratio values required are a result of the low temperature of the bypass stream selected here (300 deg. K).

A second, more involved strategy, leading to a more flexible control system, is shown in Figure 11; a second control objective would be added, namely the regulation of the bypass ratio B at a nominal value; T_f (through the preheater heat load), would now be manipulated to achieve this objective. Both control objectives should be satisfied simultaneously, this scheme constituting a MIMO one. Being that the response of the preheater is naturally slow, the following behavior can be expected: in the face of fast changes of B up and down from its nominal value, the preheater loop would not react in a net sense; instead, in the face of a sustained disturbance leading B to zero or a low value for a longer period of time (with a limit close to being reached therefore in the applicable control action), T_f would slowly be increased, shifting down the heat exchanger lines of Figure 10. A value of B too high would also be unacceptable because it would mean too much energy being wasted. T_f would be reduced in this case, and B would return to a value in the middle range in order to satisfy the main objective. Although not shown in the diagram, another control loop is required (for the preheater), for this and also for the previous strategy. The second loop mentioned above would determine the T_f set point; (for the first strategy

the T_f set point would be fixed at the value determined from the steady state relationships); the objective of the third loop would be to maintain T_f at that set point value in the face of disturbances in the flow rate, due obviously to the changes in B. The manipulative variable would be the electrical heat load.

It is seen that a good first insight is provided by the steady state relationships, as a determination of how the system will react to sustained disturbances can be made. Of course, this is only the first step in a control study, the obvious next step being the study of the system dynamics, which leads to the controller design. Results from these studies, performed with the help of a linearized model for the whole system, and a computer-aided control system design package, will be presented in the future.

References

[1] Strand, D.M. and Seinfeld, J.H., Paper 92d, 1982 Annual Meeting, A.I.Ch.E. Los Angeles, (1982)

[2] Chiang, D.N., "CO Methanation Over a Nickel Catalyst," M.Sc. thesis, Calif. Inst. of Technology, Pasadena, CA (1983)

[3] Hoiberg, J.A., Lyche, B.C. and Foss, A.S., A.I.Ch.E. Journal, 17, 1434 (1971).

[4] Khanna, R. and Seinfeld, J.H. Paper 9d, 1982 Annual Meeting, A.I.Ch.E., Los Angeles (1982)

[5] Keller, H.B., "Numerical Solution of Bifurcation and Nonlinear Eigenvalue Problems," in "Applications of Bifurcation Theory," Academic Press, New York. (1977)

[6] Powell, M.J.D., "A Hybrid Method for Nonlinear Equations" in "Numerical Methods for Nonlinear Algebraic Equations," P. Rabinowitz (ed), Gordon and Breach, New York, London (1970).

[7] Puszyński, J., Snita, D., Hlavácek, V., and Hofmann, H., Chem. Eng. Sci. 36, 1605 (1981).

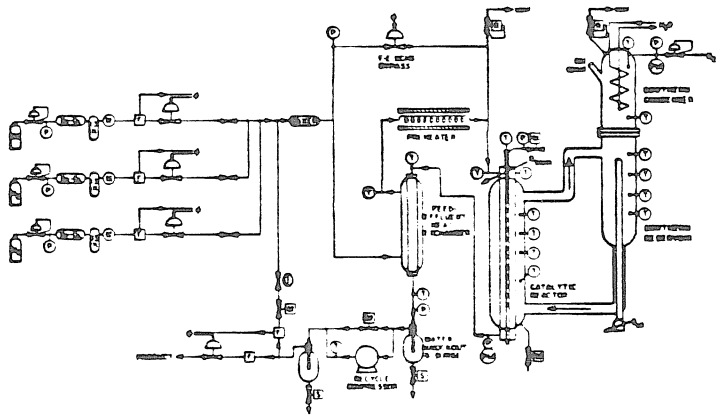

Fig. PROCESS DIAGRAM FOR EXPERIMENTAL CATALYTIC REACTOR

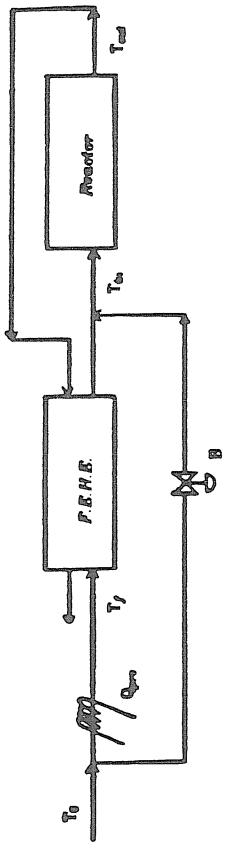

Fig. 2: Reactor/Feed-Effluent Heat Exchanger System

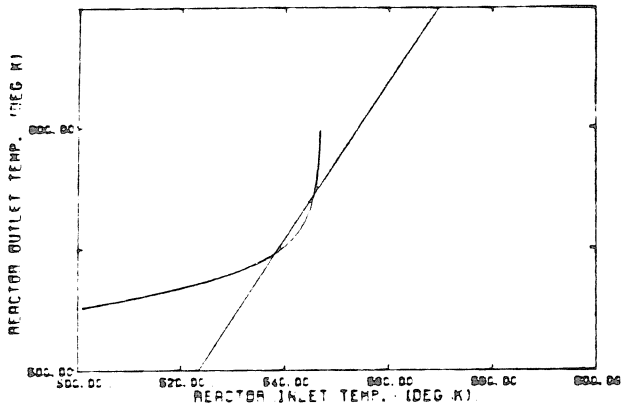

Fig 3: Steady State Relationship for Reactor/Heat Exchanger System (T_{out} vs. T_{in}) - (6% CO, 18% H_2, T_f = 534°K, B = 0, $T_{wall\ r}$ = 530°K, total flow rate: 0.022 gmol/sec)

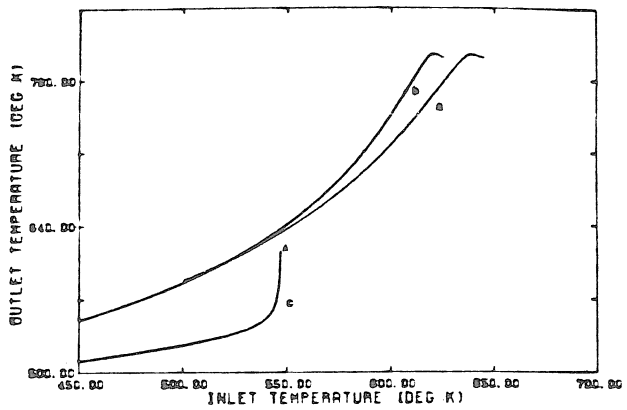

Fig. 6: Reactor Outlet vs. Inlet Temperatures for Different Values of the Activation Energy (a: Ea = 6500 cal/mol; b: Ea = 7000 cal/mol, c: Ea = 37000 cal/mol; 6% CO, 18%, H_2; T_{wall} = 530°K; flow rate: 0.022 gmol/sec).

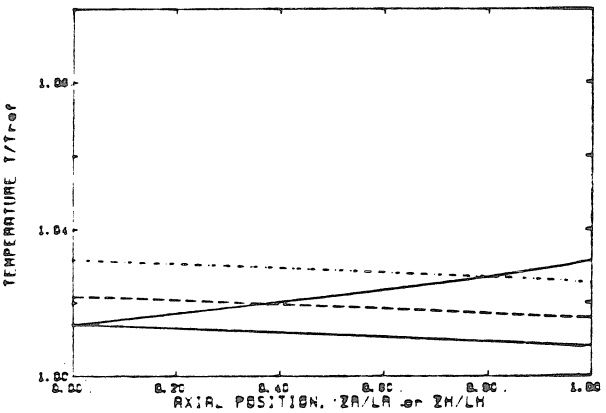

Fig 4: Profiles for Lower Steady State in Fig. 3. (solid ascending line: reactor gas temperature, descending lines: heat exchanger temperatures - - - - - effluent side, - - - - tube wall, - ——— - feed side, ——— shell wall; Tref = 530°K, LH = 0.5 m, LR = 0.3 m)

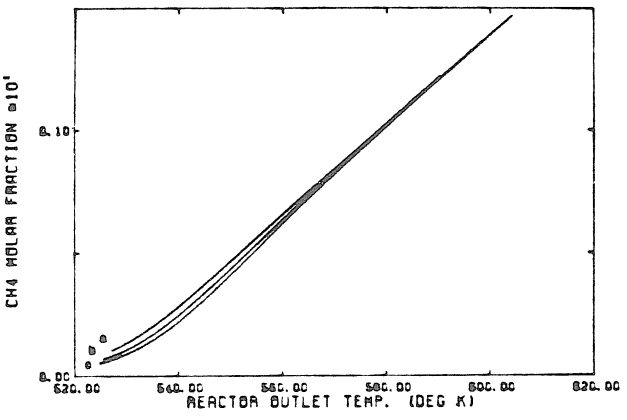

Fig. 7: Product Concentration vs. Outlet Reactor Temperature for Different Reactant Concentrations (a: 4 % CO; b: 6% CO; c: 8%. CO)

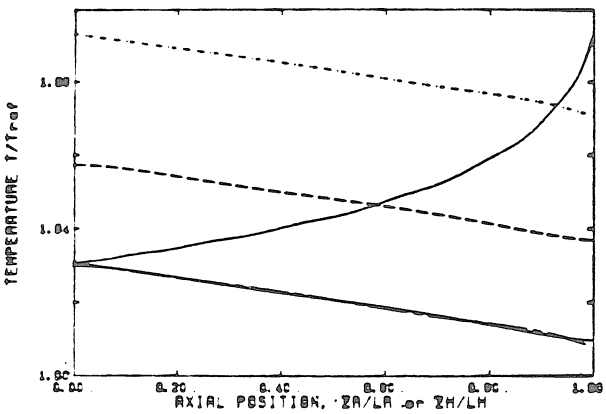

Fig. 5 Profiles for Upper (Middle) Steady State in Fig. 3.

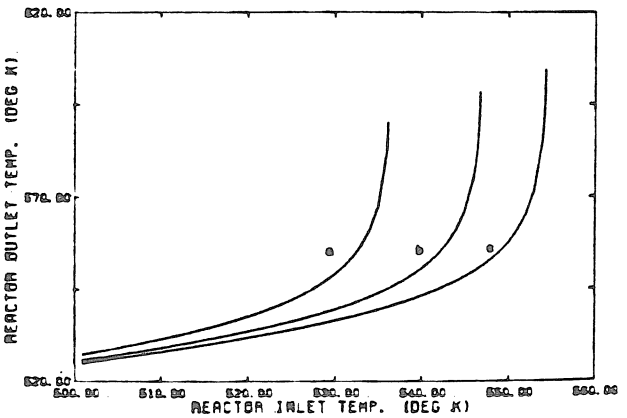

Fig. 8: Reactor Outlet vs. Inlet Temperatures, Different Reactant Concentrations (a: 4% CO, b: 6% CO; c: 8% CO)

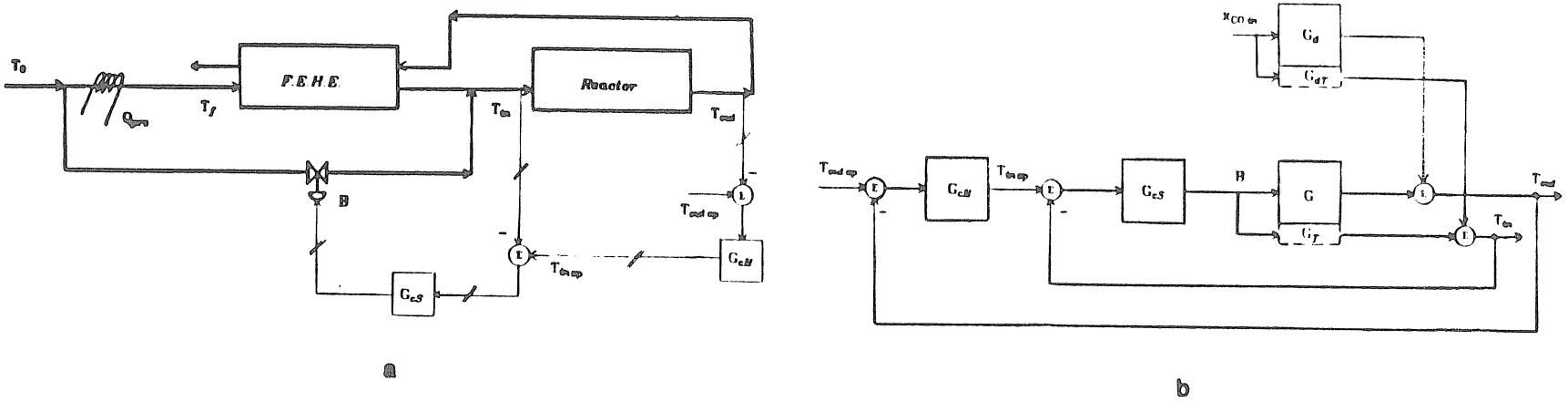

Fig. 9: First Proposed Control Strategy: a) System Configuration; b) Block Diagram

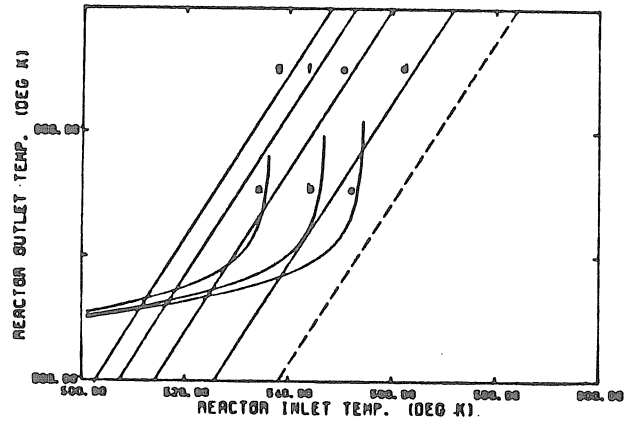

Fig. 10: Steady State Relationships for Reactor/Heat Exchanger System for Different Values of B and T_f. (a: reactor curve, 4 % CO; b: 6% CO; c: 8% CO; solid lines: T_f = 537°K; d: B = 0, e: B = 0.05, f: B = 0.08, g: B = 0.1; dashed Line: T_f = 555°K, B = 0.)

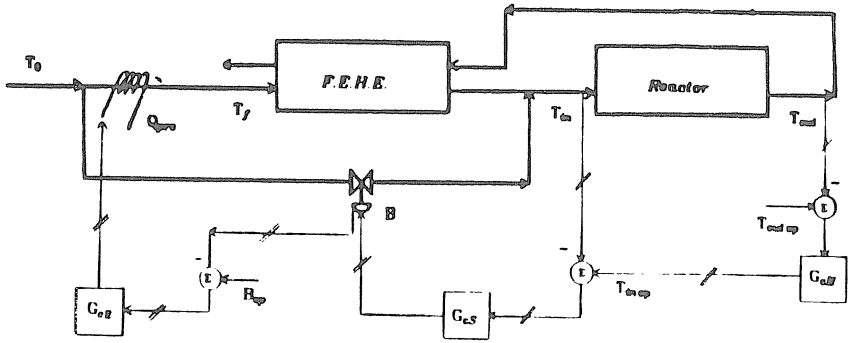

Fig. 11: Second Proposed Control Strategy

REFERENCES

Caracotsios, M. and W.E. Stewart, 1985, Sensitivity analysis of initial value problems with mixed ODE's and algebraic equations. *Comput. and Chem. Engng* **9** , 359-365.

Caracotsios, M., W.E. Stewart and J.P. Sorensen, 1985, GREG - General REGression software package for nonlinear parameter estimation. User's Manual. University of Wisconsin, Madison, WI.

Chiang, D.N., 1983, CO methanation over a nickel catalyst. M.Sc. Thesis, Calif. Inst. of Technology, Pasadena, CA.

Doyle, J.C., 1984, Lecture notes, ONR/Honeywell Workshop on Advances in Multivariable Control, Minneapolis, MN.

Doyle, J.C. and C. C. Chu, 1986, Robust control of multivariable and large scale systems. Technical report to A.F.O.S.R. for period July 1984/ October 1985.

Khanna, R., 1984, Control model development for packed-bed chemical reactors. Ph.D. Thesis, Calif. Inst. of Technology, Pasadena, CA.

Morari, M. and W.H. Ray, 1986, CONSYD - Control System Design Software. Version 3.0. Calif. Inst. of Technology, Pasadena, CA and University of Wisconsin, Madison, WI.

Pereira-Duarte, S.I., G.F. Barreto and N.O. Lemcoff, 1984, Comparison of two-dimensional models for fixed-bed catalytic reactors. *Chem. Engng Sci.* **39** , 1017-1024.

Petzold, L.R., 1982, A description of DASSL: a differential/algebraic system solver. *Sandia Tech. Rep.* 82-8637.

Rivera, D.E., 1986, Modeling requirements for process control. Ph.D. Thesis, Calif. Inst. of Technology, Pasadena, CA, in preparation.

Rivera, D.E. and M. Morari, 1985, Internal Model Control perspectives on model reduction. Proceedings of the 1985 American Control Conference, Boston, MA, pp. 1293-1298.

Strand, D.M., 1984, Personal communication. Calif. Inst. of Technology, Pasadena, CA.

Villadsen, J.V. and M.L. Michelsen, 1978, *Solution of Differential Equation Models by Polynomial Approximation* , Prentice-Hall, Englewood Cliffs, New Jersey.

Zafiriou, E. and M. Morari, 1986, Design of the IMC filter by using the structured singular value approach. Proceedings of the 1986 American Control Conference, Seattle, WA.